ISSN 0021-9673

VOL. 539 NO. 2 FEBRUARY 22, 1991

THIS ISSUE COMPLETES VOL. 539

Biochromatography and Molecular Affinity
Dijon, May 22–25, 1990

JOURNAL OF CHROMATOGRAPHY

INCLUDING ELECTROPHORESIS AND OTHER SEPARATION METHODS

ELSEVIER

JOURNAL OF CHROMATOGRAPHY

Scope. The *Journal of Chromatography* publishes papers on all aspects of chromatography, electrophoresis and related methods. Contributions consist mainly of research papers dealing with chromatographic theory, instrumental development and their applications. The section *Biomedical Applications*, which is under separate editorship, deals with the following aspects: developments in and applications of chromatographic and electrophoretic techniques related to clinical diagnosis or alterations during medical treatment; screening and profiling of body fluids or tissues with special reference to metabolic disorders; results from basic medical research with direct consequences in clinical practice; drug level monitoring and pharmacokinetic studies; clinical toxicology; analytical studies in occupational medicine.

Submission of Papers. Manuscripts (in English; *four* copies are required) should be submitted to: Editorial Office of *Journal of Chromatography*, P.O. Box 681, 1000 AR Amsterdam, The Netherlands, Telefax (+31-20) 5862 304, or to: The Editor of *Journal of Chromatography, Biomedical Applications*, P.O. Box 681, 1000 AR Amsterdam, The Netherlands. Review articles are invited or proposed by letter to the Editors. An outline of the proposed review should first be forwarded to the Editors for preliminary discussion prior to preparation. Submission of an article is understood to imply that the article is original and unpublished and is not being considered for publication elsewhere. For copyright regulations, see below.

Subscription Orders. Subscription orders should be sent to: Elsevier Science Publishers B.V., P.O. Box 211, 1000 AE Amsterdam, The Netherlands, Tel. (+31-20) 5803 911, Telex 18582 ESPA NL, Telefax (+31-20) 5803 598. The *Journal of Chromatography* and the *Biomedical Applications* section can be subscribed to separately.

Publication. The *Journal of Chromatography* (incl. *Biomedical Applications*) has 38 volumes in 1991. The subscription prices for 1991 are:

J. Chromatogr. (incl. *Cum. Indexes, Vols. 501–550*) + *Biomed. Appl.* (Vols. 535–572):
Dfl. 7220.00 plus Dfl. 1140.00 (p.p.h.) (total *ca.* US$ 4696.50)

J. Chromatogr. (incl. *Cum. Indexes, Vols. 501–550*) only (Vols. 535–561):
Dfl. 5859.00 plus Dfl. 810.00 (p.p.h.) (total *ca.* US$ 3746.50)

Biomed. Appl. only (Vols. 562–572):
Dfl. 2387.00 plus Dfl. 330.00 (p.p.h.) (total *ca.* US$ 1526.50).

Our p.p.h. (postage, package and handling) charge includes surface delivery of all issues, except to subscribers in Argentina, Australia, Brasil, Canada, China, Hong Kong, India, Israel, Malaysia, Mexico, New Zealand, Pakistan, Singapore, South Africa, South Korea, Taiwan, Thailand and the U.S.A. who receive all issues by air delivery (S.A.L. — Surface Air Lifted) at no extra cost. For Japan, air delivery requires 50% additional charge; for all other countries airmail and S.A.L. charges are available upon request. Back volumes of the *Journal of Chromatography* (Vols. 1–534) are available at Dfl. 208.00 (plus postage). Claims for missing issues will be honoured, free of charge, within three months after publication of the issue. Customers in the U.S.A. and Canada wishing information on this and other Elsevier journals, please contact Journal Information Center, Elsevier Science Publishing Co. Inc., 655 Avenue of the Americas, New York, NY 10010, U.S.A., Tel. (+1-212) 633 3750, Telefax (+1-212) 633 3990.

Abstracts/Contents Lists published in Analytical Abstracts, Biochemical Abstracts, Biological Abstracts, Chemical Abstracts, Chemical Titles, Chromatography Abstracts, Clinical Chemistry Lookout, Current Contents/Life Sciences, Current Contents/Physical, Chemical & Earth Sciences, Deep-Sea Research/Part B: Oceanographic Literature Review, Excerpta Medica, Index Medicus, Mass Spectrometry Bulletin, PASCAL-CNRS, Pharmaceutical Abstracts, Referativnyi Zhurnal, Research Alert, Science Citation Index and Trends in Biotechnology.

See inside back cover for Publication Schedule, Information for Authors and information on Advertisements.

0021-9673/91/$03.50

This issue is printed on acid-free paper.

Printed in The Netherlands

For Contents, see p. III

SPECIAL ISSUE

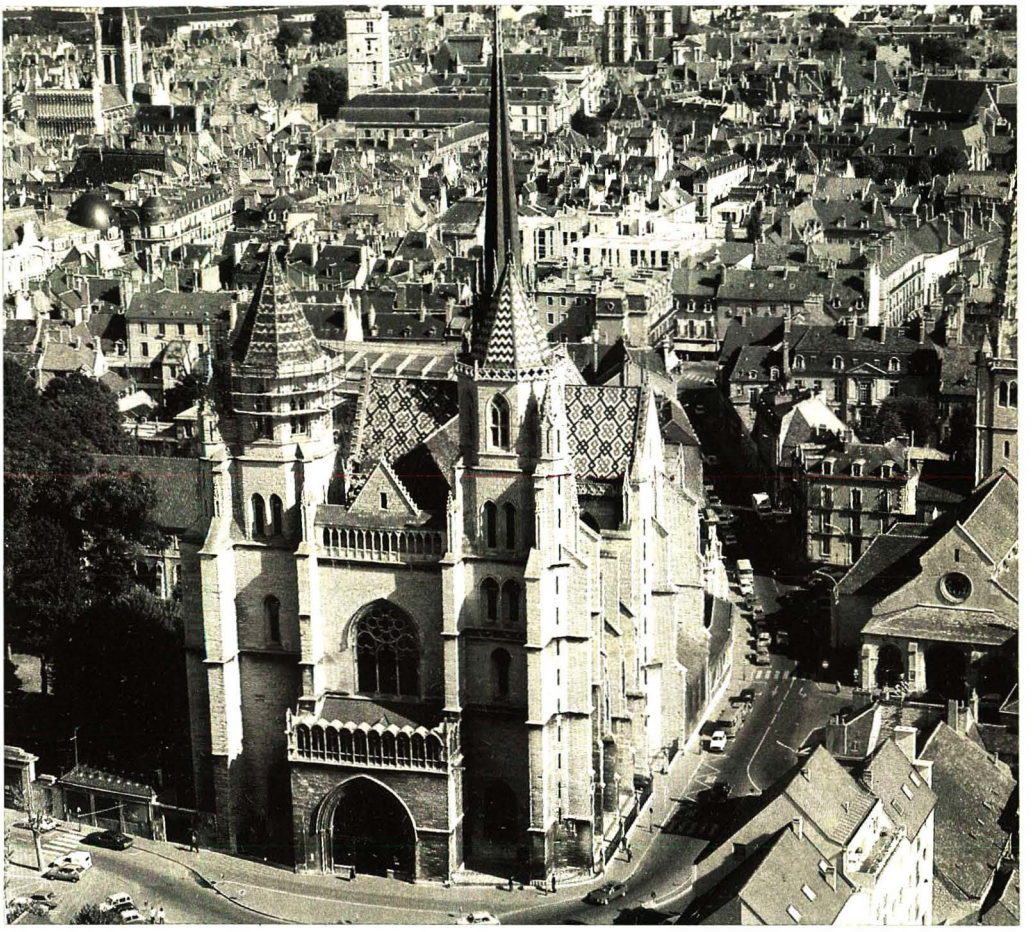

BIOCHROMATOGRAPHY AND MOLECULAR AFFINITY

THIRD MEETING OF THE FRENCH SOCIETY OF BIOCHROMATOGRAPHY

Dijon (France), May 22–25, 1990

Guest Editors

ANTE M. KRSTULOVIĆ
(Paris)

JEAN-PIERRE DANDEU
(Paris)

VOL. 539, NO. 2 JOURNAL OF CHROMATOGRAPHY FEBRUARY 22, 1991

CONTENTS

BIOCHROMATOGRAPHY AND MOLECULAR AFFINITY, 3rd MEETING OF THE FRENCH SOCIETY OF BIOCHROMATOGRAPHY, DIJON, MAY 22–25, 1990

In articles with more than one author, the name of the author to whom correspondence should be addressed is indicated in the article heading by a 6-pointed asterisk (*)

Journal of Chromatography, 539 (1991) 243
Elsevier Science Publishers B.V., Amsterdam

CHROM. 22 918

PREFACE

Recent advances in the fields of molecular biochemistry, biotechnology and gene technology have been made possible by the continuous developments in the separation sciences, which are becoming increasingly sophisticated in order to meet the required needs. Among the techniques which have been playing a key role in the analysis and isolation of biomolecules and the understanding of interactions on the molecular level, liquid chromatography has been particularly useful.

Therefore, it is not surprising that the 4-day *Third European Meeting of the Groupe Français de Bio-Chromatographie*, organized jointly with the International Society of Biorecognition Technology, and held in the beautiful capital of Burgundy, Dijon, renowned for its history, art and gastronomy, attracted some 300 prominent researchers from France, Belgium, Germany, Israel, Italy, Sweden, U.K., U.S.A., U.S.S.R. and The Netherlands.

Following a brilliant introduction on "Supramolecular chemistry: from molecular recognition towards molecular devices and self-organization", delivered by the French Nobel Laureate Professor Jean-Marie Lehn, the themes discussed were biochromatography (supports and derivatization, hydrophobic interactions), molecular recognition and affinity chromatography (biospecific affinity, immunoaffinity), pseudospecific affinity, protein conformation and chromatographic behaviour and miscellaneous topics.

In addition to the very informative lectures and posters on the latest developments in these areas, this conference also provided an ideal podium for informal exchange of experiences, much appreciated by the participants. The concurrent instrument display demonstrated state-of-the-art technological advances.

It is hoped that this special issue will be a useful source of information to researchers in this field, and an additional stimulus for the work that remains to be done for a better understanding of the intriguing facets of life.

We acknowledge the kind assistance of Professors Sebille and Muller, and as that of the reviewers, for their prompt and expert evaluation of the manuscripts.

Paris (France)

ANTE M. KRSTULOVIĆ
JEAN-PIERRE DANDEU

Journal of Chromatography, 539 (1991) 245–254
Elsevier Science Publishers B.V., Amsterdam

CHROM. 22 873

Investigation of liquid phase cooperative binding interactions on the capacity of insoluble affinity adsorbents

A. G. MAYES
Biochemistry Department, University of Bath, Claverton Down, Bath BA2 7AY (U.K.)
J. HUBBLE*
School of Chemical Engineering, University of Bath, Claverton Down, Bath BA2 7AY (U.K.)
and
R. EISENTHAL
Biochemistry Department, University of Bath, Claverton Down, Bath BA2 7AY (U.K.)

ABSTRACT

Experimental data is presented to support the theoretical prediction of an enhancement of adsorption arising from a positively cooperative liquid phase interaction between a multivalent adsorbate and free ligand. The results obtained with glyceraldehyde 3-phosphate dehydrogenase show a 4-fold increase in adsorption to 5′-adenosine monophosphate cellulose in the presence of 3 μM nicotinamide adenine dinucleotide compared with that obtained in the absence of cofactor. Although the magnitude of the effect, and the optimal free ligand concentration do not correspond to those predicted in the original model, the discrepancies may at least in part be accounted for by a maldistribution of immobilised ligand, leading to multiple cooperative interactions between adsorbate and affinity matrix. This can be qualitatively predicted by an extension to the original model.

INTRODUCTION

Separation techniques based on affinity adsorption have great potential for the production of high value, high purity bioproducts. This results from the high degree of selectivity and the consequently large purification factors which can be achieved. However, as affinity adsorption is adopted as a process scale operation the optimisation of empirically developed laboratory-scale methodology becomes important for maximising yield and quality of the end product.

Although much effort has been directed towards optimisation of the solid phase, *i.e.*, investigation of ligand immobilisation chemistry and the effect of both the length and nature of spacer arms, there appears to have been little consideration given to the possible contribution of the liquid phase to the overall performance of a system, for example the possible gains achievable by using free ligand in the liquid phase to enhance the binding of a positively cooperative enzyme to the solid phase.

The property of positive cooperativity, whereby proteins show sigmoid ligand binding isotherms is a fairly common feature of multimeric proteins in free solution.

0021-9673/91/$03.50

The performance and capacity of affinity adsorbents is strongly influenced by the affinity of the protein for the immobilised ligand. It therefore seems likely that adding free ligand to positively cooperative protein in the presence of immobilised ligand will increase the affinity of the protein for all available ligand and hence lead to tighter binding of protein to matrix ligand. This hypothesis was examined quantitatively in computer simulations by Hubble [1], which suggested that significant gains could be achieved in an appropriate system. In this paper we report attempts to obtain experimental evidence for this behaviour and compare the results with the theoretical predictions obtained from computer simulation.

MATERIALS

N^6-(6-aminohexyl)AMP, N^6-(6-aminohexyl)NAD^+, long fibrous cellulose powder, glyceraldehyde 3-phosphate dehydrogenase (GAPDH), glyceraldehyde 3-phosphate diethyl acetal and NAD^+ were obtained from Sigma (Poole, Dorset, U.K.).

Free glyceraldehyde 3-phosphate was liberated from the diethyl acetal (Sigma) by heating an aqueous solution in the presence of Dowex 50 H^+ resin, and was assayed using GAPDH and NAD^+ to check for complete hydrolysis of the acetal. This was stored in aliquots at $-20°C$ until required.

Sepharose 4B came from Pharmacia (Uppsala, Sweden). All other chemicals were of analytical grade.

METHODS

Preparation of nucleotide matrix derivatives

Sepharose 4B or long fibrous cellulose was activated with cyanogen bromide using the method of March *et al.* [2]. The final wash was with 0.1 *M* sodium bicarbonate pH 8.9 (buffer A). Matrix was resuspended in an equal volume of buffer A and sufficient N^6-(6-aminohexyl)AMP or N^6-(aminohexyl)NAD^+ added to give the desired concentration of matrix ligand. This was agitated gently for 16 h at 4°C. The matrix was washed with buffer A and the washings retained for spectrophotometric determination of unbound ligand. The washed matrix was added to 1 *M* ethanolamine and left at room temperature for 2 h to block any remaining reactive groups, then washed with water, 1 *M* sodium chloride and water again before storage at 4°C as a moist cake. Ethanolamine–Sepharose was prepared by activation followed by immediate blocking with ethanolamine.

Ligand bound to the matrices was estimated by calculation of the difference between ligand added and ligand remaining in the washings. Absorbance was measured at 267 nm and a molar absorptivity of 17.7 $mM^{-1}cm^{-1}$ used for calculations [3]. Ligand bound to Sepharose was also estimated by direct spectroscopy of a 10% suspension of matrix in glycerol–water (50:50, w/w) using a similar suspension of underivatised Sepharose as a blank. The wavelength maximum and molar absorptivity of the coupled ligand were assumed to be the same as for the free ligand. The two methods showed close agreement.

Coupling was consistently found to be 94–96% for Sepharose and 50–60% for cellulose.

Nucleotide removal from GAPDH

Nucleotides were removed by charcoal treatment using the method of Gennis [4]. Treated GAPDH had an A 280 nm/A 260 nm ratio of about 2 and was stored as an ammonium sulphate suspension at 4°C until required.

Assay of GAPDH

GAPDH was assayed at pH 8.5 and 25°C in 1 ml of a buffer containing (final concentrations) 50 m*M* sodium pyrophosphate, 5 m*M* EDTA, 10 m*M* sodium dihydrogen orthophosphate, 0.1 *M* potassium chloride, 10 m*M* cysteine, 1 m*M* NAD^+, and 1 m*M* D-glyceraldehyde 3-phosphate (2 m*M* DL racemate) which was added last to initiate the reaction. Enzyme (about 0.005 I.U.) was preincubated for 8 min in the assay buffer to ensure complete reduction of active site thiol groups. Increase in absorbance at 340 nm was followed using a Cecil 272 UV spectrophotometer fitted with a jacketed cuvette holder. Temperature was maintained using a recirculating water bath and cuvettes were left for 15 min to equilibrate prior to use.

Equilibrium batch adsorption

A quantity of matrix equal to 4 ml settled volume was added to 20 ml 50 m*M* sodium pyrophosphate buffer pH 8.5 containing 1 m*M* 2-mercaptoethanol and 1 m*M* EDTA. The total volume was measured and the suspension added to a water jacketed vessel maintained at 25 $\pm$ 0.3°C, stirred with an overhead stirrer to minimise physical matrix degradation. A known amount of GAPDH was added and allowed to equilibrate for about 10 min.

A 100-μl sample was withdrawn, spun briefly to sediment the matrix and 20-μl samples of supernatant removed for triplicate enzyme assays. The total added ligand concentration in the vessel was increased by adding a small volume of NAD^+ solution and the system allowed to re-equilibrate for 8 min before repeating the cycle. This was continued until the desired range of added ligand had been covered.

The concentration of free enzyme is found from the assays so, knowing the total amount of enzyme initially added and the system volume (recalculated after each cycle), bound enzyme can be calculated from the enzyme mass balance for each concentration of added ligand.

RESULTS AND DISCUSSION

Fig. 1 shows the simulated effect of free ligand concentration on GAPDH adsorption using theory developed by Hubble [1] and literature values for the binding constants [4]. In contrast Fig. 2a–c shows plots of bound enzyme/total enzyme against log added NAD^+ from batch adsorption experiments using AMP–Sepharose matrices with different ligand densities. In order to keep the bulk average matrix ligand concentration comparable the volume of the highest ligand density AMP–Sepharose used was lower than that used in the other two experiments. As might be expected the fractional binding in the absence of free NAD^+ (arbitrarily plotted at -6.5) increased with increasing ligand density but the predicted enhancement of binding on adding free NAD^+ was not apparent under the experimental conditions adopted for any of the matrix ligand densities tested. Similar results were obtained for NAD^+–Sepharose matrices (data not shown).

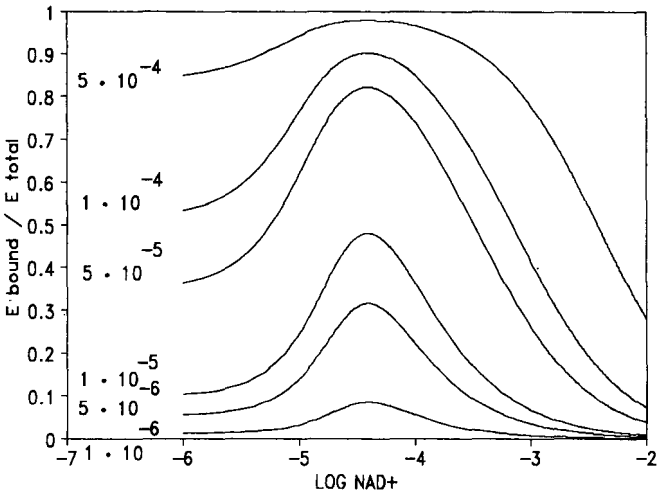

Fig. 1. The predicted effect of matrix ligand concentration on the relationship between free ligand concentration and the fraction of enzyme bound for glyceraldehyde 3-phosphate dehydrogenase. The affinity constants used were derived from the data of Gennis [4]. $K_1 = 2.6 \cdot 10^3$, $K_2 = 1.5 \cdot 10^4$, $K_3 = 1.9 \cdot 10^5$, $K_4 = 5.7 \cdot 10^3\ M^{-1}$. The matrix ligand concentrations were: $1 \cdot 10^{-6}$, $5 \cdot 10^{-6}$, $1 \cdot 10^{-5}$, $5 \cdot 10^{-5}$, $1 \cdot 10^{-4}$, $5 \cdot 10^{-4}\ M$.

The data obtained using AMP cellulose is shown in Fig. 3. Due to the low levels of binding observed in this system the scatter of points in individual experiments was greater than for the Sepharose experiments since the magnitudes of the changes in bound enzyme were similar to the magnitudes of the errors. All the individual experiments suggested that some enhancement of binding was occurring, with control experiments using blank cellulose and ethanolamine-derivatised cellulose showing no

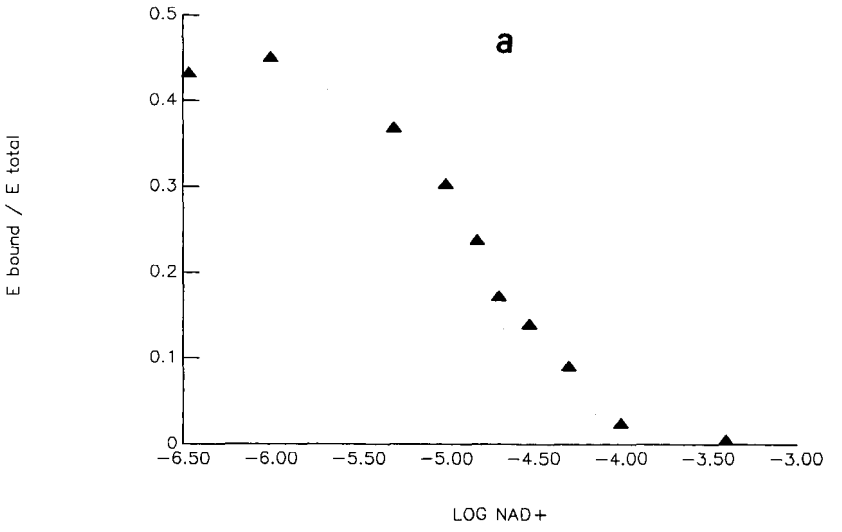

Fig. 2.

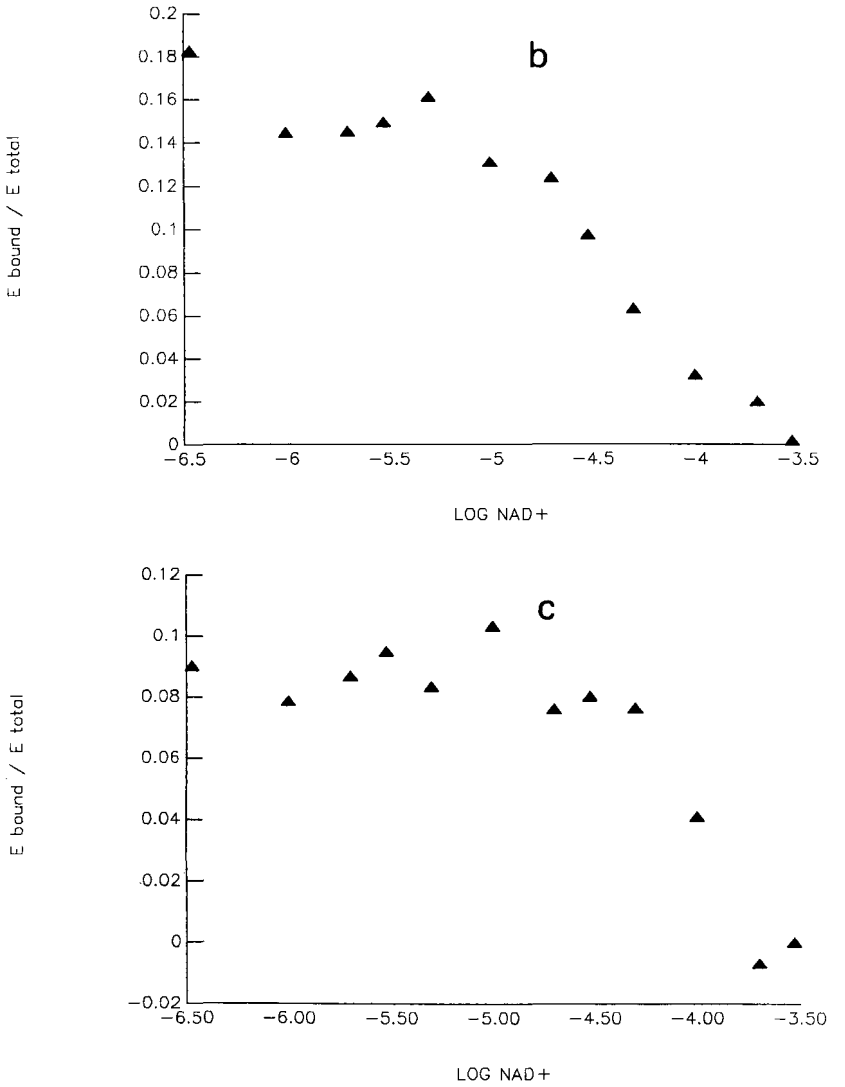

Fig. 2. Effect of added NAD^+ on the fraction of enzyme (GAPDH) bound to AMP–Sepharose. (a) High density: bulk average ligand concentration $1 \cdot 10^{-4}$ *M*. Matrix volume 6.5% of total. Matrix ligand concentration $1.5 \cdot 10^{-3}$ *M*. (b) Medium density: bulk average ligand concentration $9.3 \cdot 10^{-5}$ *M*. Matrix volume 18% of total. Matrix ligand concentration $5.2 \cdot 10^{-4}$ *M*. (c) Low density: bulk average ligand concentration $2.5 \cdot 10^{-5}$ *M*. Matrix volume 18% of total. Matrix ligand concentration $1.4 \cdot 10^{-4}$ *M*. Values for no added NAD^+ are arbitarily plotted at −6.5.

effect. On combining the data from several runs with AMP cellulose the enhancement is quite clearly seen (Fig. 3). An approximately 4-fold increase in binding was apparent on adding free ligand and this compared well with that predicted for the bulk average matrix ligand concentration used. In two other respects, however, the data were not comparable with the predicted behaviour. The fractional binding of enzyme to matrix

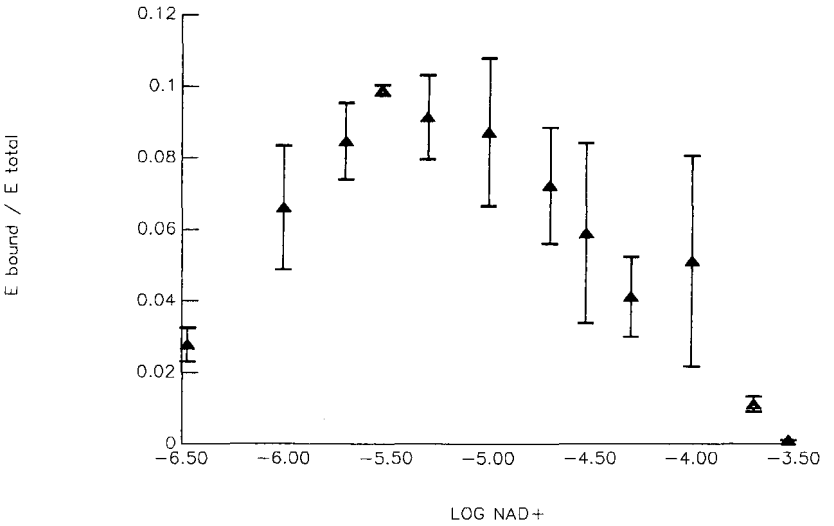

Fig. 3. Effect of added NAD^+ on the fraction of enzyme bound for GAPDH binding to AMP cellulose. The bulk average ligand concentration was $7.8 \cdot 10^{-5}$ *M* and the matrix volume = 20% of total (matrix ligand concentration $3.9 \cdot 10^{-4}$ *M*). Values plotted are means ± standard errors ($n = 3$). Values for no added NAD^+ are arbitarily plotted at −6.5.

ligand was about 10-fold lower than predicted. This observation probably results from restrictions imposed on ligand accessibility by the support matrix, and/or changes in binding constants arising from the chemical effects of immobilisation. The second deviation from the theoretical prediction is that the maximum observed binding enhancement occurs at a lower free ligand concentration. This can in part be explained by the effects of immobilised ligand maldistribution.

The difference in the behaviour of the cellulose and Sepharose matrices probably arises as a result of their different physical structures and consequent differences in the pattern of derivatisation. Sepharose beads are approximately spherical with a size range of 60–140 μm. Fibrous cellulose approximates to cylinders of length 100–250 μm and diameter about 25 μm. Sepharose 4B beads are known to be porous with pore sizes 80–230 nm, averaging about 170 nm [5]. The porosity of the cellulose used is unknown due to batch to batch variation of this natural product. It is generally composed of porous "amorphous" regions, with greater porosity than cross-linked polysaccharides like Sepharose 4B interspersed with compact "microcrystalline" regions [6]. Thus both matrices used should be freely permeable to both small molecules and GAPDH. Hence it does not appear that differences in accessibility could be a major contributor to the different behaviour of cellulose and Sepharose matrices.

The diffusional path length to the centre of a particle is up to 6 times longer for Sepharose assuming similar degrees of contortion in both matrices. Since both activating chemicals and coupling ligands must diffuse into the particle from the liquid phase it is likely that the end product will not be a uniformly derivatised particle but one with a "shell" of high ligand density at the surface and a concentration gradient running to a minimum at the centre of the particle. The shorter the path length the less

pronounced this would be expected to be. The result of this will be that the cellulose matrix will have a more uniform ligand distribution, more closely approximating the bulk average concentration than will the Sepharose matrix where the majority of the ligand will be concentrated towards the external surface of the beads. This would have two possible repercussions.

(1) The Sepharose matrix will behave as one with a higher ligand density thus tending to swamp out the cooperative effect.

(2) The higher ligand density in the Sepharose matrix will lead to an increased probability of multivalent interactions between protein and immobilised ligand.

This behaviour has been observed for a number of proteins with multiple binding sites [7–9]. A bivalent interaction will have a higher affinity constant than a monovalent one and if this is greater than or equal to the enhanced affinity of enzyme molecules partially saturated with free ligand then this will also swamp out any enhancement which might have been achieved due to the cooperative effect.

The effect of localised high concentrations of matrix ligand together with the consequences of multivalant interaction between macromolecule and resin can be qualitatively considered using an extension to the model described by Hubble [1]. In the original theoretical assessment of liquid phase cooperativity the assumption was made that with low matrix ligand densities only monovalent interactions would be possible between adsorbate and support. However, if localised high concentrations of immobilised ligand occur the possibility of multivalent interactions between enzyme and support cannot be discounted. The original model can easily be extended to consider all theoretically possible interactions between a tetravalent enzyme and both free and immobilised ligand. The broader model can be used to give a qualitative indication of the effects that these multivalent surface interactions might be expected to have on observed binding enhancements.

Development of the revised model leads to the formulation of fourteen equilibria describing interactions between individual complex species. For interaction with soluble ligand:

$$[E][L] \overset{K_1}{\rightleftharpoons} [EL]$$

$$[EL][L] \overset{K_2}{\rightleftharpoons} [EL_2]$$

$$[EL_2][L] \overset{K_3}{\rightleftharpoons} [EL_3]$$

$$[EL_3][L] \overset{K_4}{\rightleftharpoons} [EL_4]$$

A similar set of equilibria can be formulated for the interactions of E with immobilised ligand (M) using association constants $K_{m1} - K_{m4}$. Binding between enzyme and both soluble and immobilised ligand can be described in terms of six further association constants:

$$[EM][L] \overset{K_{l1}}{\rightleftharpoons} [EML]$$

$$[EML][L] \overset{K_{l2}}{\rightleftharpoons} [EML_2]$$

$$[EML_2][L] \overset{K_{l3}}{\rightleftharpoons} [EML_3]$$

$$[EM_2][L] \overset{K_{l4}}{\rightleftharpoons} [EM_2L]$$

$$[EM_2L][L] \overset{K_{l5}}{\rightleftharpoons} [EM_2L_2]$$

$$[EM_3][L] \overset{K_{l6}}{\rightleftharpoons} [EM_3L]$$

Fractional binding of enzyme to the affinity support can be described in terms of:

$$Y_m = \frac{\Sigma[EM_i] + \Sigma[EM_iL_j]}{[E] + \Sigma[EL_j] + \Sigma[EM_i] + \Sigma[EM_iL_j]}$$

where i denotes number of sites bound to immobilised ligand and j denotes number of sites bound to free ligand (for a tetramer $1 \leqslant (i + j) \leqslant 4$).

This equation can be expressed in terms of the equilibrium concentrations of L and M together with appropriate products of the individual association constants. Where the association constants are known this relationship can be used to predict the effect of free ligand concentrations on fractional binding as previously described. However, the more general form allows the effect of permitting progressively more complex multiple interactions between enzyme and adsorbate to be predicted. An example of a prediction of this type is given in Fig. 4 using the same association

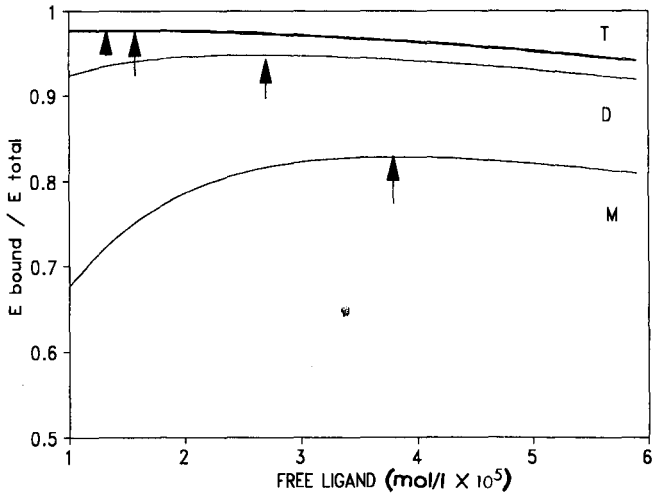

Fig. 4. The predicted effect of multivalent interactions between enzyme and matrix ligand on the relationship between free ligand concentration and fractional binding (association constants as for Fig. 1, bulk average ligand concentration $5 \cdot 10^{-5}$ M). M denotes monovalent interaction, D divalent and T tri- and tetravalent. Arrows denote the free ligand concentration giving maximal fractional binding.

constants for GAPDH as detailed for Fig. 1. The curves obtained as the number of permitted interactions with immobilised ligand is increased from 1 to 4 clearly show a shift towards a lower optimal free ligand concentration together with a masking of the enhancement effect. This was clearly observed in the Sepharose experiments where masking of enhanced binding prevented the identification of an optimum free ligand concentration.

The optimum free ligand concentration in the cellulose experiment was lower than that predicted, indicating perhaps, that even in this case some multivalent interactions were occurring.

No quantitative observations can be made at this stage concerning the levels of binding (which should increase if multivalent interactions are occurring), since the levels observed are much lower than those predicted. This may be due to changes in the intrinsic affinity constants for the interaction of protein with immobilised ligand relative to free ligand, as a result of the immobilisation process. Analysis is further complicated as onlyl a proportion of the immobilised ligand molecules will be in sufficiently close proximity to allow multiple simultaneous interactions with the enzyme. It does, however, clearly demonstrate the trends produced by multiple interactions.

CONCLUSIONS

The results presented demonstrate the occurrence of a liquid phase modification of adsorption capacities arising from the cooperative interaction of free ligand with a multivalent macromolecule. The effect observed is unlikely to be of significance in currently available affinity supports given that it is only observed under conditions of low immobilised ligand density and sub-optimal pH for binding (GAPDH shows optimal binding at about pH 7, but shows no cooperativity in the liquid phase at this pH). However, as both theoretical predictions, and the experimental results presented here suggest that cooperative effects are masked by high localised concentrations of immobilised ligand, it is possible that more significant capacity enhancements might be observed with the soluble supports used in aqueous two-phase partition [10].

In formulating the theoretical relationships described we have only considered the intrinsic cooperative properties of the adsorbate molecule. A more rigourous modelling approach would be needed to take account of the surface cooperative effects as described by Yon [11]. These arise from an increased valency of interaction even where there is no intrinsic molecular cooperativity. The concept of cooperative surface interactions resulting from immobilised ligand "clusters" in orientations suitable for multivalent interactions with a multimeric enzyme has been used to describe the binding of aldolase to phosphocellulose [11,12]. The increased apparent affinity arising from multiple surface interactions is an additional factor which will tend to mask the consequences of liquid phase cooperativity and lead to deviations from the response predicted by simple models. In generating the predictions used in this work we have assumed that the association constants between enzyme and insoluble ligands are similar to those describing the interactions with soluble ligands. Clearly this is a gross simplification even in the case of monovalent interactions with the support. When polyvalent interactions are possible determination of appropriate surface association constants becomes extremely complicated and requires much further work if accurate predictive models are to be developed.

ACKNOWLEDGEMENT

The authors wish to acknowledge the financial support of the British SERC (Grant No. GR/E 32717).

REFERENCES

1 J. Hubble, *Biotechnol. Bioeng.*, 30 (1987) 208–215.
2 S. C. March, I. Parikh and P. Cuatrecasus, *Anal. Biochem.*, 60 (1974) 149–152.
3 D. B. Craven, M. J. Harvey, C. R. Lowe and P. D. G. Dean, *Eur. J. Biochem.*, 41 (1974) 329–333.
4 L. S. Gennis, *Proc. Natl. Acad. Sci.*, 73 (1976) 3928–3932.
5 A. Demiroglou, W. Kerfin and H. P. Jennissen, in T. W. Hutchens (Editor), *Protein Recognition of Immobilised Ligands*, Alan R. Liss, New York, 1989, pp. 71–82.
6 *Whatman Technical Bulletin IE2*, 48–54.
7 D. Eilat and I. M. Chaiken, *Biochemistry*, 18 (1979) 790–794.
8 P. J. Hogg and D. J. Winzor, *Arch. Biochem. Biophys.*, 240 (1985) 70–76.
9 Y.-C. Liu and E. Stellwagen, *J. Biol. Chem.*, 262 (1987) 583–588.
10 J. M. Harris and M. Yalpani, in H. Walter, D. E. Brooks and D. Fisher (Editors), *Partitioning in Aqueous Two-Phase Systems*, Academic Press, Orlando, FL, 1985, p. 590–620.
11 R. J. Yon, *J. Chromatogr.*, 457 (1988) 13–23.
12 R. J. Yon, *Biochem. Soc. Trans.*, 16 (1988) 53.

Journal of Chromatography, 539 (1991) 255–266
Elsevier Science Publishers B.V., Amsterdam

CHROM. 22 871

Kinetic behaviour of a novel matrix ion exchanger, carboxymethyl-HVFM operated at high flow-rate

FANG MING and JOHN A. HOWELL*
School of Chemical Engineering, University of Bath, Claverton Down, Bath BA2 7AY (U.K.)

ABSTRACT

The kinetic behaviour of a novel coherent ion-exchange matrix, CM-HVFM, a carboxymethyl derivative of cross-linked regenerated cellulose, was investigated using lysozyme as a model protein. The results obtained were compared with those for two other commercial carboxymethyl cellulosic ion exchangers, HC2 (Phoenix) and CM-52 (Whatman). The flow properties of the new matrix were by far superior to those for the other materials whilst the adsorption and desorption kinetics were also faster. The new resin was able to sustain a superficial velocity of up to 8.78 m h^{-1} in a 147-mm I.D. column. In a 26-mm I.D. column, an only slightly faster velocity of 10 m h^{-1} was obtained. This contrasted with a limiting flow of less than 1.5 m h^{-1} with the other two packings. It was found that the kinetic rates of adsorption and desorption depended on the flow-rate through the matrix improving as the flow-rate increased. It was concluded that the highest flow-rates external mass-transfer resistances had been virtually removed and any remaining transfer resistance was due to diffusion through the matrix. In adsorption it was possible to achieve 90% adsorption within 8 min and 90% desorption within 5 min. Whilst the Whatman material had similar desorption rates neither of the other materials were close on the adsorption rates taking almost three times as long at the fastest sustainable superficial velocity for the CM-52 resin. These fast kinetics were achieved with a high capacity ranging from over 800 mg per dry g at a relative high salt concentration to over 2 g lysozyme per dry g for the unsalted lysozyme solution. Finally, no obvious swelling and shrinking was observed when the CM-HVFM column of 110 × 10 mm I.D. was regenerated by 2 *M* NaCl or 0.7 *M* NaOH solution for 40 min.

INTRODUCTION

The high separation efficiency and low energy requirements of ion-exchange chromatography have led to its routine use in biochemical separation processes [1,2]. In 1986 Bonnerjea *et al.* [3] studied the published purification protocols and found that ion exchange was used in 75% of all purifications. Traditional synthetic ion exchangers have a high charge density, a high degree of cross-linking and hydrophobic character that lead to low protein capacities and denaturation of adsorbed biomolecules [4]. A series of ion exchangers based on naturally occurring organic macromolecules are better at separating macromolecules as they possess macropores and a hydrophilic surfaces with lower charge density which tends not to denature the proteins. The ion exchangers based on polysaccharides possess moderately good hydraulic properties but relatively poor kinetics. Those based on cellulose, fast kinetics but poorer flow properties and those based on inorganic supports, good flow

0021-9673/91/$03.50

properties but poor capacities. There are difficulties in using several of these materials on the large scale [5].

There are few publications referring to the use of high flow-rates. Microgranular materials usually use superficial velocities of around 0.3–0.4 m h^{-1}. Levison *et al.* [6], using the Whatman microgranular QA-52, or DE-52 in a 100-ml axial flow column (66 × 44 mm I.D.) achieved a flow-rate of up to 25 ml min^{-1}, 0.99 m h^{-1} superficial velocity, beyond which higher flow was impossible due to the compressibility of the resin. Levison *et al.* [7] also reported that they used a 160 × 450 mm I.D. column packed with DE-52, a microgranular cellulose anionexchanger, at a volumetric flow-rate of about 800 ml min^{-1}, *i.e.*, only 0.3 m h^{-1} superficial velocity to separate egg white proteins. Only in analytical-scale columns significantly higher velocities are used, sometimes reaching 6 m h^{-1}.

Flow-rates used with cross-linked dextran exchangers are even slower. An example of industrial ion-exchange chromatography to produce egg white lysozyme used CM-Sephadex C-25 to adsorb the enzyme which was then eluted with 1 *M* NaCl. The cycle time depended on whether the ionic strength was adjusted by dilution or by desalting on Sephadex G-25. In the former case, the cycle time was 42 h and in the second case 15 h [8]. Both cases indicated that one of the main reasons which caused such long) cycle time was the low flow-rate.

Flow-rates through ion exchangers are usually limited by the compressibility of the matrix. The granular materials with larger particle sizes can allow fast flows but the large particles create internal transfer resistances which control the overall process. The productivity of these processes for production purposes is thus limited by either the diffusion within the particles or the flow through the bed. It will be shown in this paper that the effect of low flow-rates through the bed is to reduce further the inherent velocity of the process leading to a potential reduction in throughput and hence efficiency of use of the system.

In addition, the ion exchangers based on the cross-linked cellulose and dextran in the physical form of fibre, microgranular and sphericity show swelling and shrinking when the ionic strength and pH of the carrier fluids are varied. This leads to the resin bed being deformed and cracked and causes channeling and subsequent loss of performance.

An ideal ion exchanger is sought with the characteristics of fast kinetics, high flow-rate and stable physical form when varying the ionic strength and pH value. The novel ion-exchanger, carboxymethyl-HVFM, (CM-HVFM) supplied by Biotechnology Process Services (Durham, U.K.) is based on cross-linked regenerated cellulose and is in a coherent rather than particulate form. It is shown in this paper to exhibit high flow-rates at low pressures, and a high capacity. Because of its coherent form it is not possible to form cracks in the bed when it is subjected to changing ionic strengths.

Here we report some of these characteristics of the new matrix and leave a theoretical development for a future paper. Firstly, we examined the adsorption and desorption kinetic behaviour of CM-HVFM under a variable column flow-rate. The differential bed technique was used which allows us to assume the whole column (4 mm long) was at the same condition.

MATERIALS AND METHODS

Lysozyme (Sigma, Dorset, U.K.) was dissolved in 0.01 *M* acetic acid–sodium acetate buffer of pH 5.0.

A novel cross-linked cellulosic ion-exchanger (batch W1) (Biotechnology Process Services) was obtained in the carboxymethyl form (CM-HVFM). It was found to have a maximum lysozyme capacity of 2100 mg per dry at pH 5.0. The 3-mm high discs were supplied in diameter 2% larger than the I.D. of the columns, which were used to pack the columns. Two other carboxymethyl cellulosic ion-exchange resins were obtained commercially. CM-52, a microgranular CM ion-exchanger, was purchased from Whatman BioSystems (Kent, U.K.) and Indion HC2 (CM resin, size between 350–400 μm, batch 1246) was obtained from Phoenic Chemical, Waitaki NZ Refrigerating (Nelson, New Zealand).

A Sartorius (Surrey, U.K.) D-3400 filter holder with distributor was packed with either 2.7 g (0.3 g dry weight) CM-HVFM or 5 g of 1:1 slurry of CM-52 or 4.3 g of 1:0.8 slurry of HC2. This produced a short 5.8-ml column (4 mm × 43 mm I.D.

A 160 × 10 mm I.D. adjustable glass column (Amicon, Stonehouse, U.K.) packed with 0.5 g (dry weight) CM-HVFM was used for the 110 × 10 mm I.D. column of 8.64 ml volume. A gear micropump (Micropump, Concord, CA, U.S.A.) was used for the higher flow-rates otherwise a Millipore (Bedford, MA, U.S.A.) peristaltic pump or Autoclude peristalic pump (F.T. Scientific Instruments, Tewkesbury, U.K.) were used. A LKB (Bromma, Sweden) Uvicord II monitor was used on-line to detect the lysozyme concentration at 280 nm.

The experiments were carried out using the systems shown in Fig. 1. The sample

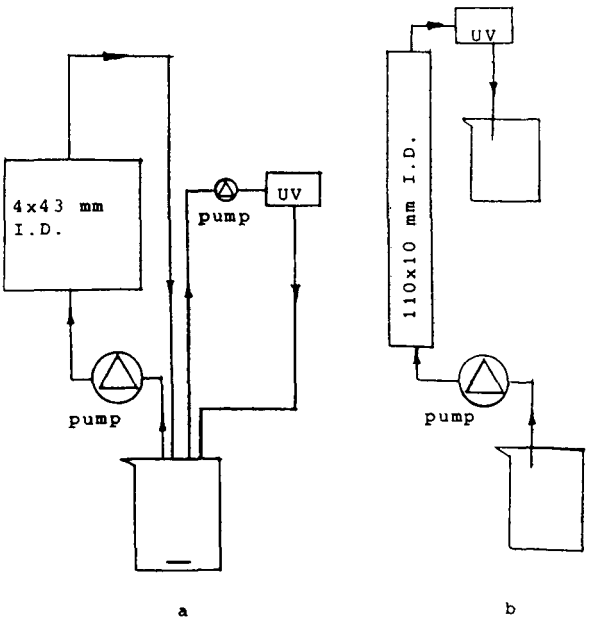

Fig. 1. Experimental devices. (a) Short column; (b) long column.

to be loaded was placed in a stirred beaker from which it was pumped upwards through the column. With the short column (Fig. 1a) a separate stream was pumped from the beaker to the UV monitor and back to the beaker at a velocity of 1800 m h^{-1} whilst for the longer column (Fig. 1b) the stream passed from the top of the column through the UV detector. The short column was operated at a fast recycle rate and acted as a differential bed in order to study the kinetics of adsorption and desorption on the ion exchangers. Before each adsorption run, the ion exchanger was equilibrated with pH 5.0 of 0.01 *M* sodium acetate buffer then the whole system (Fig. 1a) was drained before starting the run. Washing with pH 5.0 of 0.01 *M* sodium acetate buffer was followed by the adsorption and then desorption with 0.7 *M* NaCl solution. The CM-HVFM was regenerated by 2 *M* NaCl or 0.7 *M* NaOH solution. A load–wash–elution process was also performed on the longer column.

Two other larger diameter columns were used to measure the relationship between flow-rate and pressure drop through the columns. These were both about 100 mm long × 26 mm or 147 mm I.D. Pressure was increased by increasing flow.

RESULTS AND DISCUSSION

The CM-HVFM isothermal adsorption curves shown in Fig. 2 were obtained for lysozyme solutions adjusted to different ionic strengths with salt. The curve for 0.767 mS cm^{-1} ionic concentration was fitted to a Langmuir [9] isotherm with a dissociation constant, K_d, of 0.08 mg/ml and a lysozyme capacity (q_m) of 2010 mg/g. Such high protein capacity might result from the large surface area to volume ratio of the open irregualor network structure of the CM-HVFM. At a very low lysozyme concentration the CM-HVFM showed a high equilibrium protein capacity, *i.e.* 1300 mg g^{-1} in equilinium with 0.2 mg/ml lysozyme. When the ionic concentration was increased 21

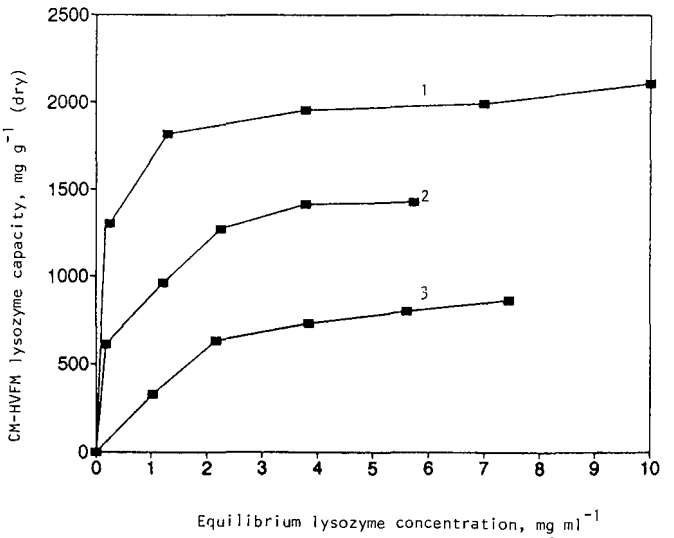

Fig. 2. CM-HVFM adsorption isotherms. Effect of ionic concentration. Curves: 1 = 0.767 mS cm^{-1}; 2 = 5.66 mS cm^{-1}; 3 = 16.3 mS cm^{-1}.

times to 16.3 mS cm^{-1}, the q_m value of CM-HVFM only dropped to 863 mg g^{-1}. Thus it is suggested from Fig. 2 that CM-HVFM could be used to recover protein from relatively low concentration streams at moderate ionic concentrations between 0.7 and 8 mS cm^{-1}.

When applying the CM-HVFM to low protein concentration streams of large volume, there are two other performance factors, kinetic process and flow-rate, which have to be considered and those will be discussed below.

The CM-52 and HC2 are also based on cross-linked cellulose thus they were chosen as the controls. The first is in the physical form of irregular microgranules (diameter 60–150 μm) and the second as almost spherical particles (diameter 350–450 μm). Fig. 3 shows the effect of pressure on superficial velocity for all three materials. The superficial velocity through the CM-HVFM or CM-52 or HC2 in the short column (4 mm × 43 mm I.D.), could reach 92.76 m h^{-1} for CM-HVFM, 32.00 m h^{-1} for Indion HC2 and only 23.64 m h^{-1} for Whatman CM-52 at an inlet pressure of 1 bar where all three kinds of ion exchangers tended to plateau and when the inlet pressure was increased to 1.7 bar no further increase in flow was observed. These materials are not suited to high-pressure chromatography.

Although very high flow-rates are obtainable for very short beds, this is not possible for long beds with the conventional materials. When the CM-HVFM or 60 g of 1:1 slurry of CM-52 or the HC2 was packed in a 100-mm deep polycarbonate column of 26 mm I.D. (Fig. 4), it can be seen that at an inlet pressure of 0.4 bar the superficial velocity of CM-HVFM could still reach 9.50 m h^{-1} in the upflow mode. However, the CM-52 and HC2 could not maintain their previous performance. The maximum superficial velocity of both of them was only about 1.00 m h^{-1} and the CM-52 inside the column was compressed to about 18% of its original length at the inlet pressure of 0.7 bar due to pressure forces within the system. This accords with the findings of Levison *et al.* [6]. The superficial velocity through the HC2 was slightly

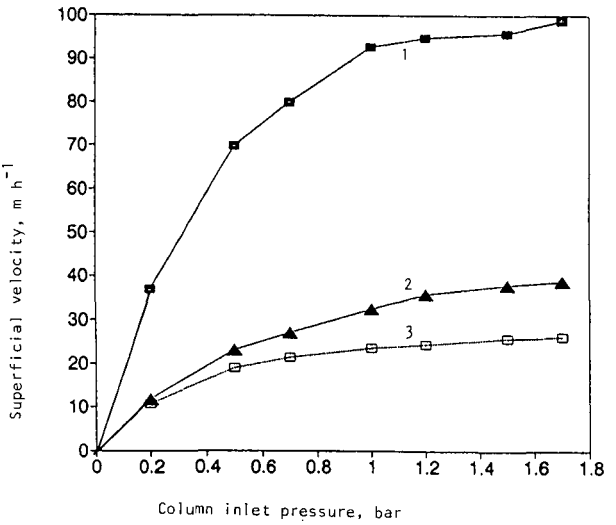

Fig. 3. The effect of pressure on superficial velocity for CM-HVFM (1), HC2 (2) and CM-52 (3) in a 4 mm × 43 mm I.D. column.

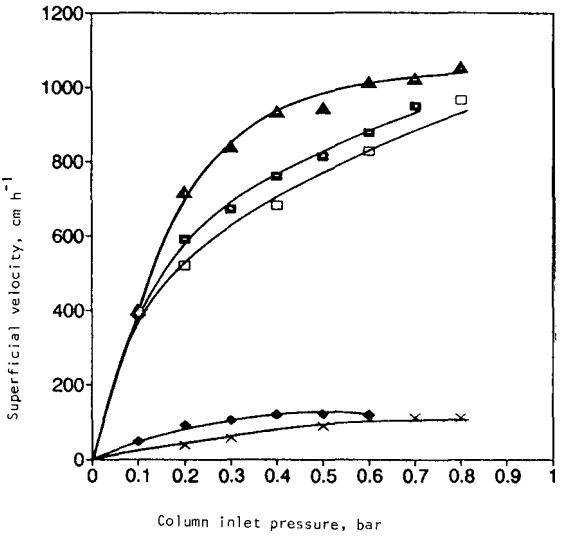

Fig. 4. The effect of column diameter and pressure on superficial velocity for CM-HVFM and comparison with 26 mm diameter columns containing CM-52 or HC. □ = 100 × 147 mm I.D. CM-HVFM, up-flow mode; □ = 100 × 147 mm I.D. CM-HVFM, down-flow mode; ▲ = 100 × 26 mm I.D. CM-HVFM, up-flow mode; × = 100 × 26 mm I.D. CM-52, up-flow mode; ◆ = 100 × 26 mm I.D. HC2, up-flow mode.

higher than that of CM-52 since the particle size of HC2 was 3–4 times larger than that of CM-52. It did not seem practical to examine the effect of increased column diameters as this would have decreased performance of these exhangers still further. It was also decided to examine the adsorption and desorption kinetics only up to a flow-rate that could be sustained in the 110-mm long column for the latter exchangers.

Scaling the column diameter up 5.7-fold to 147 mm I.D. would be expected to create a serious flow problem as the effect of the wall support is lost. Data from Levison *et al.* [7] shows that with DEAE-cellulose DE-52 the most practicable flow-rate for diameters above 100 mm is 300 mm h^{-1}. With CM-HVFM (Fig. 4) the increase in diameter only caused a further loss of flow of about 15% depending slightly on whether the flow was up or down through the column. The superficial velocity was not affected at 0.1 bar, and at 0.4 bar reached 7 m h^{-1} which suggests that a superficial velocity of 5–7 m h^{-1} might be applied on the process scale.

Figs. 5 and 6 show the relationship between the kinetic rates of adsorption and desorption and flow-rate for 5.8 ml of CM-HVFM in the differential bed (4 × 43 mm I.D. column) when first fed with 180 ml of 0.5 mg ml^{-1} of lysozyme in 0.01 *M* sodium acetate buffer at pH 5.0 to adsorb the lysozyme and then eluted with 180 ml of 0.7 *M* NaCl to desorb the adsorbed lysozyme at various superficial velocities. The same elution volume as adsorption was used so that an indication of the overall mass balance and the percentage adsorption can be gauged readily from the UV chart trace.

By using the differential bed column the column wall effect, axial dispersion and uneven distribution could be neglected due to the recycle mode of the differential bed. It is also possible to show directly how flow can affect the kinetics by altering the

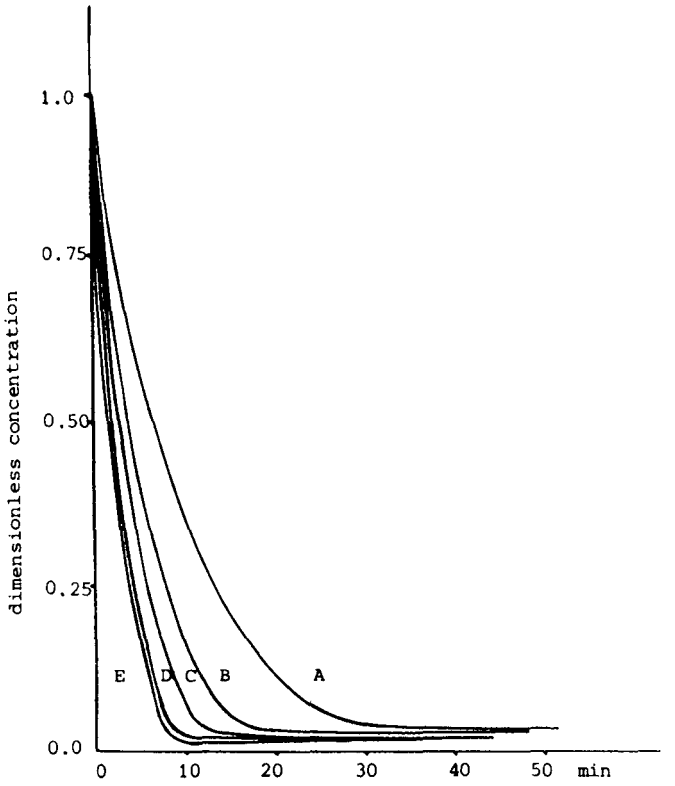

Fig. 5. The adsorption of 180 ml of 0.5 mg ml^{-1} lysozyme in 0.01 *M* sodium acetate buffer pH 5 in a 4 mm × 43 mm I.D. column A = 297 cm h^{-1}; B = 644 cm h^{-1}; C = 1388 cm h^{-1}; D = 4443 cm h^{-1}; E = 9276 cm h^{-1}.

external mass transfer coefficient. This demonstrates the significant effect which mass transfer external to the particles has on chromatographic kinetics. It is also clear that to achieve these effects on a large scale it is important to have a matrix which will sustain high velocities on a wide diameter column.

From Figs. 5 (curves A–E) and 6 (curves A–E) with the superficial velocity varying from 2.97 m h^{-1} to 92.76 m h^{-1}, it can be seen that the rates of adsorption and desorption increased with increasing superficial velocity. 80% of the total lysozyme was adsorbed in 14 min and 90% of adsorbed lysozyme was eluted in 10 min at a superficial velocity of 2.97 m h^{-1} (Figs. 5 and 6, curves A), while at a superficial velocity of 13.88 m h^{-1}. 90% of lysozyme was adsorbed in 8 min and 90% of adsorbed lysozyme was eluted in 6 min (Figs. 5 and 6, curves C), further increasing the superficial velocity to 44.43 m h^{-1} at the inlet pressure 0.21 bar required only 3.5 min for 90% of lysozyme to be adsorbed and only 5 min for 90% of the adsorbed lysozyme to be desorbed (Figs. 5 and 6, curves D). These times of adsorption and desorption were only slightly improved when the flow velocity was increased to 92.76 m h^{-1} at an inlet pressure of 1 bar (Figs. 5 and 6, curves E). It appears that the flow-rate is no longer the main limiting factor above about 50 m h^{-1}, and that at this flow-rate external film mass

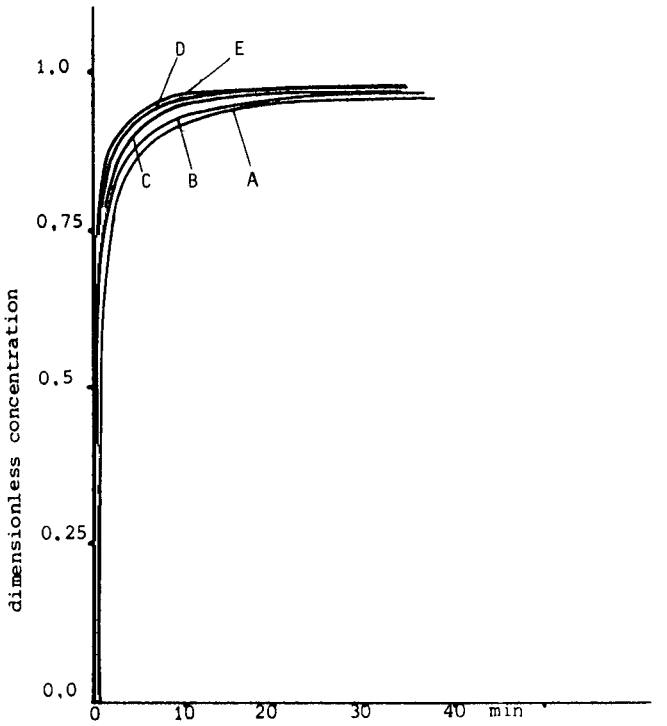

Fig. 6. The desorption of the adsorbed lysozyme with 180 ml of 0.7 *M* NaCl in a 4 mm × 43 mm I.D. column at various superficial velocities. A = 297 cm h^{-1}; B = 644 cm h^{-1}; C = 1388 cm h^{-1}; D = 4443 cm h^{-1}; E = 9276 cm h^{-1}.

transfer is no longer very significant. Conversely, at lower flow-rates the fastest kinetics are not attainable due to increased mass transfer in the fluid phase. The adsorption time for 90% lysozyme adsorption and desorption of 90% adsorbed lysozyme was reduced by factors of 5.7 and 2 respectively by increasing the superficial velocity 15-fold, from 2.97 to 44.43 m h^{-1}.

It is interesting to note that the desorption of CM-HVFM is less influenced by external mass transfer (Fig. 6). Since the commercially useful flow-rates of CM-52 and HC2 are constrained (Fig. 4), the kinetic behaviour of adsorption and desorption of CM-52 and HC2 is only described at flow velocity less than 1 m h^{-1}. Superficial velocities of 0.99 and 0.51 m h^{-1} were used but otherwise the loading and process conditions for the kinetics study of both CM-52 and HC2 were exactly the same as for CM-HVFM.

Figs. 7a and b illustrate that the kinetic processes of CM-52 are faster than those of HC2 in both cases due to the large surface area to volume ratio of microgranular material. With the same loading conditions as for the CM-HVFM, it needed 17 and 31 min to adsorb 80% of loaded lysozyme for CM-52 at the superficial velocities 0.99 and 0.51 m h^{-1}, respectively, whilst for HC2 it needed 27 min and 37 min under the same conditions (Fig. 7a). Although the CM-52 exhibits faster desorption than HC2, it still needed 10 and 14 min to elute 90% of the adsorbed lysozyme at 0.99 and 0.51 m h^{-1},

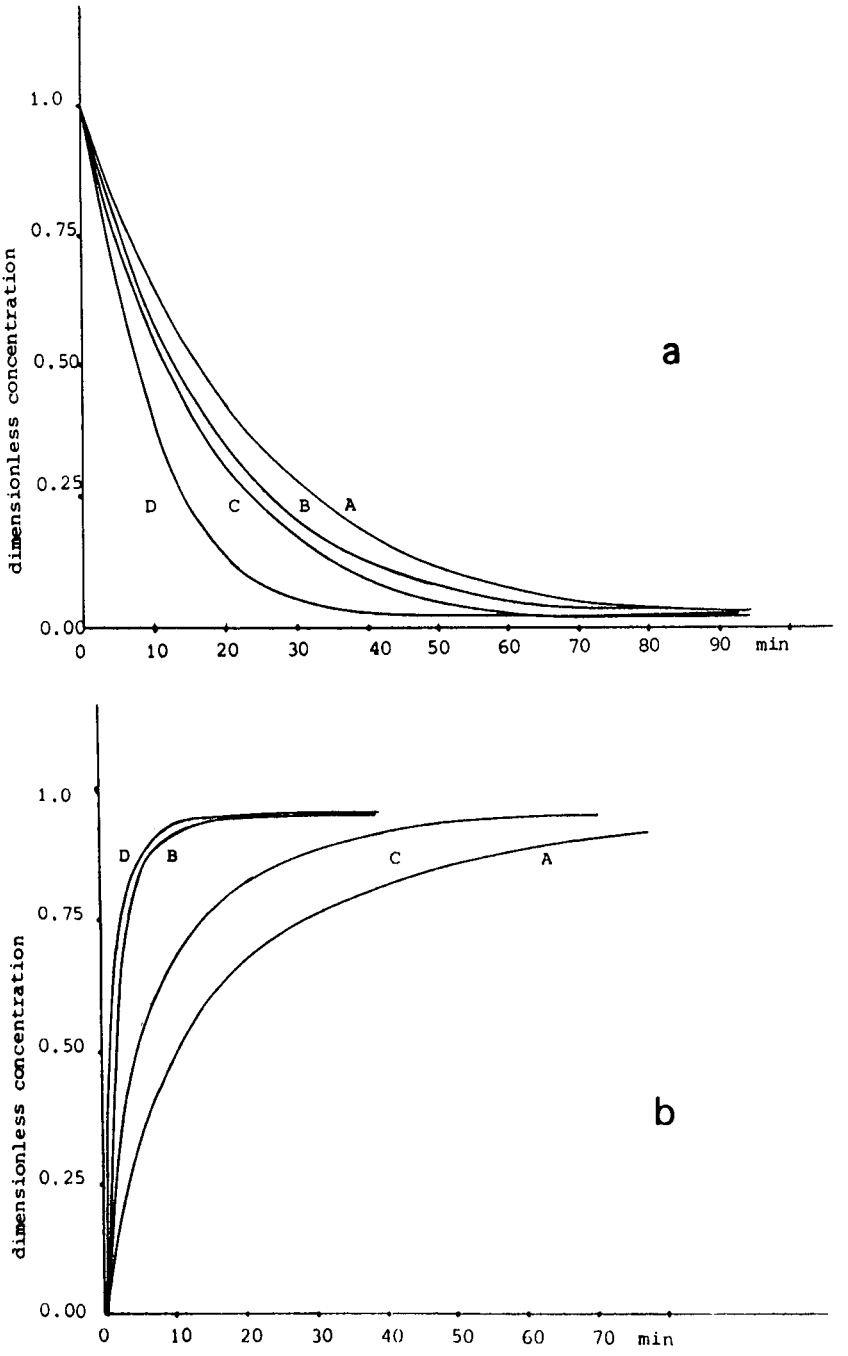

Fig. 7. (a) The adsorption of 180 ml of 0.5 mg ml^{-1} of lysozyme in 0.01 *M* sodium acetate duffer at pH 5 in a 4 mm × 43 mm I.D. column at various superficial velocities. (b) The desorption of adsorbed lysozyme with 180 ml of 0.7 *M* NaCl in a 4 mm × 43 mm I.D. column at various superficial velocities. Curves: A = HC2, 51 cm h^{-1}; B = CM-52, 51 cm h^{-1}; C = HC2, 99 cm h^{-1}; D = CM-52, 99 cm h^{-1}.

respectively. The HC2 needed more than 40 min to elute the same amount of protein. This is attributed to the larger particle sizes. The experiment described earlier (Fig. 4) indicated that it was difficult to operate the 100 × 26 mm I.D. column packed with CM-52 at a superficial velocity of more than 0.90 m h^{-1} because the microgranular material was getting increasingly compressible. This resulted in higher and higher pressures with the same flow-rates. It is apparent from the above data that this would result in significant mass transfer limitation in the external film. It was thus not possible to use the microgranular CM-52 or HC2 at their optimum kinetic rate owing to the flow restrictions.

The higher flow velocities attainable through the new matrix, CM-HVFM, allow much faster kinetics to be exhibited. Even this material has reduced flows on the larger-scale columns and whilst 40 m h^{-1} would be kinetically optimum only 7 m h^{-1} can be sustained on the 100 × 147 mm I.D. column. This is about 20 times faster than attainable on the Whatman and Indion materials.

By loading 50 mg lysozyme to the 110 × 10 mm I.D. column and then eluting with 1 *M* NaCl at various superficial velocity from 0.910 to 13.750 m h^{-1} (Fig. 8) it is found that desorption times decrease monotonically with increasing velocity. There is a point, around 5.0 m h^{-1}, in both curves beyond which the time for eluting 80% and 90% of total lysozyme is reduced only slowly.

The advantages of very high velocities and fast kinetics can be realised in a practical application. In Fig. 9, a complete adsorption desorption cycle that has not been optimised is show for 0.5 g dry weight CM-HVFM packed into the longer cylindrical column (110 × 10 mm I.D.). The feed was 340 ml of 0.588 mg ml^{-1} of lysozyme in 0.01 *M* sodium acetate buffer at pH 5.0 with a superficial velocity of 8.87 m h^{-1}, 1.7 bed volumes/min. After loading the column was washed for 2 min with 2.7 bed volumes of buffer at the same flow-rate and then eluted with 1 *M* NaCl fed at 8.41 m h^{-1}. A sharp peak and short tail for the elution are observed with complete absence

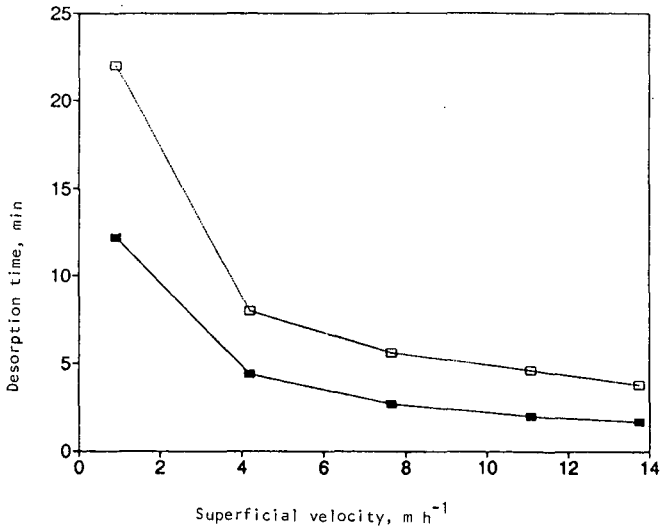

Fig. 8. Desorption time of 80% (■) and 90% (□) of total elution lysozyme at various superficial velocities.

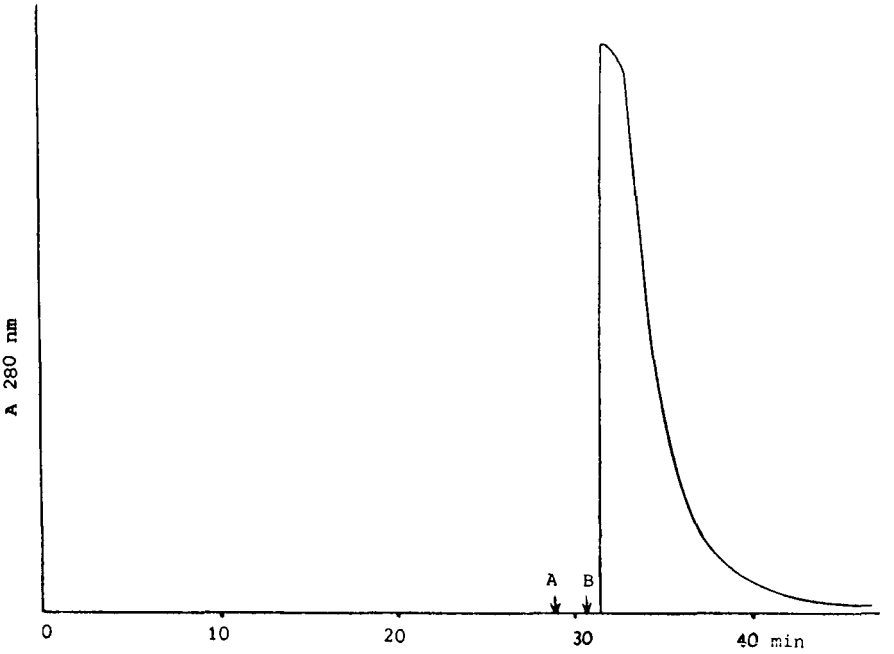

Fig. 9. Protein concentration in the column eluent. Adsorption started time 0, washing started at A, elution at B. CM-HVFM in a 110 mm × 10 mm I.D. column, loaded with 340 ml of 0.588 mg/ml lysozyme. Superficial velocity 8.87 ml h^{-1}.

of any measurable breakthrough even though the column was loaded to 50% of its total capacity with 200 mg of protein on 8.6 ml or 0.5 g of matrix. The whole process took less than 40 min. In a later experiment breakthrough was observed only when the 110 × 10 mm I.D. column had adsorbed 43 bed volumes or 365 ml of 1 mg ml^{-1} lysozyme at a superficial velocity 6.34 m h^{-1}. The column capacity at the breakthrough point was thus 365 mg of protein or 42 mg protein ml^{-1} of column. At this flow-rate that took only 45 min for the adsorption. It was thus possible to load a solution containing 1 mg ml^{-1} of protein at nearly 1 bed volume/min with total adsorption on a bed only 110 mm long.

During the above operation, the 110 × 10 mm I.D. column was regenerated by 2 *M* NaCl or 0.7 *M* NaOH for 40 min and there was no obvious swelling and shrinking observed which indicates a potential further advantage of the CM-HVFM matrix.

CONCLUSION

The new CM-HVFM matrix has several advantages over the microgranular and spherical cellulosic ion exchangers:

(1) The kinetics of adsorption of proteins by carboxymethyl cellulosic ion exchangers are controlled by external mass transfer at normal operational flow-rates. Higher flow velocities allow faster adsorption and desorption kinetics.

(2) The bed of the CM-HVFM matrix maintains an open structure at high

flow-rates, whilst the beds of microgranular and spherical matrix tend to be compressed and block. The new matrix can thus sustain a superficial velocity of over 7 m h^{-1} in a 100 mm × 147 mm I.D. column which is over five times the velocity that can be sustained by the other materials. Flow-rates are normally restricted by compression which tends to become worse in larger diameter columns leading to slower kinetics in large-scale columns than small-scale columns. The faster flows mean that longer beds are needed and thus it is important to have fast flow even in long beds. A bed of 110 mm is long enough to avoid breakthrough when over 30 column volumes have been loaded at 1 bed volume/min. The new material can thus be used to treat large volumes of solution.

(3) It is suggested that the new matrix possesses an open structure for flow which is not easily compressed but is clearly not rigid yet there are sufficiently short diffusion pathways within the material that kinetics of desorption are not slowed down. The fine structure of the new matrix is such that there are short diffusion pathways within the cellulose and a very high percentage of the surface is accessible to direct convective flow which leads to rapid kinetics that also are commensurate with the flow rate allowing very fast large scale separations. The desorption rates are intrinsically faster than adsorption and less influenced by mass transfer for the HVFM and HC2 although the large particles of HC2 are influenced by mass transfer in the external phase.

(4) CM-HVFM can withstand changes of ionic strength and pH without obvious swelling and shrinking, which can avoid the column bed being deformed and cracked.

ACKNOWLEDGEMENT

The work was supported by the SERC and BioIsolates Ltd. under a collaborative grant.

REFERENCES

1 S. Yamamoto, K. Nakaniskik and R. Matsamo, *Ion Exchange Chromatography of Proteins* (*Chromatographic Science Series*, Vol. 43), Marcel Dekker, New York, 1988, p. 3.
2 G. Sofer and L. Nystrom (Editors), *Process Chromatography —A Practical Guide*, Academic Press, London, 1989, Foreword.
3 J. Bonnerjea, S. Oh, M. Hoare and P. Dunnill, *Bio/Technology*, No. 4 (1986) 954, 958.
4 H. A. Chase, in D. Naden and M. Streat (Editors), *Ion Exchange Technology*, Ellis Horwood, Chichester, 1984, pp. 400–406.
5 G. L. Skidmore and H. A. Chase, in D. Naden (Editor), *Ion Exchange for Industry*, Ellis Horwood, Chichester 1988, pp. 520–532.
6 P. R. Levison, E. T. Butts, M. L. Kosciely and L. Lane, in Y. Briand, C. Doimel and A. Faure (Editors), *Technologies de Purification des Proteins*, Vol. 4, G.R.B.P., Clermont-Ferrand, 1990, pp. 137–142.
7 P. R. Levison, S. E. Badger, D. W. Toome, D. Carcary and E. Butts, in *Advances in Separation Processes* (*Symposium Series*, No. 118), The Institution of Chemical Engineers, U.K. Hemisphere Publ., 1990, pp. 6.1–6.11.
8 J.-C. Janson and P. Hedman, in A. Fiechter (Editor), *Advances in Biochemical Engineering*, Vol. 25, Springer, New York, 1982, pp. 64–99.
9 *Sigma Diagostics Procedure No. 690: Microprotein Determination*, Sigma, Poole, 1985.
10 I. Langmuir, *J. Am. Chem. Soc.*, 38 (1916) 2221.

Journal of Chromatography, 539 (1991) 267–277
Elsevier Science Publishers B.V., Amsterdam

CHROM. 22 876

Immobilized metal ion affinity partitioning, a method combining metal–protein interaction and partitioning of proteins in aqueous two-phase systems[a]

G. BIRKENMEIER*
Institute of Biochemistry, Karl-Marx-Universität Leipzig, Liebigstrasse 16, 7010 Leipzig (Germany)
M. A. VIJAYALAKSHMI
Laboratoire de Technologie des Séparations, Université de Technologie de Compiègne, B.P. 649, 60206 Compiègne (France)
T. STIGBRAND
Institute of Physiological Chemistry, University of Umeå, S-90187 Umeå (Sweden)
and
G. KOPPERSCHLÄGER
Institute of Biochemistry, Karl-Marx-Universität Leipzig, Liebigstrasse 16, 7010 Leipzig (Germany)

ABSTRACT

Immobilized metal ions were used for the affinity extraction of proteins in aqueous two-phase systems composed of polyethylene glycol (PEG) and dextran or PEG and salt. Soluble chelating polymers were prepared by covalent attachment of metal-chelating groups to PEG. The effect on the partitioning of proteins of such chelating PEG derivatives coordinated with different metal ions is demonstrated. The proteins studied were α_2-macroglobulin, tissue plasminogen activator, superoxide dismutase and monoclonal antibodies. The results indicate that immobilized metal ion affinity partitioning provides excellent potential for the extraction of proteins.

INTRODUCTION

Immobilized metal ion affinity chromatography (IMAC), which makes use of the selective retention of proteins on transition metal ions chelated to an insoluble matrix such as agarose, was introduced by Porath *et al.* [1]. The important contribution of Sulkowski [2] to the understanding of the underlying mechanism of this selective recognition has made this concept one of the best suited in separation technology, as evidenced by the increasing number of papers appearing in this field. While the concept of protein affinity for metal chelates has been extensively studied by the chromatography of proteins [3], peptides [4] and, more recently, of whole cells [5], very few attempts have been made to introduce this affinity principle to the other analytical and preparative separation methods [6]. The utilization of aqueous

[a] This paper is dedicated to Professor P.-Å. Albertsson on the occasion of his 60th birthday.

0021-9673/91/$03.50

two-phase systems for the affinity purification of many molecules, using pseudo-specific ligands such as triazine dyes, is now well established [7]. Hence, it is of considerable interest to exploit the affinity of proteins for immobilized (chelated) metals in such partitioning systems. Both of these aspects are the subject of this paper.

However, certain requirements have to be met in order to exploit successfully the IMA principle in affinity partitioning. First, an appropriate chemistry must be developed for the preparation of soluble polymers with covalently coupled chelating groups. Second, the impact of the protein surface topography on their recognition by metal chelates has to be considered. Moreover, the microenvironment of the electron donor grouping [5] on the protein surface may result in a variable mechanism of protein recognition by a metal ligand.

EXPERIMENTAL

Polyethylene glycol (PEG) 6000 and 1540 were obtained from Serva (Heidelberg, Germany). Dextran T-70 was obtained from Pharmacia (Uppsala, Sweden) and bromoacetic acid from Aldrich (Steinheim, Germany).

α_2-Macroglobulin (α_2-M) was purified from fresh plasma [8]. Copper–zinc superoxide dismutase (SOD) was a gift from Symbicom (Umeå, Sweden). Single-chain tissue plasminogen activator (t-PA) was kindly provided by Professor P. Wallen, University of Umeå, Sweden.

Preparation of metal chelate PEG

Iminodiacetate-PEG (IDA-PEG) was synthesized by reaction of bromoacetic acid with aminomonomethoxy-PEG (amino-M-PEG) 5000. Amino-M-PEG was prepared according to Cordes [9]. Briefly, 60 g of M-PEG 5000 (Sigma) were melted at 65°C and water was removed under vacuum. After addition of 3 ml of distilled thionyl chloride, the sample was rotated for 6 h at 65°C under a nitrogen atmosphere to exclude moisture. After removing excess of thionyl chloride by evaporation, the residue was dissolved in 3 l of absolute ethanol and precipitated at 4°C. The dried Cl-M-PEG was dissolved in 150 ml of water and 150 ml of ammonia solution (25%) were added. The solution was placed in a sealed plastic tube and left for 100 h at 55°C in a dry oven. After evaporation of the solvent, 53 g of amino-M-PEG were obtained.

For the preparation of IDA-PEG, 15 g of amino-M-PEG dissolved in 100 ml of water were reacted with 15 g of bromoacetic acid at pH 8.5 for 12 h and room temperature. Then, 100 ml of water were added and the IDA-M-PEG was extracted three times with 300 ml of chloroform. Phase separation was accelerated by centrifugation. The combined chloroform phases were dried over anhydrous sodium sulphate and the solvent was removed by distillation. After two crystallizations in absolute ethanol, 12–13 g of IDA-PEG were obtained.

Metal charging of IDA-PEG was done by dissolving 2 g of IDA-PEG in 10 ml of 50 m*M* sodium acetate (pH 4.0) containing the respective metal ions (Cu^{2+}, Zn^{2+}, Ni^{2+}, Fe^{3+}) in a 10–20-molar excess over the IDA-PEG. The solution was stirred for 1 h and then extracted with chloroform. The chloroform was dried and evaporated, yielding 1.9 g of metal–IDA-PEG.

The metal content in solutions was determined by flame photometry using appropriate standards.

Preparation of two-phase systems

The two-phase systems were prepared from stock solutions of polymers in water–40% (w/w) PEG and 20% (w/w) dextran. The polymer solutions were mixed with buffer, water and protein sample to give the final concentration as indicated in the legends to the figures. Affinity partitioning was performed by replacing part of the total PEG with metal–IDA-PEG. The systems were equilibrated by 40 inversions at 22°C. Phase separation was accelerated by centrifugation at 2000 *g* for 2 min. Aliquots were withdrawn from the top and bottom phases and analysed for the metal or protein content. Similarly, two-phase systems composed of PEG and salt were prepared from stock solutions and treated as described above.

Determination of the partition coefficient

The partition coefficient, K, was calculated as the ratio of the concentration or radioactivity of a species in the upper and lower phase. The effect of the affinity of a protein for the metal–IDA-PEG was expressed in terms of $\Delta \log K$, given by $\Delta \log K = \log K_{aff} - \log K_0$, where K_{aff} and K_0 are the partition coefficients of the protein in the presence and absence of metal–IDA-PEG in the system, respectively, other conditions being identical. The concentrations of α_2-M and monoclonal antibodies were determined by enzyme-linked immunoadsorbent assay (ELISA).

Iodination

SOD and t-PA were iodinated with 0.5 mC of ^{125}I (Amersham, U.K.), applying the Iodobeads technique [10].

RESULTS

Preparation of metal–IDA-PEG

The soluble chelating polymer was synthesized by three steps starting from monomethoxy-PEG as outlined in Fig. 1. Under the conditions used, mostly monosubstituted chelating PEG was formed. The nitrogen content of IDA-PEG as determined by elemental analysis was 0.32%, which is higher than expected (theoretical value 0.28%). Partial dimethylation during the reaction may account for this discrepancy.

The tridentate IDA-PEG may occupy a maximum of three coordination sites in the metal coordination sphere, leaving three coordination sites free for interaction withe water or proteins at least in the case of a hexacoordinate central metal ion. The amounts of the metal ions such as Cu^{2+}, Zn^{2+}, Ni^{2+} and Fe^{3+} chelated by the IDA-PEG are given in Table I. With Cu^{2+} and Zn^{2+}, about 1 mol of metal ion is chelated per mol of the polymer; Ni^{2+} and Fe^{3+} gave lower binding ratios.

Partitioning of metal–IDA-PEG in two-phase systems

The partition coefficients of metal–IDA-PEG complexes in PEG–dextran and PEG–salt sysems are compared in Table II. In PEG–dextran systems, the metal ions partition in favour of the PEG-rich top phase owing to chelation with IDA-PEG. Even in PEG–salt systems, a high partition coefficient was observed at least for Cu^{2+}. On the other hand, Zn^{2+}, Ni^{2+} and Fe^{3+} are probably released from the chelating polymer, as deduced from their low K values in systems containing high concentrations of phosphate.

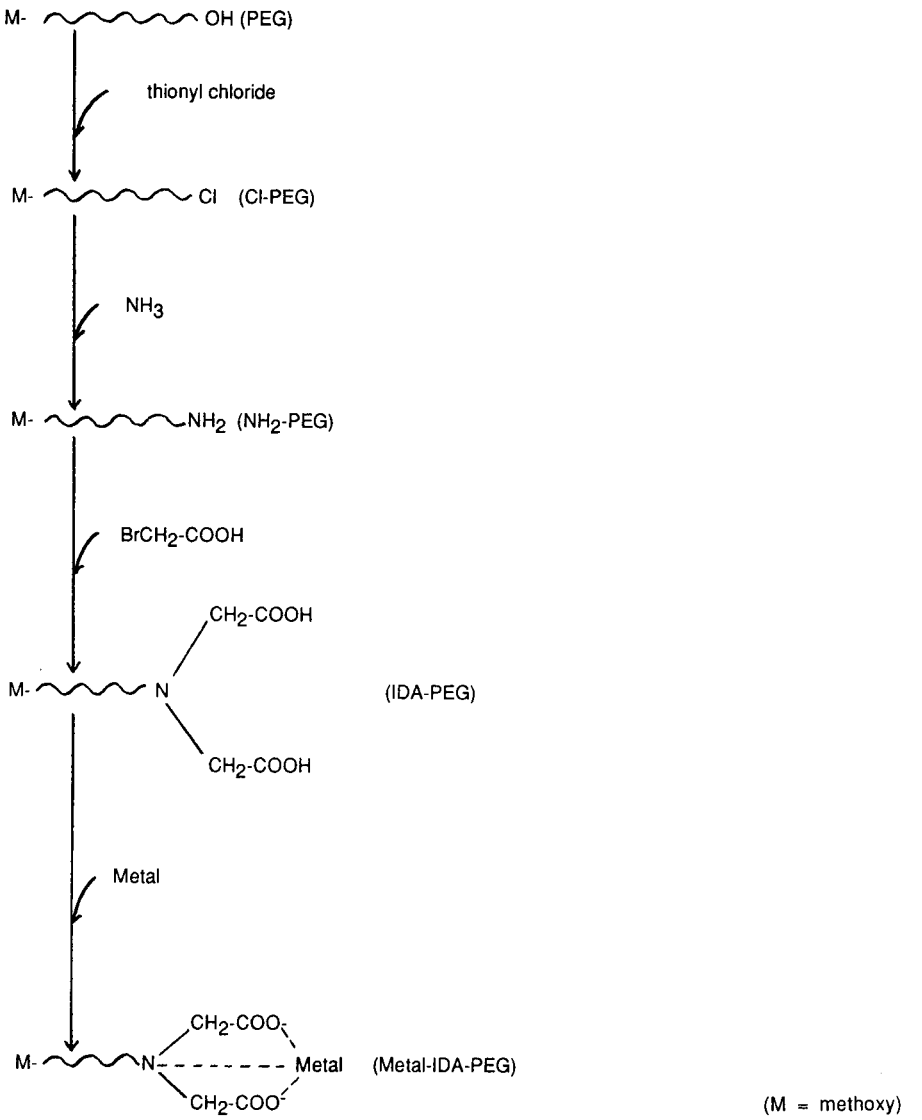

Fig. 1. Synthesis of metal–IDA-PEG.

Effect of metal–IDA-PEG on partitioning of α_2-M

The proteinase inhibitor α_2-M was used as a model protein to study the principles of metal chelate affinity partitioning. When α_2-M was added to a system containing increasing concentrations of metal–IDA-PEG, different extraction curves were obtained (Fig. 2). Cu^{2+}–IDA-PEG causes a change in the partition coefficient of more than 1000-fold ($K_0 = 0.085$; $K_{aff} = 85$) yielding a maximum $\Delta \log K$ of *ca.* 3.0. The complexed metals Zn^{2+} and Ni^{2+} give rise to lower efficacy; Fe^{3+} seems to have a negligible affinity to the protein.

TABLE I

METAL ION CONTENT OF IDA-PEG AFTER CHARGING WITH Cu^{2+}, Zn^{2+}, Ni^{2+} AND Fe^{3+}

The metal content is expressed as μmol of the respective metal per μmol of IDA-PEG. The nitrogen content of IDA-PEG as determined by elemental analysis was 0.32%, giving rise to the assumption of monosubstituted PEG.

Metal ion	Metal ion content (μmol/μmol IDA-PEG)
Cu^{2+}	0.92
Zn^{2+}	0.80
Ni^{2+}	0.27
Fe^{3+}	0.40

Effect of pH and salt concentration on affinity partitioning of α_2-M

Coordinate binding of proteins to transition metals is expected to be sensitive to the pH of the medium. The magnitude of such pH effects can be exactly measured by titration experiments as shown in Fig. 3. The binding of α_2-M to Cu^{2+}–IDA-PEG is diminished as the pH of the phase system is decreased. The effect of salts such as NaCl and Na_2SO_4 on the partitioning of α_2-M was two-fold. At pH values above 5, the binding of α_2-M to Cu^{2+}–IDA-PEG was strengthened in the presence of salts, indicated by the higher $\Delta \log K$ values obtained. At lower pH values, salts seemed to suppress the binding, probably owing to quenching of non-coordination bonds.

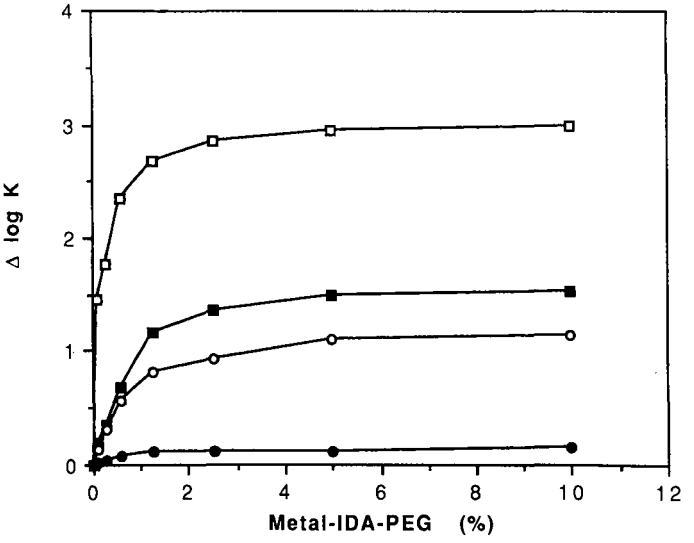

Fig. 2. Effect of metal–IDA-PEG on partitioning of α_2-M in PEG–dextran systems. Two-phase systems of 2 g were composed of 5% PEG 6000, 7.5% dextran T-70, 0.1 *M* Na_2SO_4, 0.01 *M* sodium phosphate buffer (pH 7.0), 20 μg of α_2-M and increasing amounts of metal–IDA-PEG. The concentration of the liganded polymer is expressed as a percentage of the total PEG in the system. □ = Cu^{2+}–IDA-PEG; ■ = Zn^{2+}–IDA-PEG; ○ = Ni^{2+}–IDA-PEG; ● = Fe^{3+}–IDA-PEG.

TABLE II

PARTITION COEFFICIENTS OF METAL–IDA-PEG COMPLEXES IN PEG–DEXTRAN AND PEG–SALT SYSTEMS

PEG–dextran system: 5% PEG 6000, 7.5% dextran T-70, 0.1 *M* Na_2SO_4, 0.01 *M* sodium phosphate buffer (pH 7.0); 20% of the total PEG 6000 was replaced with different metal–IDA-PEG derivatives. PEG–salt system: 11% PEG 1540, 13.5% K_2HPO_4–KH_2PO_4 (pH 7.0), 2% PEG 6000; 20% of the total PEG 6000 was replaced with different metal–IDA-PEG derivatives. The partitioning was performed at 22°C. Aliquots were removed from the top and bottom phases, appropriately diluted and subjected to flame photometry. Blanks were systems without metal–IDA-PEG.

Metal–IDA-PEG	*K*	
	PEG–dextran	PEG–salt
Cu^{2+}–IDA-PEG	11.1	10.2
Zn^{2+}–IDA-PEG	5.5	0.55
Ni^{2+}–IDA-PEG	10.6	0.25
Fe^{3+}–IDA-PEG	11.3	0.44

Partitioning of α_2-M in PEG–salt systems in the presence of metal–IDA-PEG

Aqueous two-phase systems may also be formed by mixing PEG with high concentrations of salts such as sodium sulphate or sodium phosphate. In such systems the polymer is highly concentrated in the top phase, whereas the bottom phase is formed by the salt solution. Even there, Cu^{2+}–IDA-PEG was found to be very effective in extracting the protein from the salt-rich bottom phases (Fig. 4A and B). The highest $\Delta \log K$ values obtained are comparable to that yielded in PEG–dextran systems. The difference in the steepness of the partition curves indicates that the affinity of α_2-M for Cu^{2+}–IDA-PEG is obviously higher in PEG–sulphate than PEG–phosphate systems. This may reflect different effects of these salts on the water structure in the medium.

Dissociation of protein–metal–IDA complexes

Transition metal ions, particularly Cu^{2+}, Zn^{2+} and Ni^{2+}, bind with electron-donor atoms such as N, O and S in available amino acid residues in proteins. Hence, it would be expected that the dissociation of the metal chelate–protein complexes could be accomplished by competing electron donors, *e.g.*, free amino acids. As shown in Fig. 5, cysteine strongly diminished the binding of α_2-M to Cu^{2+}–IDA-PEG with increasing concentration in the two-phase system. In comparison, imidazole and tryptophan were less effective. No influence on the affinity partitioning of α_2-M was observed by the addition of ammonium ions at the pH of the experiment. As one would expect, the addition of EDTA at concentrations above 2 m*M* abolished the binding of α_2-M to Cu^{2+}–IDA-PEG.

Immobilized metal ion affnity partitioning of other proteins

The binding properties of different proteins towards selected chelated transition metals are compared in Table III. The partitioning experiments were conducted in PEG–dextran and PEG–salt systems. Apparently, uncharged IDA-PEG had only

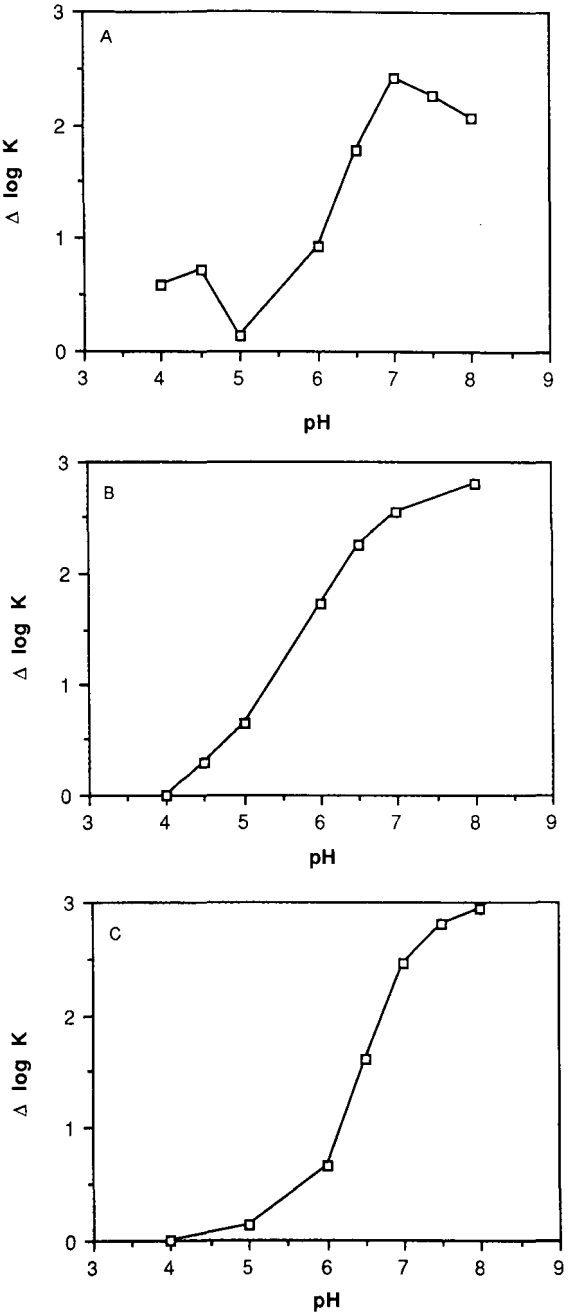

Fig. 3. Effect of pH and salt on affinity partitioning of α_2-M. Two-phase systems of 12 g, composed of 5% PEG 6000, 7.5% dextran T-70, 240 μg of α_2-M in the presence or absence of salt and Cu^{2+}–IDA-PEG, were adjusted to pH 8.0 with 0.1 *M* NaOH with continuous stirring at 22°C. After 5 min of equilibration, the pH was decreased stepwise by adding 0.1 or 0.01 *M* HCl, and aliquots of 1 ml were withdrawn, immediately centrifuged and analysed for the protein in the top and bottom phases. Composition of the systems: (A) 2.5% Cu^{2+}–IDA-PEG, no salt; (B) 2.5% Cu^{2+}–IDA-PEG, 1 *M* NaCl; (C) 2.5% Cu^{2+}–IDA-PEG, 0.1 *M* Na_2SO_4.

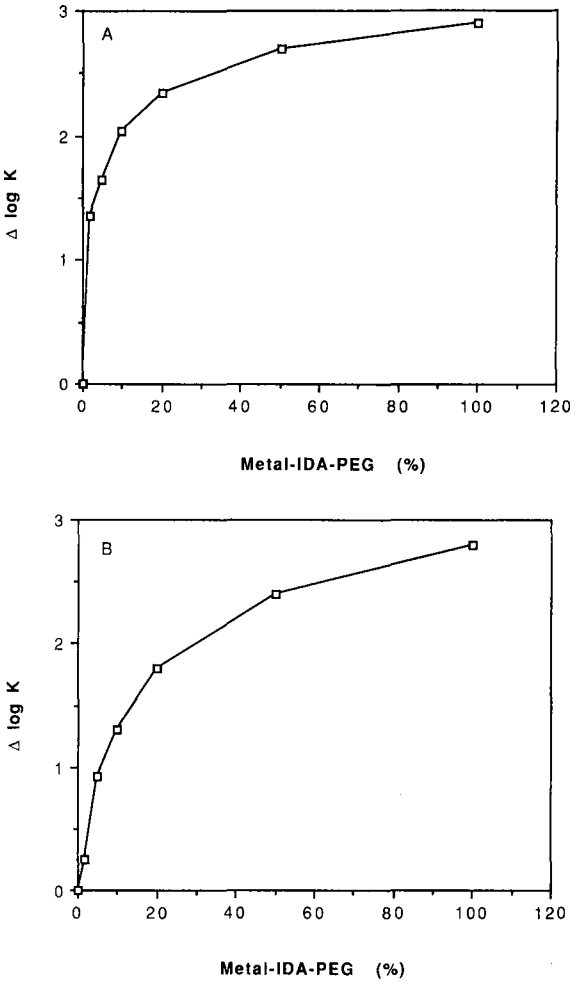

Fig. 4. Effect of metal–IDA-PEG on partitioning of α_2-M in PEG–salt systems. Two-phase systems of 2 g were composed of either (A) 10% PEG 1540, 10% Na_2SO_4, 2% PEG 6000, 10 m*M* sodium phosphate buffer (pH 7.0) and 20 μg of α_2-M or (B) 11% PEG 1540, 13.5% K_2HPO_4–KH_2PO_4, 2% PEG 6000 and 20 μg of α_2-M. The given percentage of liganded PEG expresses that part of the total PEG 6000 which was replaced with Cu^{2+}–IDA-PEG. Log *K* for α_2-M was -1.17 and -1.1 for the PEG–sulphate and PEG–phosphate systems, respectively.

marginal effects on the partitioning of the proteins in both kinds of two-phase systems. As expected, the binding properties of the proteins differed significantly owing to their different surface properties. In general, Cu^{2+}–IDA-PEG was found to be the most effective ligand with both PEG–dextran and PEG–salt systems. Zn^{2+}–, Ni^{2+}– and Fe^{3+}–IDA-PEG were less effective, especially when used in conjunction with PEG–phosphate systems. This is probably due to the formation of metal phosphates because Zn^{2+} and Ni^{2+} are known to be bound less strongly than Cu^{2+} by

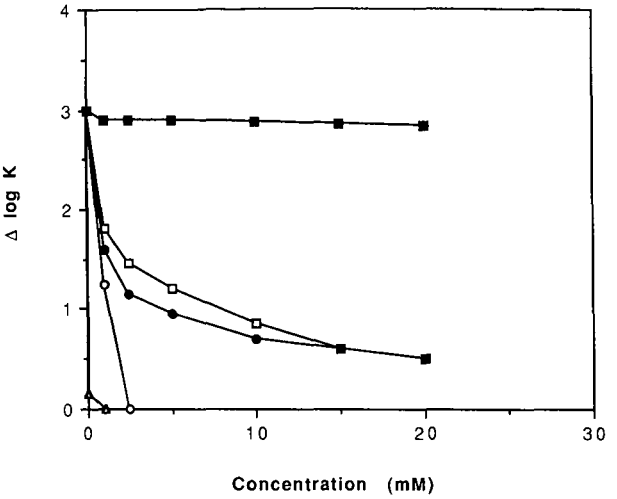

Fig. 5. Dissociation of the protein–metal–IDA-PEG complexes. The two-phase systems of 2 g were composed of 5% PEG 6000 including 2.5% Cu^{2+}–IDA-PEG, 7.5% dextran T-70, 0.1 *M* Na_2SO_4, 0.01 *M* sodium phosphate buffer (pH 7.0), 20 μg of α_2-M and different additives in the concentrations given on the abscissa. □ = Imidazole; ● = tryptophan; ○ = cysteine; △ = EDTA; ■ = ammonium ion. The $\Delta\log K$ values were calculated in comparison with systems of the same composition but without Cu^{2+}–IDA-PEG (log K_0).

iminodiacetate chelator. Among the proteins tested, α_2-M displayed the strongest binding to metal–IDA-PEG. t-PA interacted preferentially with chelated Cu^{2+}. Its affinity to chelated Ni^{2+} was higher than that to chelated Zn^{2+}. SOD bound fairly selectively to Cu^{2+}–IDA-PEG whereas no interaction was found with chelated Zn^{2+}

TABLE III

EFFECT OF METAL–IDA-PEG ON PARTITIONING OF DIFFERENT PROTEINS IN PEG–DEXTRAN AND PEG–SALT SYSTEMS

PEG–dextran system: 5% PEG 6000, 7.5% dextran T-70, 0.1 *M* Na_2SO_4, 0.01 *M* sodium phosphate buffer (pH 7.0); for the calculation of $\Delta\log K$, 20% of the total PEG was replaced with uncharged IDA-PEG or metal–IDA-PEG. PEG–salt system: 11% PEG 1540, 2% PEG 6000, 13.5% K_2HPO_4-KH_2PO_4 (pH 7.0); for the calculation of $\Delta\log K$, 50% of the total PEG 6000 was replaced with uncharged IDA-PEG or metal–IDA-PEG.

Protein	$\Delta\log K$							
	PEG–dextran: metal–IDA-PEG				PEG–salt: metal–IDA-PEG			
	Cu^{2+}	Zn^{2+}	Ni^{2+}	None	Cu^{2+}	Zn^{2+}	Ni^{2+}	None
α_2-Macroglobulin	3.00	1.50	1.10	0.17	2.4	0.06	0.18	0.02
Tissue plasminogen activator	1.59	0.78	1.20	0.14	1.23	0.46	0.31	0.03
Superoxide dismutase	1.30	0.05	0.18	0.08	0.83	0.10	0.20	0.05
Monoclonal antibody ($IgG_{1\kappa}$)	1.15	0.12	0.05	0.10	n.d.[a]	n.d.	n.d.	n.d.

[a] n.d. = Not determined.

and Ni^{2+}. When we tested a range of monoclonal antibodies, different partition coeffients were obtained. However, all displayed the strongest binding to chelated Cu^{2+}, as exemplified for a monoclonal antibody of the immunoglobulin (Ig) $G_{1\kappa}$ type. No correlation was found between the magnitude of binding ($\Delta \log K$) to chelated metal ions and a certain class or subclass specificity.

DISCUSSION

In this study the feasibility of complexation of proteins with chelated metal ions was exploited for affinity extraction in aqueous two-phase systems; so far the only published application is the extraction of haemoglobin [11].

Using α_2-M as a model protein, the effect of the transition metal ions Cu^{2+}, Zn^{2+}, Ni^{2+} and Fe^{3+} chelated to IDA-PEG on the partitioning of this protein was clearly shown. The results reveal that the type and concentration of the chelated metal ions are important parameters which influence the partition coefficient of the protein. The strong effect exerted by chelated Cu^{2+} on the partitioning of proteins in comparison with other metal ions parallels its strong tendency to coordinate predominantly with histidine residues on the protein surface. It is fairly clear that the accessibility of surface-exposed histidine residues is the dominant factor governing the binding strength of metal chelates to proteins [12]. Accordingly, the differences in the $\Delta \log K$ values obtained for α_2-M, t-PA, SOD and a monoclonal antibody may account for this fact.

To perform affinity partitioning, specific or pseudo-biospecific ligands such as inhibitors, antibodies or dyes were used [7]. However, the difficulty of reversing the ligand–protein interaction is often encountered with this technique. In the case of immobilized metal ion affinity partitioning (IMAP), several possibilities exist for dissociating the metal–protein complex under nondenaturing conditions. The addition of free electron-donating amino acids or EDTA was as effective as lowering the pH of the two-phase system (Figs. 3 and 5).

As shown in Fig. 4 and Table III, the binding of proteins to chelated metal ions occurs at high concentrations of salts in the phase system. In addition, a promoting effect of the water structure-forming salts such as sodium phosphate and sodium sulphate on binding of α_2-M to Cu^{2+}–IDA-PEG was observed. This offers interesting possibilities for performing IMAP also in PEG–salt systems, which can be handled and scaled up more easily than PEG–dextran systems.

Liquid–liquid partitioning in conjunction with metal affinity extraction should be an interesting approach for downstream processing of proteins including those of clinical and industrial interest. The growing use of recombinant DNA technology allows the modification of protein products in order to facilitate their purification. The introduction of "affinity tails" of desirable chromatographic properties, such as histidine-containing peptides, will make the use of IMAP a very attractive alternative for large-scale purifications [13].

ACKNOWLEDGEMENTS

Part of this work was carried out under the collaborative research programme between Karl-Marx-University of Leipzig, and the University of Technology of

Compiègne. G.B. gratefully acknowledges the hospitality offered to him at Umeå University. T.S. was supported by the Swedish Medical Research and Cancer Research Council. We acknowledge useful discussions with Dr. E. Sulkowski during the preparation of the manuscript.

REFERENCES

1 J. Porath, J. Carlsson, I. Olsson and G. Belfrage, *Nature (London)*, 258 (1975) 598.
2 E. Sulkowski, *Trends Biotechnol.*, 3 (1985) 1.
3 E. Sulkowski, *BioEssays*, 10 (1989) 170.
4 M. Belew, T. T. Yip, L. Andersson and J. Porath, *J. Chromatogr.*, 403 (1987) 197.
5 H. Goubran-Botros and M. A. Vijayalakshmi, *J. Chromatogr.*, 495 (1989) 113.
6 S. S. Suh and F. H. Arnold, *Biotechnol. Bioeng.*, 35 (1990) 682.
7 G. Birkenmeier, G. Kopperschläger and G. Johansson, *Biomed. Chromatogr.*, 1 (1986) 64.
8 F. Van Leuven, J.-J. Cassiman and H. Van den Berghe, *J. Biol. Chem.*, 256 (1981) 9016.
9 A. Cordes, *Thesis*, Technical University Carozo-Wilhelmina, Braunschweig, 1985.
10 *Pierce Manual: ImmunoTechnology Catalog and Handbook*, Pierce, Rockford, IL, 1989, p. C-53.
11 S. D. Plunkett and F. H. Arnold, *Biotechnol. Tech.*, 4 (1990) 45.
12 E. S. Hemdan, Y.-J. Zhao, E. Sulkowski and J. Porath, *Proc. Natl. Acad. Sci. U.S.A.*, 86 (1989) 1811.
13 C. Ljungquist, A. Breitholtz, H. Brink-Nilsson, T. Moks, M. Uhlen and B. Nilsson, *Eur. J. Biochem.*, 186 (1989) 563.

Journal of Chromatography, 539 (1991) 279–287
Elsevier Science Publishers B.V., Amsterdam

CHROM. 22 898

Interactions of the mitochondrial membrane rat liver D-3-hydroxybutyrate dehydrogenase with glass beads during adsorption chromatography

Relationships with the activation of the enzyme by phospholipids

P. ADAMI and B. NASSER
Laboratoire de Biochimie et Biologie Moléculaire (UA CNRS 531), Université de Franche Comté, 25030 Besançon Cedex (France)
and
N. LATRUFFE*,[a]
Laboratoire de Biologie Moléculaire et Cellulaire, Université de Bourgogne, B.P. 138, 21004 Dijon (France)

ABSTRACT

D-3-Hydroxybutyrate dehydrogenase (BDH) is an NAD^+-dependent dehydrogenase of the mitochondrial inner membrane involved in the energetic balance between the liver and peripheral organs in mammals. It allows the conversion of ketone bodies (acetoacetate and D-3-hydroxybutyrate) and it is one of the best documented lipid-requiring enzymes with a dependence on lecithins. After release of proteins from the membrane by phospholipase A2 treatment of salt-treated mitochondria, the rat liver enzyme is absorbed on controlled-pore glass beads. After batch washing, the enzyme, devoid of lipids (apoBDH), is specifically eluted at pH 8.05–8.15 with a 0.1 *M* Tris–1 *M* LiBr buffer under reducing conditions (5 m*M* dithiothreitol). It appears that during BDH absorption, the glass beads mimic the phospholipid surface of biomembranes.

INTRODUCTION

D-3-Hydroxybutyrate dehydrogenase (BDH), EC 1.1.1.30, is a ketone body converting enzyme (for a review, see ref. 1). This mammalian NAD(H)-dependent enzyme plays a central role in the energetic balance between hepatic and peripheral tissues under physiological and pathological conditions. Indeed, the concentrations of the ketone bodies (acetoacetate and D-3-hydroxybutyrate) in the plasma and in the cells depend on the interrelationships between the metabolic pathways of lipids, of

[a] Present address: Laboratoire de Biologie Moléculaire et Cellulaire, Faculté des Sciences de la Vie–Mirande, Université de Bourgogne, B.P. 138, 21004 Dijon, France.

0021-9673/91/$03.50

carbohydrates and of some ketogenic amino acids [2]. Under normal conditions, D-3-hydroxybutyrate dehydrogenase is essential in the oxidization of D-3-hydroxybutyrate in the brain of newborns, providing energy and biosynthetic precursors (acetyl-CoA) of cholesterol and myelin. In addition, extrahepatic tissues such as the kidney, heart and skeletal muscle use ketone bodies preferentially as energy fuels. It is also well known that an overproduction of ketone bodies appears in diseases or non-physiological conditions, *e.g.*, diabetes mellitus, starvation or hyperlipidic diet [3].

Lehninger *et al.* [4] showed that D-3-hydroxybutyrate dehydrogenase is located in the inner mitochondrial from mammalian tissue. Later, it was found that the orientation of the catalytic site is on the matrix side of the inner membrane [5].

BDH is one of the few enzymes so far known which show a specific lipid dependence (absolute requirement for phosphatidylcholine for enzymatic activity).

The enzyme cannot be released from the membrane by sonication, osmotic shock or high ionic strength [4]. Three methods have been used to solubilize the BDH from mitochondrial membrane: cholate treatment [6], phospholipid hydrolysis by snake venom phospholipase A_2 [7] which released BDH almost completely, although only 30–40% of phospholipids were hydrolysed whatever the nature of the hydrolysed phospholipid, and incubation of mitochondria at high pH which partially released the enzyme [8].

In order to understand the phospholipid–apoBDH interaction at the molecular level, it was necessary to obtain a purified homogeneous and lipid-free apoenzyme. With this aim, Fleischer's group [9] proposed an original technique for purifying beef heart apoBDH based on the release of the enzyme by treatment of mitochondria with phospholipase A_2, adsorption of the enzyme on untreated controlled-pore glass beads (CPG) and selective elution of the protein from the column by lithium bromide, a chaotropic agent, at defined pH. Purified beef heart apoBDH, devoid of phospholipids and water soluble under defined conditions, consists of a single polypeptide chain of 31 500 dalton as shown by sodium dodecyl sulphate polyacrylamide gel electrophoresis (SDS-PAGE) [9]. Several purification procedures, partial or complete, were successively proposed by different groups in order to improve the purity, stability, yield, time required or simplicity, or to adapt the technique to BDH from different species [10–18].

However, some of these purification procedures were not suitable for studying lipid–protein interactions as BDH was purified as a mitochondrial phospholipid complex and not as apoBDH [10–14]. To our knowledge, no-one has tried to explain the nature of specific interactions between BDH and the glass surface of CPG which are essential in the purification process. In this paper, we describe the purification procedure adapted in our laboratory for the rat liver mitochondrial membrane-bound BDH and show a relationship between phospholipid–BDH interaction and glass–BDH adsorption.

EXPERIMENTAL

Materials

Controlled-pore glass beads (CPG-10-350; mesh size 120–200; pore diameter *ca.* 350 Å) were obtained from Electro-Nucleonics (Fairfield, NJ, U.S.A.). These beads were not treated with polyethylene glycol or polyethylene oxides as indicated for

exclusion chromatography [19]. Chemicals were of the highest grade available. Solutions were prepared in ultrapure water.

Methods

Rat liver mitochondria were prepared on a large scale as described previously [20] and were stored frozen (−70°C) at 40 mg ml^{-1} in 0.25 *M* sucrose until used. Protein was determined as described by Lowry *et al.* [21] and modified by Ross and Schatz [22] for assays containing free thiols. Lipid phosphorus was determined according to Chen *et al.* [23].

Mitochondrial lipids (MPL) were extracted from rat liver mitochondria. Aqueous dispersions of MPL were prepared by the dialysis or the sonication procedures described previously [24].

SDS-PAGE was performed according to Laemmli [25].

D-3-Hydroxybutyrate dehydrogenase activity was measured spectrophotometrically at 334 nm at 20 or 37°C as described previously [26], in a "cocktail medium" containing 10 m*M* potassium phosphate, 0.05 m*M* EDTA, 0.04% bovine serum albumin, 1.27% (v/v) ethanol, 0.3 m*M* dithiothreitol (DTT) and 2 m*M* NAD^+ (final volume 450 μl). The reaction was started by addition of 50 μl of 0.2 *M* D,L-3-hydroxybutyrate.

Preparation of "crude intrinsic mitochondrial membrane proteins fraction"

Frozen–thawed mitochondria were submitted to a high ionic strength (1 volume of 3 *M* KCl) in order to remove soluble and membrane-associated proteins. Crude intrinsic mitochondrial membrane proteins fraction (about 20% of the original protein) was obtained after ultracentrifugation for 30 min at 100 000 *g*. This pellet was frozen at −80°C

Solubilization and purification of D-3-hydroxybutyrate apodehydrogenase

Frozen crude intrinsic mitochondrial membrane protein fraction (20 g of original mitochondrial protein) from about 150 rats was thawed by gentle swirling in a water-bath at 37°C. This suspension (*ca.* 0.5 l) was added to a beaker containing 0.1 *M* Tris–HCl (pH 7.4), 1 m*M* NAD^+, 3 m*M* $CaCl_2$, 5 m*M* DDT and water to give a final volume of 1 l at 30°C. The mitochondrial membrane fraction was digested by addition of 80 ml (equivalent to 80 mg of original snake venom) of phospholiphase A_2 [8], *i.e.*, in a ratio of 4 μl per milligram of original mitochondrial protein, at 30°C for the optimum time (usually 3–4 min) previously determined in a trial digestion [8]. Digestion was terminated by adding the mixture to a cold carboy (*ca.* 5 l capacity) containing 36.66 ml of 0.3 *M* EDTA, 55 ml of 2 *M* KCl and 125 ml of "ice cubes" (−20°C) consisting of 0.1 *M* KCl, 20 m*M* EDTA and 2 m*M* DTT, to cool the mixture rapidly to *ca.* 8°C. The pH was reduced by addition of 30.66 ml of 2 *M* potassium phosphate (pH 6.5).

An aliquot was removed to determine the amount of solubilized D-3-hydroxybutyrate apodehydrogenase in the supernatant after ultracentrifugation (3 min) at 140 000 *g* in a Beckman Airfuge. The digested suspension was stirred slowly with a paddle and 100 ml (packed volume) of untreated CPG previously degassed in water and stored under nitrogen were added with an equal volume of buffer VI (see Table I). Adsorption of the apodehydrogenase on the glass beads was nearly complete (90%) after 30 min.

The glass beads with bound enzyme were recovered in 1-l centrifuge bottles by centrifugation for 30 s at 1000 rpm in a Sorvall RC5B and GS3 rotor. The first five washed with potassium phosphate buffers (buffers I–VI; see Table I) were carried out batchwise in the centrifuge bottles so as to remove mitochondrial membrane fragments trapped in the sedimented glass beads.

The glass beads were then packed into a column (*ca.* 20 cm × 8 cm I.D.) already containing 50 ml of packed CPG as scavenger, under a nitrogen atmosphere, and washing was continued with buffer VII at a flow-rate of *ca.* 3 ml cm^{-2} min^{-1}.

The enzyme was eluted (see Table I) using 1.0 *M* LiBr–0.1 *M* Tris–HCl–2.5 m*M* DTT elution buffer with an initial pH of 8.00 and a flow-rate of *ca.* 3 ml cm^{-2} min^{-1}, then with pH 8.05 buffer until enzymatic activity was detected in the effluent (usually after 5–7 column volumes). Elution was continued with buffer in the pH range 8.10–8.15 until the activity began to decrease, at which point the pH of the effluent was increased to a maximum of 8.15. Elution was terminated when the enzymatic activity per litre fell below 1% of the initial activity solubilized by phospholipase A_2. A small amount of additional enzymatic activity could be eluted at higher pH (8.20–8.30), but elution of contaminants began to predominate, attended by a yellow band which migrated slowly down the second column during the course of elution of the enzyme.

When the activity was first detected in the eluate from the purification column, the eluate was passed directly into a 1-l stirred vessel and titrated with 1 *M* HCl to pH 7.2. This titrated effluent was applied directly to a second column [concentration column, consisting of 50 ml of CPG-10 packed in buffer A (see Table I), column dimensions *ca.* 18 cm × 3.5 cm I.D.] at a flow-rate to match the elution rate of the

TABLE I

BUFFERS USED FOR PURIFICATION OF D-3-HYDROXYBUTYRATE APODEHYDROGENASE ON CONTROLLED-PORE GLASS BEADS

Buffer description	Buffer composition (containing 2.5 m*M* DTT)	pH	Elution volume (ml)	
			Purification column	Concentration column
Washing buffers				
I = A	1 *M* potassium phosphate	6.5	1500	200
II	1.5 *M* potassium phosphate	8.15	1500	Omitted
B	1 *M* potassium phosphate	7.5	Omitted	200
III = C	1 *M* potassium phosphate	8.15	3000	600
IV = D	0.75 *M* potassium phosphate	6.5	1500	600
V = E	0.2 *M* potassium phosphate	6.5	1500	200
VI = F	0.02 *M* potassium phosphate	6.5	750	200
VII = G	0.01 *M* Tris	7.75	750	200
Elution buffers				
8.00	0.1 *M* Tris–1 *M* LiBr	8.00 at 4°C	750	200
8.05	0.1 *M* Tris–1 *M* LiBr	8.05 at 4°C	750	400
8.10	0.1 *M* Tris–1 *M* LiBr	8.10 at 4°C	750	400
8.15	0.1 *M* Tris–1 *M* LiBr	8.15 at 4°C	3000	1400
8.20	0.1 *M* Tris–1 *M* LiBr	8.20 at 4°C	750	600
8.30	0.1 *M* Tris–1 *M* LiBr	8.30 at 4°C	500	600

purification column. After all the eluate had been applied, the column was washed with buffers A–G.

The second (concentration) column was then eluted with 1 *M* LiBr–0.1 *M* Tris–HCl–5 m*M* DTT (pH 8.00–8.15) buffers. Fractions containing enzymatic activity were pooled, adjusted to 5 m*M* 4-(2-hydroxyethyl)-1-piperazineethane sulphonic acid (HEPES), titrated to pH 7.0 with 1 *M* HCl and concentrated to a volume of *ca.* 50 ml using 400-ml Amicon stirred cells with a PM-10 membrane. The enzyme solution was adjusted to 0.4 *M* LiBr, 5 m*M* HEPES (pH 7.0) and 5 m*M* DTT as essential reducing agent to prevent BDH disulphide bond formation, and concentrated to a final volume of 4–5 ml (*ca.* 1–2 mg protein/ml) in a 60-ml Amicon stirred cell using a PM10 membrane.

The concentrated enzyme was ultracentrifuged (Type 40 rotor for 30 min at 105 000 *g*). A small opalescent glass bead pellet was obtained which had a low protein content. The supernatant, containing the purified apodehydrogenase, was quick-frozen in small aliquots and stored in a liquid nitrogen refrigerator.

RESULTS AND DISCUSSION

Purification scheme and properties of purified apoBDH

The purification of D-3-hydroxybutyrate dehydrogenase from rat liver mitochondria has been adapted from methods described 15 years ago for beef heart mitochondria BDH [9,19] and for other proteins [27]. Although the basic elements of the method have remained unchanged, the procedure has been improved and simplified: a previous treatment of mitochondria with a high ionic strength of KCl already removes 80% of contaminating proteins. The enzyme is then released from the mitochondrial inner membrane with the use of phospholipase A_2. The ammonium sulphate precipitation step [8] has been omitted. BDH solubilized in the supernatant is now directly adsorbed in batch to controlled pore glass beads (CPG-10), which are then washed to remove the mitochondrial membranes and any other non-adsorbed proteins. The first five elution buffers are applied batchwise prior to packing the CPG-10 with adsorbed proteins into a column for the chromatographic elution. From 20 g of rat liver mitochondrial protein, we obtain more than 10 mg of the purified enzyme with a specific activity at 37°C of about 80 μmol min^{-1} mg $protein^{-1}$ when reactivated with mitochondrial phospholipids. The procedure has been appreciably shortened; the entire preparation now takes *ca.* 18–20 h with an additional 8 h for concentration and centrifugation.

Fig. 1 shows the elution profile of apoBDH from the CPG concentration column. The purification procedure results in the elution of two separate fractions of enzyme (apoBDH) from the second column. The first fraction elutes in the pH 8.15, 1 *M* phosphate buffer (contaminated phosphate fraction) and the second (highest activity) in the 1.0 *M* LiBr–0.1 *M* Tris–HCl (pH 8.05–8.15) buffer (called pure "LiBr–BDH fraction").

After diafiltration and concentration, the pooled "LiBr–BDH" active fractions are checked for purity and for lipid dependence. Fig. 2 shows that after two CPG adsorption–elution cycles (purification column and concentration column), BDH appears to be at least 95% pure. Fig. 3 indicates that the purified lipid-free apoBDH is catalytically inactive and requires reassociation with either total mitochondrial

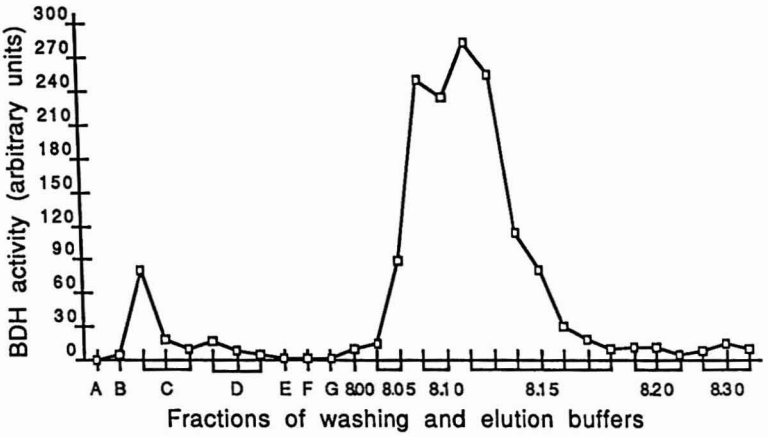

Fig. 1. Elution profile of apoBDH from a controlled-pore glass bead concentration column. Buffers A–G are washing buffers and buffers 8.00–8.30 correspond to elution buffers (see Table I). Each bar on the abscissa corresponds to a fraction of 200 ml. BDH activity is expressed in arbitrary units and corresponds to 40 μl of fraction reactivated with 1.8 μg of lipid phosphorus MPL and measured as described under Experimental.

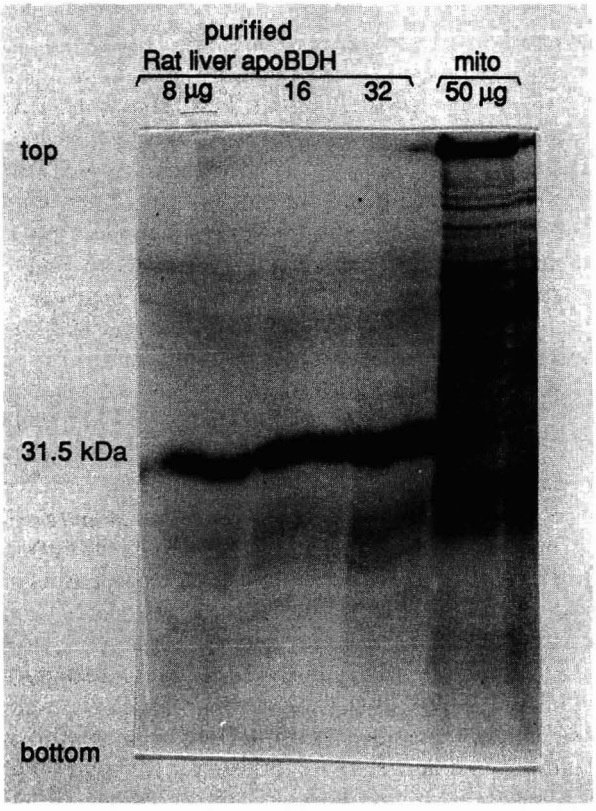

Fig. 2. Purified apoBDH separated by 10% SDS-PAGE and stained with Coomassie Brilliant Blue. For conditions, see Experimental. kDa = Kilodalton.

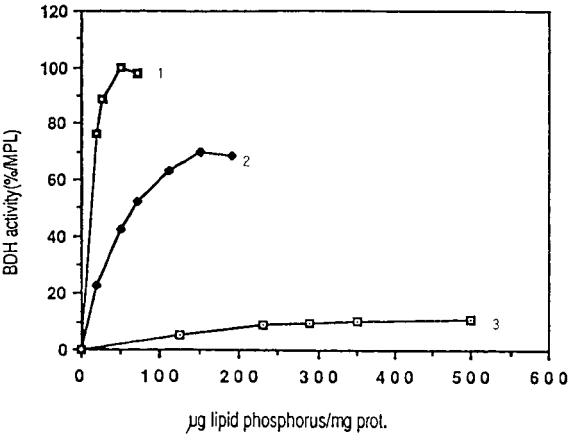

Fig. 3. BDH reactivation by differents amounts of natural [MPL (1), mitoPC (2)] or synthetic DMPC (3) phospholipids. The apoBDH (10 µg) was incubated for 10 min at room temperature in 100 µl (final volume) containing 20 m*M* Tris–HCl–1 m*M* EDTA–5 m*M* DTT (pH 8.1) and the appropriate phospholipid concentrations. The 100-µl aliquot was added at 37 C to a cuvette containing 450 µl of "cocktail" medium as described under Experimental. Then the enzyme reaction was started by addition of 50 µl of 0.2 *M* DL-β-hydroxybutyrate at 37°C and the activity was followed by measuring the increase in absorbance at 334 nm.

phospholipid containing lecithin (MPL), or pure mitochondrial lecithin (mitoPC), or synthetic lecithin (dimyristoylphosphatidylcholine, DMPC). The different extents of reactivation according to the nature of the lipid have been explained previously [28–32].

Several other attempts to purify rat liver apoBDH by different methods have been tried in our laboratory. All of them failed, including Burnett and Khorana's method involving DEAE-cellulose chromatography [17] or an immunoaffinity procedure based on the use of rabbit monospecific anti-rat liver BDH antibody [33].

Relationships between glass beads–BDH adsorption and phospholipid–BDH reactivation

Taking into account the specificity of BDH for either CPG or phospholipids it was important to establish whether there was any relationship between the two interacting mechanisms.

Fig. 4 shows that the addition of CPG prevents the reactivation of purified apoBDH by phospholipids while not modifying the enzymatic activity of BDH previously reconstituted with MPL. These results indicate that the interaction between CPG and the BDH polypeptide chain changes the conformation of the enzyme or, more probably, that the glass surface interacts with phospholipid-binding sites of BDH. However, there is an important difference between glass beads and membrane phospholipid surfaces, as only the latter is able to reactivate BDH.

On the other hand, Fig. 5 shows that LiBr is needed to reactivate BDH by lecithin (PC) or phospholipid containing lecithin (MPL), previously associated with phospholipid containing no lecithin [phosphatidylethanolamine–diphosphatidylglycerol–phosphatidylinositol (PE–DPG–PI)]. This displacement of BDH from a non-reactivating phospholipid surface to a reactivating phospholipid surface is due to the

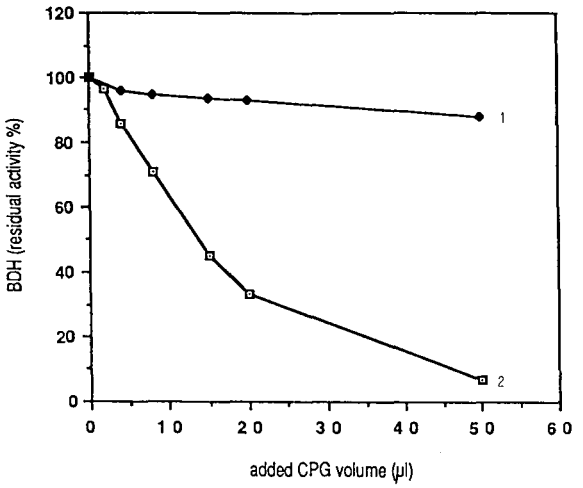

Fig. 4. Effect of controlled-pore glass beads (CPG) on BDH enzyme activity. The untreated glass beads (CPG) were added at room temperature to a cuvette containing 20 m*M* Tris–HCl–1 m*M* EDTA–5 m*M* DTT (pH 8.1) and 20.4 µg of the enzyme (apoBDH or BDH–MPL complex), final volume 450 µl. After 15 min of gentle shaking, the enzyme activity was measured at 334 nm either immediately for BDH–MPL complex assay (1), or after previous incubation (10 min) of MPL (80 µg of lipid phosphorus per mg protein) in the assay containing CPG–apoBDH (2).

ionic strength and to the chaotropic effect of LiBr in addition to the alkaline pH. An evident similarity is found with BDH elution from the glass bead column (Fig. 1). To our knowledge, such a relationship between BDH reactivation by phosholipid and BDH purification by glass beads adsorption has not been reported before.

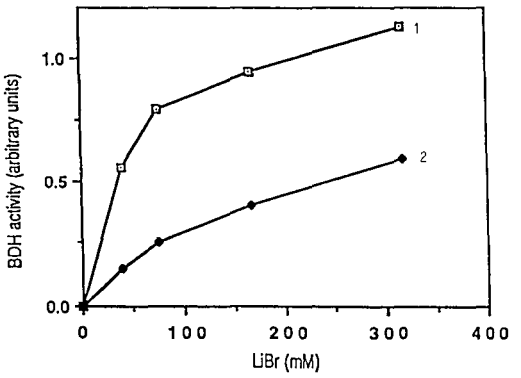

Fig. 5. Displacement of the non-active complex BDH–PE–DPG–PI by reactivating phospholipid [PC (2) or MPL (1)] in the presence of LiBr. ApoBDH (35 µg) was incubated for 15 min at room temperature in a medium (650 µl) containing a microdispersed PE–DPG–PI preparation (200 µg lipid phosphorus per mg protein) and 20 m*M* Tris–HCl–1 m*M* EDTA–5 m*M* DTT (pH 8.1). At the end of incubation, 50 µl of the mixture were removed and added to a medium (650 µl final volume) containing the same buffer and a fixed amount (180 µg lipid phosphorus per mg protein) of reactivating phospholipid (MPL or PC) and an increasing concentration of LiBr. After incubation for 15 min at room temperature, an aliquot of 70 µl was removed and measured as described under Experimental.

It appears that glass beads mimic phospholipids in their interaction with BDH. Indeed, it is well known that a phospholipid membrane is amphipathic and shows a polar surface mostly negatively charged and a hydrophobic domain. On the other hand, untreated glass beads show a negatively polarized surface of the silicate network in addition to a hydrophobic character.

The combination of a high pH (8.05–8.15), high ionic strength and the chaotropic effect of LiBr is able to break the bonds between surface negative charges and positive amino groups of the BDH amino acid side-chain.

This work extends our knowledge of both the basic principles of the adsorption chromatography of membrane proteins and the mechanism of lipid–protein interactions.

ACKNOWLEDGEMENTS

This work was supported by grants from CNRS (040531), INSERM (877005) and the Fondation pour la Recherche Médicale. Thanks are due to Drs. J. M. Berrez and M. S. El Kebbaj (Besançon) and Drs. J. O. McIntyre and S. Fleischer (Nashville) for advice and initial experiments.

REFERENCES

1 N. Latruffe, J. M. Berrez and M. S. El Kebbaj, *Biochimie*, 68 (1986) 481.
2 A. Page, H. A. Krebs and D. H. Williamson, *Biochem. J.*, 121 (1971) 49.
3 A. Kante, M. Cherkaoui Malki, C. Coquard and N. Latruffe, *Biochim. Biophys. Acta*, 1033 (1990) 291.
4 A. L. Lehninger, H. C. Sudduth and J. B. Wise, *J. Biol. Chem.*, 235 (1960) 2450.
5 Y. Gaudemer and N. Latruffe, *FEBS Lett.*, 54 (1975) 30.
6 I. Sekuzu, P. Jurtshuk and D. E. Green, *J. Biol. Chem.*, 238 (1963) 975.
7 S. Fleischer and B. Fleischer, *Methods Enzymol.*, 10 (1967) 406.
8 G. S. Gotterer, *Biochemistry*, 6 (1967) 2139.
9 H. G. O. Bock and S. Fleischer, *Methods Enzymol.*, 32 (1974) 374.
10 N. C. Nielsen and S. Fleischer, *J. Biol. Chem.*, 248 (1973) 2549.
11 H. M. Menzel and G. G. Hammes, *J. Biol. Chem.*, 248 (1973) 4885.
12 C. S. Hexter and R. Goldman, *Biochim. Biophys. Acta*, 307 (1973) 421.
13 A. K. Grover and G. G. Hammes, *Biochim. Biophys. Acta*, 356 (1974) 309.
14 M. Levy, M. Joncourt and J. Thiessard, *Biochim. Biophys. Acta*, 424 (1976) 57.
15 J. C. Vidal, E A. Guglielmucci and A. O. M. Stoppani, *Mol. Cell. Biochem.*, 16 (1977) 153.
16 M. Miyahara, K. Utsumi and D. W. Deamer, *Biochim. Biophys. Acta*, 641 (1981) 220.
17 B. K. Burnett and H. G. Khorana, *Biochim. Biophys. Acta*, 815 (1985) 51.
18 J. O. McIntyre, N. Latruffe, S. C. Brenner and S. Fleischer, *Arch. Biochem. Biophys.*, 262 (1988) 85.
19 H. G. O. Bock and S. Fleischer, *J. Biol. Chem.*, 250 (1975) 5774.
20 S. Fleischer, J. O. McIntyre and J. C. Vidal, *Methods Enzymol.*, 55 (1979) 32.
21 O. M. Lowry, N. J. Rosebrough, A. L. Farr and R. J. Randall, *J. Biol. Chem.*, 193 (1951) 265.
22 E. Ross and G. Schatz, *Anal. Biochem.*, 32 (1973) 91.
23 P. S. Chen, T. Toribara and H. Warner, *Anal. Chem.*, 28 (1956) 1756.
24 G. Rouser and S. Fleischer, *Methods Enzymol.*, 10 (1967) 385.
25 U. K. Laemmli, *Nature (London)*, 227 (1970) 680.
26 M. S. El Kebbaj, N. Latruffe and Y. Gaudemer, *Biochem. Biophys. Res. Commun.*, 108 (1982) 42.
27 H. G. O. Bock, P. Skene, P. Cassidy, S. Fleischer and S. Harshman, *Science*, 191 (1976) 380.
28 J. M. Berrez, N. Latruffe and Y. Gaudemer, *Biochimie*, 66 (1984) 717.
29 J. M. Berrez, F. Pattus and N. Latruffe, *Arch. Biochem. Biophys.*, 243 (1985) 62.
30 M. S. El Kebbaj, J. M. Berrez, T. Lakhlifi, C. Morpain and N. Latruffe, *FEBS Lett.*, 182 (1985) 176.
31 M. S. El Kebbaj and N. Latruffe, *Arch. Biochem. Biophys.*, 244 (1986) 622.
32 M. S. El Kebbaj, N. Latruffe, M. Monsigny and A. Obrenovitch, *Biochem. J.*, 237 (1986) 359.
33 C. Coquard, P. Adami, M. Cherkaoui Malki, D. Fellmann and N. Latruffe, *Biol. Cell*, 59 (1987) 137.

Journal of Chromatography, 539 (1991) 289–296
Elsevier Science Publishers B.V., Amsterdam

CHROM. 22 893

Immobilization of dermatan sulphate on a silica matrix and its possible use as an affinity chromatography support for heparin cofactor II purification

V. SINNIGER and J. TAPON-BRETAUDIÈRE

Laboratoire d'Hématologie, C.H.U. Necker-Enfants Malades, 156 rue de Vaugirard, 75015 Paris Cedex 15 (France)

F. L. ZHOU

Laboratoire de Recherche sur les Macromolécules, Université Paris-Nord, Av. J.B. Clément, 93430 Villetaneuse (France)

A. BROS

Laboratoire d'Hématologie, C.H.U. Necker-Enfants Malades, 156 rue de Vaugirard, 75015 Paris Cedex 15 (France)

D. MULLER and J. JOZEFONVICZ

Laboratoire de Recherche sur les Macromolécules, Université Paris-Nord, Av. J.B. Clément, 93430 Villetaneuse (France)

and

A. M. FISCHER*

Laboratoire d'Hématologie, C.H.U. Necker-Enfants Malades, 156 rue de Vaugirard, 75730 Paris Cedex 15 (France)

ABSTRACT

Dermatan sulphate (DS) is a glycosaminoglycan which catalyses specifically thrombin inhibition by a plasmatic inhibitor, Heparin cofactor II (HCII). DS was insolubilized on a silica matrix to study its interaction with HCII. The immobilization of DS was performed with a good yield on a silica previously coated with polysaccharides in order to neutralize the negatively charged silanol groups. The value of the affinity constant of insolubilized DS for HCII, measured by the adsorption isotherm, is consistent with the value obtained for soluble DS. The DS bound to the silica matrix was also tested as a chromatographic support for the purification of HCII from human plasma: the optimum conditions for HCII adsorption and desorption were determined. The eluted HCII was obtained with a good yield (21%) and with no contamination by antithrombin III, the other main plasmatic inhibitor of thrombin.

INTRODUCTION

Heparin cofactor II (HCII) is a human plasma glycoprotein, the properties of which were reported in the 1980s [1,2]. Although its physiological role is not yet well established, it is known that HCII inhibits thrombin in the presence of heparin or dermatan sulphate (DS) [2,3]. HCII has a structure and a mechanism of inhibition

0021-9673/91/$03.50

close to those of antithrombin III (ATIII), a well known potent thrombin inhibitor. However, these two plasmatic inhibitors have different properties: whereas ATIII inhibits all the serine proteases of the intrinsic coagulation cascade [4], HCII activity is specific to thrombin. The inhibition by HCII is specifically catalysed by DS, a glycosaminoglycan (GAG) of the vascular endothelium, which has no effect on thrombin inhibition by ATIII.

The potentiation of HCII by DS is related to a specific polysaccharide sequence [5,6], as a minimum of twelve residues is required for the HCII catalysis whereas an octasaccharide is sufficient to bind to HCII. The presence of sulphate groups in the DS structure appears to be of importance in HCII catalysis [7]. One Lys and four Arg residues are involved in the GAG binding site of HCII [8,9]. However, the precise mechanism oof interaction between HCII and DS is not yet known. The low plasma concentration of HCII and its chemical properties close to those of ATIII do not allow an easy purification process. Most of the procedures used to isolate HCII [2,9,10] involve several steps (at least five) including a first step of protein fractionation followed by ion-exchange and gel permeation chromatography; HCII and ATIII are separated by their different affinities for heparin on an insolubilized heparin sorbent. The contaminating ATIII can also be eliminated on an anti-ATIII immunoabsorbent.

In this work, we studied the interaction between insolubilized DS and HCII in order to understand better the specificity and binding mechanism between this GAG and HCII. DS was insolubilized on a dextran- or agarose-coated silica support which combines all the advantages of traditional supports and the important mechanical properties of silica [11]. The affinity of the immobilized DS for HCII was determined from the adsorption isotherm under static conditions. Then, preliminaty studies of the isolation of HCII from human plasma were carried out in order to set up an easy, fast and efficient purification procedure.

EXPERIMENTAL

Materials

Silica beads XO15M, purchased from IBF Biotechnics (Villeneuve la Garenne, France), had an average pore diameter of 1250 Å and were spherical (40–100 μm). The polysaccharides used for the coating were dextrans T500 (Pharmacia France, Bois d'Arcy, France) and Indubiose agarose A37 HAA (IBF Biotechnics). The activating agents were 1,4-butanediol diglycidyl ether (BDGE) and 1,1'-carbonyldiimidazole (CDI). Dermatan sulphate NF 112 from bovine intestinal mucosa was provided by Pharmuka (Gennevilliers, France). Human purified thrombin, chromothrombin and monospecific antibodies against HCII were purchased from Diagnostica Stago (Asnieres, France); bovine factor Xa from Biotrol (Diagnostic Reagents, U.K.) and chromogenic substrate, S2222 from Kabi-Vitrum (Stockholm, Sweden). A pool of platelet-poor plasma was prepared by centrifugation at 2000 *g* of blood from fifteen normal subjects, collected on 0.13 *M* sodium citrate. This pool was used to establish the adsorption isotherm and the calibration graphs for HCII and ATIII assays.

Preparation of coated silica supports and immobilization of DS

The synthesis of the active supports was realized in two successive steps. In the

first, silica beads were coated with dextran or agarose substituted with DEAE functions in order to neutralize the ion-exchange capacity of native silica, as described previously [11,12]. Two types of coated silica were prepared: the silica with a single layer of substituted polysaccharides as described above, and the same silica with a double coating in which the second layer consisted of a neutral polysaccharide [13]. Silica with a double coating is a new type of support; preliminary studies have demonstrated a decrease in the non-specific interactions with these supports. The amount of polysaccharides was determined by elemental analysis of carbon. In the second step, the coated silica phases were activated and coupled with DS. Before immobilization of DS, the contaminating heparin was removed from DS by a deamination treatment with nitrous acid [14]. The coated silica supports were then activated by hydroxyl groups with either 0.3 g of CDI or 3 μl of BDGE per gram of coated silica. DS coupling was performed by using 3 g of activated support and 250 mg of GAG suspended in 14.5 ml of 0.1 *M* sodium carbonate (pH 8.7). The amount of bound DS was determined by elemental analysis of the sulphur content.

Adsorption isotherm and determination of affinity constant

Adsorption experiments were performed at 4°C to prevent the loss of HCII activity. The isotherm was established from measurement of HCII adsorption using the following procedure: 400 μl of the support suspension were incubated with 0.02 *M* Tris–HCl (pH 7.4)–0.05 *M* NaCl buffer. Several dilutions of plasma, corresponding to different HCII concentrations (0.02–0.4 U/ml), were incubated with the support suspension for 90 min at 4°C. After sedimentation, the amount of residual HCII in the supernatant was determined by an HCII assay, as described under *Chromatographic experiments*. The amount of adsorbed protein corresponds to the difference between the initial and remaining concentrations of active HCII in the supernatant. The adsorption isotherm was then established. The affinity constant was calculated from the initial slope and plateau of the isotherm and the binding capacity of the support was measured from the plateau value.

Chromatographic experiments

The chromatographic experiments were performed using an LKB system. A 13 × 1.1 cm I.D. column containing 5 ml (2.5 g dry weight) of the affinity sorbent was packed using a slurry method. Each support was washed with 25 ml of initial buffer. In order to define the optimum conditions for the interaction between HCII and its ligand, different buffers (0.02 or 0.05 *M* Tris–HCl) with pH values of 6.5, 7.4 or 8.5 and NaCl concentrations of 0 or 0.05 *M* were tested. A 5-ml aliquot of human plasma was loaded on the column. Elution was performed at a flow-rate of 20 ml/h at 4°C using a 40-ml linear gradient increasing from the molarity of the initial buffer used to 1 *M* NaCl. The eluted proteins were detected at 280 nm and the chromatographic fractions collected to perform ATIII and HCII assays. The protein concentration was measured by Lowry's method [15]. The biological activity of HCII in the eluted fractions was assayed at 37°C by measuring the thrombin inhibition in the presence of DS as follows: 150 μl of a diluted sample were added to 150 μl of 0.05 *M* Tris–HCl (pH 8.4)–0.1 *M* NaCl containing 0.2 g/l of DS. After incubation for 2 min with 150 μl of human purified thrombin (3 U/ml), 150 μl of chromothrombin (1.5 μM) were added and the amidolysis of the substrate was measured at 405 nm. The results were

reported with respect to a calibration graph established under the same conditions, with dilutions of a normal plasma. By definition, the concentration of plasmatic HCII is 1 unit/ml. The biological activity of ATIII was determined by measuring its anti-factor Xa activity in the presence of heparin: 100 μl of a diluted sample were added to 100 μl of 0.05 *M* Tris–HCl (pH 8.4)–0.05 *M* NaCl containing 6 U/ml of heparin and incubated for 2 min. Then 100 μl of bovine factor Xa were added and after incubation for 1 min 100 μl of S2222 (4 m*M*) were added. Hydrolysis of the substrate was measured at 405 nm. The calibration graph was established under the same conditions, using the same pool of normal plasma as previously described. The concentration of HCII antigen was measured by electroimmunodiffusion [16] with monospecific antibodies raised against human HCII. HCII purity was checked by immunoelectrophoresis [17] with anti-human HCII and anti-human serum antibodies and by sodium dodecyl sulphate polyacrylamide gel electrophoresis (SDS-PAGE) [18].

RESULTS AND DISCUSSION

Characterization of the affinity supports

To neutralize the negatively charged silanol groups on the silica surface, a polysaccharide (dextran or agarose) was used to coat the silica. The characteristics of the coated silica are presented in Table I. A larger amount of polymer is bound to the silica when the coating polysaccharide is dextran. However, the coverage of the silica surface is more efficient with agarose, which has a greater number of DEAE groups.

The immobilization of DS was performed using CDI or BDGE as activating agents. Table II shows the amounts of immobilized DS for three differents supports. Coupling of DS by BDGE seems more efficient than that by CDI. BGDE mainly activates hydroxyl groups whereas CDI acts essentially on primary amino groups. The greater efficiency of BDGE shows that DS is mainly immobilized by its hydroxyl groups rather than by its primary amino groups. This is certainly due to the large number of hydroxyl groups on the DS compared with the small number of primary amino groups, which are mostly acetylated amino groups.

The affinity of insolubilized DS for HCII was studied by measuring the affinity constant from the Langmuir isotherm. Fig. 1 shows the adsorption of HCII on the affinity support. The adsorption isotherm obtained corresponds to the Langmuir model. The value of the affinity constant for HCII is $7 \cdot 10^5$ l/mol, which is consistent with the published value for soluble DS of $6.6 \cdot 10^5$ l/mol according to Pratt *et al.* [19].

TABLE I

CHARACTERISTICS OF COATED SILICA SUPPORTS

Support	Coating polymer	DEAE (%)	Amount of fixed polymer (mg/g silica)
SiD-DS 1	DEAE-dextran	4	121
SiD-DS 2	DEAE-dextran	4	138
ASiA-DS 1	DEAE-agarose	10	45
	Agarose	–	35

TABLE II

INSOLUBILIZATION OF DERMATAN SULPHATE ON COATED SILICA

Support	Activating agent	Amount of dermatan used (mg)	Amount of dermatan fixed (mg)	Yield (%)
SiD-DS 1	BDGE	250	195	78
SiD-DS 2	CDI	250	133	53
ASiA-DS 1	CDI	250	94	38

these similar values indicate that the non-specific interactions make only a small contribution to the overall adsorption process. Moreover, it seems that the binding sites for HCII in the DS structure are not masked or are not involved in the immobilization of DS on the coated silica. Compared with the affinity constant of soluble DS for ATIII, which is $1 \cdot 10^3$ l/mol [19], the affinity constant of HCII is higher and shows that DS has a very weak affinity for ATIII. However, the affinity constant of insolubilized DS for HCII is not in the range of 10^7 or 10^8 l/mol, which would demonstrate a very high affinity for HCII. As reported in the literature, the native DS used in this study has a weak affinity for HCII; this could be explained, as was noted by Griffith and Marbet [20], by the fact that perhaps only a small fraction of the DS is involved in the HCII binding. The binding capacity of the tested supports was of 0.5 U of HCII per gram of support.

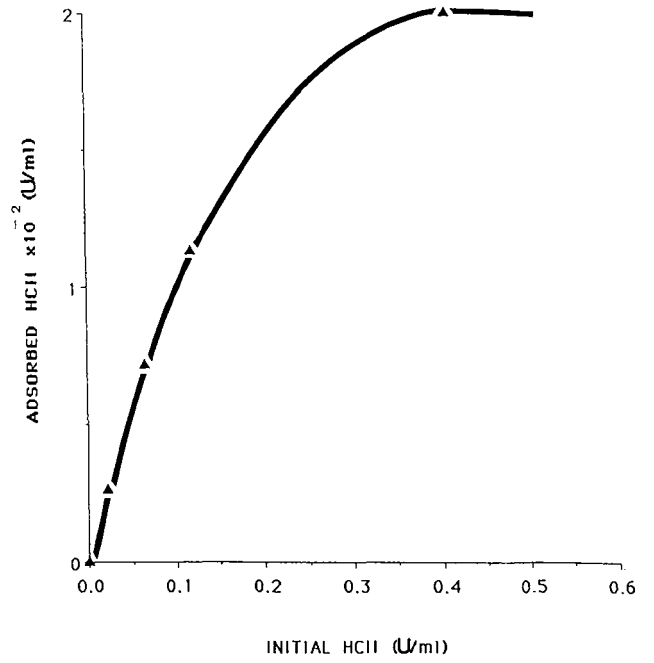

Fig. 1. Adsorption isotherm of HCII on the insolubilized DS support.

TABLE III

INFLUENCE OF INITIAL BUFFER ON THE HCII AND ATIII ADSORPTION ON AFFINITY SORBENT

Initial buffer	ATIII adsorbed (U/ml)	HCII adsorbed (U/ml)
0.02 *M* Tris (pH 7.4)	0	0.30
0.05 *M* Tris (pH 7.4)	0	0.81
0.02 *M* Tris (pH 7.4)–0.05 *M* NaCl	0	0.84
0.02 *M* Tris (pH 6.5)–0.05 *M* NaCl	0.03	0.01
0.02 *M* Tris (pH 8.5)–0.05 *M* NaCl	0	0

Isolation of HCII from human plasma

Several initial buffers were used to determine the optimum conditions of adsorption of HCII on the affinity sorbent (Table III). A minimum concentration of 0.05 *M* is required for optimum adsorption of HCII on the insolubilized DS. A buffer of 0.02 *M* [0.02 *M* Tris–HCl (pH 7.4) led to a very weak adsorption of HCII whereas buffers of 0.05 *M* Tris–HCl (pH 7.4) and 0.07 *M* [0.05 *M* Tris–HCl (pH 7.4)–0.02 *M* NaCl] allow a better adsorption of HCII. From these results and those of Sculy *et al.* [7], who showed that a maximum activity of HCII, in the presence of soluble DS, was obtained with 0.05 *M* NaCl, it seems that the optimum buffer for HCII adsorption is 0.02 *M* Tris–HCl (pH 7.4)–0.05 *M* NaCl. Under these optimum conditions, up to 21% of the initial HCII is adsorbed on the insolubilized DS. This low molarity required to obtain optimum adsorption of HCII is consistent with the weak affinity constant of the support for this inhibitor. At pH 8.5, the total activity of ATIII and HCII is recovered in the washing buffer, showing that at a basic pH neither HCII nor ATIII is adsorbed on the affinity sorbent. In contrast, when the pH is lowered to 6.5, the two inhibitors adsorbed on the insolubilized DS. The influence of pH and molarity on the adsorption of HCII on DS seems to indicate that the interaction between the inhibitor and the DS is mainly an ionic interaction. This interaction is probably due to the negative sulphate and carboxyl groups of DS, and also to the positive amino groups of HCII Lys residues.

In all the chromatographic experiments, under conditions of optimum pH and molarity, ATIII was never adsorbed on the affinity sorbent. The total amount of ATIII loaded on the column was always recovered in the washing buffer. Under these dynamic conditions, insolubilized DS has no affinity for ATIII, which is not adsorbed on the support. Thus, on our supports, we can separate HCII from ATIII. Whereas ATIII is totally recovered in the washing buffer, HCII binds to the support and can be eluted with a buffer gradient. HCII is eluted in a range from 0.12 to 0.48 *M* NaCl (Table IV) from the immobilized DS whereas is eluted from insolubilized heparin between 0.13 and 0.28 *M* NaCl. A higher molarity seems to be required to desorb HCII from insolubilized DS than from insolubilized heparin, which means that insolubilized DS has a greater affinity for HCII than for insolubilized heparin. The specific activities of the eluted HCII (mean of three experiments for each support) were 0.05

TABLE IV

CONDITIONS AND YIELD OF HCII ELUTION

Support	Molarity of HCII desorption (*M* NACl)	HCII yield (%)[a]	ATIII yield (%)
SiD-DS 1	0.12–0.38	15	0
SiD-DS 2	0.28–0.40	7	0
ASiA-DS 1	0.21–0.48	17	0

[a] Mean values of three experiments.

U/mg for SiD-DS2, 0.22 U/mg for ASiA-DS1 and 0.34 U/mg for SiD-DS1. The highest specific activity of the eluted HCII is obtained with the SiD-DS1 support; this is probably due to a lower non-specific interaction of this support than the others. However, the specific activities of the eluted HCII are not very high compared with those obtained in the classical purification processes in which specific activities of 0.9 [10] to 10 U/mg [2] were obtained. The HCII activity yields obtained with our supports were 7% for SiD-DS2, 17.5% for SiD-DS1 and 21% for ASiA-DS1, whereas no ATIII activity was found in the elution gradient. These yields are in the same range as those obtained in the previously described purification procedures of 3–30% yields [9,10]. Although SiD-DS1 and ASiA-DS1 were not prepared under the same conditions, these two supports gave comparable yields and specific activities.

The purified HCII was tested by electroimmunodiffusion. The HCII activity/HCII antigen ratio was between 0.6 and 1; a ratio of less than 1 indicates partial inactivation of the HCII after the elution with a salt gradient. The eluted HCII was also tested by SDS-PAGE and immunoelectrophoresis, which revealed two contaminating proteins, IgA and an α_2-globulin, which has not been identified as another coagulation inhibitor (ATIII or α_2-macroglobulin).

CONCLUSIONS

The interaction between DS and HCII is not well understood. It was interesting to study this interaction by immobilizing this GAG on a silica support. DS has been insolubilized on a silica phase, a synthesis which has never been achieved before. Silica beads were previously coated with polysaccharides in order to neutralize silanol groups, according to data obtained in our laboratory [13]. DS can be immobilized on silica, regardless of the coating polymer used, dextran or agarose. The GAG seems to bind to the matrix by its hydroxyl groups more than by its amino groups.

Under static conditions, the affinity constant of insolubilized DS for HCII is similar to that of soluble DS. When used as a chromatographic support under optimum conditions of pH and molarity, insolubilized DS has no affinity for ATIII. HCII is adsorbed on the affinity sorbent and can be eluted by a salt gradient between 0.12 and 0.48 *M* NaCl. With only one chromatographic step, the yield of the eluted HCII is identical with those obtained in previously described purification processes, with no contaminating ATIII. However, the specific activity is lower than those given by other published procedures.

We have shown that insolubilized DS, used as an affinity chromatography support, may allow the separation of HCII from ATIII, which is important for the study of each inhibitor. However, the native DS, soluble or insolubilized, has a weak affinity for HCII and it will be of interest to isolate a fraction of this GAG with a high affinity for HCII. The insolubilization of such a fraction might allow a very efficient isolation procedure for HCII in a single chromatographic run.

ACKNOWLEDGEMENTS

The authors thank M. Delvallée for expert secreterial help and C. Millien and C. Sternberg for technical assistance. This work was in part supported by grant No. 885006 from INSERM and by a grant from the Groupement d'Intérêt Public "Therapeutiques Substutives".

REFERENCES

1 D. M. Tollefsen and M. K. Blank, *J. Clin. Invest.*, 68 (1981) 589.
2 D. M. Tollefsen, P. W. Majerus and M. K. Blank, *J. Biol. Chem.*, 257 (1982) 2162.
3 D. M. Tollefsen, C. A. Pestka and W. J. Monafo, *J. Biol. Chem.*, 258 (1983) 6713.
4 R. D. Rosenberg, *Semin. Haematol.*, 14 (1977) 427.
5 D. M. Tollefsen, M. E. Peacock and W. J. Monafo, *J. Biol. Chem.*, 261 (1986) 8854.
6 H. Munakata, C. C. Hsu, C. Kodama, J. Aikawa, M. Sakurada, N. Ototani, M. Isemura, Z. Yosizawa and N. Hayashi, *Biochim. Biophys. Acta*, 925 (1987) 325.
7 M. F. Scully, V. Ellis and V. V. Kakkar, *Thromb. Res.*, 46 (1987) 491.
8 F. C. Church, G. B. Villanueva and M. J. Griffiith, *Arch. Biochem. Biophys.*, 246 (1986) 175.
9 R. Yamagishi, T. Koide and N. Sakuragawa, *FEBS Lett.*, 225 (1987) 109.
10 P. Wunderwald, W. J. Shrenk and H. Port, *Thromb. Res.*, 25 (1982) 177.
11 F. L. Zhou, D. Muller, X. Santarelli and J. Jozefonvicz, *J. Chromatogr.*, 476 (1989) 195.
12 X. Santarelli, F. L. Zhou, D. Muller and J. Jozefonvicz, *Colloq. INSERM*, 175 (1989) 155.
13 F. L. Zhou, D. Muller and J. Jozefonvicz, *J. Chromatogr.*, 510 (1990) 71.
14 D. Lagunoff and G. Warren, *Arch. Biochem. Biophys.*, 99 (1962) 396.
15 O. Lowry, N. Rosenberg, A. Farr and R. Randall, *J. Biol. Chem.*, 193 (1951) 265.
16 C. B. Laurell, *Anal. Biochem.*, 15 (1966) 45.
17 P. Grabar and C. A. Williams, *Biochim. Biophys. Acta*, 10 (1953) 193.
18 U. K. Laemmli, *Nature (London)*, 227 (1970) 681.
19 C. W. Pratt, H. C. Whinna, J. B. Meade, R. E. Treanor and F. C. Church, *Ann. N.Y. Acad. Sci.*, 556 (1989) 104.
20 M. J. Griffith and G. A. Marbet, *Biochem. Biophys. Res. Commun.*, 112 (1983) 663.

Journal of Chromatography, 539 (1991) 297–306
Elsevier Science Publishers B.V., Amsterdam

CHROM. 22 870

Review

Polymer ligands for mild hydrophobic interaction chromatography —principles, achievements and future trends

P. HUBERT*, R. MATHIS and E. DELLACHERIE
Laboratoire de Chimie-Physique Macromoléculaire, URA CNRS 494, ENSIC, B.P. 451, 54001 Nancy Cedex (France)

ABSTRACT

Mildly hydrophobic polymers, such as those generally used in the "partition between aqueous two-phase systems" technique, can be immobilized on inert supports to afford stationary phases which are less denaturing towards biomolecules than those involved in traditional hydrophobic chromatography. Various aspects of this technique are reviewed. Examples of successful fractionations are presented to illustrate its principles, and the main trends for future studies in this field are discussed.

CONTENTS

1. INTRODUCTION

Since the initial work of Er-el *et al.* [1], hydrophobic interaction chromatography (HIC) on agarose gels has become an important separation method [2–6]. Hydrophobic ligands, such as *n*-alkyl or phenyl groups, are chemically attached to the agarose matrix and the separations are based on differences in the surface hydrophobicity of proteins [7]. However, strong hydrophobic interactions sometimes result in almost irreversible adsorption [3,6,8] or denaturation during the elution with often harsh mobile phase conditions (*e.g.*, low pH, chaotropic agents, detergents, organic solvents, etc.).

Therefore, it can be envisaged that ligands with intermediate hydrophobic character would be of interest, as they would provide an adequate binding strength

0021-9673/91/$03.50

without the above drawbacks. "Partition between aqueous two-phase systems", a separation technique extensively described by Albertsson [9], exploits these mild hydrophobic interactions. The systems are composed of either two polymers, or a polymer and a salt. Poly(vinyl alcohol)–dextran, polyethylene glycol–dextran and polyethylene glycol-$MgSO_4$ are among the most widely used biphasic systems. However, although many successful purification experiments have been reported, it is clear that the high viscosity of the solutions affords one likely explanation, among others, for its limited practical use. Recent improvements might, however, result in some revival of this technique in the near future [10,11].

Its seems logical that the principles of the partition technique could be transposed to a chromatographic procedure if one of these polymers were immobilized on the chromatographic support. This idea is not totally new, as Morris [12] and more recently Anker [13] exploited this concept many years ago. However, probably owing to the difficulties caused by the fact that the aqueous polymer phase was merely soaked up by the support beads, the idea received no further attention for about 10 years.

It was only in the early 1980s that different groups revived this concept [14–19] and started to immobilize covalently various mildly hydrophobic polymers on chromatographic supports, to produce stationary phases less denaturing towards biomolecules than those used in traditional HIC.

This paper is intended to review our own work in this field over the past few years [20–24]. The synthesis and physico-chemical characterization of the stationary phases, fractionation achievements and future trends will be discussed.

2. STATIONARY PHASES: SYNTHESIS AND PHYSICO-CHEMICAL CHARACTERIZATION

Water-soluble polymers, such as those involved in aqueous two-phase systems, are generally regarded as hydrophilic species, obviously because of their solubility in this solvent. However, a closer look at thermodynamics-related parameters, such as surface tension, reveals the relative nature of the hydrophilicity–hydrophobicity concept. The surface tension of polyethylene glycols (PEGs) for instance, in the range $\gamma_{sv} \approx 42$–46 mJ/m^2 [25], is situated mid-way between those of water ($\gamma_{sv} \approx 70$ mJ/m^2) and of low-energy materials such as C_6–C_{16} alkanes ($\gamma_{sv} \approx 18$–28 mJ/m^2) [26]. PEGs are slightly more hydrophobic than various other water-soluble polymers such as poly(vinyl alcohol) (PVA), polyvinylpyrrolidone (PVP), polyacrylamide or dextran [27], but less hydrophobic than, for instance, polystyrene ($\gamma_{sv} \approx 32$ mJ/m^2) [28] and *a fortiori* than the C_6–C_{16} alkanes, which are the most commonly used ligands in traditional HIC.

From this point of view, it is clear that PEGs, and also the other polymers used in the partition technique, and which all fall within a narrow range on the hydrophobicity scale, may definitely be considered as hydrophobic materials. Conversely, when compared with alkyl chains, their designation as "mild hydrophobic ligands" [15] is perfectly justifiable (Fig. 1).

As many other groups, we selected the polyethers as ligands for mild hydrophobic chromatography studies. PVA is the only other polymer, used in a few instances in this field [15,19].

The polyether class includes the following: polyethylene glycols (PEGs), $HO(CH_2CH_2O)_nH$; polypropylene glycols (PPGs), $HO[CH_2(CH_3)CHO]_nH$; poly-

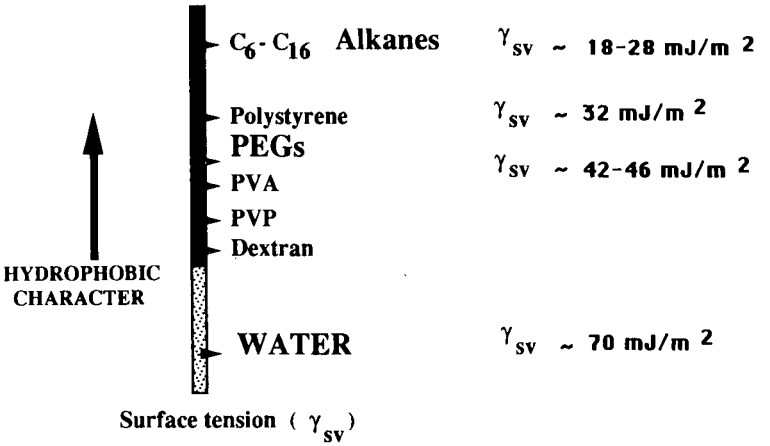

Fig. 1. Schematic hydrophobicity scale based on surface tension of various chemicals.

tetramethylene glycols (PTMGs), $HO(CH_2CH_2CH_2CH_2O)_nH$; and various PEG–PPG copolymers which are also commercially available as Pluronics (Serva) or Jeffamines (Texaco).

The hydrophobic character of these polymers increases with increasing number of carbon atoms (2–4) in the repeating unit: PEGs < PEG–PPG copolymers < PPGs < PTMGs. Further, as all these polymers are available with a large range of molecular masses, the polyethers thus form a family of wide potential.

Covalent immobilization of polyethers on Sepharose requires a preliminary activation of either the matrix or the polymer. As we are dealing with mild hydrophobic interactions, much care should obviously be taken not to introduce strongly interacting spacer arms on the gels, as they would lead to erroneous interpretations of the phenomena observed.

This was effectively experienced [20,21] when performing the activation reaction with certain commonly used bisepoxides such as 1,4-butanediol diglycidyl ether or ethylene glycol diglycidyl ether (Fig. 2). In fact, these activation groups remained in large amounts on the gel after the coupling step and, owing to the presence of $(CH_2)_n$ units in their structure ($n = 2$ or 4), acted as hydrophobic ligands, to afford strongly adsorbing stationary phases, even in the absence of any immobilized polyether. No

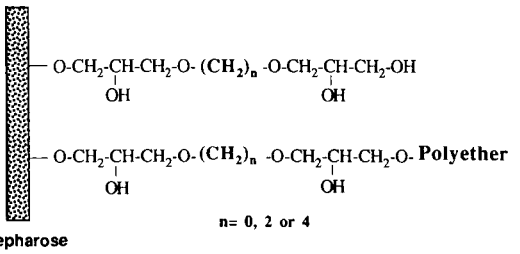

Fig. 2. Schematic representation of the stationary phases obtained by coupling a polyether to Sepharose previously activated by various bisepoxides.

such undesirable side-effect was observed when (±)-1,3-butadiene diepoxide was used ($n = 0$) (Fig. 2).

Unambiguous immobilization of polyethers on chromatographic supports, by means of spacer arms not liable to interfere in the hydrophobic interaction, can be obtained using carbonyldiimidazole (CDI) or *p*-nitrophenyl chloroformate as activation reagents. However, the reaction of the matrix thus activated, with polyethers, directly via their terminal hydroxyl groups, would result in both instances in carbonate spacer arms which are sensitive to hydrolysis. More stable immobilization is afforded by the urethane group, formed when the coupling of the activated matrix is carried out with the polyethers, after prior transformation into their corresponding amino derivatives [29].

3. QUANTIFICATION OF IMMOBILIZED POLYETHERS

Obviously, the quantification of polyethers immobilized on inorganic supports such as siliceous materials presents no major difficulties, as their high content of carbon atoms allows their direct measurement by elemental analysis. Conversely, with polysaccharide supports such as agarose, no such distinctive feature can be exploited, and one must therefore turn to more sophisticated methods.

The agarose thermoreversible gel results from the rigid helical conformation adopted by the molecule when the solution conditions (temperature, ionic strength, solvent, etc.) are no longer favourable to the coil state [30]. A direct non-destructive NMR analysis in solvents [dimethyl sulphoxide (DMSO) or hot water] preventing the formation of the ordered conformation may, therefore, be considered, provided that immobilized polyethers contain distinctive CH_3 or CH_2 groups, resulting in signals sufficiently resolved from the peaks corresponding to the saccharide backbone. All polyethers, except PEGs, fullfil this condition.

This approach affords perfect calibration graphs when artificial mixtures of Sepharose and various amounts of polyethers are analysed. Unfortunately, all the Sepharose–polyether stationary phases obtained are no longer soluble, either in hot water or in DMSO. This phenomenon can be explained either by a profound modification of the physico-chemical properties of the Sepharose (water solubility cannot be re-established even on addition of strong aggregation-disrupting agents such as urea or NaSCN [31]) or by a cross-linking phenomenon, due to the bifunctional character of the polyethers and despite their large excess used during the coupling step. The synthesis of a stationary phase starting from strictly monofunctional polyethers (such as monomethoxy PEGs) would allow one to distinguish between these two hypotheses. However, the commercially available "monofunctional compounds" have been proved to be contaminated by various amounts of difunctional species, sometimes as high as 20% [32].

As ether bonds are sensitive to acidic cleavage, many degradation techniques can be considered. We attempted to hydrolyse our stationary phases with formic or hydrochloric acid treatment and subsequently analyse the resulting mixture by ^1H or ^{13}C NMR, according to the procedure described by Shibusawa *et al.* [18]. The construction of a calibration graph is a prerequisite for this approach. It permits a comparison of the integral of the distinctive CH_3 (or CH_2) signal of the polyether in the hydrolysed stationary phase spectra with those obtained with artificial mixtures

containing Sepharose and known amounts of polyether. In our own experience, reproducible linear correlations are difficult to obtain for the calibration graph itself. This unreliability is due, in our opinion, to the experimental conditions under which the crude hydrolysis mixture is prepared for the NMR sample. It seems likely that some of the hydrolysis fragments are sufficiently volatile to be eliminated along with the solvent during its removal at 70°C under reduced pressure. Clearly, a far better approach consists in performing the hydrolysis experiment in dilute $^2H_2SO_4$, according to the procedure described by Andrade [33]. In fact, in this instance, the hydrolysis mixture can be directly analysed by NMR, without further work-up liable to produce undesirable effects.

In order to determine the PEG content of Sepharose–PEG samples, we tested another method, based on degradation by boron tribromide (BBr_3), proposed by Drevin and Johansson [34]. The cleavage fragments (*e.g.*, for PEGs, 2-bromoethanol and 1,2-dibromoethane) are subsequently analysed by gas chromatography (GC). Satisfactory results were reproducibly obtained with our own Sepharose–PEG samples with this method. Its ability to afford reliable results with more complex mixtures resulting from BBr_3 cleavage of PPGs (three types of fragments) or PEG–PPG copolymers (five types of fragments) is currently under investigation.

4. FRACTIONATION ACHIEVEMENTS

Up to now, most of the work devoted to mild HIC by other groups has been carried out on standard protein mixtures or simple extracts, and has been mainly intended for physico-chemical or thermodynamic investigations. Obviously, this approach is of great value for a better understanding of the principles governing this new technique.

We started with a different strategy, attempting to investigate the ability of this non-specific technique to cope with actual fractionation problems with complex mixtures, and to afford high purification ratios together with a high recovery of enzymatic activities. Fractionation challenges concerning enzymes acting on hydrophobic substrates were selected in the steroid and lipid fields.

A crude extract of *Pseudomonas testosteroni*, containing $\Delta_{5\to4}$ 3-oxosteroid isomerase (isomerase), was chromatographed on a Sepharose–PEG stationary phase with various concentrations of dextran T70 in the mobile phase. The chromatographic behaviour of this enzyme, and that of contaminants, may be correlated with batch partition studies in PEG–dextran two-phase systems. Earlier experiments [35] showed that contaminants favoured the dextran-rich bottom phase (partition coefficient $K_{\text{contaminants}} \approx 0.4$), whereas isomerase established preferential interactions with the PEG-rich top phase ($K_{\text{isomrase}} \approx 4$). The chromatographic elution profile was in agreement with this partition result.

An increased dextran concentration in the mobile phase resulted in an enhanced separation of the peaks corresponding to isomerase and contaminants. Complete resolution could even be obtained with high concentrations of dextran in the mobile phase (Fig. 3).

Solutions of potassium phosphate [20], a salt known to produce two-phase systems with PEG, may advantageously be used as the mobile phase instead of the viscous dextran solutions. In this instance, total retention of isomerase was obtained

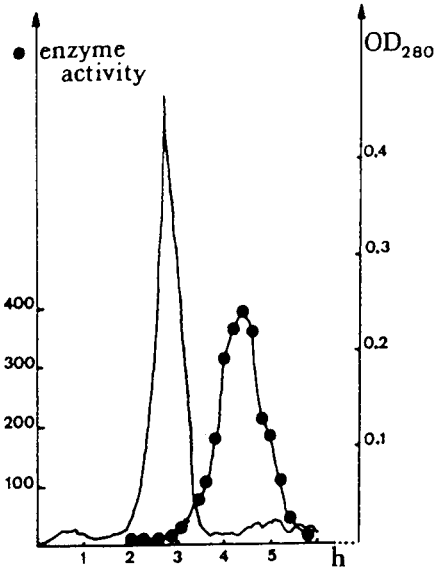

Fig. 3. Extraction of isomerase from a *Pseudomonas testosteroni* crude extract on Sepharose–PEG, with 12% (w/v) dextran T70 in the mobile phase. See ref. 20 for more detailed experimental conditions.

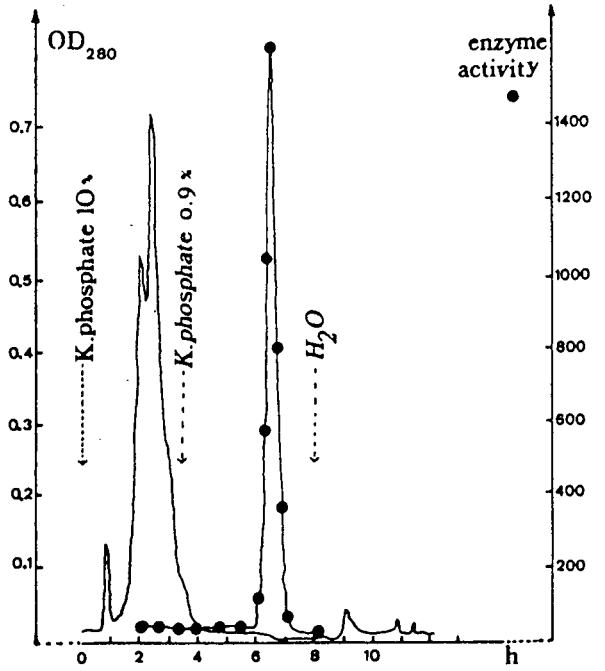

Fig. 4. Stepwise elution of the isomerase-containing sample with various potassium phosphate concentrations on Sepharose–PEG stationary phase. See ref. 20 for more detailed experimental conditions.

(potassium phosphate *ca.* 10%), whereas this enzyme was only retarded in the previous experiment with dextran. Stepwise elution with a decreased potassium phosphate concentration (*ca.* 1%) resulted in the recovery of isomerase in good yield (*ca.* 60%) and the removal of most of contaminants (*ca.* 7 μg compared with *ca.* 5 mg in the injected sample) (Fig. 4).

Similar purification results were obtained for an esterase from *Bacillus pumilus* (86% yield, 140-fold purification) on a Sepharose–Pluronic stationary phase [22].

Further, more sophisticated fractionations were attempted on Sepharose–PEG and Sepharose–Pluronic with three different enzymes [isomerase, 3α-hydroxysteroid dehydrogenase (α-HSD) and 3β,17β-hydroxysteroid dehydrogenase (β-HSD)] contained in the same *Pseudomonas testosteroni* crude extract. According to the hydrophobicity scale proposed by Bigelow [36], the purification of these three enzymes represents a real challenge [37].

Their chromatographic behaviours were predicted using "partition between aqueous two-phase systems" experiments [24]. These two-phase systems were prepared by mixing potassium phosphate (final concentration 10, 15 or 20%, w/w) with PEG and Pluronic mixtures of various compositions. The resulting systems are thus composed of a phosphate-rich bottom phase and a polyether-rich top phase, of increasing hydrophobicity with its Pluronic content. The partition coefficient of any considered enzyme therefore gives a direct estimation of its ability to establish preferential interactions with the polyethers. Consequently, when chromatography is carried out using Sepharose–PEG or Sepharose–Pluronic stationary phases and a potassium phosphate mobile phase, high partition coefficients ($K > 1$) should correspond to retention or retardation. Conversely, biomolecules with low partition coefficients ($K < 1$) favour the phosphate-rich bottom phase and should be eluted with no retardation.

The main information obtained from batch partition analysis was as follows: (1) $K_{\text{isomerase}} > K_{\beta\text{-HSD}} \gg K_{\alpha\text{-HSD}}$ in all experiments; (2) the possibility of shifting the partition coefficient of α-HSD above 1 by increasing the phosphate concentration or (and) the hydrophobic character (*i.e.*, the Pluronic content) of the top phase; and (3) enhanced ΔK ($K_{\text{isomerase}} - K_{\beta\text{-HSD}}$) as the hydrophobic character of the polyether-rich top phase is increased. This perfectly paralleled the chromatographic experiments, *i.e.*, (1) elution in the order α-HSD, β-HSD, then isomerase; (2) retention or not of α-HSD, according to the ionic strength in the mobile phase and the nature of the stationary phase (PEG or Pluronic); and (3) better separation of β-HSD from isomerase on Sepharose–Pluronic than on Sepharose–PEG.

This preliminary information allowed us to develop a strategy for optimum chromatographic resolution (Fig. 5). Good enzymatic activity recovery (α-HSD, 60%; β-HSD, 40%; isomerase, 65%) together with almost quantitative removal of contaminants in each fraction could thus be obtained (residual contaminants expressed as a percentage of total protein in the starting crude extract: α-HSD, 1.5%; β-HSD, 2%; isomerase, not detectable).

5. FUTURE TRENDS

As mild HIC has already proved to be very efficient for sophisticated fractionation problems with complex mixtures, our future concern in this field ought

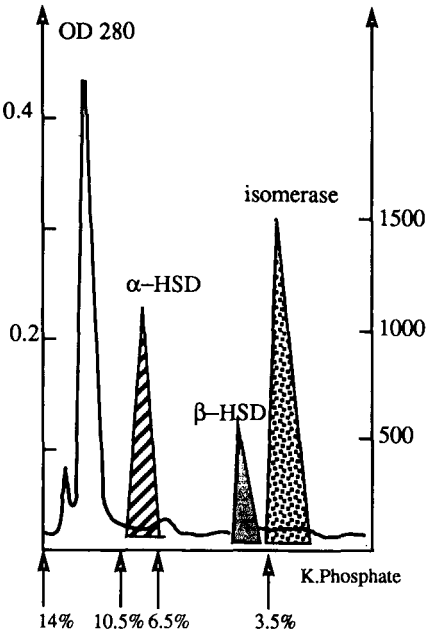

Fig. 5. Stepwise elution of the *Pseudomonas testosteroni* crude extract on Sepharose–Pluronic with various potassium phosphate concentrations. See ref. 24 for more detailed experimental conditions.

to turn to physico-chemical characterizations, rather than to additional biological studies. However, other polyethers such as PPGs or PTMGs have been immobilized on Sepharose and the resulting stationary phases should be tested, in order to obtain a complete study through the whole polyether family.

Further, the determination of immobilized polymers remains an important question, as the ligand concentration on the gel plays a prominent role in the interaction process. The solutions already exist but, in our opinion, should be more thoroughly investigated.

Ultimately, it would be of interest to quantify the hydrophobic character of the stationary phases. If the hydrophobicity of the polyethers is an important parameter, the interaction of the solute with the stationary phase is probably a global process, in which not only the nature of the immobilized polyether, but also the support itself and the amount of hydrophobic ligands, also play a role.

Surface tension is one of the most indicative measure of this hydrophobic character. Whereas the measurement of surface tension of liquids in straightforward, that of solid surface and especially of beads is far more complicated. However, certain methods already exist, such as contact angle measurements [38], reverse GC [39] and the sedimentation volume technique [40,41], and we are currently working on their application to the problems posed by our stationary phases.

This determination of the surface tension of the stationary phase (γ_{sv}) could be the first step in characterizing, in terms of thermodynamics, a three-component (sorbent–mobile phase–protein) system. In fact, the adsorption of a protein on

a sorbent being comparable to an adhesion process, the free energy of association may be given by the expression [42]

$$\Delta F_{smp} = \gamma_{sp} - \gamma_{sm} - \gamma_{mp}$$

where γ is the interfacial tension and the subscripts s, m and p represent sorbent, mobile phase and protein, respectively. All these interfacial tensions may be calculated through an equation of state [43] from the measurable individual surface tensions of the stationary phase (γ_{sv}), the protein (γ_{pv}) and the mobile phase (γ_{mv}). This makes possible explicit thermodynamic predictions of the relative extent of adhesion of the considered biomolecule (p) to a given sorbent (s), under various mobile phase (m) conditions.

In addition, as the measurement of chromatographic parameters such as retention volumes and capacity factors also leads to the determination of the association constant or the free energy of association [19,44], a second approach is therefore available for characterizing the three-component system in terms of thermodynamics.

REFERENCES

1 Z. Er-el, Y. Zaidenzaig and S. Shaltiel, *Biochem. Biophys. Res. Commun.*, 49 (1972) 383.
2 S. Hjertén, *Adv. Chromatogr.*, 19 (1981) 111.
3 B. H. J. Hofstee, *Pure Appl. Chem.*, 51 (1979) 1537.
4 J. Porath, L. Sundberg, N. Fornstedt and P. Ohlsson, *Nature (London)*, 245 (1973) 465.
5 G. Halperin, M. Breitenbach, M. Tauber-Finkelstein and S. Shaltiel, *J. Chromatogr.*, 215 (1981) 211.
6 R. J. Yon, *Int. J. Biochem.*, 9 (1978) 373.
7 W. Melander and Cs. Horváth, *Arch. Biochem. Biophys.*, 183 (1977) 200.
8 T. Laas, *J. Chromatogr.*, 111 (1975) 373.
9 P. A. Albertsson, *Partition of Cell Particles and Macromolecules*, Almqvist & Wiksell, Stockholm, and Wiley-Interscience, New York, 2nd ed., 1971.
10 T. G. I. Ling, H. Nilsson and B. Mattiasson, *Carbohydr. Res.*, 11 (1989) 43.
11 A. Foucault and K. Nakanishi, *J. Liq. Chromatogr.*, 11 (1988) 2455.
12 C. J. O. R. Morris, *Protides Biol. Fluids*, 10 (1963) 325.
13 H. S. Anker, *Biochim. Biophys. Acta*, 229 (1971) 290.
14 S. H. Chang, K. M. Gooding and F. E. Regnier, *J. Chromatogr.*, 120 (1976) 321.
15 T. G. I. Ling and B. Mattiasson, *J. Chromatogr.*, 254 (1983) 83.
16 N. T. Miller and B. L. Karger, *J. Chromatogr.*, 326 (1985) 45.
17 J. P. Chang, Z. El Rassi and Cs. Horváth, *J. Chromatogr.*, 319 (1985) 396.
18 Y. Shibusawa, U. Matsumoto and M. Takatori, *J. Chromatogr.*, 398 (1987) 153.
19 T. Suzuki, N. Muroi and T. Tomono, *J. Biomater. Sci. Polym. Ed.*, 1 (1989) 3.
20 R. Mathis, P. Hubert and E. Dellacherie, *J. Chromatogr.*, 319 (1985) 43.
21 R. Mathis, P. Hubert and E. Dellacherie, *J. Chromatogr.*, 347 (1985) 291.
22 R. Mathis, A. Mourey and P. Hubert, *Appl. Environ. Microbiol.*, 54 (1988) 1307.
23 R. Mathis, P. Hubert and E. Dellacherie, *J. Chromatogr.*, 474 (1989) 396.
24 R. Mathis, P. Hubert and E. Dellacherie, *J. Chromatogr.*, 538 (1991) 456.
25 G. Körösi and E. Kovats, *J. Chem. Eng. Data*, 26 (1981) 323.
26 N. Jarvis, R. B. Fox and W. A. Zesnian, in *Contact Angle, Wettability and Adhesion (Advances in Chemistry Series)*, American Chemical Society, Washington, DC, 1979, p. 323.
27 B. Yu. Zalavsky, A. V. Baevskii, S. V. Rogozhin, A. V. Gedrovich, A. V. Shishkov, A. A. Gasanov and A. A. Masimov, *J. Chromatogr.*, 285 (1984) 63.
28 S. N. Omenyi, A. W. Neumann and C. J. van Oss, *J. Appl. Phys.*, 52 (1981) 789.
29 A. F. Buckmann, M. Morr and G. Johansson, *Makromol. Chem.*, 182 (1981) 1379.
30 S. Arnott, A. Fulmer, W. E. Scott, I. C. M. Dea, R. Moorhouse and D. A. Rees, *J. Mol. Biol.*, 90 (1974) 269.

31 C. Rochas and M. Lahaye, *Carbohydr. Polym.*, 10 (1989) 289.
32 R. de Vos and E. J. Goethals, *Polym. Bull.*, 15 (1986) 547.
33 J. D. Andrade, in J. D. Andrade (Editor), *Surface and Interfacial Aspects of Biomedical Polymers (Surface Chemistry and Physics*, Vol. 1), Plenum Press, New York, 1985, p. 61.
34 I. Drevin and B. L. Johansson, *J. Chromatogr.*, 295 (1984) 210.
35 P. Hubert, E. Dellacherie, J. Neel and E. E. Baulieu, *FEBS Lett.*, 65 (1976) 169.
36 C. C. Bigelow, *J. Theor. Biol.*, 16 (1967) 187.
37 J. Boyer, D. N. Baron and P. Talalay, *Biochemistry*, 4 (1965) 1825.
38 A. W. Neumann, R. J. Good, C. J. Hope and M. Sejpal, *J. Colloid Interface Sci.*, 49 (1974) 291.
39 E. Papirer, H. Balard, Y. Rahmani, A. P. Legrand, L. Facchini and H. Hommel, *Chromatographia*, 23 (1987) 639.
40 D. R. Absolom and R. A. Barford, *Anal. Chem.*, 60 (1988) 210.
41 E. I. Vargha-Butler, T. K. Zubovitz, H. A. Hamza and A. W. Neumann, *J. Dispersion Sci. Technol.*, 6 (1985) 357.
42 J. Visser, *Adv. Colloid Interfacial Sci.*, 15 (1981) 157.
43 C. A. Ward and A. W. Neumann, *J. Colloid Interface Sci.*, 49 (1974) 286.
44 Cs. Horváth, W. Melander and I. Molnar, *Anal. Chem.*, 49 (1977) 142.

Journal of Chromatography, 539 (1991) 307–314
Elsevier Science Publishers B.V., Amsterdam

CHROM. 22 874

Comparative affinity chromatographic studies using novel grafted polyamide and poly(vinyl alcohol) media

D. MÜLLER-SCHULTE*
Institut für Organische Chemie der RWTH Aachen, Prof-Pirlet-Strasse 1, W-5100 Aachen (Germany)
and
S. MANJINI and M. A. VIJAYALAKSHMI
Université de Technologie de Compiègne, Departement Genie Biologique, B.P. 649, 60206 Compiègne Cedex (France)

ABSTRACT

Radiation-grafted polyamide in microparticulate form was used for the affinity chromatographic separation of fibronectin, human immunoglobulin IgG1 and human serum albumin using gelatin, histidine and Cibacron Blue F3G-A as affinity ligands. The chromatographic properties, in particular the protein adsorption capacities of the grafted carriers, were tested in comparison with several commercial media (Sepharose, Spherosil, Eupergit, Fractogel, VA-Epoxy). As a result of grafting, long molecular spacers are introduced into the polymer carrier, leading to high ligand binding and protein loading capacities well above those achieved with commercial media. A novel support based on poly(vinyl alcohol) carrying a blood group-specific trisaccharide ligand for the removal of blood group antibodies from human serum is described. The poly(vinyl alcohol) carrier exhibits excellent antibody binding capacities when compared with supports carrying protein G and protein A ligands. New perspectives opened up by the new support with regard to *in vivo* haemoperfusion are discussed.

INTRODUCTION

A number of carrier media based on silica gels, polysaccharides or synthetic organic materials have been described for diverse chromatographic applications [1]. The increasing importance of separation technology in different areas has led to improved chromatographic media which are mainly used for the production of biologically active substances. Prominent examples include the purification of antibodies, blood components, growth factors, interferon, insulin and fibronectin. If one considers technical applications, affinity chromatography offers enormous advantages over other separation methods.

Depending on the degree of biorecognition of the ligand, the separation of biomolecules can be obtained in a single step, thereby simplifying the commonly used separation procedures which generally require several purification steps. Affinity chromatography can therefore offer a significant reduction in cost, time and technical effort.

Despite the enormous effort invested in the field of affinity chromatography,

0021-9673/91/$03.50

a few aspects still remain critical, including insufficient ligand binding capacity of the support, the cost, the physical and chemical stability and the lack of biospecificity of the affinity ligand [2]. Another essential point is the different coupling method, the drawbacks of which have been critically discussed [1].

We have demonstrated recently that radiation-grafted polyamide-6 in microparticulate form and newly developed poly(vinyl alcohol) carriers exhibit distinctly higher protein and ligand binding capacities than those achieved with well established commercial media [2,3].

In this work, the performances of grafted polyamide-6 (Biograft) and poly(vinyl alcohol) (PVA) gels as carriers were tested in comparison with several commercial media.

Gelatin, Cibacron Blue F3G-A and *l*-histidine were used as affinity ligands for the separation of human fibronectin (Fn), human serum albumin (HSA) and human immunoglobulin IgG1. Likewise, a trisaccharide hapten specific against blood group A antibodies was coupled to different supports, the aim being to assess the feasibility of these carriers for *in vivo* haemoperfusion.

EXPERIMENTAL

Materials

The materials were purchased from the following sources: Sepharose and Superose media, Pharmacia–LKB (Freiburg, Germany); Fractogel TSK HW-75F, Merck (Darmstadt, Germany); Eupergit C, Röhm Pharma (Darmstadt, Germany); VA-Epoxy and VA-Hydroxy, Riedel-de Haën (Selze, Germany); Synsorb A and blood group A trisaccharide, Chembiomed (Edmonton, Canada); Spherosil, Rhône Poulenc (Paris France); IgG1 protein solution from human placenta, Institut Merieux (Lyon, France); and PVA, Hoechst (Frankfurt/M, Germany). All other chemicals were supplied by Fluka (Freiburg, Germany) and Merck.

Preparation of grafted polyamide and poly(vinyl alcohol) carriers

The grafting of polyamide-6 and the synthesis of the PVA carriers were carried out according to previously described procedures [4,5]. For grafting, 2-hydroxyethyl methacrylate together with N-vinylpyrrolidone and acrylamide were used, resulting in a graft uptake of 74% (w/w). Activation was carried out with epichlorohydrin in 1 *M* sodium hydroxide solution [4].

PVA was synthesized as follows [5]: PVA was dissoved with heating in ethylene glycol to obtain a 5% solution. The hot solution was dispersed in vegatable oil with stirring at 400–1000 rpm. The suspension was cooled and the beads formed were separated from the oil by several extractions with acetone. The diameter of the beads depends on the stirring speed, and ranges from 50 to 500 μm. Cross-linking was performed using epichlorohydrin in 3 *M* sodium hydroxide solution. Epoxy-activation with epichlorohydrin was performed as for the grafted polyamide.

Preparation of affinity supports

Gelatin support. Ten millilitres of a 1% gelatin (porcine skin, Fluka) solution in 1 *M* potassium phosphate (pH 7.5) were added to 3 ml of epoxy-activated support (Biograft, Eupergit C or VA-Epoxy) and the mixture was left for 30 h at 30°C with

gentle stirring. The excess of protein was removed by washing with 0.5 *M* potassium phosphate. The remaining oxirane groups were blocked by incubation for 2 h with 1 *M* ethanolamine solution (pH 8.0). The support was stored in 0.05 *M* Tris–HCl buffer (pH 7.5) containing 0.02% sodium azide.

Fractogel TSK HW-75F was activated for coupling with gelatin using 2-fluoro-1-methylpyridinium toluenesulphonate according to the method described by Ngo [6].

Cibacron Blue support. Coupling of Cibacron Blue F3G-A to 3 ml of Biograft and PVA was effected in a solution containing 20% sodium chloride and 1 *M* sodium carbonate for 2 days at 40°C [7]. In order to ensure maximum binding, a high dye concentration (100 mg/ml resin) was used. Extensive washing with water and 4 *M* sodium chloride solution containing 40% (v/v) ethylene glycol followed until all unbound dye had been removed. Before use, the matrices were equilibrated in 0.01 *M* potassium phosphate (pH 7.5).

Histidine support. Histidine was covalently coupled to epoxy-activated Biograft as described elsewhere [8]. Two coupling agents were used, epichlorohydrin and 1,4-butanediol diglycidyl ether.

Blood group A immunoadsorbent. For the preparation of the immunoadsorbents, 0.5 ml of epoxy carrier (Biograft or Eupergit C) was incubated with 1 ml of borate buffer (pH 9.5) containing 0.5 mg of the blood group hapten. After reaction for 20 h at room temperature, the adsorbent was washed several times with 1 *M* sodium chloride solution. Fractogel TSK HW-75F was activated with 2-fluoro-1-methylpyridinium toluenesulphonate as described above.

The activation of PVA using 1,6-hexamethylene diisocyanate dissolved in dimethyl sulphoxide and the subsequent coupling of the blood group hapten were carried out as described previously [2]. After the reaction, the matrix was washed with water and dimethyl sulphoxide. Before use, all supports were equilibrated with physiological sodium chloride solution.

Determination of immobilized Cibacron Blue

The amount of Cibacron Blue F3G-A coupled to the support was determined spectrophotometrically by measuring the differences in absorbance at 610 nm between added and unbound dye [7].

Chromatographic procedures

Gelatin support. Gelatin affinity support (3 ml) was packed into a chromatographic column (5 × 0.9 cm I.D.). After equilibration with 50 ml of phosphate-buffered saline (pH 7.5) containing 0.01 *M* citric acid and 0.02% sodium azide (buffer A), 20 ml of freshly prepared pooled citric human plasma (obtained by centrifugation for 10 min at 3000 *g*) were loaded on the column at a flow-rate of 50 cm/h. After the major unretained peak had eluted and the absorbance monitored at 279 nm had reached zero, the Fn was eluted with 3 *M* urea in buffer A. The Fn content of the eluted fraction was determined by a standard turbidimetric immunoassay test [9]. Briefly, antiserum to human Fn is added to the plasma sample and the absorbance is measured with a Behring laser nephelometer. The Fn content is automatically evaluated from the corresponding protein concentration of a standard dilution [9].

Cibacron Blue support. Cibacron Blue F3G-A affinity resin (3 ml) was packed into the column described above and equilibrated in 0.05 *M* sodium phosphate buffer

(pH 7.0) at a flow-rate of 25 cm/h. A 10-ml volume of sample solution containing 30 mg of HSA was loaded on the column. Unadsorbed protein was washed off the column with 20 ml of buffer solution. The bound HSA was subsequently eluted with 10 ml of 4 *M* sodium chloride and the fractions were collected at a flow-rate of 25 cm/h. The protein content was determined spectrophotometrically at 280 nm.

Histidine support. A 20 × 1 cm I.D. column was packed with 1 ml of support. Adsorption and washing were performed in 0.025 *M* Tris–HCl buffer (pH 7.4). The same buffer containing 0.2 *M* sodium chloride was used for desorption. The experiments were conducted at 4°C, except for Spherosil columns, for which the optimum retention was obtained at room temperature. The concentration of the eluted IgGl was determined spectrophotometrically at 280 nm.

Blood group immunoadsorbent. Pooled human serum type O (1 ml) was added for 10 min at room temperature to a given amount of support (batch procedure; for details see Table IV). The content of antibody adsorbed was determined by the agglutination test as described previously [2].

RESULTS AND DISCUSSION

The performance of Biograft and PVA carriers was tested in comparison with seven different commercial supports: Sepharose, Superose, Fractogel, Eupergit C, VA-Epoxy, Synsorb A and Spherosil. As the commercial matrices chosen here are frequently used in practice, the results obtained should provide important data with regard to the performance of Biograft and PVA.

All supports were coupled under identical conditions, with the exception of gelatin Sepharose, protein A/protein G Sepharose and Synsorb A, which were used as supplied by the manufacturer.

As shown in Table I, the Fn adsorption capacity of gelatin Biograft is about 80% higher than that of Gelatin Sepharose. VA-Epoxy shows the best performance among the commercial media, which is in line with recent findings regarding the performance of this matrix in immunoaffinity chromatography [2]. Although the study of the different supports under identical test conditions is the main topic, it should be stressed that the performance of the separation can still be optimized by modifying certain test

TABLE I

ADSORPTION CAPACITY OF FIBRONECTIN ON DIFFERENT GELATIN AFFINITY RESINS

Human plasma (20 ml) was applied to 3 ml of adsorbent at a linear flow-rate of 50 cm/h at room temperature. The Fn concentration in the elution fraction was determined using an immunoturbidimetric standard test method [9]

Support	Approximate bead size (μm)	Capacity (mg Fn/ml gel)
Biograft	150	2.8
Gelatin Sepharose 4B	70	0.6
Fractogel TSK HW-75F	40	0.9
Eupergit C	150	1.4
VA-Epoxy	110	2.1

TABLE II

ADSORPTION CAPACITY OF HSA ON DIFFERENT CIBACRON BLUE F3G-A GELS

Flow-rate: 25 cm/h.

Support matrix	Approximate bead size (μm)	Ligand bound (mg/ml gel)	HSA adsorbed (mg/ml gel)
Biograft	150	0.5	0.59
PVA	80	1.4	0.81
Sepharose CL-6B	70	0.2	0.19
Fractogel TSK HW-75F	40	0.3	0.65
VA-Hydroxy	110	0.3	0.21

parameters, *e.g.*, amount of ligand bound, flow-rate, temperature and amount of protein loaded onto the column, as recently demonstrated by Regnault *et al.* [10] for the separation of Fn. This leaves room for further improvements when using grafted polyamide carriers.

HSA adsorption capacities on different Cibacron Blue resins are given in Table II. Biograft binds about three times as much HSA as VA-Hydroxy and Sepharose CL-6B. This correlates directly with the ligand uptake of these supports: 0.5 mg/ml (Biograft), 0.3 mg/ml (VA-Hydroxy) and 0.2 mg/ml Cibacron Blue (Sepharose) under the chosen test conditions. PVA shows the highest protein adsorption with 0.81 mg/ml, yet this amount is relatively low considering the large amount of the ligand bound (1.4 mg/ml). The performance of Fractogel TSK HW-75F is not in accordance with the other results of this test series, insofar as it adsorbs relatively large amounts of HSA (0.65 mg/ml), which is in contrast to its low Cibacron Blue uptake. An explanation of this could be the non-specific adsorptions due to the partly non-polar nature of the

TABLE III

COMPARISON OF IgG1 ADSORPTION CAPACITIES OF DIFFERENT HISTIDINE-COUPLED AFFINITY RESINS

For details see Experimental.

Support	Approximate bead size (μm)	Capacity (mg IgCl/ml gel)
Biograft	150	0.69
Sepharose 4B		
Without spacer[a]	70	0.05
With spacer[b]		0.23
Superose 12 with spacer[b]	30	0.29
Spherosil		
Without spacer[c]	80	0.15
With spacer[d]		0.28

[a] Activated with epichlorohydrin.

[b] Activated with 1,4-butanediol diglycidyl ether.

[c] Activated with γ-glycidyloxypropyltrimethoxysilane.

[d] Activated with γ-glycidyloxypropyltrimethoxysilane and subsequently reacted with aminocaproic acid; coupling of histidine was conducted using carbodiimide [8].

Fractogel structure. A reason for the relatively low protein adsorption achieved with PVA regarding the very high ligand binding density could be that a high ligand density, owing to steric effects, prevents an appropriate interaction of the non-polar moiety of the ligand with the non-polar region of HSA [11].

A comparison of the IgGl binding capacities on different histidine affinity supports is shown in Table III. Grafted polyamide adsorbs about three times more IgGl than Sepharose 4B, Superose 12 and Spherosil. The influence of a spacer molecule on the protein binding efficacy is demonstrated by comparing the results obtained with 1,4-butanediol diglycidyl ether, which functions as a spacer, and epichlorohydrin. The differences between these two coupling modes are obvious, especially with Sepharose 4B: 0.05 mg IgGl/ml bound without spacer and 0.23 mg IgGl/ml bound with spacer. In contrast, the grafted support does not require an additional spacer-like coupling agent, which would also contribute to the overall high costs of affinity media.

The above-described ligands have one common feature, namely that they are all pseudo-specific. However, as they are inexpensive and are readily available, they are frequently used in the laboratory. This applies especially to the use of some textile dyes such as Cibacron Blue, Remazol Yellow and Procion Red [12]. Although these ligands interact with a number of proteins [7], Cibacron Blue F3G-A has been applied successfully to the separation of HSA, enzymes, growth and coagulation factors and interferon [12]. HSA is technically produced by a chromatographic process using Cibacron Blue columns [13]. A comparison of the performances of different Cibacron Blue supports is hence of fundamental interest with regard to technical applications.

By adopting defined adsorption or desorption modes, a resolution and degree of purification comparable to those of immunoadsorption can be obtained with pseudo-specific ligands. This applies especially to histidine, which interacts through its carboxyl, amino and imidazole groups with several proteins at or around their isoelectric point and has shown particular efficacy in separating IgG subclasses [14]. This mode of chromatography also has some potential if one considers its technical application [15].

TABLE IV

REMOVAL OF BLOOD GROUP A ANTIBODIES FROM HUMAN SERUM

Pooled human serum type O (1 ml) was incubated for 10 min at room temperature (batch procedure). The antibody content was determined by agglutination test [3].

Support	Sample volume (ml)	Approximate bead size (μm)	Antibody bound (%)
PVA	1.0	500	>90
Biograft	0.5	150	>90
Eupergit C	0.5	150	>90
Fractogel TSK HW-75F	0.5	40	<30
Synsorb A	1.0	500	<50
Protein A Sepharose CL-4B[a]	0.3	70	<10
Protein G Sepharose 4[a]	0.3	70	<10

[a] Used as supplied by the manufacturer without blood group hapten.

The reason for the overall superior performance of the grafted supports in comparison with well established media lies in their special molecular structure. Grafting leads to long tentacle-like molecular chains which function automatically as spacer arms [4]. These grafted chains obviously possess a high accessibility for ligands and proteins, as shown in recent enzyme and antibody immobilization tests [3,16].

Affinity chromatography has also been successfully used in the medical field. In bone marrow transplantation, ABO incompatibilities can be circumvened by anti-A and anti-B antibody removal from blood and serum. For this purpose, a novel PVA carrier was developed to which a specific blood group oligosaccharide was attached

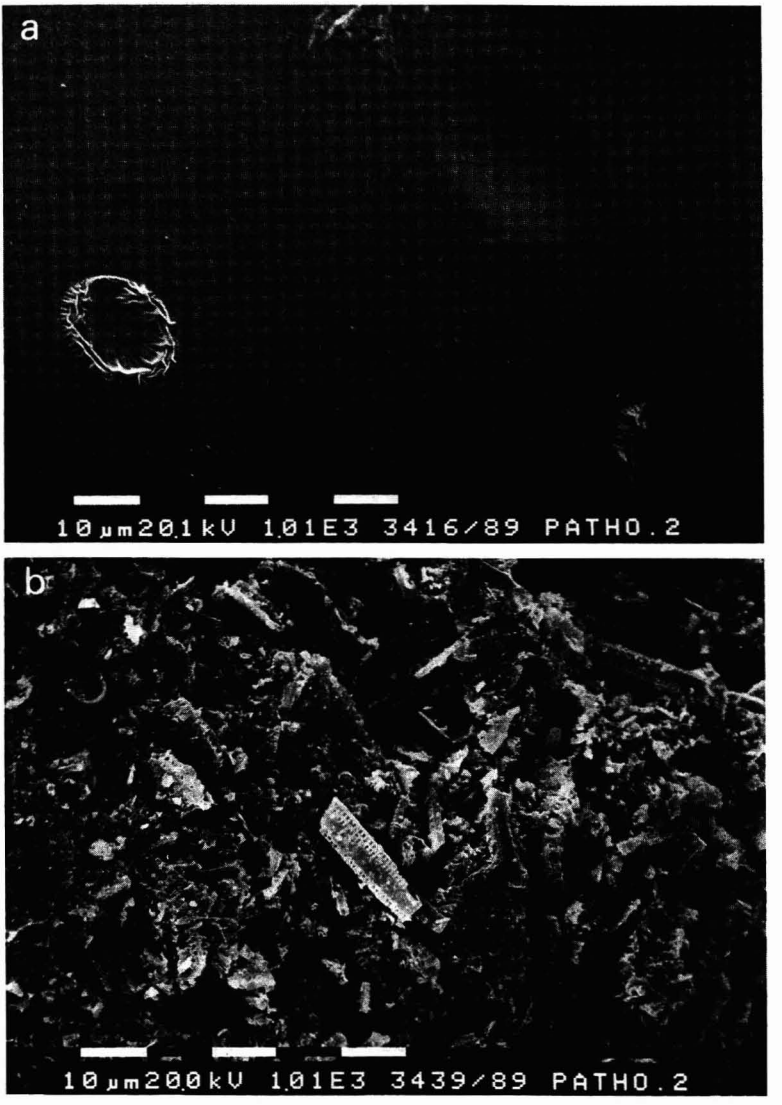

Fig. 1. Scanning electron micrographs of (a) PVA and (b) Synsorb A immunosorbent carriers, showing the smoothness of the surface morphology of PVA beads in comparison with Synsorb.

[2,17]. A comparative study of the blood group antibody adsorption capacities on different immunosorbents is shown in Table IV.

PVA, Biograft and Eupergit C bind over 90% of the antibody, whereas Fractogel and Protein A and Protein G Sepharose adsorb relatively low protein contents (<30% and <10%, respectively). The PVA protein binding ability is outstanding if one considers the large bead size of this gel (*ca.* 500 μm). This underlines both the efficacy of the isocyanate coupling technique and the suitability of PVA as an affinity support. Further, it becomes obvious that the blood group trisaccharide ligand exhibits distinctly better specificity and hence binding properties than protein A and protein G, ligands frequently used for IgG separations [18].

Although Biograft and Eupergit C also show good protein adsorptions, these carriers are only suitable for *in vitro* usage owing to their small bead sizes. Synsorb A, a commercial immunosorbent based on silica gel [19], also has a bead size of *ca.* 500 μm and shows reasonable adsorption properties. However, this support might not be useful for *in vivo* application as it consists of very small single building blocks (Fig. 1) which produce a rough surface morphology. The surface morphology, however, is vital for biocompatibility as it directly influences the mode of blood flow. Rough surfaces can cause micro turbulences and thus promote thrombus formation [20]. Another detrimental reaction is the activation of the complement system [21]. Hence PVA remains the only choice for practical haemoperfusion because of its excellent adsorption capacity, smooth surface morphology (Fig. 1) and good blood compatibility, which is superior to that of common carrier types [21].

Apart from the biochemical performance, the newly developed media possess excellent chemical stability. Treatments in 1–6 *M* sodium hydroxide are possible without detectable destruction [5]. This is a unique feature among all common chromatographic supports and it seems that these media are useful alternatives to currently used supports.

REFERENCES

1 J-X. Huang and G. Guiochon, *J. Chromatogr.*, 492 (1989) 431.
2 D. Müller-Schulte, *J. Chromatogr.*, 510 (1990) 115.
3 D. Müller-Schulte and H. G. Thomas, *Radiat. Phys. Chem.*, 35 (1990) 93.
4 D. Müller-Schulte, Continuation in part USA, Patent, Serial Number 07150, 417 (1988).
5 D. Müller-Schulte, *Ger. Pat. Appl.*, P3900945.9-43 (1989).
6 T. T. Ngo, *Makromol. Chem. Macromol. Symp.*, 17 (1988) 229.
7 P. D. G. Dean and D. H. Watson, *J. Chromatogr.*, 165 (1979) 301.
8 M. A. Vijayalakshmi, *These*, Docteur ès Science, Université Technologie de Compiègne, 1980, p. 95.
9 *Immunoturbidimetric Assay*, Behring Werke, Marburg, 1988.
10 V. Regnault, C. Rivat and J. F. Stoltz, *J. Chromatogr.*, 432 (1988) 93.
11 G. Kopperschläger, H. J. Böhme and E. Hofmann, *Adv. Biochem. Eng.*, 10 (1982) 101.
12 Y. D. Clonis, *Bio/Technology*, 5 (1987) 1290.
13 *Products for Biotechnology*, Institut Biologique Français (IBF), La Garenne, 1987.
14 S. Kanoun, L. Amourache, S. Krishnan and M. A. Vijayalakshmi, *J. Chromatogr.*, 376 (1986) 259.
15 M. A. Vijayalakshmi, *Trends Biotechnol.*, 7 (1989) 71.
16 D. Müller-Schulte and F. A. Horster, *Polym. Bull.*, 7 (1982) 395.
17 R. U. Lemieux, *Chem. Soc. Rev.*, 7 (1978) 423.
18 S. Ohlson, R. Nilsson, U. Niss, B. M. Kjellberg and C. Freiburghaus, *J. Immunol. Methods*, 114 (1988) 175.
19 *Product Brochure*, Chembiomed, Edmonton, Canada, 1989.
20 B. D. Ratner, A. B. Johnston and T. J. Lenk, *J. Biomed. Mater. Res.*, 21 (1987) 59.
21 H. Meltzer, Technical University Aachen, unpublished results.

Journal of Chromatography, 539 (1991) 315–325
Elsevier Science Publishers B.V., Amsterdam

CHROM. 22 875

Microfiltration membranes as pseudo-affinity adsorbents: modification and comparison with gel beads

B. CHAMPLUVIER and M.-R. KULA*
Institut für Enzymtechnologie, Heinrich-Heine Universität Düsseldorf, P.O. Box 2050, W-5170 Jülich (Germany)

ABSTRACT

Microfiltration membranes were studied as alternative adsorbents to the usual spherical hydrogels beads for the purification of proteins. Assumption of monolayer adsorption onto the internal area allowed the capacity measured by adsorption of model proteins to be predicted. The membrane could be modified with triazine dyes to yield an affinity-like support. The capacity of the dyed membrane was similar to the capacity of dyed Sepharose and the membrane could be used repeatedly. Enzymes from a crude extract of baker's yeast were selectively adsorbed in both batch and continuous experiments, allowing purification factors of at least ten.

INTRODUCTION

Dye ligand chromatography has long been known as a versatile and robust tool for purifying proteins from the analytical to the preparative scale [1]. In order to shorten the process time, more efficient adsorbents have been sought. The application of beads with small diameters allows the restrictions set by diffusive transport of the proteins to the ligand to be reduced considerably [2]. However, high operating pressures are required. Alternatively, porous polymer matrices modified as ion exchangers (Memsep, Millipore; Zetaprep, Cuno) have been introduced recently because of their high surface area, convective solute transport and low pressure drops [3].

Microfiltration membranes are potentially attractive adsorbents because they offer the same advantages as the matrices mentioned above together with mechanical strength, a highly porous structure and a large range of configurations for operation. Moreover, membranes are capable of handling unclarified solutions. Capillary membrane modules modified to yield affinity supports allowed, for instance, antibodies to be isolated from a cell culture medium [4].

In this work, microfiltration membranes made of nylon were tested as affinity-like adsorbents. The available capacity of the basic material was evaluated in two ways: from measurements of the inner surface area available in principle for adsorption and from experiments involving adsorption of model proteins. Modification of a nylon membrane with various pseudo-affinity ligands (triazine dyes) was

0021-9673/91/$03.50

performed and the modified membranes were tested as adsorbents. A proprietary dye ligand membrane was used for enrichment of enzymes from a crude yeast extract. Batch and filtration mode experiments were compared with the different membranes and their reusability was assessed. The results were compared with those obtained with pseudo-affinity agarose gels.

EXPERIMENTAL

Materials

Microfiltration membranes (Ultipor) were obtained from Pall (Dreieich, Germany). According to technical information from the manufacturer, Ultipor are isotropic membranes made of nylon 66 with a high surface concentration of amine and carboxylate groups in a 1:1 ratio. Modified nylon membranes with a positively charged surface, Zetapor (0.2 μm) and Zetabind (0.45 μm), were acquired from Cuno Europe (Cergy-Pontoise, France). Zetabind is intended for DNA and protein blotting. Samples from a proprietary nylon-based membrane modified with triazine dyes were a gift from Sartorius (Göttingen, Germany).

Cibacron Blue F3G-A was purchased from Ciba Geigy (Basle, Switzerland), Procion dyes from ICI (Frankfurt, Germany), polyethylenimine (PEI) from Sigma Chemie (Deisenhofen, Germany) and glutaraldehyde from Fluka (Neu-Ulm, Germany). All other reagents were of analytical-reagent grade.

Bovine serum albumin (BSA), fraction V (Boehringer Mannheim, Tutzing, Germany) was dissolved in water and hen egg lysozyme (Fluka) in 1 m*M* potassium phosphate buffer (pH 7.0).

A crude enzyme extract was prepared from commercial baker's yeast (*Saccharomyces cerevisiae*). A 40% (w/v) suspension in 100 m*M* potassium phosphate buffer (pH 6.0)–1 m*M* EDTA–5 m*M* mercaptoethanol was disintegrated in a high-pressure homogenizer, centrifuged and filtered through a 0.2-μm filter. The extract was stored at −20°C. Before use, samples were again clarified by centrifugation and diluted 4-fold with a 1 m*M* EDTA solution.

Dye ligand immobilization

The dye ligands were coupled to Ultipor membranes (0.1-μm nominal pore size) either directly or using PEI as spacer. The latter was first bound to membranes previously activated by glutaraldehyde at pH 8.0 [5]. The dyeing was carried out in two steps: a 1-h dye adsorption at room temperature from 6% NaCl solution, followed by reaction for 1 h at 50°C after raising the pH to 10.8 with carbonate buffer. A large excess of reagents were used and the membranes were rinsed repeatedly after every reaction step. After a final rinse with water and methanol, the membranes were stored dry at room temperature. The amount of dye coupled to the membrane was determined spectrophotometrically after dissolution of samples in phenol–methanol. Dyeing of Sepharose CL-4B was performed as described for the membranes.

Batch adsorption experiments

Samples of membrane were contacted with the solution of proteins in a shaken vessel for about 3 h. No significant change in protein concentration in the liquid occurred typically after 90 min up to 24 h. The amount adsorbed was calculated from

the mass balance. The experiments were performed in flasks for BSA and lysozyme and in micro test-tubes (Eppendorf) for yeast extract. The support volume was about 2% of the solution volume. Blanks without membranes were incubated in parallel to check that no deactivation or unexpected losses occurred. Before the adsorption experiments, the membranes were equilibrated with the corresponding solution without protein.

Adsorption and desorption in filtration mode

Membranes discs of 25 mm diameter were used; the effective filtration area was 3.3 cm^2.

To perform the adsorption experiments with lysozyme, filter holders (Sartorius, SM16517E) connected to a syringe were used. The following solutions (5 ml) were successively passed through the filter: buffer, 0.1 g/l lysozyme, 1 *M* sodium chloride and then 10 ml buffer. Residual liquids were flushed out of the holder with air. Lysozyme adsorption was measured by the decrease in concentration on filtration. The above cycle was performed three times.

For the experiments with the yeast extract, a filter holder with a minimum dead volume was constructed and inserted into an a fast protein liquid chromatography (FPLC) system (Pharmacia, Uppsala, Sweden). One to ten membranes could be fitted in the holder. Samples of 500 μl were injected. The membrane was washed with 10 ml of buffer. Unless stated otherwise, elution was carried out with a 10-ml linear gradient from 0 to 0.25 *M* KCl, a 5-ml step with 2 *M* KCl in buffer and a 5-ml step with starting buffer. Fractions of 5 ml were collected. Before the next run, a few milliliters of starting buffer were passed through the module without collecting the fractions.

Assays

Lysozyme concentrations were measured at 280 nm. BSA and yeast proteins were assayed with the Coomassie or with the micro-BCA test using kits purchased from Pierce (Oud Beijerland, The Netherlands). Malate dehydrogenase (MDH) and glucose-6-phosphate dehydrogenase (G6PDH) activities were measured according to Bergmeyer [6] and adenylate kinase according to Ito *et al.* [7].

RESULTS

Preliminary evaluation of membrane capacity for model proteins

The capacity of the membranes considered as adsorbents for proteins was evaluated in two ways: first by calculating the amount that could be adsorbed in a close-packed monolayer using literature data for the physical dimensions of model proteins and measuring the surface area available within the matrix; and second by measuring the adsorption of BSA under conditions favourable to adsorption.

The internal surface areas of the membranes were measured by nitrogen adsorption [8] using a Sorptomatic apparatus (Carlo Erba, Milan, Italy). The results for Ultipor membranes of various nominal pore sizes are shown in Fig. 1. Together with monolayer adsorption values calculated from the BSA and lysozyme dimensions (3.8 nm diameter × 15.0 nm length and 4.5 × 4.4 × 3.0 nm, respectively [9,10]), the overall surface would allow *ca.* 150 μg of lysozyme and 150–600 μg of BSA to bind to a 1-cm^2 piece of membrane with 0.1-μm nominal pore size. The two values for BSA

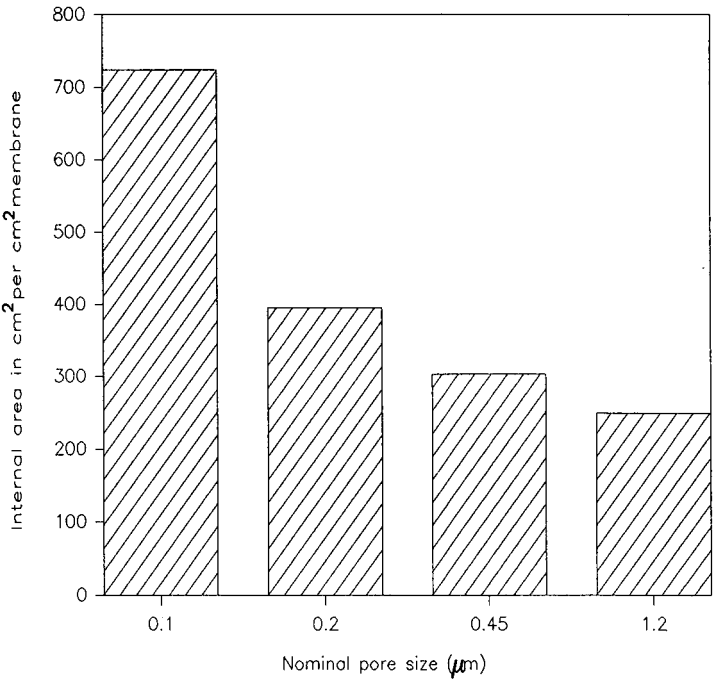

Fig. 1. Inner surface area of microfiltration membranes (Ultipor, Pall) with differents pore sizes, determined by nitrogen adsorption.

refer to adsorption of the protein molecule with its main axis parallel or perpendicular to the support surface.

The adsorption measured with BSA in aqueous solution at concentrations of 0.25 and 0.5 g/l on two positively charged membranes (Zetapor, Zetabind) and an amphoteric membrane (Ultipor) are shown in Table I. At the end of the experiment, an excess of BSA remained in solution. On doubling the initial concentration, the increase in the amount adsorbed was small relative to the concentration left in solution for Ultipor and Zetapor, therefore indicating saturation.

Immobilization of dye ligands to Ultipor membrane

The amounts of crude dye immobilized on the Ultipor membrane in two batches were in good agreement (Table II). A five to ten times higher dye concentration was bound when PEI was used as spacer. Dye concentrations in the same range were obtained with mono- (Cibacron, Procion H) and dichlorotriazinyl (Procion MX) dyes.

Adsorption of lysozyme to dyed Ultipor membrane

Batch adsorption was performed in duplicate. Adsorption in the filtration mode was repeated three times with every membrane specimen, the membrane being washed with sodium chloride solution and buffer between runs. As the amounts adsorbed did not show any trend, the averages from three data are reported. The amounts of

TABLE I

AMOUNTS OF BSA ADSORBED IN BATCH FROM 0.25 AND 0.5 g/l SOLUTIONS IN WATER ON CATIONIC (ZETAPOR, 0.2 μm; ZETABIND, 0.45 μm) AND AMPHOTERIC (ULTIPOR, 0.1 μm) NYLON MEMBRANES

Membrane	Introduced ($\mu g/cm^2$)	Adsorbed ($\mu g/cm^2$)	Remaining in solution ($\mu g/ml$)
Ultipor	159	80	126
	320	108	337
Zetapor	158	144	22
	320	176	264
Zetabind	132	47	161
	264	106	307

lysozyme introduced in the experiment were similar in the batch and filtration modes, namely 126 and 152 μg per square centimetre of filter, although the initial concentration was 2.5 times higher in the batch experiment. Table III shows that the amounts of lysozyme adsorbed per square centimetre of filter were very similar in the batch and filtration modes. Adsorption was systematically higher on the dyed membrane. The highest adsorption was observed with the blue membrane modified first with PEI.

Adsorption of yeast proteins to dyed membranes or Sepharose CL-4B

The proprietary membrane from Sartorius and Sepharose CL4-B carrying the blue (Cibacron F3G-A) or the yellow ligand (Procion Yellow HE3-G) were compared in batch experiments. A large excess of bulk protein was incubated in contact with the support in order to test the selectivity of the binding for the target enzymes. About 1000 times more protein than the expected capacity was used. As a consequence, the concentration change in solution was negligible and a mass balance would not allow the amount of proteins adsorbed to be measured. Also, an overestimation of protein

TABLE II

AMOUNTS OF DYE LIGANDS COUPLED TO ULTIPOR MEMBRANES (0.1 μm) IN μg OF CRUDE DYE PER mg OF DRY MEMBRANE

Ligands were coupled directly or using polyethylenimine as a spacer (denoted PEI-).

Dye	Dye coupled (μg/mg membrane)	
	Batch 1	Batch 2
PEI-Cibacron Blue F3G-A	21.4	15.5
Cibacron Blue F3G-A	2.71	2.57
Procion Blue MX-R	6.65	6.6
Procion Red MX-5B	4.04	3.38
Procion Red HE3-B	4.14	5.4
Procion Yellow HE3-G	0.56	1.1

TABLE III

AMOUNTS OF LYSOZYME ADSORBED ON DYED MEMBRANES FROM A BUFFER SOLUTION (POTASSIUM PHOSPHATE, pH 7.0, 1 m*M*) IN BATCH AND FLOW-THROUGH MODES

The amounts introduced were 126 and 152 $\mu g/cm^2$ membrane, respectively. Membrane sample: Ultipor (0.1 μm). Average and standard deviation are from duplicate and triplicate experiments, respectively.

Dye	Amount of lysozyme adsorbed ($\mu g/cm^2$ membrane)	
	Batch	Flow-through
PEI-Cibacron Blue F3G-A	122 ± 4	110 ± 18
Cibacron Blue F3G-A	78 ± 2	83 ± 4
Procion Blue MX-R	90 ± 22	92 ± 11
Procion Red MX-5B	85 ± 15	81 ± 38
Procion Red HE3-B	94 ± 21	102 ± 2
Procion Yellow HE3-G	87 ± 4	87 ± 8
Not dyed	40 ± 13	62 ± 6

desorption values (about 50%) was caused by the transfer of a significant amount of bulk proteins with interstitial liquids in the supports. Desorption was attempted by resuspending the drained support in buffer containing 0.5 *M* KCl. The amount of proteins and enzyme activity adsorbed or desorbed were related to the unit volume of support derived from the membrane dimensions or from weighing the drained gel and assuming a density of unity, respectively.

TABLE IV

COMPARISON OF PROPRIETARY DYE LIGAND MEMBRANES WITH SEPHAROSE CL-4B AS CARRIERS WITH BLUE OR YELLOW LIGANDS, FOR THE ADSORPTION OF ENZYMES FROM A CLARIFIED YEAST HOMOGENATE

Amounts of MDH, adenylate kinase, G6PDH activities and protein adsorbed and desorbed per millilitre of support. Variations are standard deviations.

Support	MDH (U/ml)	Adenylate kinase (U/ml)	G6PDH (U/ml)	Proteins (mg/ml)
Adsorption				
Sartorius blue	800 ± 100	350 ± 60	120 ± 10	nd[a]
Sartorius yellow	990 ± 120	260 ± 70	70 ± 10	nd
Sepharose blue	250 ± 50	430 ± 30	20 ± 10	nd
Sepharose yellow	780 ± 140	100 ± 70	20 ± 10	nd
Desorption				
Sartorius blue	200 ± 30	50 ± 1	5 ± 0.5	10.7 ± 0.5
Sartorius yellow	610 ± 30	50 ± 10	10 ± 1	12.0 ± 0.9
Sepharose blue	240 ± 10	210 ± 10	2 ± 0.4	13.4 ± 1.3
Sepharose yellow	620 ± 10	140 ± 10	4 ± 0.3	14.1 ± 1.0

[a] nd = Not determined.

The results in Table IV show that the amounts of proteins or individual enzymes involved in adsorption or desorption were of the same order regardless of the support material. The ligand had no general effect on the binding. However, more MDH was bound to the yellow ligand on both supports and more adenylate kinase to the blue gel.

On desorption, a low recovery (below 20%) was found for G6PDH on all the supports and for adenylate kinase on the membranes. The MDH recovery was higher than that of the other enzymes, and better with the gel supports.

The comparison of the specific activities in the original extract and the corresponding values in the desorption solutions (data not shown) revealed that significant enrichments occurred for MDH irrespective of the support, with a factor of 5 on the blue ligand and 12–14 on the yellow ligand. Enrichment factors for adenylate kinase were about 3 with membranes and 6–9 with gels, as a result of the better recovery on the latter. No significant enrichment of G6PDH could be measured.

Binding of yeast proteins to dyed membranes in filtration mode

The reusability of the dyed membrane was tested by repeated loading and elution (0 to 0.25 *M* KCl gradient and then a step with 2 *M* KCl) of proteins from the yeast

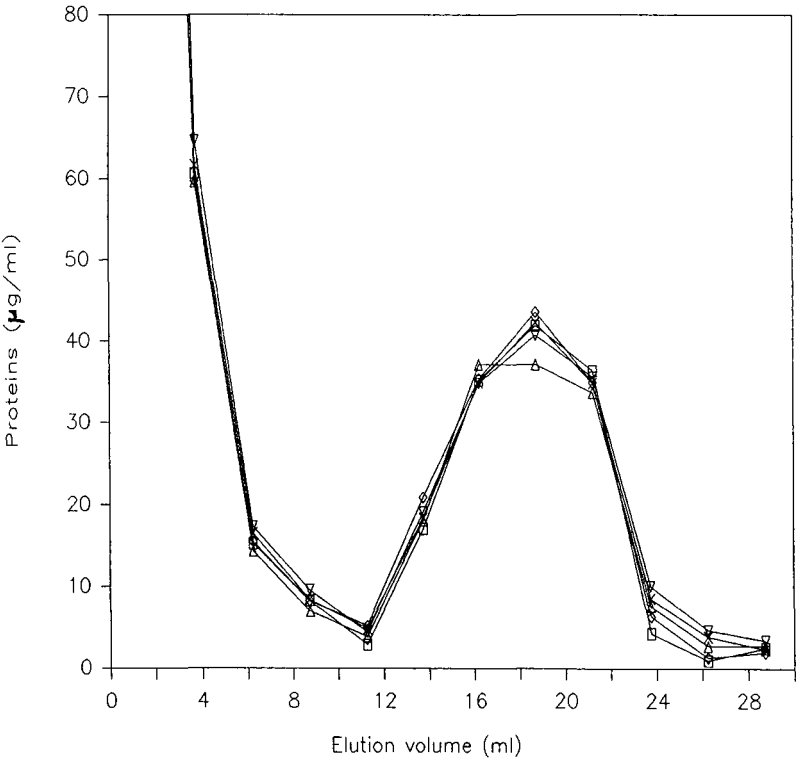

Fig. 2. Repeated use of a stack of ten membranes as stationary phase for binding proteins from the yeast extract. A 500-µl aliquot of the extract was loaded on the membrane, previously equilibrated with starting buffer; the membrane was washed with 10 ml of starting buffer followed by a 10-ml KCl gradient up to 0.25 *M*, a 5-ml step with 2 *M* KCl and a 5-ml step with starting buffer. Linear velocity, 0.3 cm/min. Succession of runs: □, ◇, △, ×, ▽.

TABLE V

REUSABILITY OF A MEMBRANE SPECIMEN (3.3 cm^2) FOR BINDING ENZYMES FROM THE YEAST EXTRACT

A 500-μl aliquot of the extract was loaded on the membrane previously equilibrated with starting buffer; the membrane was washed with 20 ml of starting buffer followed by a 40-ml KCl gradient up to 2 *M*. Proteins, G6PDH, MDH and adenylate kinase recovered in the eluted peak.

Run No.	Proteins (μg)	G6PDH (U)	MDH (U)	Adenylate kinase (U)
1	308	0.21	16.36	1.89
2	319	0.21	12.24	1.69
3	294	0.28	12.24	0.05

crude extract. A stack of ten membranes was used in the FPLC system. The elution profiles observed in five successive runs were highly reproducible (Fig. 2). The amount of proteins recovered was constant within 3% error. However, the elution peak was spread over about 7.5 ml.

The same kind of experiment was repeated with only one disc of membrane in the holder and using 20 ml of starting buffer to wash unbound proteins and a 40-ml linear gradient up to 2 *M* for elution. A frontal application of the sample was used to overload the support capacity as in the batch adsorption experiments. The flow-rate for elution was 1.0 ml/min in the first two runs and 0.05 ml/min in the third. MDH, G6PDH, adenylate kinase and the bulk of the eluted proteins were recovered in a typical broad peak without apparent separation from each other. The amount of proteins and enzymes found in the gradient was stable, in general (Table V). However, the recovery of adenylate kinase was lower in the third run, possibly because of deactivation over several hours.

The data in Table V, when related to the support volume, yield 3.6 U/ml G6PDH, 205 U/ml MDH and 27 U/ml adenylate kinase (first two runs only), in good agreement with the desorption from the blue membrane in the batch mode (Table IV). The desorption of protein, yielding 4.65 mg/ml, was notably lower than in the batch mode, but the latter value was biased, as mentioned above. In consequence, the enrichment factors were found to be about twice as high as in the batch mode.

DISCUSSION

Preliminary evaluation of the capacity of microfiltration membranes as adsorbents for proteins showed that experimental values obtained with BSA were in good agreement with the calculated value of 150 $\mu g/cm^2$ membrane, based on the actual inner area of the support and the assumption of adsorption in a monolayer of BSA on the surface. Under the conditions chosen, namely a low ionic strength, electrostatic attraction of protein to the support with the cationic membranes was expected to yield a high affinity of BSA for the support (Table I). The positively charged membrane Zetapor showed prompt saturation, as a very small increase in adsorption was observed while the remaining concentration in solution differed by a factor of about 10. On the other hand, the small residual concentration left in

solution with the smallest amount of BSA introduced showed that the affinity was very high. In fact, the concentration in the support matrix was about 470 times higher than that in the solution. The Ultipor membrane showed saturation to a lesser extent, but the amphoteric nature of the membrane made a net electrostatic attraction less evident as the unadjusted pH of the aqueous solution was close to the isoelectric point of the membrane, reported as 6.5 [11]. The Zetabind membrane surprisingly showed no saturation at all, despite the excess of BSA remaining in the solution. The latter shows that the affinity for BSA was low in comparison with the other two membranes. Gershoni and Palade [12] found a steady increase in BSA binding up to 500 $\mu g/cm^2$ when a large excess (up to 37 mg/cm^2) was contacted with a Zetabind membrane, which was then rinsed before counting the I^{125}-labelled BSA. The requirement for such a high concentration to achieve high adsorption values and the resistance to rinsing are contradictory if one assumes an equilibrium between adsorbed and soluble BSA. The binding mechanism on that membrane could therefore be particular, *i.e.*, a form of low affinity but irreversible insolubilization on the surface. Our experimental set-up based on mass balance to determine adsorption did not allow that range of concentrations to be investigated. Nevertheless, the high concentrations of BSA remaining in solution (Table I) indicated that no binding sites with high affinity were left on any of the membranes.

The lysozyme capacity on dyed membranes (Table III) was consistent with the monolayer capacity calculated for the Ultipor membrane. Moreover, the monolayer values predicted well the capacity measured on the proprietary ligand membrane (see Table V, values for 3.3 cm^2 sample area) with a protein mixture.

Fig. 1 suggests that the capacity of Ultipor membranes with larger pore sizes up to 1.2 μm would correspond to only a three times reduction in capacity.

The modification of nylon membranes with triazine dyes is reproducible, regardless of the dye reactivity (Table II). Concentrations of 0.5–3.6 $\mu mol/ml$ membrane can be calculated for Cibacron Blue without and with PEI as spacer. The values reported for agarose gels were in the range 1–10 $\mu mol/ml$ [1].

The adsorption of lysozyme under conditions favourable to electrostatic attraction showed the positive effect of the dye ligand on the membrane capacity (Table III) as a 2-fold adsorption was observed compared with the parent membrane. The value measured on the latter cannot be considered as a background for dyed membranes as the original binding sites could be masked by dye ligands. The maximum values in Table III can be converted to a concentration of 8.6 mg/ml support, which corresponds to about 60% of the maximum concentration reported on blue Sepharose CL-6B [13].

The good correlation between batch and flow-through data for lysozyme adsorption (Table III) indicated two important properties of the membranes as dye ligand adsorbents: first, no irreversible binding occurred, as washing of the support with 1 *M* NaCl restored the initial capacity; second, flow-through conditions allowed the adsorption to be achieved in a few minutes, even with a more dilute solution. The first point was confirmed with the proprietary dye ligand membrane and yeast proteins and enzymes (Fig. 2, Table V).

Batch and flow-through experiments with the latter membrane showed the applicability of the support to the isolation of specific enzymes from crude mixtures. The amounts of enzymes recovered were similar in both procedures (Tables IV and V).

Enrichment factors in the region of 10 would be very attractive in early separations as a large proportion of the bulk proteins would be discarded.

The volumetric capacity of the membranes was found to be comparable to that of the corresponding Sepharose gels, at least as measured by enzyme adsorption or protein desorption (Table IV).

The method adopted here to desorb enzymes showed a poor performance; in batch adsorption the recovery was not complete and notably inferior on membranes than on gels; in the flow-through mode, extensive peak spreading occurred. The latter may reflect sequential desorption of different proteins or axial dispersion in the holder or the lines. However, individual enzyme peaks were fairly broad also, covering at least 5 ml for the data in Table IV, and axial dispersion would account only for peaks of 2.5 ml duration as measured in complementary experiments (data not shown). In fact, no optimization of the desorption step has been attempted so far. Several possibilities exist for improving the desorption behaviour: optimization of the buffer composition and pH for a particular enzyme or eluting specifically with substrate or cofactor.

This paper demonstrates that the inner surface of microfiltration membranes made of nylon could be modified with dye ligands and used for adsorption of proteins, yielding volumetric capacities close to those of the corresponding agarose support. The binding capacity could be used repeatedly and no irreversible fouling was apparent. However, desorption using high salt concentrations was not satisfactory and notably worse than with dye ligand gels. Optimizing the desorption step is still possible.

Interestingly, the available area was not dramatically reduced when membranes with larger nominal pore sizes were considered. This might yield a very favourable opportunity to optimize the space–time yield of membrane adsorbents, as membranes with high permeabilities could be chosen without affecting the capacity.

ACKNOWLEDGEMENTS

B.C. was supported by a grant from the European Commission, DG XII. We thank Cuno, Pall and Sartorius for the gift of membranes. R. Regenbogen (Deutsches Wollforschung Institut, Aachen, Germany) is gratefully acknowledged for the nitrogen adsorption measurements.

REFERENCES

1 Y. D. Clonis, T. Atkinson, C. J. Bruton and C. R. Lowe (Editors), *Reactive Dyes in Protein and Enzyme Technology*, Stockton Press, New York, 1987.
2 P. Hedman, J. C. Janson, B. Arve and J. G. Gustafsson, in G. Durand, L. Bobicnon and J. Florent (Editors), *Proceedings of the 8th International Biotechnology Symposium, Paris, 1988*, Vol. 1, Société Française de Microbiologie, Paris, 1988, pp. 623–643.
3 H. A. Chase, in A. E. Rodrigues, M. D. Le Van and D. Tondeur (Editors), *Adsorption: Science and Technology*, Kluwer, Dordrecht, 1989, p. 539.
4 S. Brandt, R. A. Goffe, S. B. Kessler, J. L. O'Connor and S. E. Zale, *Bio/Technology*, 6 (1988) 779.
5 P. D. G. Dean, W. S. Johnson and F. A. Middle (Editors), *Affinity Chromatography —A Practical Approach*, IRL Press, Oxford, 1985, Ch. 3, p. 64.
6 H. U. Bergmeyer, *Methods of Enzymatic Analysis*, Vol. II, Verlag Chemie, Weinheim, 1983, p. 246.
7 Y. Ito, A. G. Tomasselli and L. H. Noda, *Eur. J. Biochem.*, 105 (1980) 85.
8 S. J. Gregg and K. S. W. Sing, *Adsorption, Surface Area and Porosity*, Academic Press, London, 1st ed., 1967, Ch. 2, p. 35.

9 F. MacRitchie, *J. Colloid Interface Sci.*, 38 (1972) 484.
10 T. Imoto, L. N. Johnson, A. C. T. North, D. C. Phillips and J. A. Rupley, in P. D. Boyer (Editor), *The Enzymes*, Academic Press, London, 3rd ed., 1972, Ch. 21, p. 666.
11 A. C. J. Orchard, in *Proceedings of International Conference on Membrane Separation Processes, Brighton, May 24–26, 1989*, BHRA Information Services, Bedford, U.K., and Springer, Berlin, 1989, p. 79.
12 J. M. Gershoni and G. E. Palade, *Anal. Biochem.*, 124 (1982) 396.
13 H. A. Chase, *J. Chromatogr.*, 297 (1984) 179.

Journal of Chromatography, 539 (1991) 327–334
Elsevier Science Publishers B.V., Amsterdam

CHROM. 22 907

Recognition of phosphate groups by immobilized aluminium(III) ions

LENNART ANDERSSON
Biochemical Separation Centre, Biomedical Centre, University of Uppsala, P.O. Box 577, S-751 23 Uppsala (Sweden)

ABSTRACT

Aluminium ions, immobilized on iminodiacetate-agarose, were used as a chromatographic adsorbent. At pH 6.0, in strong salt solution, phosphoamino acids, phosphopeptides, phosphoproteins and nucleotides that contained terminally bound phosphate were retained. At pH 7.5 most of the phosphorus compounds were desorbed. Conversely, phosphate-free compounds were unretained at both pHs and the same behaviour was displayed by nucleotides which contained only internally bound phosphate. These findings might be useful as a basis for the development of a procedure for isolating phosphoproteins.

INTRODUCTION

Studies of the chromatographic behaviour on immobilized Cu(II), Ni(II), Zn(II) and Co(II) ions of selected thiol-free model proteins have demonstrated that surface histidyl groups are the primary electron donors in the interaction between metal and protein [1]. Other metals, such as Fe(III) and especially Al(III), can be assumed to have a higher affinity for oxygen as the electron donor [2]. Chromatography of model compounds on immobilized Fe(III) seems to support this hypothesis. For instance, phosphate compounds are strongly bound, presumably via oxygen [3,4]. Immobilized Al(III) has limited use for the separation of biological molecules. The free metal ion is known to form strong complexes with phosphate, citrate and other oxygen-rich compounds [5]. This property is the basis upon which a new separation method has been attempted. This paper describes the properties of Al(III) immobilized on agarose gel and its possible utility as an adsorbent for phosphorus-containing compounds.

EXPERIMENTAL

Iminodiacetic acid(IDA)-agarose (Chelating Sepharose Fast Flow) was obtained from Pharmacia–LKB (Uppsala, Sweden), or was prepared in this laboratory [6]. The Cu(II)-binding capacity was 30 and 70 μmol/ml wet gel, respectively. A glass column (20 × 10 mm I.D.) containing Chelating Superose was purchased from Pharmacia. The gel consists of the high-performance matrix Superose 12 onto which iminodiaetic acid is coupled. Carboxymethylaspartyl-agarose (CM-asp-agarose) was

0021-9673/91/$03.50

described previously [7] and tris(carboxymethyl)ethylenediamine (TED)-agarose were synthesized according to a previous report [8]. Binding capacities were 42 and 90 μmol of Cu ions per millilitre, respectively. However, CM-asp-agarose displayed poor aluminium binding and was not studied further. Aluminium binding to TED-agarose was strong but neither the model compounds, *i.e.*, phosphoprotein and phosphoamino acids, nor the other proteins used in this work were bound to TED–Al(III)–agarose. Those results confirm some observations made earlier [9].

Ovalbumin, pepsin (4300 U/mg protein), pepsinogen (porcine stomach, grade 1-S, 3900 U/mg protein), rabbit muscle phosphorylase *a* and phosphorylase *b* were purchased from Sigma (St. Louis, MO, U.S.A.). Chicken muscle glycogen phosphorylase was prepared following the procedure of Petell *et al.* [10]. Assays for phosphorylase *a* and phosphorylase *b* activity were carried out according to the procedure of Hedrick and Fischer [11], slightly modified. It was found that the chicken muscle extract contained high phosphorylase *b* activity. Alkaline phosphatase (calf intestine, grade I) was obtained from Boehringer (Mannheim, Germany). Ovalbumin was fractionated on immobilized IDA–Fe(III) into components containing no, one and two phosphate groups, according to an earlier report [3]. L-Amino acids, phospho-L-serine, phospho-L-threonine, phospho-L-tyrosine, nucleotides and nucleotide derivatives were of analytical-reagent grade. The synthetic peptides Arg–Arg–Ala–Ser–Val–Ala and its phosphorylated analogue Arg–Arg–Ala–P–Ser–Val–Ala were a gift from Dr. B. Fransson of this institute.

The aluminium concentration in the column eluates was determined according to a procedure in which the metal is complexed with Alizarin S [12]. Dephosphorylation of ovalbumin and pepsinogen was done by incubation with alkaline phosphatase (1–2 units/mg protein). Protein samples were analysed by sodium dodecyl sulphate–polyacrylamide gel electrophoresis (SDS-PAGE) on microplates (Phast System, Pharmacia), or by electrophoresis in 1% agarose gel slabs. Staining was done in solutions of Coomassie Brilliant Blue.

Preparation of columns and chromatography

Metal-free gel was suspended in water, degassed and poured into a chromatographic column (60 × 10 mm I.D., bed volume 5 ml). Columns were charged with a solution of aluminium chloride (50 m*M*) in distilled water. The charging was considered to be complete when a precipitate of aluminium hydroxide was formed from a small aliquot of the eluate after addition of one drop of 5% sodium carbonate solution. After washing out unbound metal with three column volumes of water, the column was equilibrated with five column volumes of starting buffer. Freeze-dried and salt-free samples were dissolved in starting buffer; in some instances they were desalted in this buffer on a small Sephadex G-25 column prior to chromatography. Runs were made at room temperature with a flow-rate of 15–20 ml/h. Fractions of 1.0 or 1.5 ml were analysed for protein and enzymic activity. The metal was removed after each run with 0.1 *M* EDTA (0.5 *M* NaCl; pH 7) and occasionally with a portion of 0.1 *M* sodium hydroxide. Chromatographic runs on Chelating Superose were accomplished using an LKB high-performance liquid chromatographic system consisting of pump (Model 2150), a controller (Model 2152) and a two-channel recorder (Model 2210).

The following buffer systems were used, unless indicated otherwise: pH 5.0, 0.05

M acetic acid–NaOH (1 *M* NaCl); pH 6.0, 0.05 *M* MES–NaOH (1 *M* NaCl); pH 7.0, 0.05 *M* PIPES–HCl (1 *M* NaCl); and pH 8.0, 0.05 *M* Tris–HCl (1 *M* NaCl), where MES = 4-morpholinoethanesulphonic acid and PIPES = 1,4-piperazinodiethanesulphonic acid.

RESULTS AND DISCUSSION

Aluminium binding and stability of the chelating gel

The binding capacity was determined by frontal analysis. The copper- and aluminium-binding capacities were 30 and 14 μmol per millilitre wet gel, respectively, for Chelating Sepharose or Superose and 70 and 32 μmol/ml, respectively, for the "home-made" IDA-agarose. The stability of the metal chelates was checked by measuring the aluminium ion concentration at pH 5.0, 6.0, 7.0 and 8.0 in eluates from a column that was completely loaded with metal. The leakage from Chelating Sepharose was found to be 0.015, <0.004, <0.004 and 0.020 μmol/ml, respectively, which indicates good stability in this pH range. From TED-agarose it was less than 0.004 μmol/ml eluate at these pH values.

Chromatography of low-molecular-mass compounds

Amounts of 0.5–1 mg of compounds containing bound phosphate and phosphate-free analogues, amino acids, nucleosides, nucleotides and peptides were dissolved in starting buffer and chromatographed, one by one, on Al(III)–IDA-agarose at different pH values. The results are given in Table I. Evidently none of the phosphate-free substances was retained. All the substances that were retained at pH 6.0 (1 *M* NaCl) contain an external (terminal) phosphate group. The absence of retention of GpU, ApG, NAD and UDPG indicates that internal phosphate groups do not contribute significantly to adsorption. The increased affinity of ADP, GTP and ATP might be due to metal chelation. Strong chelating of Al(III) ions to ADP has been reported [2]. Compounds adsorbed on Al(III)–IDA–agarose and containing mono-esterified phosphate group(s) could be desorbed either by increasing the pH to 8 or by adding 20 m*M* phosphate. ADP, ATP and GDP, once adsorbed, resisted desorption at pH 8 or 9, but their elution proceeded reasonably well at pH 11.

Chromatography of model proteins

Porcine pepsinogen and pepsin are single-chain polypeptides composed of 370 and 329 amino acid residues, respectively. In each protein there is a single phosphorylated serine that is positioned fairly near the amino-terminus. On activation, pepsinogen loses its 41-residue N-terminal peptide. Both pepsinogen and pepsin were weakly retained in MES buffer (pH 6.0) (1 *M* NaCl). The retention became strong if 0.5 *M* potassium phosphate was substituted for 1 *M* sodium chloride. Both enzymes were desorbed with good recoveries (<90% for pepsinogen, 70% for pepsin) by 20 m*M* phosphate buffer (0.5 *M* K_2SO_4). In a control experiment, dephosphorylated pepsinogen was run under similar conditions. Fig. 1 shows that pepsinogen was strongly retained but the dephosphorylated enzyme unretained at pH 6. Presumably, little or no conformational change takes place after the dephosporylation because there is no significant loss in activity. These results suggest that immobilized Al(III) can recognize a seryl-phosphate group among more than 300 residues.

TABLE I

RETENTION OF LOW-MOLECULAR-MASS SUBSTANCES ON Al(III) IONS IMMOBILIZED ON CHELATING SEPHAROSE FAST FLOW

Substance[a]	pH of buffers in 1 *M* NaCl			
	5.0	6.0	7.0	8.0
L-Amino acids	–	–	–	–
Phosphoserine	+	+	–	–
Phosphothreonine	+	+	–	–
Phosphotyrosine	+	+	–	–
Arg–Arg–Ala–Ser–Val–Ala	–	–	–	–
Arg–Arg–Ala–P–Ser–Val–Ala	+	+	–	–
Nucleosides	–	–	–	–
AMP	+	+	+	–
ADP	+	+	+	+ –
ATP	+	+	+	+ –
GMP	+	+	+	–
GDP	+	+	+	+ –
CMP	+	+	+	–
NAD^+	n.d.	–	–	–
NADP	n.d.	+	–	–
FAD	–	–	–	–
GpU	–	–	–	–
ApG	–	–	–	–
UDPG	–	–	–	–
cAMP	–	–	–	–

[a] Standard abbreviations; also GMP = guanosine 5′-phosphate; CMP = cytidine 5′-monophosphate; NADP = nicotinamide adenine dinucleotide phosphate; FAD = flavin adenine dinucleotide; GpU = guanosine phosphate uridine; ApG = adenosine phosphate guanosine; UDPG = uridine diphosphate glucose; cAMP = cyclic adenosine 3′,5′-monophosphate.

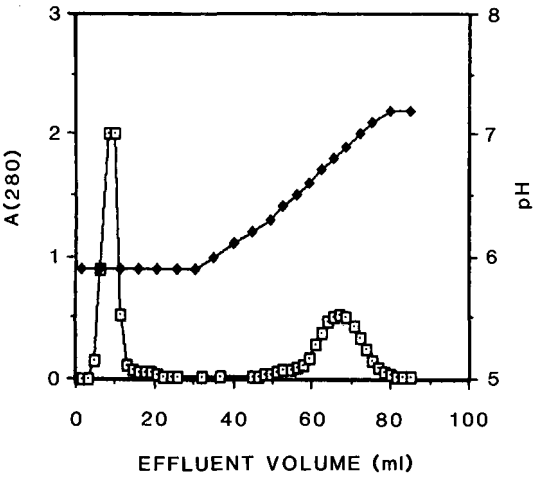

Fig. 1. Chromatography of pepsinogens on Al(III)–IDA γ-agarose. A sample of 4 mg of pepsinogen in 5 ml was applied and the column was washed with 45 ml of 0.05 *M* MES–NaOH (0.5 *M* K_2SO_4) (pH 6.0). The column was then rinsed with 20 m*M* phosphate buffer (0.5 *M* K_2SO_4) (pH 7); the buffer change is indicated by an arrow. □ = Porcine pepsinogen; ◆ = dephosphorylated porcine pepsinogen.

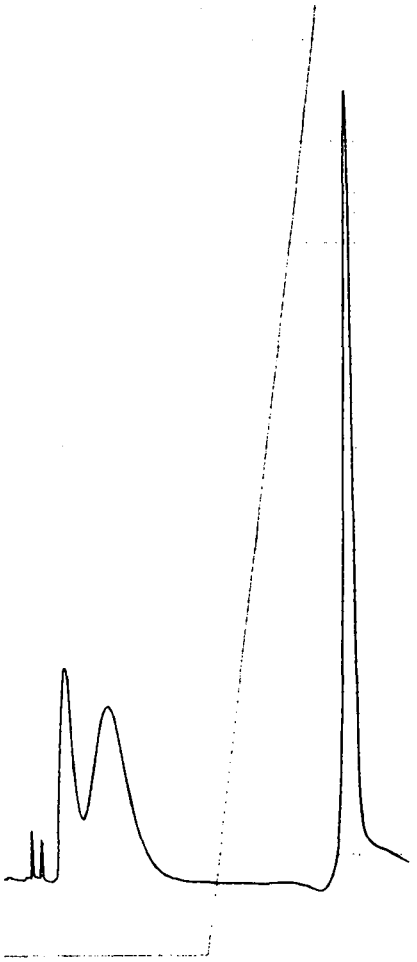

Fig. 2. Recorder trace from chromatography of ovalbumin on Al(III)–IDA-Superose column. 2 mg of ovalbumin were dissolved in 0.05 *M* MES–NaOH (1 *M* NaCl) buffer (pH 6.0) and injected into the column. The column was then rinsed with starting buffer and developed with a pH gradient formed by mixing starting buffer with 0.05 *M* PIPES–HCl (1 *M* NaCl) buffer (pH 7.2). The flow-rate was 0.25 ml/min. Time scale: 1 cm = 10 min.

Native ovalbumin was chromatographed on Al(III)–Chelating Superose. A 2-mg amount was dissolved in MES buffer (pH 6.0) (1 *M* NaCl) and applied. After washing out weakly bound protein, the column was developed with a pH gradient from 6.0 to 7.3. The results are illustrated in Fig. 2. Purified ovalbumins with no, one and two phosphate groups were chromatographed, one by one, in the same way. By comparison, the first peak in Fig. 2 was identified as ovalbumin with no phosphate, the second peak as the monophosphate ovalbumin and the third peak as the diphosphate ovalbumin. The poor retention of the monophosphate ovalbumin might be due to partial masking of the phosphate group. The resolution was greatly dependent on the

flow-rate, which suggests slow desorption kinetics. The overall protein recovery was always near 100%. It was found, by analysis, that diphosphate ovalbumin scavenged some aluminium from the adsorbent.

Muscle glycogen phosphorylase may exist in the form of phosphorylase *a*, which is produced from phosphorylase *b* phosphorylation of one seryl residue per subunit, *A priori*, this enzyme seems rather complicated to choose as a model protein. Both the *a* and *b* forms contain one bound pyridoxal phosphate; however, this group is contained deep within the interior of the protein. Depending on the conditions, the *a* and *b* enzyme may be built up of two four subunits. Phosphorylase *b* was unretained when chromatographed on Al(III)–IDA-agarose under the usual conditions. Phosphorylase *a*, on the other hand, was always adsorbed. However, depending on the enzyme source, the adsorption was sometimes strong and sometimes weak. This variation might be due to the different aggregation and/or conformational states that have been reported [13]. These states are assayed only with difficulty and therefore any further interpretation seems impossible. However, the outcome of these experiments does not contradict the hypothesis that binding occurs via phosphate groups.

Some other model proteins that are known to interact through histidyl groups with Cu(II)– and Ni(II)–IDA-agarose gel were chromatographed using the same procedure. None of them, *i.e.*, horse cytochrome *c*, human serum albumin, whale myoglobin and hen's egg lysozyme was, however, adsorbed at pH 6.0, 7.0 or 8.0. This means that immobilized Al(III) does not recognize one or several surface histidyl side-chains.

Adsorption of proteins in crude extracts

A 3-ml volume of dialysed human serum were chromatographed on Al(III)–Chelating Sepharose at pH 6.0 in the presence of 1 or 2 *M* sodium chloride or 0.5 *M* potassium sulphate. After washing with 25 ml of starting buffer desorption was effected with 20 m*M* phosphate (1 *M* NaCl) (pH 7) and subsequently with 0.1 *M* EDTA (0.5 *M* NaCl). However, only small amounts of protein (0.1–0.5%) were desorbed and therefore no attempt was made to analyse this material. Hen's egg white was filtered and diluted 10-fold with 0.05 *M* MES (1 *M* NaCl) (pH 6.0). A 1-ml volume was applied, the column was washed with buffer and proteins were desorbed with 0.05 *M* Pipes (1 *M* NaCl) (pH 7.2) (Fig. 3a). The desorbed material was analysed by SDS-PAGE and was found to be homogeneous with the same molecular mass as standard ovalbumin (not shown). Agarose gel electrophoresis revealed that the material behaved as diphosphate ovalbumin (Fig. 3b). The experiments on extracts suggest that Al(III)–Chelating Sepharose has a high selectivity for the phosphoprotein.

Rat liver acetone powder (Sigma L 1380) was extracted with MES buffer (pH 6.0) (1 *M* NaCl) at room temperature for 20 min. After centrifugation the extract was applied to the Al(III) column and chromatographed. A large amount of UV-absorbing material was desorbed on increasing the pH. The UV spectrum and protein analysis showed that this material contained a mixture of nucleotides but no protein.

Extracts of chicken muscle were transferred to MES buffer (pH 6.0) (1 *M* NaCl) to remove EDTA and phosphate ions. Ten millilitres were chromatographed on Al(III)–IDA-agarose gel in the same buffer. There was virtually no adsorption of protein and all of the applied phosphorylase b activity appeared in the breakthrough

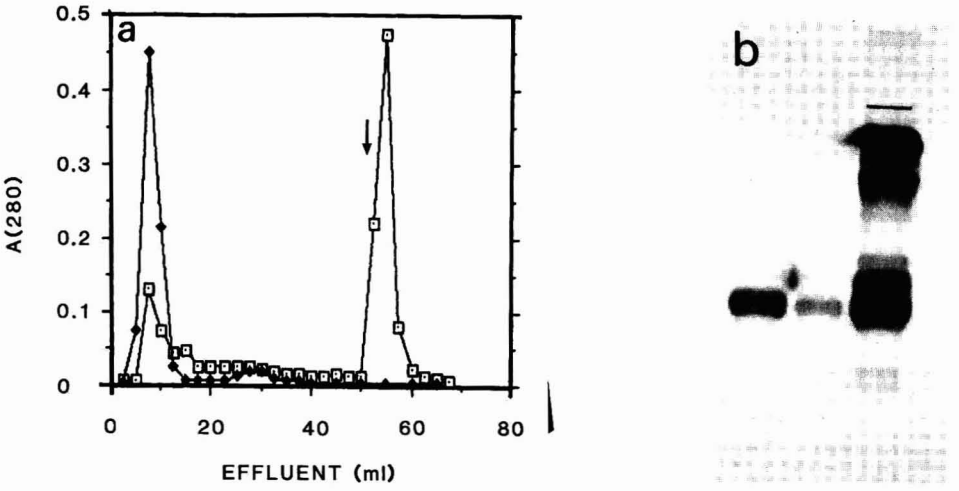

Fig. 3. (a) Chromatography of crude egg white on Al(III)–IDA γ-agarose. A 1-ml sample of diluted egg-white extract was applied and the column was rinsed with 25 ml of starting buffer. The column was then developed with a pH gradient formed by mixing 25 ml of starting buffer with 25 ml of 0.05 *M* PIPES–HCl (1 *M* NaCl) buffer (pH 7.2). Finally, the column was rinsed with the second buffer. (b) Agarose electrophoresis of hen's egg-white proteins. Lanes: 1 = crude extract of egg white; 2 = pooled fractions from peak 2 (at 55 ml) in (a).

peak. In another experiment the extraction procedure was done in the absence of EDTA but in the presence Mn(II) ions. This extract displayed phosphorylase a activity. After chromatography on Al(III)–IDA γ-agarose gel in the same buffer as before, all of the phosphorylase a was found to be adsorbed. It was, however, difficult to recover the enzyme in the usual manner. However, even in this complicated case, immobilized Al(III) appears to recognize bound phosphate groups.

In summary, it seems that aluminium ions can recognize a phosphate group having an external position within a molecule. With proper handling, the adsorbent might be useful for the group isolation of certain compounds, including proteins, containing a small number of externally bound phosphate groups. All evidence in this work suggests that the specificity for phosphorylated protein among other proteins is remarkably high, let alone the possible interference of nucleotides containing an external phosphate group that may be present in biological extracts.

The data from this and from previous studies [3,8,14,15] allow some comparison between the properties of immobilized Fe(III) and immobilized Al(III). Obviously, the latter adsorbent has a superior selectivity for phosphoprotein. On the other hand, binding of phosphorylated proteins to Al(III)–IDA γ-agarose gel seems comparatively weaker and therefore requires the presence of high concentrations of salt. Therefore, it may be advantageous that both adsorbents, combined, be used for the purpose of purifying proteins, especially phosphoproteins.

ACKNOWLEDGEMENT

This work was financially supported by the Swedish Natural Science Research Council.

REFERENCES

1 E. S. Hemdan, Y.-J. Zhao, E. Sulkowski and J. Porath, *Proc. Natl. Acad. Sci. U.S.A.*, 86 (1989) 1811.
2 R. G. Pearson, *J. Am. Chem. Soc.*, 85 (1968) 643.
3 L. Andersson and J. Porath, *Anal. Biochem.*, 154 (1986) 250.
4 G. Muszynska, L. Andersson and J. Porath, *Biochemistry*, 25 (1986) 6850.
5 R. B. Martin, *Clin. Chem.*, 32 (1986) 1797.
6 J. Porath, J. Carlsson, I. Olsson and G. Belfrage, *Nature (London)*, 258 (1975) 598.
7 J. Porath, *Trends Anal. Chem.*, 7 (1988) 254.
8 J. Porath and B. Olin, *Biochemistry*, 22 (1983) 1621.
9 J. Porath, B. Olin and B. Granstrand, *Arch. Biochem. Biophys.*, 225 (1983) 543.
10 J. K. Petell, M. S. Sardo and H. G. Lebherz, *Prep. Biochem.*, 11 (1981) 69.
11 J. L. Hedrick and E. Fischer, *Biochemistry*, 4 (1965) 1337.
12 C. A. Parker and A. P. Goddard, *Anal. Chim. Acta*, 4 (1950) 517.
13 R. J. Fletterick and N. B. Madsen, *Annu. Rev. Biochem.*, 49 (1980) 31.
14 E. Sulkowski, *Macromol. Chem. Macromol. Symp.*, 17 (1988) 335.
15 G. Chaga, L. Andersson, B. Ersson and J. Porath, *Biotechnol. Appl. Biochem.*, 11 (1989) 424.

Journal of Chromatography, 539 (1991) 335–341
Elsevier Science Publishers B.V., Amsterdam

CHROM. 22 896

Highly active enzyme preparations immobilized via matrix-conjugated anti-Fc antibodies

BEKA SOLOMON*, ERAN HADAS, RELA KOPPEL, FIDI SCHWARTZ and GIDEON FLEMINGER

Department of Biotechnology, Tel-Aviv University, Ramat Aviv, Tel-Aviv 69978 (Israel)

ABSTRACT

A novel method for enzyme immobilization to achieve highly active enzyme preparations is described. The enzyme is first reacted in solution with a specific monoclonal antibody (mAb) which does not interfere with its enzymic activity and which possesses a high affinity towards the enzyme. The immunocomplex is then reacted with immobilized anti-Fc antibodies which are coupled to the matrix by methods that preserve maximum immunological activity. Horseradish peroxidase (HRP) immobilization on epoxy-activated beads (CB6200) was chosen as a model system for this approach. Coupling of HRP via its mAbs to anti-Fc antibodies immobilized yielded the best results, corresponding to binding of 325 ng of fully active enzyme per bead. Binding of the enzyme to anti-HRP mAb directly immobilized on the beads was considerably lower.

INTRODUCTION

During the last two decades, reactions which involve catalysis by immobilized enzymes have been widely used on both the laboratory and industrial scales with preparative, analytical and diagnostic applications. Many matrices and covalent binding methods have been developed in order to achieve highly active enzyme–matrix conjugates [1]. However, enzymes often tend to lose their biological activity on coupling to a matrix owing to masking of their active sites or multi-point attachments which restrict local movements necessary for the activity of the enzyme. In such cases, coupling of the enzymes via monoclonal antibodies (mAbs) which do not affect their activity and possess a high binding affinity towards the enzyme may be advisable [2].

Previously we have shown that the binding of such antibodies to insoluble carriers, *e.g.*, Eupergit C, yields matrix-conjugated mAb preparations which efficiently bind the corresponding enzymes to yield highly active immobilized enzymes [3]. In such preparations, the enzyme is bound via specific preselected and well defined sites. Apparently, in this instance, mAbs form an extended spacer separating the enzyme from the carrier. In addition, the mAbs bind the respective enzymes via epitopes remote from the active site so that the active sites face the outer solution. Multi-point attachments are also eliminated and the enzymes are relatively free to move to express higher activity.

0021-9673/91/$03.50

Since, in principle mAbs, which do not affect enzymatic activity and which bind the enzymes at high affinity, may be prepared against almost any enzyme, this technique may represent a general solution to the preservation of high activity of immobilized enzymes. At present, the main restriction on the use of mAbs is their high cost, but improvements of the techniques for their large-scale production is expected to lead to a marked decrease in price [4].

We expected that the formation of soluble complexes of enzymes with specific mAbs, followed by immobilization via reaction with anti-Fc antibodies, should lead to a higher capacity for enzyme binding than direct coupling of the enzyme to immobilized antibodies. Further, optimization of anti-Fc immobilization onto the solid carrier with respect to antigen binding activity should eventually lead to even higher activity of the immobilized enzyme. We have tested various methods for antibody immobilization in order to achieve the highest antigen binding activity.

The carrier used in this study was Eupergit C1Z-coated poly(methyl methacrylate) beads (6 mm, CB6200). These beads are especially suitable for application in immunodiagnostic assays. Immunoassays performed with such beads are expected to be more reproducible and reliable than those performed with enzyme-linked immunosorbent assay (ELISA) microtitre plates owing to the covalent binding, rather than hydrophobic adsorption, of the first antibody to the surfact of the matrix. Nevertheless, assays based on these beads have to be optimized with respect to protein-binding capacity, antigen-binding activity of the immobilized antibodies and reproducibility of the results.

As a model system we chose immobilization of horseradish peroxidase (HRP) via specific mAbs. Two approaches were examined and compared; (a) binding of HRP to immobilized mAb and (b) binding of a soluble complex of HRP with its mAb to immobilized anti-Fc antibodies. This enzyme, which is commonly used in immunodiagnostics as a reporter enzyme, contains only a small number of lysine residues and a blocked N-terminus [5] and, therefore, does not react directly with the oxirane groups of the matrix. Thus any matrix-associated enzymatic activity may be attributed to antibody-modulated immobilization of the enzyme.

EXPERIMENTAL

Materials

Eupergit C1Z-coated poly(methyl methacrylate) beads (6 mm, CB6200) were obtained from Rohm-Pharma (Darmstadt, Germany). Horseradish peroxidase (HRP) was purchased from Sigma (St. Louis, MO, U.S.A.).

Chemical modification of CB6200 beads

Fifty beads were incubated with 25 ml of 0.1 *M* adipic dihydrazide (ADH), hexamethylenediamine (HMD) or hydrazine hydrate (HH) in 0.2 *M* phosphate buffer (pH 8.8) for 16 h at room temperature. The beads were then extensively washed and unreacted oxirane groups were blocked with 0.2 *M* β-mercaptoethanol. The modified beads were extensively washed and kept for further use in phosphate-buffered saline (pH 7.4) (PBS) at 4°C.

Assay of the enzymic activity of horseradish peroxidase

HRP (10–100 μl, 0.1–10 ng) was incubated in ELISA microtitre plates with 100 μl of HRP substrate solution [2 mg/ml of *o*-phenylenediamine (Fluka, Buchs, Switzerland) and 0.008% hydrogen peroxide in 50 m*M* citrate buffer (pH 5.0)] for 1 min at room temperature. Colour development was stopped by the addition of 4 *M* hydrochloric acid (50 μl) into each well. The intensity of the colour developed was measured with an ELISA reader (SLT, Grodig, Austria) at 492 nm (with a reference beam at 405 nm).

Preparation and purification of monoclonal antibodies

The preparation of anti-HPR antibodies has been described previously [6]. A monoclonal antibody (HRP2) which did not interfere with the enzymic activities of HRP was selected using the microassay described above. This antibody was purified by high-performance immunoaffinity chromatography using Eupergit C-bound HRP as described previously [7]. The apparent binding constant of this antibody was determined according to the procedure of Pinckard and Weir [8], *i.e.*, as derived from the reciprocal of the free monoclonal antibody concentration at which 50% of the maximum binding to HRP was achieved.

Immobilization of anti-Fc antibodies on CB6200 beads

Polyclonal anti-Fc antibodies were coupled to oxirane groups of the beads either directly or after reversible protection of their amino groups by reaction with dimethylmaleic anhydride (DMA). By the direct immobilization procedure the antibodies (0.1 mg) were incubated with ten beads in 5 ml of 1 *M* potassium phosphate buffer (pH 7.4) for 16 h at 4°C. Blocking of unreacted oxirane groups was achieved by incubation with 0.2 *M* β-mercaptoethanol (pH 8.0) for an additional 4 h at room temperature. By the DMA procedure the antibodies (0.1 mg) were incubated first with DMA for 1 h and then coupled to the beads as described previously [9].

Alternatively, oriented immobilization of anti-Fc antibodies was achieved by coupling of periodate-oxidized antibodies to ADH-, HH- or HMD-modified CB6200 beads as described previously [6].

Anti-Fc antibodies were also coupled to chemically modified CB6200 by incubation of the antibodies (0.1 mg) with ten beads in the presence of 10% glutaraldehyde in water for 16 h at room temperature.

Immobilization of the monoclonal antibody HRP2 on CB6200 beads

Monoclonal antibody HRP2 was coupled to CB6200 beads either directly (as described above for the anti-Fc antibodies) or via its immunological reaction with the immobilized anti-Fc antibodies. Beads containing anti-Fc antibodies were incubated with increasing amounts of mAb HRP2 (1–10 μg per bead) for 1 h at 37°C. The amount of antibodies bound to the beads was determined by the difference in the amounts of protein measured before and after coupling by a microassay described by Bradford [10].

Immobilization of horseradish peroxidase on CB6200 beads

Two approaches were used for the coupling of HRP to CB6200. First, HRP was coupled to matrix-conjugated anti-HRP mAb (see above). Alternatively, the enzyme

was reacted with the antibody in solution and then the immunocomplex was immobilized onto the CB6200 beads via reaction with immobilized anti-Fc antibodies.

Coupling of HRP to the beads by immunological reaction with immobilized mAb HRP2 was carried out by incubation of the enzyme (5 μg in 200 μl of low-fat milk) with the beads containing increasing amounts of antibody (0.3–1000 μg pr bead) for 1 h at room temperature with gentle agitation. For coupling of HRP to soluble antibody, 5 μg of the enzyme were incubated with 10 μg of antibody in PBS for 1 h at 37°C. The immunocomplex formed was the incubated with immobilized anti-Fc for a further 1 h in PBS at 37°C with gentle agitation. In a control experiment, the direct binding of HRP to the beads was tested. A 5-μg amount of HRP was incubated with each bead in 1 *M* potassium phosphate buffer (pH 7.4) for 16 h at 4°C, followed by washing with 1% Triton X-100 in PBS. The enzymic activity of bound HRP was determined by incubation of each of the beads with 0.5 ml of *o*-phenylenediamine [2 mg per ml of 0.1 *M* phosphate buffer (pH 8.0) containing 0.008% hydrogen peroxide for 1 min at room temperature. Colour development was stopped by the addition of 4 *M* hydrochloric acid (0.5 ml) to each test-tube. The intensity of the colour developed was measured with the ELISA reader using a calibration graph based on the activity of known amounts of soluble HRP measured under the same experimental conditions.

RESULTS AND DISCUSSION

Binding of HRP via specific antibodies immobilized on CB6200 beads

Immobilization of HRP on CB6200 beads via its mAb HRP2, which does not interfere with its enzymic activity and binds to the enzyme with a high binding constant (10^9 l/mol), provides an efficient model system for immobilization of enzymes. In order to determine the protein-binding capacity of CB6200 beads, increasing amounts of ^{125}I-labelled immunoglobulin G (IgG) were incubated with the beads. The beads were then extensively washed with a solution of 10% SDS in 8 *M* urea in order to remove any non-covalently bound protein. The amount of covalently linked antibodies was determined by measuring the gamma irradiation of the beads. As shown in Table I, the amount of bound IgG increased with protein input up to 2.2 μg bound to each bead.

Increasing amounts of anti-HRP antibody (HRP2) were coupled to the CB6200

TABLE I

BINDING OF HORSERADISH PEROXIDASE ON mAb HRP2 DIRECTLY IMMOBILIZED ON CB6200 BEADS

mAb HRP2			HRP bound (μg)	HRP/mAb HRP2 (mol/mol)
Input (μg)	Bound			
	μg	%		
0.3	0.3	100	0.055	0.73
1.0	0.9	90	0.110	0.49
3.0	1.3	43	0.175	0.54
10.0	1.8	18	0.100	0.22
30.0	2.2	7	0.025	0.05

beads and its immunological activity was determined by the ability to bind HRP. As shown in Table I, when HRP was immobilized via bound mAb HRP2, the amount of enzyme bound to the beads increased with the amount of matrix-conjugated antibody up to 1.3 μg per bead. The specific antigen-binding activity of the immobilized antibody decreased markedly with increasing amount of antibody bound to the beads (Table I). Even at a low antibody concentration (0.3 μg per bead) the molar ratio of bound antigen to antibody did not exceed 0.73, compared with 2.0 mol/mol obtained for the same antigen–antibody complex in solution (see below). At higher antibody concentrations, the amount of bound enzyme decreased, apparently owing to steric hindrance effects (see Fig. 1).

In order to improve the antigen-binding capacity of the bound antibodies and increase the activity of the immobilized enzyme, different binding methods were attempted. Binding of mAb HRP2 via its carbohydrate moieties [6] or after reversible blocking of its most reactive amino groups [9] did not improve the antigen-binding activity of the immobilized antibody.

Binding of HRP–anti-HRP immunocomplex to anti-Fc antibodies immobilized on CB6200 beads

Oriented immobilization of mAb HRP2 via anti-Fc antibodies led to a considerable enhancement of the enzymic activity of immobilized HRP. Anti-Fc antibodies were immobilized on CB6200 beads using various immobilization methods. Immunocomplexes between mAb HRP2 and HRP were formed in solution to achieve the highest antigen-binding capacity (2 mol enzyme/mol antibody) and then incubated with anti-Fc immobilized on the beads by various methods, as presented in Table II. By this procedure the enzymic activity of immobilized HRP was expected to be dependent on the immunological capability of the immobilized anti-Fc antibodies to bind the immunocomplex between HRP and its mAb. The enzymic activity of bound HRP was determined by a specific microassay using a calibration graph constructed with soluble enzyme under the same experimental conditions. As shown in Table II, immobilization of anti-Fc antibodies via a small spacer (hydrazine hydrate) failed to improve their immunological activity. The activity of anti-Fc antibodies immobilized via large

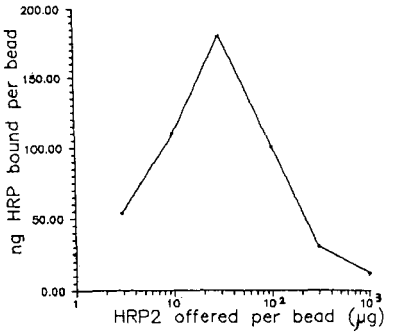

Fig. 1. Effect of amount of antibody offered per bead on the activity of the immobilized antibody. Increasing amounts of HRP2 (anti-HRP mAb) were offered to the beads. Following washing, the beads were incubated with HRP and the amount of immobilized HRP was determined as described under Experimental.

TABLE II

ENZYMIC ACTIVITY OF THE COMPLEX OF HORSERADISH PEROXIDASE WITH mAb HRP2 IMMOBILIZED ON CB6200 BEADS VIA ANTI-Fc ANTIBODIES

Immobilization method[a]	HRP	
	Enzymic activity (O.D. 492)	Bound enzyme (ng)
Oxirane (no anti-Fc)	0.020	2
Oxirane + anti-Fc	1.060	132
Oxirane + DMA–anti-Fc	1.949	244
Hydrazine hydrate + oxidized anti-Fc	0.728	91
Hydrazine hydrate + GA + anti-Fc	1.083	135
HMD + GA + anti-Fc	2.600	325
ADH + oxidized anti-Fc	1.145	143
ADH + GA + anti-Fc	2.596	324

[a] Abbreviations: ADH, adipic dihydrazide; HMD, hexamethylenediamine; DMA, dimethylmaleic anhydride; GA, glutaraldehyde.

spacers, *e.g.*, glutaraldehyde coupled to ADH or HMD, was found to be considerably higher than the activity of antibodies bound direclty via oxirane groups.

Binding of anti-Fc antibodies to oxirane groups of the matrix by using the reversible blocking with DMA led also to preparations which possessed high immunological activity. The method [9] is based on reversible blocking of most reactive amino groups of the antibodies, usually located on Fab regions, with DMA prior to the coupling reaction. After coupling to matrix via another amino group that remained unblocked during reaction with DMA, the blocking agent was removed by changing the pH and the active amino groups were available for the immunological reaction with the antigen.

The amount of HRP coupled to the various preparations of CB6200-conjugated anti-Fc varied between 90 and 325 ng per bead, depending on the immunological activity of the anti-Fc antibodies.

We have shown that enzymes may be immobilized via anti-Fc antibodies by a two-step reaction. First, the enzyme is allowed to react in solution with a properly selected specific monoclonal antibody, which binds it with high affinity and which does not interfere with its activity. Then the immunocomplex formed is bound to highly active anti-Fc antibodies. The resulting preparation of immobilized enzyme should possess high enzymic activity.

The soluble immunocomplex of enzymes and its monoclonal antibodies function as markers to quantify and purify the antibodies, and also to determine small amounts of enzymes present in the biological fluids. The use of other soluble immunocomplexes, such as glucose oxidase–antibodies for the immunohistochemical detection of antigen [11], alkaline phosphatase–antibodies in quantitative immunoassay [12] or β-galactosidase–antibodies for the purification of enzymes or antibodies [13], has been reported previously. The smaller amounts of antibodies or enzymes detected in these systems depend on the affinity of the antibody tested and on the location of the antigenic site on

the enzyme molecule. The method is applicable using crude preparations of enzymes and unpurified ascitic fluids containing the desired antibodies which decrease the cost of the test considerably. The immobilized immunocomplex of monoclonal antibodies and enzymes offers a streamlined purification system for the commercial-scale isolation of specific proteins (enzymes) found in complex mixtures. Utilization of other Eupergit C derivatives, such as the 30 N type, which possess high flow-rates and operating pressures suitable for high-performance liquid chromatography, for binding of enzymes and antibodies, provides an excellent chromatographic system [7]. The isolation of the soluble immunocomplex from the reaction mixtures or other biological fluids, using the highly active anti-Fc antibodies immobilized on the above system, is under investigation.

REFERENCES

1 K. Mosbach, *Methods Enzymol.*, 136 (1987) 117.
2 B. Solomon, R. Koppel and E. Katchalski-Katzir, *Biotechnology*, 2 (1984) 709.
3 B. Solomon, R. Koppel, G. Pines and E. Katchalski-Katzir, *Biotechnol. Bioeng.*, 28 (1986) 1213.
4 S. C. Roberts and A. R. Rees, *Nature (London)*, 332 (1987) 323.
5 K. G. Welinder, *FEBS Lett.*, 72 (1976) 19.
6 G. Fleminger, E. Hadas, T. Wolf and B. Solomon, *Appl. Biochem. Biotechnol.*, 23 (1990) 123.
7 G. Fleminger, T. Wolf, E. Hadas and B. Solomon, *J. Chromatogr.*, 510 (1990) 271.
8 R. N. Pinckard and D. M. Weir, in D. M. Weir (Editor), *Handbook of Experimental Immunology*, Blackwell Scientific, Oxford, 1978, p. 16.1.
9 E. Hadas, R. Koppel, F. Schwartz, O. Raviv and G. Fleminger, *J. Chromatogr.*, 510 (1990) 303.
10 M. Bradford, *Anal. Biochem.*, 72 (1976) 248.
11 C. A. Clark, E. C. Downs and F. J. Primus, *J. Histochem. Cytochem.*, 30 (1982) 17.
12 J. E. Butler, P. L. McGiven and P. Swanson, *J. Immunol. Methods*, 20 (1978a) 365.
13 T. Ternynk, J. Gregoire and S. Avrameas, *J. Immunol. Methods*, 58 (1983) 109.

Journal of Chromatography, 539 (1991) 343–353
Elsevier Science Publishers B.V., Amsterdam

CHROM. 22 872

Purification of *E. coli* 30S ribosomal proteins by high-performance liquid chromatography under non-denaturing conditions

CLAIRE CACHIA, PIERRE-JACQUES FLAMION* and JEAN-PIERRE SCHREIBER
Laboratoire de Biophysique, U.F.R. des Sciences Pharmaceutiques et Biologiques, 7 Boulevard Jeanne d'Arc, 21000 Dijon (France)

ABSTRACT

High-performance ion-exchange chromatography was applied to the separation of proteins from the 30S ribosomal subunit under non-denaturing conditions. It was shown that a single chromatographic step only allows the purification of nine proteins. To increase the number of separated proteins, a prefractionation step was added that depends on the physical characteristics of the proteins to be purified. Sixteen out of 21 proteins could be purified by using prefractionation (gel permeation and lithium chloride salt washing). This method is well suited to preparing fresh samples on demand for optical studies owing to the simplicity of the buffers used and the amounts of proteins recovered in the eluted peaks (0.05–0.1 mg/ml).

INTRODUCTION

The extraction and separation methods used in the preparation of isolated proteins are of crucial importance for the study of their structures, in particular for the 30S ribosomal proteins which have a prominent role in 16S rRNA and 30S subunit conformations [1–6]. Structural studies require a biological material that is as native as possible without denaturing during extraction, purification and preservation processes for sample preparation. To achieve this goal, it is now well established that proteins have to be extracted from 30S subunits by LiCl salt washing [7,8] (instead of with 3.5 *M* LiCl–4 *M* urea or 66% acetic acid, which are harsh extraction conditions). It has been shown, by nuclear magnetic resonance (NMR) and circular dichroism studies, that salt-extracted 30S ribosomal proteins have a better defined tertiary structure than urea-treated proteins [9,10]. Dijk and Littlechild [11] published a purification procedure involving traditional chromatographic methods, based on this salt extraction. Unfortunately, it required large amounts of 30S subunits, large volumes of solvents and was also time consuming.

In recent years, high-performance liquid chromatographic (HPLC) techniques have been developed, and numerous separations of 30S ribosomal proteins have been published using high-performance size-exclusion chromatography (HPSEC) [12,13], high-performance ion-exchange chromatography (HPIEC) [14,15] and re-

0021-9673/91/$03.50

versed-phase HPLC (RP-HPLC) [16–18]. HPSEC separations are generally performed under native conditions but lead to poor resolution in contrast to HPIEC and RP-HPLC, which offer higher resolution but under denaturing conditions, by using urea for HPIEC and trifluoroacetic acid (TFA) mixed with solvents for RP-HPLC. Apart from HPSEC, no HPLC separation of total 30S ribosomal proteins has been carried out under non-denaturing conditions.

We recently described the use of HPLC in the ion-exchange mode for the separation of eight "core" *E. coli* 30S ribosomal proteins (S4, S7, S8, S15, S16, S17, S18 and S19) under non-denaturing conditions [19]. In contrast to the conventional preparation [11], we have shown that HPIEC is a fast preparation method using small amounts of material with only a few purification steps. In this paper, we demonstrate the advantage of using two chromatographic steps to prepare pure proteins from specific groups (*e.g.*, high-molecular mass protein group or core proteins) with acceptable yield and purity and without the need to recover the other groups.

EXPERIMENTAL

Chemicals

Spectroscopic-grade TFA and HPLC-grade acetonitrile were purchased from Merck (Darmstadt, Germany) and Aldrich-Chimie (Strasbourg, France) respectively. Urea was for biochemical use (Merck) and all other chemicals were of analytical-reagent grade (Merck).

Buffers

The following buffers were used: TSM [0.01 *M* tris(hydroxymethyl)aminomethane–0.03 *M* succinic acid–0.01 *M* $MgCl_2$ (pH 8)]; TMK [0.03 *M* Tris–0.02 *M* $MgCl_2$–0.35 *M* KCl–0.006 *M* β-mercaptoethanol (pH 7.4)]; buffer A [0.05 *M* ammonium acetate (pH 5.6)] and buffer B (buffer A + 1 *M* NaCl).

Isolation of ribosomal proteins

The 30S subunits of *E. coli* MRE 600 ribosomes were isolated by zonal sucrose gradient centrifugation as described previously [20] and stored in TSM at −80°C in small aliquots (200 A_{260} units/ml).

Extraction of total proteins (TP30) was carried out on 30S subunits with 4.5 *M* LiCl–6 m*M* β-mercaptoethanol for 20 h at 4°C. The precipitate of 16S rRNA was removed by centrifugation (5000 *g*, 5 min). It has been shown that the residual protein in the precipitate is less than 1.5% [19]. The supernatant is used as it is for application to the permeation column, or equilibrated in buffer A with 0.15 or 0.25 *M* NaCl using a Pharmacia PD10 column (Pharmacia–LKB, Uppsala, Sweden) before application to the ion-exchange column.

Fractionation of 30S subunits into two main groups (core particles and split proteins) was done with 3.5 *M* LiCl–6 m*M* β-mercaptoethanol as described previously [19,21]. Both groups can be recovered in two different ways. For quantitative preparations (up to 15 mg of 30S), centrifugation (300 000 *g*, 10 h) was used and the resulting pellets of core particles were dissolved in TSM, whereas split proteins remained in the supernatant. HPSEC was preferred for analytical preparations: in a single run of 2 h, core particles which migrate in the void volume and split proteins

were separated. Before application to the ion-exchange column, the core proteins were extracted and treated as for TP30 whereas the split proteins were equilibrated in buffer A with 0.15 or 0.25 *M* NaCl using the Pharmacia PD10 column.

Chromatography

Chromatography was performed using a Pharmacia fast protein liquid chromatography (FPLC) system. The absorbance of the eluate was monitored with a Pharmacia UV-1 detector or a Waters Assoc. Model 480 spectrophotometer at 254 or 280 nm. All separations were carried out at room temperature. Sample volumes greater than 1 ml were injected with a 10-ml superloop obtained from Pharmacia.

HPSEC

HPSEC was performed using a Pharmacia Superose 12 column (300 × 10 mm I.D.) or a Pharmacia Superdex XK 16/70 column (60 × 1.6 cm I.D.). Generally, sample solutions were eluted in TMK or in buffer A with 0.15 or 0.25 *M* NaCl at flow-rates of 0.5 ml/min for the Superose column and 1.0 ml/min for the Superdex column. The volumes of the collected fractions were 0.5 ml for the Superose column and 1 ml for the Superdex column. Before application to the ion-exchange column, the collected fractions were pooled and concentrated in Sartorius Centrisart (cut-off 5000) to 1–5 ml if the recovered volumes were greater than 10 ml.

HPIEC

HPIEC was carried out using a LKB Ultropac TSK CM-3SW (150 × 7.5 mm I.D.). Samples in buffer A containing 0.15 or 0.25 *M* NaCl to prevent precipitation were eluted at a flow-rate of 1.0 ml/min using a gradient from buffers A and B. The gradient shape is shown in Fig. 1. Changing the gradient shape at 0.4 *M* increases the resolution in the range 0.4–0.65 *M* where most of proteins are eluted.

RP-HPLC

RP-HPLC was performed using a Pharmacia ProRPC HR 5/10 column (5-μm silica, 300 Å pore size, C_1/C_8-bonded phase) (100 × 5 mm I.D.). Solvent I was 0.1% TFA in water (pH 2.0) and solvent II was 0.1% TFA in acetonitrile–water (1:1, v/v). Proteins were eluted at room temperature using a linear gradient from 30% to 90% II in 120 min at a flow-rate of 0.2 ml/min. Before injection, the column was equilibrated with 30% II, and then the fractions from HPIEC were loaded directly onto the column. The optimum protein concentration injected was 0.1 mg per 100 μl.

Identification of ribosomal proteins

RP-HPLC was used in combination with polyacrylamide gel electrophoresis (PAGE) at pH 4.5 [22] and urea HPIEC [14] to assess the identity of chromatographic fractions.

Degrees of purification and yields

Degrees of purification and yields were calculated from spectrophotometric measurements. The amounts of proteins recovered were determined from absorbances determined from peak areas on the chromatograms or by direct measurements of eluted peaks on a Varian Cary 2200 spectrophotometer (Varian, Mulgrave, Australia).

The protein concentrations were determined by using the molar absorptivities of each protein calculated from the composition of tryptophans, tyrosines and cysteines in the corresponding protein and with respective values of the molar absorptivities of 5600, 1400 and 127 l/mol · cm at 278 nm [23]. It has been shown that these residues are the only ones that contribute significantly to absorbance over the range 276–282 nm [23] and that the molar absorptivities calculated on this basis are very close to the measured values, with an average relative standard deviation of 3.8% [24]. Purification yields were calculated from ion-exchange chromatograms with reference to the amount of 30S subunits used. Degrees of purity were determined from reversed-phase chromatograms by comparing the amounts of all the other eluted proteins with the amount of wanted protein.

RESULTS AND DISCUSSION

TP30 were extracted from subunits with 4.5 *M* LiCl, which is the upper limit of LiCl concentration that can be employed for salt washing without denaturation of proteins [25,26]. The 21 salt-extracted 30S proteins were resolved into sixteen major peaks by using HPIEC with buffers A and B. Samples ranging from 50 to 200 μg of proteins gave typical chromatograms such as that presented in Fig. 1. Peak fractions were analysed by both RP-HPLC and one-dimensional PAGE. Under non-denaturing conditions, the elution was performed with a ionic strength 20% higher than that under denaturing conditions for the same duration of elution. The elution orders for cation-exchange HPLC on carboxymethyl (CM) supports eluted with 6 *M* urea buffers [13,17] are very similar to the conventional orders. Under non-denaturing conditions, a more pronounced difference exists (Table I). Because HPLC produces selective and rapid separations, it was expected that a single run would be sufficient to purify the major part of total ribosomal proteins but, as can be seen from Table I, only three peaks are pure (S4, S5 and S8). Attempts to increase the resolution by using a shallower gradient were unsuccessful. As has been reported previously using traditional methods [11], HPIEC offers higher resolution than classical chromatography, in which proteins disturb the chromatography, mainly S2, S3, S5 and S17 which are not eluted as single peaks, owing to complex formation or partial precipitation. It was found that only S4, S8, S10, S14 and S16 can be recovered with acceptable degrees of purity and yields by this method (see Table III).

To isolate the other proteins in a simple way with only two purification steps we carried out an initial fractionation of TP30 into two groups of various compositions according to the selected proteins. The choice of the prefractionation method is very important because it determines the final yield of the prepared proteins (see Table III). Two methods are generally used to split TP30 [11,21], HPSEC and LiCl salt washing, which are poorly selective and just allow the concentrations of the wanted proteins to increase in one of the groups to the detriment of the other. We shall give two examples to illustrate the purification methods with prefractionation.

Fractionation of TP30 by HPSEC is well suited to purifying the ribosomal proteins with a molecular mass ranging from 15 000 to 40 000 daltons. Fig. 2A shows a typical elution profile obtained from the Pharmacia Superose 12 column (the Superdex column gave similar results), where TP30 migrate in three groups (G1, G2 and G3). Table II presents the elution characteristics and the composition of the three

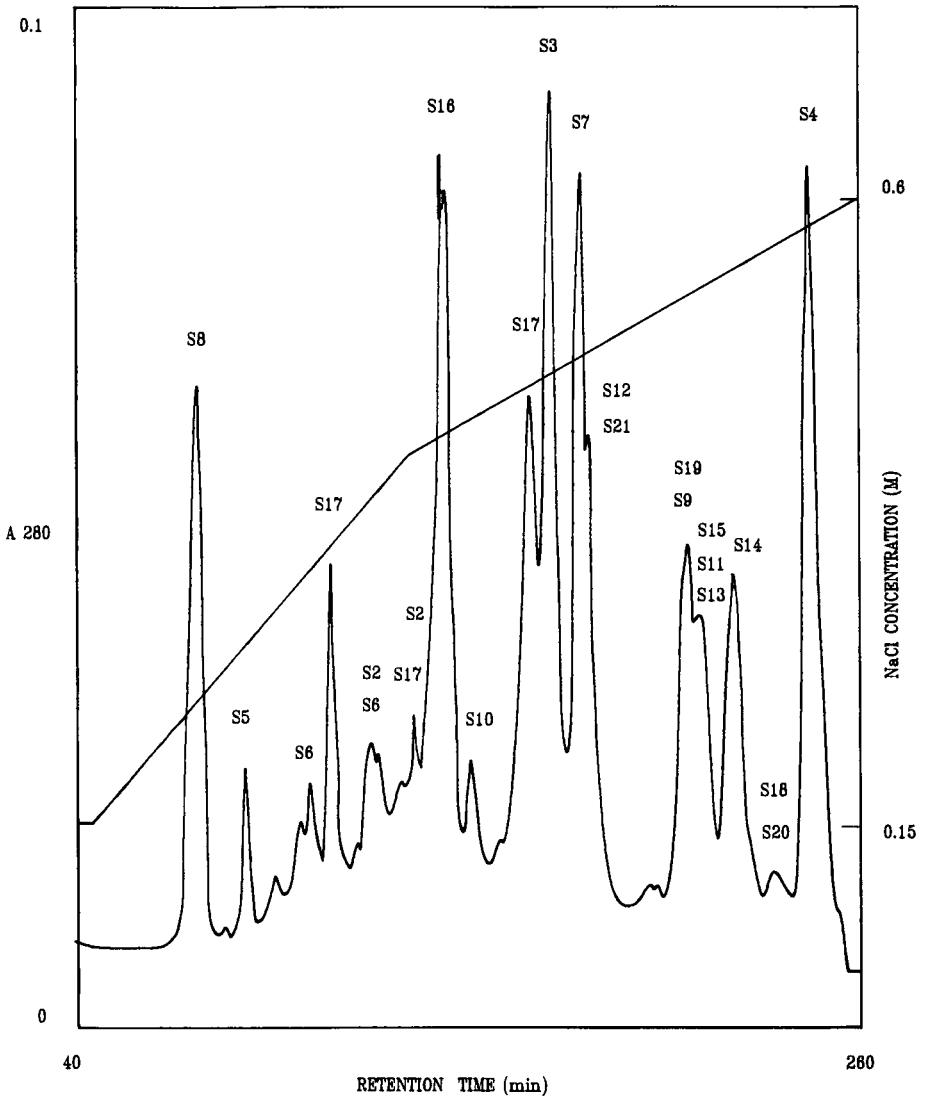

Fig. 1. HPIEC on TSK CM-3SW (150 × 7.5 mm I.D.) of TP30 under non-denaturing conditions. 50–200 μg of TP30 in 5–10 ml of buffer A with 0.15 *M* NaCl were applied to the CM column. Following a 30-min equilibration with buffer A–0.15 *M* NaCl, gradients were applied from 0.15 to 0.4 *M* over 50 min and from 0.4 to 0.6 *M* over 140 min. Note that absorbance scale (A_{280}) was changed to 0.2 unit after 145 min (elution time of S16).

selected groups, the first group consisting only of protein S1. Proteins are eluted roughly according to their molecular masses (M_r), with some exceptions. The principal anomaly is the presence of S7 (M_r = 19 732 [21]) in the third group, which is mainly constituted by proteins with molecular masses ranging from 8000 to 14 000 daltons. It should be noted that the resolution on silica-based columns such as TSK G2000 SW seems higher than that on organic-based material such as Pharmacia Superose or

TABLE I

CHARACTERISTICS OF ION-EXCHANGE HPLC OF TP30 PROTEINS UNDER NON-DENATURING CONDITIONS

Elution conditions as in Fig. 1.

Proteins	Peak No.															
	1	2	3	4	5	6	7	8	9	10	11	12	13	14	15	16
Main[a]	S8 (1)	S5 (3)	S6	S17	S2 (2)	S17	S16 (5)	S10 (1)	S17	S3 (4)	S7	S19	S15	S14 (6)	S18	S4 (7)
Others			S2	S2 S6	S17	S2	S2	S3 S5	S3 S5	S17 S14	S21 S12	S15 S9	S14 S13	S18	S20	
NaCl (%)[b]	23	26	32	34	37	40	41	42	45	46	47	51	52	54	56	57

[a] Previous results in parentheses [11].

[b] NaCl concentration in buffer B as reference.

Superdex [27]. It has been demonstrated [28] that the elution on a silica-based column not only depends on the protein sizes but also is strongly affected by the electrostatic interactions between the proteins and the support. This could explain the observed differences in resolution and elution order between the two types of supports, but here the difference is mainly due to the extraction methods for TP30, which was native in this work and denaturing in the studies of Kamp and Wittmann-Liebold [27].

Groups G2 and G3 were then rechromatographed by HPIEC as described above, to obtain purified proteins. Fig. 2B and C show the elution profiles of groups G2 and G3, respectively. Group G2 gives S2, S3, S4, S5 and S6 with degrees of purity better than 90% calculated from reversed-phase chromatograms and a small amount of S19–S13 complex. Group G3, mainly constituted of S7, S10, S14, S15, S16, S17, S18, S19 and S20, is more complicated to resolve because many proteins migrate together, *e.g.*, S7, S21, S12 and S19, S15, S13. If proteins of group G3 are wanted, a more suitable prefractionation must be applied using HPSEC to simplify the ion-exchange HPLC, by only collecting the fractions where the wanted proteins are eluted.

Fractionation of TP30 by LiCl salt washing was performed with concentrations of LiCl ranging from 1.5 to 3.5 *M*, which allowed the removal of increasing amounts of proteins from the subunits [7,8]. The major problem is that the composition of the groups is not well defined because it depends not only on LiCl concentration but also on Mg^{2+} concentration and ribosome subunit preparation. In addition, this fractionation is not selective and several proteins are present in two groups in various amounts. An example is 3.5 *M* LiCl treatment of 30S subunits. The two resulting groups are the core particles which are constituted of 16S rRNA in association with S4, S7, S8, S15, S16 and S17 and in reduced amounts with S6, S11, S18 and S19, and the split proteins, *i.e.*, S1, S2, S3, S5, S9, S10, S12, S13, S14, S20, S21 and S6, S11, S18, S19. Small amounts of core proteins S4, S7, S16 and S17 were always recovered in the split fraction. As shown previously (Fig. 3 [19]), from the group of core proteins we can purify S8, S17, S16, S7, S4, S15, S19 and S18 by using one HPSEC and one HPIEC step, but the purification of the other proteins from the split group was not greatly facilitated by this procedure owing to the bad selectivity of salt washing. To purify

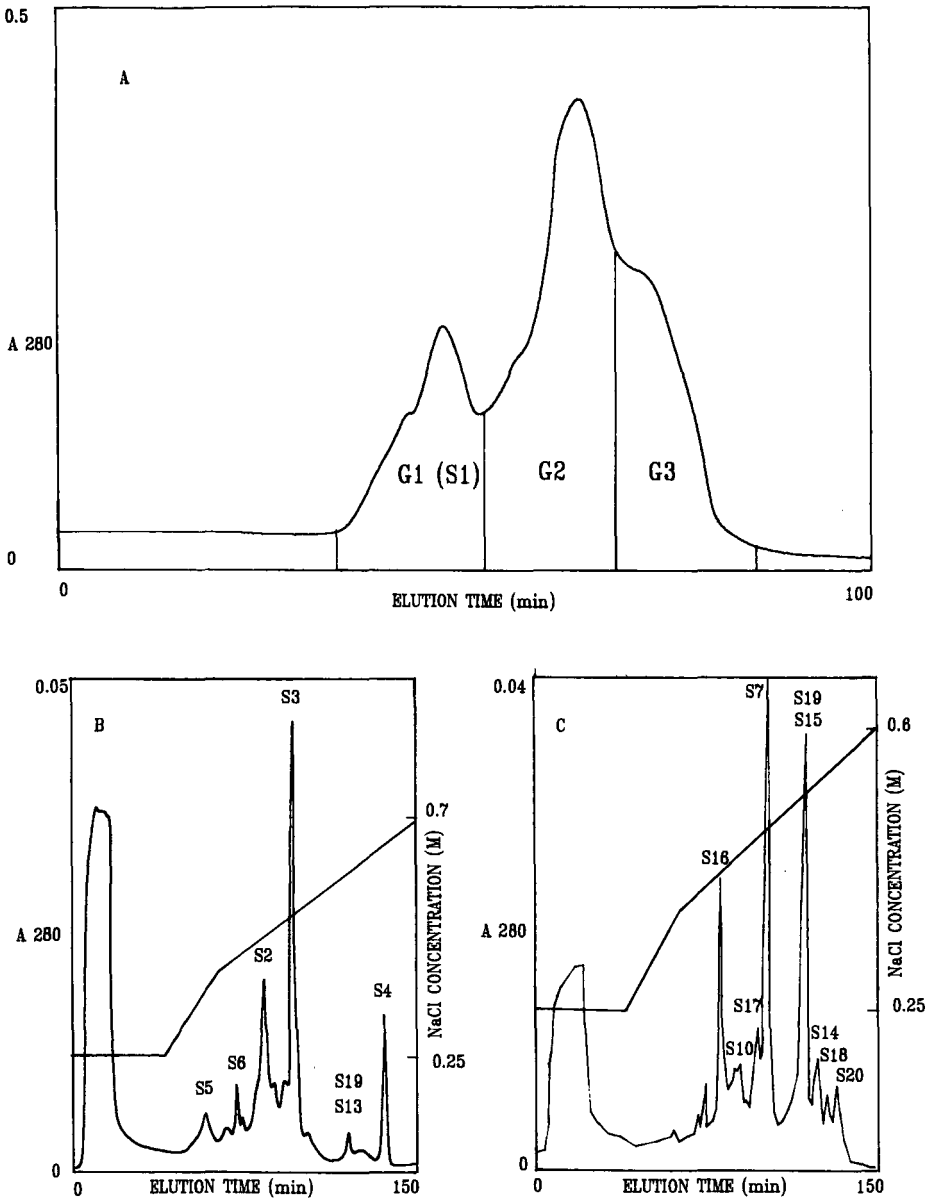

Fig. 2. (A) HPSEC of TP30 on Pharmacia Superdex XK 16/70 (60 × 1.6 cm I.D.) under non-denaturing conditions. About 1–10 mg of TP30 extract were injected in 4 ml of 4.5 *M* LiCl–TMK mixture. The proteins were eluted in TMK or buffer A with 0.15 *M* NaCl at a constant flow-rate of 1.0 ml/min. (B) Ion-exchange HPLC of the G2 proteins under non-denaturing conditions. 1–10 ml of concentrated G2 proteins in buffer A with 0.25 *M* NaCl were applied to the CM column. The gradient was started with eluent A–0.25 *M* NaCl over 30 min and then linearly increased to 0.4 *M* over 40 min and to 0.6 *M* over 80 min. (C) Ion-exchange HPLC of the G3 proteins under the same conditions in (B).

TABLE II

CHARACTERISTICS OF GEL PERMEATION HPLC OF TP30 UNDER NON-DENATURING CONDITIONS

Protein (molecular mass)	Elution volume (ml)													
	G1	G2					G3							
	52[a]	62	68	70	73	75	77	79	81	83	85	87	89	91
S1 (61 159)	★★[b]													
S2 (26 613)		★[b]	★★	★★										
S2 (25 852)			★★	★★	★★									
S4 (23 138)			★★	★★	★★									
S5 (17 514)			★	★★	★★	★								
S6 (15 200)			★	★★	★★	★								
S7 (19 732)								★	★★	★★	★			
S8 (12 196)						★	★★	★★	★					
S9 (14 569)				★	★	★	★	★	★	★				
S10 (11 736)									★	★★	★★	★		
S11 (13 788)						★	★★	★★	★					
S12 (13 608)											★	★★	★★	★
S13 (12 968)			★	★	★	★	★	★	★					
S14 (11 200)					★	★★	★★	★						
S15 (10 000)											★	★★	★★	★
S16 (9192)								★	★★	★★	★			
S17 (9573)								★	★★	★★	★			
S18 (8896)				★	★★	★★	★							
S19 (10 239)					★	★★	★★	★						
S20 (9553)									★	★★	★★	★		
S21 (8369)							★	★★	★★	★				

[a] Elution volume corresponding to the maximum value of A_{280}.

[b] The presence of large amounts of protein is indicated by two asterisks and of smaller amounts by one asterisk.

proteins of the split group more easily, a lower LiCl concentration must be used during the salt-washing step to reduce the number of split proteins and the concentration value adjusted with respect to the wanted proteins.

Table III lists the isolation conditions, yields and degrees of purity of sixteen proteins of the 30S subunit. It is clear that the core proteins are the easiest to prepare under non-denaturing conditions because of their good solubilities (1–5 mg/ml) and weak interactions between them, a single HPIEC run on TP30 can give S4, S8, S10, S14 and S16 and also S3, S5 and S17 with a degree of purity better than 90% but with poor yields because of co-migrations, the pre-fractionation by gel permeation leads to the purification of S1, S2, S3, S4, S5 and S6 with a lower yield than by direct HPIEC owing to the loss of material during HPSEC and the additional concentration step before the ion-exchange separation, the prefractionation by LiCl salt washing allows the purification of core proteins with yields greater than those obtained by the classical method and S9, S11, S12, S13 and S21 were not recovered in a pure form under these conditions.

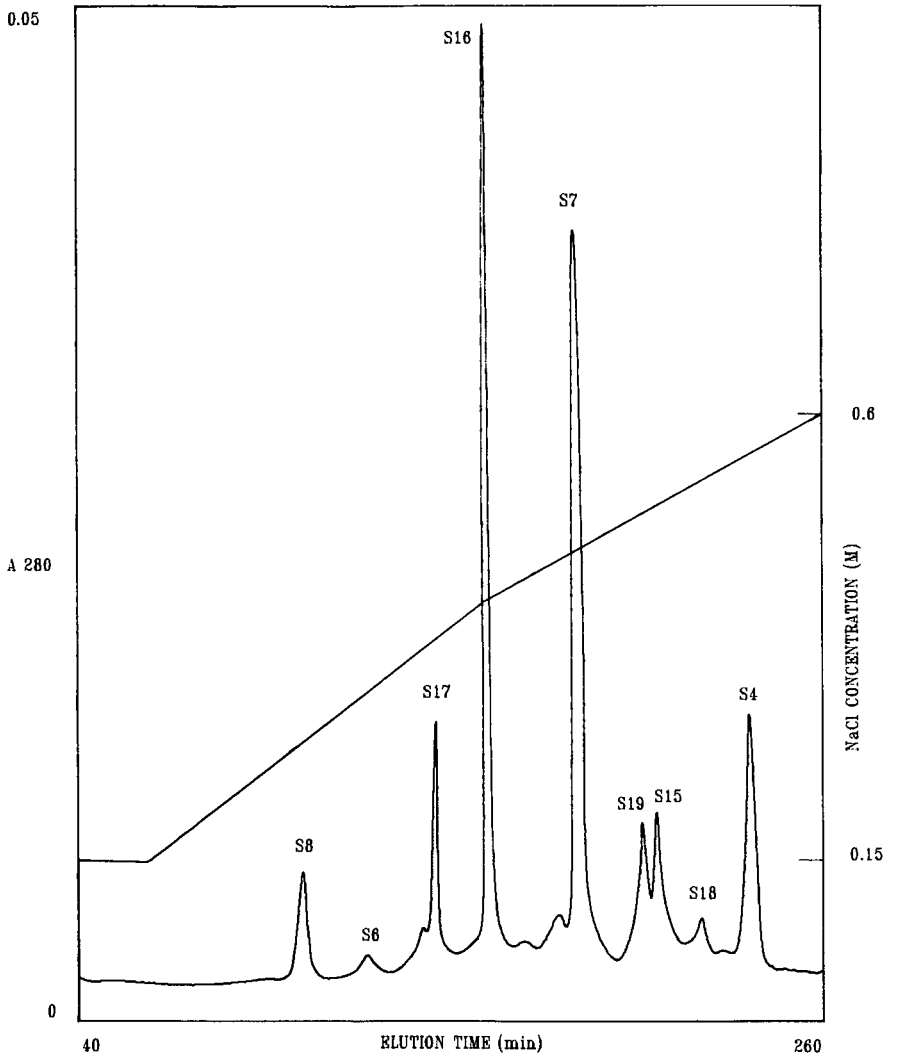

Fig. 3. HPIEC of core proteins under non-denaturing conditions. 50 A_{280} of core proteins (obtained by centrifugation) in 2–3 ml of buffer A with 0.15 *M* NaCl were applied to the CM column. An elution gradient identical with that in Fig. 1 was used.

CONCLUSIONS

We have shown that it is possible to prepare fresh samples of sixteen 30S proteins under non-denaturing conditions. Under these conditions, HPIEC is the most suitable technique for the isolation of 30S proteins. RP-HPLC was only used here as an analytical technique. Although the selectivity and rapidity of HPIEC improved the separation in comparison with conventional chromatographic methods, this was not sufficient to eliminate completely co-migration along the column owing to complex

TABLE III

SEPARATION METHODS FOR TP30 WITH YIELDS AND DEGREES OF PURITY

Protein	Ion-exchange on TP30		Size-exclusion + ion exchange (groups G1, G2, G3)		Salt washing[a] + ion exchange (core proteins)	
	Yield (%)	Purity (%)	Yield (%)	Purity (%)	Yield (%)	Purity (%)
S1			24	>95		
S2			23	>95		
S3	25	>90	26	>95		
S4	70	>95	15	>95	50	>95
S5	25	>95	10	>95		
S6			5	>95	15	>95
S7	20	>90			60	>95
S8	95	>95			90	>95
S9						
S10	44	>95				
S11						
S12						
S13						
S14	70	>95				
S15					>50	>90
S16	90	>95	22	>95	100	>95
S17	25	>90			40	>95
S18					50	>95
S19					40	>90
S20			27	>95		
S21						

[a] Previous results [19].

formation and partial precipitation. It was found that prefractionation of the proteins into groups by salt washing or by HPSEC improves significantly the fraction purity, but this does not lead to major simplification of the procedure, but only allows the composition of one group to be made suitable in relation to the proteins to be purified. Protein recoveries are generally higher than those obtained by the conventional method (see Table III), with values ranging from 10 to 90%. Further, it was possible to purify several proteins such as S7, S15 and S18 that are not recovered by traditional methods in good yield.

Samples prepared by this method can be used directly for optical studies, in particular for circular dichroism spectroscopy, owing to the simplicity of the buffers used. The amounts recovered, ranging from 0.05 to 0.1 mg/ml, allow the direct use of the peak fractions for these optical studies, whereas NMR studies requiring larger amounts of proteins need a preparative-scale separation.

REFERENCES

1 A. Liljas, *Prog. Biophys. Mol. Biol.*, 210 (1982) 161.
2 V. Mandiyan, S. Tumminia, J. S. Wall, J. F. Hainfeld and M. Boublik, *J. Mol. Biol.*, 210 (1989) 323.
3 V. D. Vasiliev and V. E. Koteliansky, *FEBS Lett.*, 76 (1977) 125.

4 R. A. Zimmerman, in G. Chambliss, G. R. Craven, J. Davies, K. Davis, L. Kahan and M. Nomura (Editors), *Ribosomes, Structure, Functions and Genetics*, University Park Press, Baltimore, 1980, p. 135.
5 R. Brimacombe, J. Atmadja, W. Stiege and D. Schuler, *J. Mol. Biol.*, 199 (1988) 115.
6 S. Stern, B. Weiser and H. F. Noller, *J. Mol. Biol.*, 204 (1988) 447.
7 T. Itoh, E. Otaka and S. Osawa, *J. Mol. Biol.*, 33 (1968) 109.
8 A. Atsmon, P. Spitnik-Elson and D. Elson, *J. Mol. Biol.*, 25 (1967) 161.
9 J. Dijk, J. A. Littlechild, A. M. Freund, J. Pouyet, M. Daune and S. W. Provencher, *Biochim. Biophys. Acta*, 874 (1986) 227.
10 J. A. Littlechild, A. Malcolm, K. Paterakis, I. Ackermann and J. Dijk, *Biochim. Biophys. Acta*, 913 (1987) 245.
11 J. Dijk and J. A. Littlechild, *Methods Enzymol.*, 59 (1979) 481.
12 A. R. Kerlavage, C. J. Weitzmann, T. Hasan and B. S. Cooperman, *J. Chromatogr.*, 266 (1983) 225.
13 R. M. Kamp, A. Bosserhoff, D. Kamp and B. Wittmann-Liebold, *J. Chromatogr.*, 317 (1984) 181.
14 P. J. Flamion and J. P. Schreiber, *Anal. Biochem.*, 147 (1985) 458.
15 M. Capel, D. Datta, C. R. Nierras and G. R. Craven, *Anal. Biochem.*, 158 (1986) 179.
16 B. S. Cooperman, C. J. Weitzmann and M. A. Buck, *Methods Enzymol.*, 164 (1988) 523.
17 R. J. Ferris, C. A. Cowgill and R. R. Traut, *Biochemistry*, 23 (1984) 3434.
18 P. Stiegler, M.-L. Hartmann and J.-P. Ebel, *Biochimie*, 68 (1986) 587.
19 C. Cachia, P.-J. Flamion and J.-P. Schreiber, *J. Chromatogr.*, 498 (1990) 417.
20 S. J. S. Hardy, C. G. Kurland, P. Voynow and G. Mora, *Biochemistry*, 8 (1969) 2897.
21 S. Yu. Venyaminov and Z. V. Gogia, *Eur. J. Biochem.*, 126 (1982) 299.
22 P. S. Leboy, E. C. Cox and J. G. Flaks, *Proc. Natl. Acad. Sci. U.S.A.*, 52 (1964) 1367.
23 H. Edelhoch, *Biochemistry*, 6 (1967) 1948.
24 S. C. Gill and P. H. Von Hippel, *Anal. Biochem.*, 182 (1989) 319.
25 S. Maruyama, K. Kuwajima, K. Nitta and S. Sugai, *Biochim. Biophys. Acta*, 494 (1977) 343.
26 F. Ahmad, *J. Biol. Chem.*, 258 (1983) 11143.
27 R. M. Kamp and B. Wittmann-Liebold, *Methods Enzymol.*, 164 (1988) 542.
28 F. Regnier, *Methods Enzymol.*, 91 (1983) 137.

Journal of Chromatography, 539 (1991) 355–362
Elsevier Science Publishers B.V., Amsterdam

CHROM. 22 905

Immobilized Cibacron Blue —leachables, support stability and toxicity on cultured cells

I. HULAK
IBF-Biotechnics, 35 Avenue Jean Jaurès, 92390 Villeneuve la Garenne (France)
C. NGUYEN
IMEDEX, B.P. 38, 69630 Chaponost (France)
and
P. GIROT and E. BOSCHETTI*
IBF-Biotechnics, 35 Avenue Jean Jaurès, 92390 Villeneuve la Garenne (France)

ABSTRACT

Although immobilized dyes are widely used on the laboratory scale and have good potential for industrial applications, they are still subject to some reservations. Little information is available about dye leakage and toxicity, which seriously hinders the use of such supports in the production of pure proteins. Investigations of the leakage mechanism and the *in vitro* toxicity of the native dye and of that leached from the column are reported. The possible presence of traces of dye in the purified biological materials necessitates the availability of sensitive analytical tests. The preparation and preliminary isolation of dye antibodies as a first step in the development of an immunohistochemical assay of leached dyes are also described.

INTRODUCTION

Chromatography is probably the most widely used method for the purification of enzymes and proteins. Interest is linked to the possibility of obtaining very pure substances, not only on the laboratory scale but also at the industrial level. Today, process chromatography is applied to the purification of many biological materials used in diagnostics and therapeutics.

It is obvious that at the level of industrial exploitation leading to the purification of a therapeutic product, the polymeric chromatographic support must be sufficiently stable and not release oligomers or other trace chemicals that could be toxic or have a secondary action. From this point of view, a number of experiments were performed in our laboratories to determine the level of leachables and undesirable products that might be present in the chromatographic supports.

An example of studies of leaching and toxicity is provided by immobilized dyes. Cibacron Blue F3 GA (Ciba Geigy) immobilized on a solid matrix provides adsorbents with high efficiency and specificity such that these supports are very attractive for application at the preparative level [1,2]. However, the dye may be leached under certain physico-chemical conditions and it is then necessary not only to determine the

0021-9673/91/$03.50

amount of ligand in the column effluents but also to establish its possible toxicity. This paper reports results on measurements of leached dye on agarose-based sorbents, the *in vitro* toxicity of the leached dye and preliminary results on the preparation and purification of specific antibodies against the dye.

EXPERIMENTAL

Native Cibacron Blue F3 GA was obtained from Fluka (Buchs, Switzerland), immobilized dyes on agarose-cross-linked beads from suppliers such as Pharmacia–LKB (Uppsala, Sweden) and Amicon (Danvers, MA, U.S.A.), foetal bovine serum culture media and all other chemicals for eukaryotic cell culture from Gibco-BRL (Paisley, U.K.) and biological materials such as bovine serum albumin (BSA), human haemoglobin and antibodies from Sigma (St. Louis, MO, U.S.A.). All other chemicals were of analytical-reagent grade. Chromatographic sorbents such as DEAE-Trisacryl Plus, protein A–Spherodex and Blue-Trisacryl were supplied by IBF-Biotechnics (Villeneuve la Garenne, France).

Determination and collection of leached dye

Agarose-immobilized Cibacron Blue was washed repeatedly on a Büchner funnel with water and packed into 50-ml columns. The sorbent was then perfused with acidic, neutral and alkaline solutions for several hours at room temperature and the effluents were collected. The dye present in the effluents was determined by spectrophotometry at 608 nm using a calibration curve from native Cibacron Blue. The sensitivity of this determination was close to 1 mg/l of dye.

In vitro cell culture

MRC-5 human cells were cultured in classical conditions in DMEM medium containing 10% foetal bovine serum at 37°C. Following WHO recommendations, MRC-5 cells were taken at the 29th passage and cultured over 25 days up to the 35th passage. Parallel cultures were realized: in the absence of any additive (standard culture), in the presence of 25 μg/ml of native Cibacron Blue and in the presence of 25 μg/ml of leached dye from agarose beads. Growth curves were determined by counting the cells and by calculating the cell division rate. The morphology of MRC-5 cells was also checked during the *in vitro* culture.

Determination of polyploidia level

At the 36th passage and after 72 h, cultured MRC-5 cells were submitted to another passage during which the mitosis were blocked. Under these conditions and after a hypotonic shock, chromosomes were fixed and spread out, then submitted to an acidic hydrolysis and subsequently stained. The proportion of polyploidic cells was determined on each culture slide.

Determination of in vitro genotoxic effect

The genotoxic effect of free Cibacron Blue was determined using the SOS-Chromotest. The standard genotoxic agent used was 4-NQO (4-nitroquinoline oxide) as recommended by the *in vitro* test supplier.

Preparation of polyclonal antibodies

Polyclonal antibodies of Cibacron Blue were prepared using a protein–dye conjugate. The free dye is actually non-antigenic and the preparation of antibodies can be accomplished only with an appropriate carrier.

As carrier we used BSA, which was first mannosylated and then couped with the dye. The latter operation was effected by simple contact of albumin and the dye (Cibacron is a preactivated dye) under alkaline conditions overnight. The solution was then neutralized and desalted by gel filtration through a Trisacryl GF 05 column to remove the excess of free dye. The resulting albumin–dye covalent complex was used for the immunization of rabbits under classical conditions and in association with Freund's additive. The methodology of immunization used was classical: injection of 1 mg of antigen per week for 3 weeks. Another injection was also effected after 3 weeks of rest. The antibodies were detected in the rabbit blood by an enzyme-linked immunosorbent assay (ELISA) test using as competitor a complex of human haemoglobin and Cibacron Blue obtained as described above for BSA.

Purification of Cibacron Blue antibodies

The chromatographic strategy followed to separate antibodies from hyper-immunized rabbit serum was based on three principles: whole rabbit immunoglobulins G (IgG) could be separated from plasma in one step on DEAE-Trisacryl Plus as previously described [3]; whole rabbit immunoglobulins G could be separated specifically in a single step using immobilized protein A; and antibodies against Cibacron Blue should be biospecifically adsorbed on immobilized dye and then separated from other proteins.

In the first series of trials rabbit immunized serum was injected directly onto a column of DEAE-Trisacryl Plus previously equilibrated with 0.025 *M* Tris–HCl buffer (pH 8.5) containing 25 m*M* sodium chloride. Different fractions obtained under a salt elution gradient were collected and then analysed (Fig. 3A).

In a second series of trials, an affinity purification was effected on a column of protein A–Spherodex. The whole immunized rabbit serum was first diluted with an equal volume of 1.5 *M* glycine–NaOH buffer containing 2 *M* sodium chloride (pH 8.9) and then injected into the affinity column previously equilibrated with the same buffer. After washing, the adsorbed immunoglobulin G was eluted by injecting 1 *M* acetic acid (Fig. 3B).

As a third approach, a column containing 7 ml of Blue-Trisacryl was equilibrated with phosphate-buffered saline (PBS) and then the whole immunized rabbit serum was injected after PBS equilibration (2 ml of rabbit serum). After washing with PBS until elimination of non-adsorbed proteins, a first elution was done using 0.1 *M* sodium chloride. A second elution using the same buffer containing 1 *M* sodium chloride followed (Fig. 3C). All the fractions collected from the three columns were analysed by gel electrophoresis and by Ouchterlony double diffusion [4] against Cibacron Blue-substituted haemogolobin and BSA.

RESULTS AND DISCUSSION

It has been clearly demonstrated that most of the leached dye resulted from the acidic washings of the agarose-based sorbents. The amount of leached dye was

between 0.2 and 1.7 μg per millilitre of sorbent (depending on the pH). In comparison, a dye coupled to a synthetic sorbent did not show any leakage effect when exposed to the same acidic conditions. This phenomenon was correlated with the sensitivity of agarose to acidic media (pH < 4) as demonstrated previously [5]. An NMR spectrum of the column effluent showed that the dye containd a certain number of osidic linkages (*i.e.* linkages between sugars) related to the presence of a glycosidic part on the dye [6] (results not shown). This result indicates that the dye leakage was in fact the result of partial hydrolysis of the agarose chain supporting a molecule of dye covalently immobilized.

The *in vitro* cell culture of MRC-5 human cells showed that the lethal dose of dye was *ca.* 200–250 μg/ml. At this concentration, the cells did not adhere to the surface of the dish and then died. This is why we used 25 μg/ml of dye in the culture medium, which was compatible with cell adherence. At this concentration, the MRC-5 culture study showed a significant decrease in the division time when the medium contained 25 μg/ml of leached dye (Fig. 1). The size of the cells at the end of the culture was smaller when compared with a standard culture (microscopic observation). Conversely, the native dye did not seem to influence the cell division. The growth curve was very similar to the standard one. In addition, no morphological modification was detected [6]. A chromosome analysis (polyploidia) of MRC-5 collected after the 36th passage (after 22 days of culture) over thousands of metaphases indicated that no modification was induced in the presence of the native Cibacron Blue. The polyploidia level was actually of 6/512 (average) and was very close to the standard cell culture (7/520 on average). Both results were significantly lower than the WHO reommendations (17/520). The polyploidia level of the cells cultured in the presence of leached dye was significantly higher, however, above the limits of acceptance (see Table I).

Genotoxic studies performed with the SOS-Chromotest indicated the absence of any toxicity at concentrations far higher than those usually utilized. The dye genotoxic activiy, when compared with that of 4-NQO, was about three orders of magnitude lower (Fig. 2).

These studies were carried out at high concentrations of dye (from 25 to 500

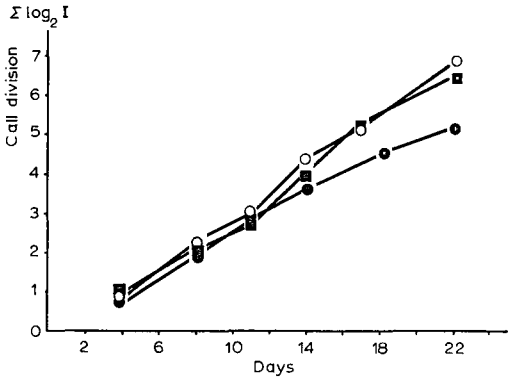

Fig. 1. Growth curves of MRC-5 human cells *in vitro* over six passages in classical conditions (from the 29th to the 35th passage). Cultures were effected in DMEM medium containing 10% of foetal bovine serum in the presence of 25 μg/ml of (■) native Cibacron Blue (NCB) or (●) leached dye (LCB). (○) Standard curve obtained in the absence of dye (FBS).

TABLE I

POLYPLOIDIA RESULTS FOR CULTURED MRC-5 CELLS IN THE PRESENCE OF CIBACRON BLUE AT THE 36th PASSAGE

Slide No.	Standard curve	MRC-5 + NCB[a] (25 μg/ml)	MRC-5 + LCB[b] (25 μg/ml)
1	9/538	5/536	23/528
2	5/503	6/503	15/512
3	8/510	9/513	17/522
4	5/529	5/502	18/508
Average	7/520	6/513	18/517

[a] NBC = Native Cibacron Blue.
[b] LBC = Leached Cibacron Blue.

μg/ml) whereas the amounts that possibly leaked during a chromatographic run were usually less than 1 μg/ml.

These preliminary data made it clear that the toxicity studies whould be extended to other determinations *in vitro* and/or *in vivo*. However, to improve the accuracy of these investigations, we thought that a more sensitive method of dye detection was essential, because the spectrophotometry is not sensitive enough and there is no easy means of localizing the dye once it has been incorporated into the cell. Hence the preparation of antibodies against Cibacron Blue was investigated. It was found that when the dye coupled with BSA was injected directly into rabbits, no antibody response was detected. However, in association with Freund's additive, a positive response was obtained in three out of four rabbits. The amount of secreted antibodies (determined empirically by measurement of the detection limit) was not constant from

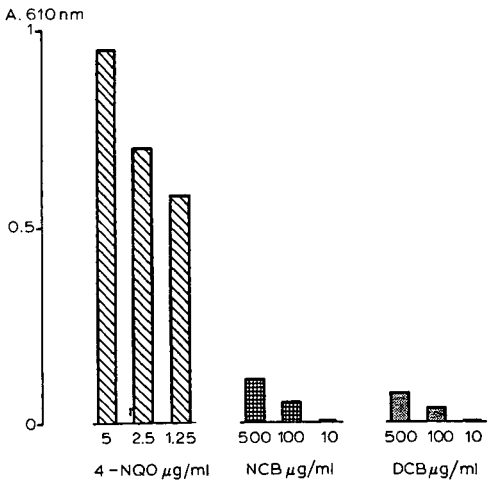

Fig. 2. Genotoxic results obtained using SOS-Chromotest. The standard genotoxic agent was 4-NQO. NBC = native Cibacron Blue; DCB = deactivated Cibacron Blue. The absorbance at 610 nm was the result of the final enzymatic activity induced by the genotoxic effect of the chemicals.

TABLE II

DETECTION DILUTION LIMITS OF SECRETED ANTI-CIBACRON BLUE ANTIBODIES

Days of immunization	Dilution limit of antibody detection	
	Rabbit 1	Rabbit 2
51	800	800
70	800	1600
85	800	3200
105	1600	3200
140	3200	6400
189	3200	N.D.

rabbit to rabbit (see Table II), but in more than 50% of the rabbits the secretion level was acceptable and increased week after week.

Table III and Fig. 3 show the main results of the isolation of anti-Cibacron Blue antibodies using three different approaches. Whole immunoglobulins G with good purity were obtained using DEAE-Trisacryl Plus, protein A–Spherodex or Blue-Trisacryl. In the first instance, most of the IgG, including specific Cibacron Blue antibodies, were present in the flow-through as expected [3]. This fraction contained only a few contaminants in small amounts; the purity determined by electrophoresis was in fact 95%. In the second instance the IgG fraction, obtained by acidic elution, contained most of the rabbit IgG and all Cibacron Blue antibodies. The purity of this fraction was similar to those obtained by ion exchange; however, the yield was higher (about 60%) than in the DEAE-Trisacryl Plus fractionation.

Blue-Trisacryl allowed us to obtain fairly pure antibodies (about 95% by electrophoresis) in one step using the described conditions. The fraction containing the Cibacron Blue antibodies was obtained by elution with 0.1 *M* sodium chloride. This fraction was not contaminated by the presence of albumin, which is known to have a high affinity for Cibacron Blue [7,8]; albumin was actually eluted quantitatively by 1 *M* sodium chloride washing. The agarose double diffusion experiments show that the

TABLE III

MAIN RESULTS ON THE SEPARATION OF IgG FROM IMMUNIZED RABBIT BY VARIOUS CHROMATOGRAPHIC PROCEDURES

Protein fraction	Chromatography	IgG purity (average) (%)	Presence of Cibacron Blue antibodies	IgG Yield (average) (%)
Whole serum	–	18–20	+	100
Flow-through DEAE-Trisacryl	Ion-exchange	95	+	>40
Fraction adsorbed on protein A-Spherodex	Affinity Fc fragment	95	+	>60
0.1 *M* NaCl elution on Blue-Trisacryl	Affinity Fab fragment	90	+	>90

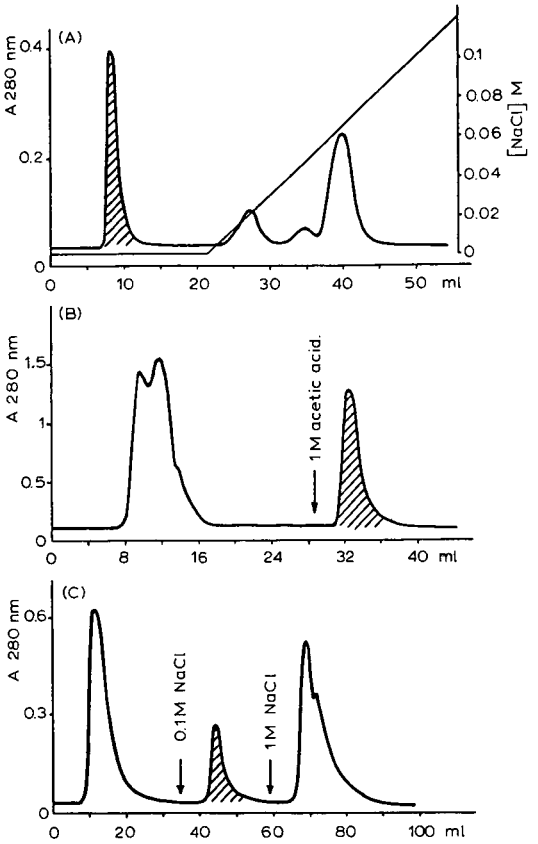

Fig. 3. Chromatographic profiles of IgG separation from immunized rabbit serum against Cibacron Blue. (A) Fractionation obtained by ion-exchange chromatography on DEAE-Trisacryl Plus; (B) fractionation obtained by affinity chromatography of IgG on protein A–Spherodex; (C) fractionation of anti-Cibacron Blue antibodies by affinity chromatography on Blue-Trisacryl. The sample in all instances was whole rabbit serum, previously equilibrated with the starting buffer. The grey areas indicate the localization of anti-Cibacron Blue antibodies. For further details, see Experimental.

anti-Cibacron Blue antibodies present in the flow-through of the DEAE-Trisacryl Plus column and in the absorbed fraction of protein A–Spherodex were contaminated by anti-BSA antibodies and other immunoglobulins. These sorbents in fact do not discriminate between the different categories of immunoglobulins G. On the other hand the Blue-Trisacryl active fraction (Fig. 3C) did not show any cross-reaction with BSA, demonstrating the absence of BSA antibodies. The latter were found in the flow-through of this column.

These antibodies of different purity will be used for the preparation of an ELISA-like or immunometric detection assay for free and leached dye from specific affinity sorbents.

CONCLUSION

This preliminary work demonstrated that at acidic pH, the agarose-based immobilized dyes are not stable. This instability seems to be related more to the matrix instability than to linkage breaking between the dye and the support. The leaked dye, which seemed to be associated with a small part of polysaccharide, modified the growth rate of the *in vitro* human MRC-5 cell culture and increased significantly the number of polyploidic cells. As these effects were not observed with a free native dye, a preliminary conclusion could be made that the osidic part of the leached dye was responsible for the difference. At this stage, models of dyes coupled with sugars should be synthesized and submitted to similar tests. On the other hand, we demonstrated that it was possible to synthesize and purify active antibodies against dyes, which represents a useful alternative to a spectrophotometric assay for the determination of traces of dyes.

ACKNOWLEDGEMENTS

This work was partially supported by a grant from the French Minister of Research and Technology as a part of EUREKA project EU-384.

REFERENCES

1 R. K. Scopes, *Anal. Biochem.*, 165 (1987) 235.
2 R. F. Sherwood, R. G. Melton, S. H. Alwan and P. Hugues, *Eur. J. Biochem.*, 148 (1985) 447.
3 G. Corthier, E. Bochetti and J. Charley-Poulain, *J. Immunol. Methods*, 66 (1984) 75.
4 O. Ouchterlony, *Prog. Allergy*, 5 (1958) 1.
5 E. Boschetti in C. Doinel (Editor), *Protein Purification Technologies*,G.R.B.P., Paris, Vol. 3, 1988, p. 23.
6 S. Oulieu, F. Viliamier, M. Allary, E. Boschetti and C. Nguyen, preliminary communication, *Proc. Symp. Protein–Dye Interactions, Compiègne,* 1988, unpublished results.
7 J. Travis and R. Pannell, *Clin. Chim. Acta*, 49 (1973) 49.
8 J. Saint-Blancard, E. Boschetti, P. Riberon, P. Claudel, P. Girot and M. Allary, *Sci. Tools*, 32 (1985) 37.

Journal of Chromatography, 539 (1991) 363–371
Elsevier Science Publishers B.V., Amsterdam

CHROM. 22 894

Tandem immunoaffinity and reversed-phase high-performance liquid chromatography for the identification of the specific binding sites of a hapten on a proteic carrier

M. YVON
Station de Recherches Laitières, CRJ–INRA, 78352 Jouy-en-Josas (France)
and
J. M. WAL*
Laboratoire de Nutrition et Sécurité Alimentaire, CRJ–INRA, 78352 Jouy-en-Josas (France)

ABSTRACT

Immunoaffinity (IA) and reversed-phase (RP) high-performance liquid chromatography were combined for the identification of the specific binding sites of benzylpenicilloyl (BPO) groups on human serum albumin (HSA). Tryptic hydrolysates of BPO–HSA were loaded on the IA column. BPO-peptides were desorbed and concentrated directly on the RP column, coupled via a switching valve, then separated by using gradient elution and identified by the amino acid sequences. This single-step procedure permitted more than 95% recovery of the BPO-peptides present in minute amounts, with good specificity.

INTRODUCTION

Like most drugs, penicillin is not immunogenic by itself. Allergic accidents occurring after penicillin therapy or consumption of food from penicillin-treated animals are mainly due to benzylpenicilloyl (BPO)–protein conjugates. These allergenic compounds result from the cleavage of the β-lactam ring of penicillin G and formation of covalent bond between the carbonyl of BPO and ε-amino groups of proteins. In man or animals treated with penicillin, the main proteic carrier for BPO is the serum albumin. *In vitro*, under physiological conditions of pH and temperature, human serum albumin (HSA) can also be penicilloylated to form HSA–BPO conjugates similar to those occurring *in vivo*. The mechanism of protein penicilloylation, based on a nucleophilic attack of penicillin by NH_2 groups of albumin, needed to be confirmed as previous observations suggested that among the various (*ca.* 60) ε-amino groups of lysine present in albumin, only a few of them were available for penicillin aminolysis [1].

The study of the specific binding sites of a ligand (such as a hapten) covalently bound on a proteic carrier needs first the preparation and the chromatographic separation and purification of peptides from the original conjugate and second hapten detection on each peptide using a specific method. This procedure was used by Walker

0021-9673/91/$03.50

[2] to identify the binding site of acetylsalicylic acid on human serum albumin. We have localized BPO groups on a fragment of albumin from a penicillin-treated patient by the same method, which needs numerous steps and is time consuming [3].

Several workers have used a two-step approach; the first is affinity chromatography and the second. reversed-phase high-performance liquid chromatography (RP-HPLC) to separate the peptides retained on the affinity column. This approach was used by Iberg and Flückiger [4] to identify the glycosylated sites on albumin from a diabetic patient and by Lafaye and Lapresle [5] to search for BPO-binding sites on HSA from penicillin-treated patients. However, the separation of peptides on a low-pressure affinity column takes several hours and often needs large amounts of material (100–300 mg of proteins).

Tandem immunoaffinity and RP-HPLC have already been used for various studies such as the determination of recombinant leucocyte interferon α-2 in complex mixtures [6] and to discriminate between similar structural forms of proteins [7]. We have tried to use this method to isolate specifically penicilloylated peptides from hydrolysates of BPO–HSA conjugates obtained from penicillin-treated patients. Only very small amounts of such samples were available. We compared this binding with that occurring on a conjugate prepared *in vitro*.

EXPERIMENTAL

Reagents and penicilloylated albumins

For HPLC, all the chemicals used were of HPLC grade. For amino acid analysis and for recurring Edman degradation, the chemicals used were of Sequanal grade (Pierce). Other reagents were of analytical-reagent grade.

Penicilloylated albumins prepared from sera from three penicillin-treated patients [1,3] were obtained from the Institut Pasteur (Paris, France). A BPO–HSA conjugate was prepared *in vitro* as described [3].

Approximately two BPO groups were covalently fixed per mole of HSA in the case of the *in vitro* conjugate. Concerning the penicilloylated albumins obtained from the patients, 2.8–3 BPO groups were determined per mole of HSA. However, it should be noted that in each instance, these penicilloylation rates are mean values corresponding to the average number of BPO groups measured on the whole population of penicilloylated albumin molecules. It does not mean that all the molecules have fixed two (or three) BPO groups; some might have fixed more BPO groups whereas others might have fixed only one group.

Digestion of penicilloylated albumins

Cyanogen bromide digestion of penicilloylated albumins and HPLC separation of fragments

Cyanogen bromide (CNBr) cleavage was carried out on 2 mg of BPO–albumin and separation of fragments $A_{299\text{-}585}$, $B_{1\text{-}123}$ and $C_{124\text{-}298}$ was performed by RP-HPLC as described previously [8].

Reduction and carboxymethylation of the CNBr fragment C

Denaturation, disulphide cleavage and alkylation were performed as described by Swenson *et al.* [9]. A 10-nmol sample of fragment C was dissolved in 1 *M* Tris–HCl buffer (pH 8.0) containing 6 *M* urea and a 10-fold molar excess of dithiothreitol over the SH concentration and kept overnight at 40°C under a nitrogen atmosphere.

Iodoacetic acid in 1 *M* NaOH (1.3-fold molar excess over total thiols) was added and the mixture was maintained in the dark for 4 h, before the reaction was stopped by addition of 5 μl of β-mercaptoethanol. Desalting of the mixture was performed by RP-HPLC: 100 μl were injected onto an Aquapore RP-300 (7 μm) column (30 × 4.6 mm I.D.) (Brownlee), equilibrated in a mixture of 50% solvent A [0.05% aqueous solution of trifluoroacetic acid (TFA)] and 50% solvent B [acetonitrile–2-propanol–0.05% TFA in water (2:1:2, v/v/v)]. Elution of fragment C was achieved with a 30-min linear gradient from 50 to 100% of solvent B at a flow-rate of 1.0 ml/min. Runs were performed at room temperature and peptides were detected at 215 nm. The reduced C-containing fractions were pooled and the solvent was removed using a Speed-Vac evaporator.

Tryptic digestion

Tryptic digestion was performed on reduced fragment C in 0.1 *M* phosphate buffer (pH 7.8) overnight at room temperature using L-1-tosylamide-2-phenylethyl chloromethyl ketone (TPCK)–trypsin (Sigma) (molar ratio enzyme/substrate, E/S = 1/50). The enzymatic reaction was stopped by heating at 100°C for 10 min.

Isolation and separation of the penicilloylated fragments from tryptic digest

Preparation of immunoaffinity column (IAC)

Purification of antipenicilloyl antibodies. Rabbit anti-BPO antisera were obtained as described previously [10]. An HSA–BPO conjugate (5 mol BPO/mol HSA) was prepared at alkaline pH and in the presence of a 10-fold molar excess of penicillin.

An Ultraffinity-EP column (50 × 46 mm I.D.) (Beckman) was derivatized by recycling a solution of HSA–BPO conjugate (200 mg) in 20 ml of 1 *M* potassium phosphate buffer (pH 7.0) at 0.2 ml/min for 18 h. The derivatized column was then washed with 0.1 *M* potassium phosphate (pH 7.0) at 1.0 ml/min for 1 h and converted to the loading buffer [0.02 *M* phosphate–0.2 *M* NaCl (pH 7.0)].

Rabbit anti-BPO antisera were dialysed with the loading buffer and 5–10 ml were loaded onto the column at 1.0 ml/min. The column was washed with 10 ml of loading buffer at the same flow-rate. The anti-BPO antibodies were eluted with 7 ml of 0.01 *M* HCl (pH 2) at the same flow-rate. The column was then re-equilibrated with loading buffer.

Column derivatization with antipenicilloyl antibodies. A 13-mg sample of antipenicilloyl antibodies purified as described before was dissolved in 18 ml of 1 *M* phosphate buffer (pH 7.0) and recycled through an Ultraffinity-EP column (50 × 4.6 mm I.D.) overnight at 0.2 ml/min. An 8-mg sample of antibodies was then immobilized. The column was washed with 1 *M* phosphate buffer (pH 7.0) at 1.0 ml/min for 1 h and stored in the same buffer until needed. It was equilibrated with 10 m*M* phosphate buffer (pH 7) containing 8 g/l NaCl [phosphate-buffered saline (PBS)] before use.

Apparatus

The immunoaffinity column was connected to a reversed-phase column (Nucleosil $5C_{18}$, 250 × 46 mm I.D.) (Société Française Chromato Colonne, Neuilly-Plaisance, France) via a six-way valve (Rheodyne, Cotati, CA, U.S.A.) as described by Rybacek *et al.* [6]. The switching valve contained the affinity column in place of a sample loop. The position of the switching valve determined whether the immunoaffinity and analytical columns would be used in series or separately.

Production and separation of the penicilloylated fragments

The tryptic digests of peptides C were loaded onto the affinity column in PBS at a flow-rate of 1.0 ml/min. The column was then washed with 10–15 ml of PBS at the same flow-rate. Non-retained peptides were collected to check the absence of BPO, then the valve was switched to place both columns in-line. The bound antigens were desorbed from the immunoaffinity column into the analytical column with 0.1% TFA solution at a flow-rate of 1.0 ml/min. After 10 min, the valve was switched, placing the immunoaffinity column off-line to permit the analysis of the antigens by gradient elution on the analytical column. The reversed-phase chromatographic separation was performed with a 30-min linear gradient from 0 to 100% of acetonitrile–isopropanol–0.1% TFA in water (2:1:2, v/v/v) at a flow-rate of 1.0 ml/min. All runs were performed at room temperature and peptides were detected at 215 nm. Fractions were collected every 0.25 min and analysed for BPO concentration. Simultaneously, the affinity column was equilibrated with loading buffer.

RP-HPLC at pH 7.0 was performed on the same column equilibrated with 0.01 *M* phosphate buffer (pH 7.0). Elution was achieved with a 30-min linear gradient from 0 to 100% of acetonitrile–0.01 *M* phosphate buffer (pH 7) (60:40, v/v) at a flow-rate of 1.0 ml/min.

Detection of penicilloyl groups

BPO detection was performed using an enzyme immunoassay (EIA) directly derived from the radioimmunoassay as described [10].

Identification of peptides and location of BPO-binding sites

Sequencing was achieved using a Model 477 Sequanator connected to a Model 120 A PTH HPLC analyzer (Applied Biosystems).

A recurring Edman degradation using Tarr's procedure [11] was performed on each peptide and the EIA for BPO detection was realized at each cycle on the phenylthiohydantoin (PTH) derivative

RESULTS

Isolation and separation of penicilloylated peptides

The isolation and separation of penicilloylated peptides from C tryptic digests were achieved using the dual-column chromatographic system described above. Fig. 1 shows the RP-HPLC patterns of (a) the entire tryptic hydrolysate generated on the

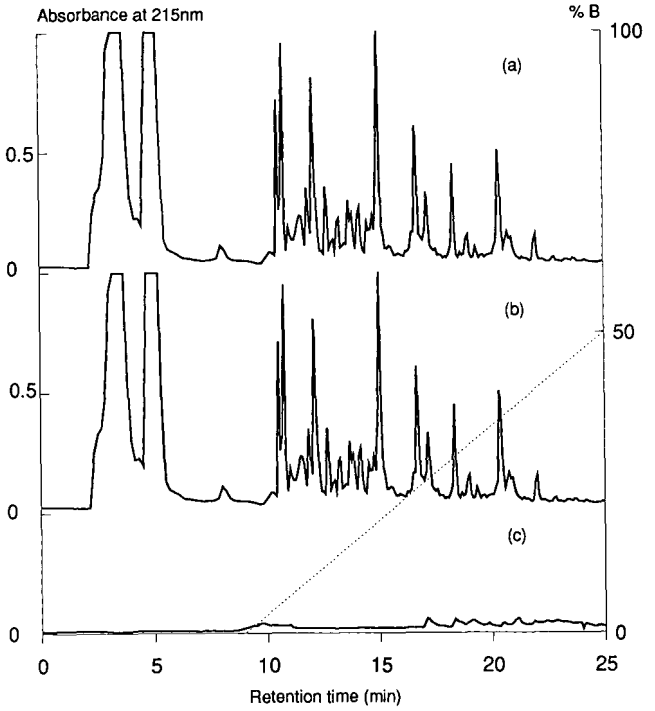

Fig. 1. RP-HPLC profile of (a) the entire tryptic hydrolysate of HSA fragment C, (b) the non-retained fraction and (c) the retained fraction on the immunoaffinity column. See text for the chromatographic conditions. The dotted line indicates the gradient of solvent B.

reversed-phase column alone, (b) the non-retained fraction on the IAC and (c) the retained fraction. Almost all the peptides of the hydrolysate did not bind to the IAC, as the chromatograms of the entire hydrolysate and of the non-retained fraction were nearly identical. The immunoenzymatic assay applied to the non-retained fraction showed no BPO present in this fraction whereas the loaded sample contained 1.2 μg of BPO.

The chromatogram of the retained peptides and the BPO assay in the collected fractions (Fig. 2) show two major BPO-containing peaks, *i.e.*, Pep 17 and Pep 21 at retention times of 17.1 and 21.1 min, respectively. The sum of the BPO in all the collected fractions was 1.12 μg, which represents about 95% of the loaded amount.

Identification of peptides and location of BPO-binding sites

Each of the BPO–peptides was analysed for its amino acid sequence. In order to confirm the BPO-binding site, BPO determinations were performed again at each cycle of the Edman degradation. The amino acid sequencing permitted the following peptides to be identified.

Pep 17 consists of a mixture of two peptides corresponding to the sequences 187–195 and 191–197 of HSA. They can be separated by RP-HPLC at pH 7.0 into two

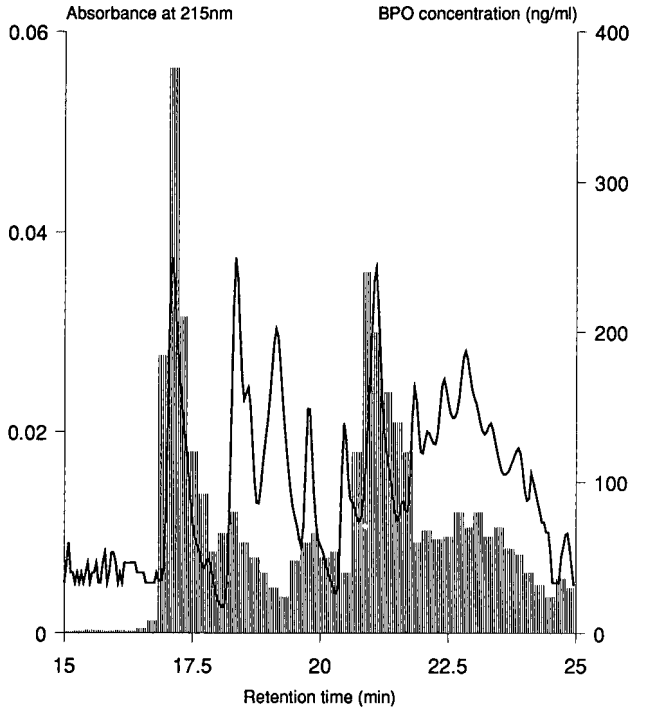

Fig. 2. RP-HPLC separation of the retained fraction on the immunoaffinity column. Columns and running conditions as in Fig. 1. Solid line, absorbance at 215 nm; hatched peaks, BPO concentration in each fraction.

peaks with retention times of 12.0 min (Pep 12) and 15.0 min (Pep 15). The sequence of Pep 21 corresponds to that of fragment 198–205.

Pep 12: $\underrightarrow{Asp_{187}}\text{–}\underrightarrow{Glu_{188}}\text{–}\underrightarrow{Gly_{189}}\text{–}\rightarrow\text{–}\underrightarrow{Ala_{191}}\text{–}\underrightarrow{Ser_{192}}\text{–}\underrightarrow{Ser_{193}}\text{–}\underrightarrow{Ala_{194}}\text{–}\underrightarrow{Lys_{195}}$

Pep 15: $\underrightarrow{Ala_{191}}\text{–}\underrightarrow{Ser_{192}}\text{–}\underrightarrow{Ser_{193}}\text{–}\underrightarrow{Ala_{194}}\text{–}\rightarrow\text{–}\underrightarrow{Gln_{196}}\text{–}\underrightarrow{Arg_{197}}$

Pep 21: $\underrightarrow{Leu_{198}}\text{–}\rightarrow\text{–}\underrightarrow{CMCys_{200}}\text{–}\underrightarrow{Ala_{201}}\text{–}\underrightarrow{Ser_{202}}\text{–}\underrightarrow{Leu_{203}}\text{–}\underrightarrow{Gln_{204}}\text{–}\underrightarrow{Lys_{205}}$

No amino acid could be detected in the fourth cycle of Pep 12 and in the fifth cycle of Pep 15 during the sequencing whereas BPO was found in these fractions. These data indicate that binding of BPO occurs at Lys 190 and Lys 195.

It should be emphasized that no tryptic cleavage occurs on a penicilloylated lysine and that lysine 190 and 195 are never found penicilloylated at the same time (or on the same peptide). On Pep 12 only Lys 190 is penicilloylated and not Lys 195, whereas when Lys 195 is penicilloylated (on Pep 15) Lys 190 is not penicilloylated. The peptide 187–197 where both lysine 190 and 195 could be penicilloylated is never observed.

In Pep 21 no amino acid is detected at the second cycle of the sequencing while BPO is found in the corresponding fraction, proving that the BPO binding site is located on lysine residue 199.

DISCUSSION

The *in situ* derivatization of the prepacked Ultraffinity-EP column is very easy and very fast. This column can also be used for the preparation of several milligrams of proteins in addition to the isolation of micro amounts of peptides. For the purification of antipenicilloyl antibodies, a large amount (30 mg) of HSA–BPO conjugate has been immobilized. This derivatized column permitted in each run (*e.g.*, 30 min), 6 mg of immunoglobulins to be purified from about 10 ml serum. The same type of column can also be derivatized with a much smaller amount of ligand. Only 13 mg of antipenicilloyl antibodies were used to prepare the immunoaffinity column.

In the preparation of the affinity column no chemical agent was used for blocking excess reactive groups on the Ultraffinity support, although this technique is classically used in low-pressure chromatography to prevent irreversible loss of sample materials on remaining active sites. We only verified that such a procedure was not necessary in the present instance as the BPO recovery was good and the non-specific binding of protein material on the column was small. In HPLC the elution time is much shorter than that in low-pressure chromatography, so that the contact between the sample material and the support might be too short to allow a non-specific reaction with the formation of a covalent bond. This would not be a difficulty when high specificity and affinity occur between the phase and the ligand such as in an antigen–antibody binding.

All the penicilloylated peptides appeared to bind to this column as no BPO was detected in the non-retained fraction. The recovery of these peptides was very good, as 95% of the amount of penicilloyl loaded were obtained in the fractions eluted from the reversed-phase column. Moreover, in order to establish the effect of the previous steps (*i.e.*, CNBr cleavage, subsequent trypsin treatment and heating) on the binding of BPO to protein fragments, total BPO was determined in each of these different steps in the overall procedure.

CNBr cleavage is known to occur specifically on methionine residues, which should not affect BPO bound to lysine residues. No data are available concerning the stability of the pseudo peptidic BPO–protein bond in formic acid, but under the acidic conditions in which sequencing is operated (TFA, HCl and heating) the bond appears to be stable and no BPO is lost. However, during the repeated steps of samples drying, evaporation of residual CNBr and formic acid and then redissolution of the dried hydrolysate, part of the protein material is lost. This loss (*ca.* 40%) is accompanied by the same loss of total BPO. The BPO recovery is therefore not complete during the CNBr cleavage but no particular peptidic fragment or binding site appears to be specifically involved.

Trypsin cleavage occurs on peptidic bonds involving a lysine or an arginine residue but not on pseudo peptidic bonds such as BPO–Lys. This was checked using a standard conjugate, *i.e.*, BPO–ε-aminocaproate. After trypsin hydrolysis, performed under the experimental conditions, more than 80% of the intact conjugate was recovered, which can be considered to be quantitative. Moreover, during the separation and identification of penicilloylated peptides, cleavage never occurred on a BPO–Lys. Trypsin cleaves neither the peptidic bond of penicilloylated lysine residue nor the pseudo peptidic BPO–lysine bond.

The chromatograms of the entire digest and of the peptides which were not

bound by the immunoaffinity column were nearly identical. This indicates that the non-specific binding of peptides was very low. However, the chromatogram of the retained fraction observed at a much greater sensitivity (*e.g.*, 0.06 a.u.f.s.) showed that some peptides which were bound to the immunoaffinity column did not contain a BPO group as detected by EIA. These peptides only represent a few percent (1–2%) of those injected. Janis and Regnier [7] also observed a non-specific binding of peptides on a covalently immobilized immunoaffinity column. This non-specific binding of peptides was probably more important than in our study, as they observed significant differences between the chromatogram of the non-retained peptides and the chromatogram of the entire tryptic digest. They indicated that treatment with Tween 20 of the immunoaffinity column decreased the non-specific binding of peptides but did not totally eliminate it. The non-specific binding of peptides is common in affinity chromatography and it is necessary to check the presence of hapten on peptides which bind to the IAC by a specific test applied subsequently.

However, the immunoaffinity step permits most of the non-penicilloylated peptides which represent about 98% of the peptides in the entire digest to be discarded. In a previous study, the isolation and separation of penicilloylated peptides from the tryptic digest of HSA fragment C needed three steps of HPLC purification. The first was a reversed-phase separation at pH 7.0. Each of the three penicilloylated fractions was then purified by ion-exchange chromatography and a third step of purification and desalting was done by reversed-phase chromatography using TFA–acetonitrile–isopropanol as the eluent. In each step all the eluted fractions must be collected and analysed for BPO. This means a total of seven chromatographic analyses and of about 700 samples to be analysed for BPO. Taking into account drying steps, dilution steps, etc., it took more than 6–7 days to obtain the purified penicilloylated peptides.

Moreover, it must be noted that very often the contamination of one peptide by another is only detected in the last step of the analysis during the identification. An entirely new procedure for the separation, detection and identification of each BPO peptide is then necessary, which means much more work. Using the dual column system, the same three penicilloylated peptides were obtained in a single step.

As the HSA molecule cannot be digested directly by trypsin because of its compact structure, we used several steps for its digestion. The CNBr cleavage permitted the molecule to be cut into three fragments and then to obtain tryptic digests containing a smaller number of peptides As the penicilloylated peptides represent only a few percent (1–2%) of the peptides, it is better to work on hydrolysates which are not too complex in order to decrease the proportion of non-specific contamination and the risk of eluting several peptides at an identical retention time.

The tryptic hydrolysates of the CNBr fragments A and B of HSA were analysed by this methodology [12] and three new binding sites for penicilloyl groups were unequivocally established: Lys 432, Lys 541 and Lys 545. It is worth noting that the same sites have been identified for the three *in vivo* and for the *in vitro* penicilloylated albumins, hence BPO-binding sites appear to be located only on lysine residues and only six different Lys residues out of a total of 59 can be penicilloylated.

As noted, all these potential binding sites cannot be penicilloylated at the same time (*e.g.*, on the same albumin molecule). This explains why six sites could have been detected while the measured average penicilloylation rate among the total population of penicilloylated albumin molecules was "only" two or three BPO groups per mole of HSA.

The data obtained give indications of the possible mechanism in penicillin allergy. A nucleophilic attack of the drug and then a covalent binding of BPO groups to proteins, *e.g.*, serum albumin, are necessary for the formation of the allergenic metabolite. However, this binding needs particular amino acid sequences and/or conformation of the protein molecule that are constant and somehow universal as they have also been described in several β-lactamases and protein-binding proteins [13].

It can be observed that four BPO–Lys out of six are located near serine from which they are separated by two amino acids. This position represents the configuration in which in an α-helix, Lys and Ser residues are the nearest. These results suggest a cooperation between these two residues in the mechanism of formation of the allergen metabolite of penicillin and therefore support the mechanism of penicilloylation proposed by Yamana *et al.* [14].

The BPO-binding sites are very few, located in small regions of the albumin molecule where they are concentrated, which certainly limits their bioavailability for specific antibodies. Some of them are not specific for penicillin: Lysine 199 is site of glycosylation, acetylation and aspirin binding.

All these considerations could suggest that under normal conditions the reacting molecules could rather be masked inside the protein carrier which would protect the organism against immunological disorders. Diseases and therapeutic, nutritional or environmental factors could unmask these determinants. Competition between ligands and modifications of the spatial structure of albumin can increase the number, the presentation and the chemical reactivity of reacting sites and thus permit an allergic process to be triggered.

CONCLUSION

The combination of affinity and RP-HPLC methods provides a rapid technique for the analysis of the binding sites of a hapten and more generally of any ligand covalently bound to a proteic carrier, and thus it provides a methodological approach for studying mechanisms of formation of allergenic determinants from drugs. The sensitivity of this association permits the analyses of very small amount of samples (*ca.* 100–200 μl of serum) which is especially useful for clinical studies in man.

REFERENCES

1 C. Lapresle and J. M. Wal, *Biochim. Biophys. Acta*, 586 (1979) 106.
2 J. E. Walker, *FEBS Lett.*, 66 (1976) 173.
3 M. Yvon, P. Anglade and J. M. Wal, *FEBS Lett.*, 247 (1989) 273.
4 N. Iberg and R. Flückiger, *J. Biol. Chem.*, 261 (1986) 13542.
5 P. Lafaye and C. Lapresle, *FEBS Lett.*, 234 (1988) 305.
6 L. Rybacek, M. D'Andrea and S. J. Tarnowski, *J. Chromatogr.*, 397 (1987) 355.
7 L. J. Janis and F. E. Regnier, *J. Chromatogr.*, 444 (1988) 1.
8 M. Yvon and J. M. Wal, *FEBS Lett.*, 239 (1988) 237.
9 R. P. Swenson, M. Williams, V. Massey, S. Rouchi, Minchiotti, M. Galliano and B. Curti, *J. Biol. Chem.*, 257 (1982) 8817.
10 J. M. Wal, G. Bories, S. Mamas and F. Dray, *FEBS Lett*, 57 (1975) 9.
11 G. E. Tarr, in M. Elzinga (Editor), *Methods in Protein Sequence Analysis*, Humana Press, Clifton, NJ, 1982, p. 223.
12 M. Yvon, P. Anglade and J. M. Wal, *FEBS Lett.*, 263 (1990) 237.
13 B. Joris, J. M. Ghuysen, G. Dive, A. Renard, O. Dideberg and P. Charlier, *Biochem. J.*, 250 (1988) 313.
14 T. Yamana, A. Tsuji, E. Miyamoto and E. Kiya, *J. Pharm. Pharmacol.*, 27 (1975) 771.

Journal of Chromatography, 539 (1991) 373–381
Elsevier Science Publishers B.V., Amsterdam

CHROM. 22 877

Purification of DNA and group separation of normal and modified DNA components by size-exclusion chromatography

M. POLVERELLI, L. VOITURIEZ, F. ODIN, J.-F. MOURET and J. CADET*
Laboratoires de Chimie, DRF, Centre d'Études Nucléaires, 85 X, F-38041 Grenoble Cédex (France)

ABSTRACT

DNAs and their normal or modified constituents are separated in one chromatographic run on a TSK HW 55F column with a 0.1 *M* ammonium formate (pH 6.5) volatile solvent. A group separation between 2'-deoxyribonucleotides, 2'-deoxyribonucleosides and nucleobases was achieved. A good resolution of photoinduced decomposition products of (pyrimidine) nucleobases was obtained on a TSK G 1000 PW column. Separation of nucleic acid components is thought to be governed by mechanisms involving both size exclusion, weak hydrophobic interactions and ionic repulsion between the matrix and the charged molecules.

INTRODUCTION

Purification of chemically modified DNA is required prior to analysis for a specific type of base damage. Ultracentrifugation [1], electrophoresis [2] and liquid chromatography on various supports [3] are techniques generally used to obtain pure DNA. Once purified, DNA may be submitted to acidic hydrolysis [4] or enzymatic digestion [5]. Whatever the hydrolytic method choosen, a reliable measurement of a specific modified nucleoside is possible only after simple monitoring of the completeness of DNA hydrolysis. Subsequently, the separation of the biopolymer from the released low-molecular-mass components is generally achieved by precipitation of the macromolecule using ethanol–salt mixtures [6].

When analysed with a Fractogel TSK HW 55F column eluted with 0.1 *M* ammonium formate (pH 6.5), DNAs (with molecular masses of above 10^5 dalton) are excluded in the void volume (V_0). With this volatile solvent, the excluded DNA may be digested enzymatically directly in the chromatographic eluate, adding only a concentrated nuclease buffer and metallic cofactors. The enzymatic hydrolysate may be analysed with the same chromatographic system.

We achieved a separation of the finally remaining unhydrolysed DNA from its digestion products (2'-deoxyribonucleotides or nucleosides) in a single chromatographic run. Whereas DNAs are excluded according to the well known size-exclusion mechanism, Fractogel TSK HW 55F and TSK G 1000 PW columns may be used for

0021-9673/91/$03.50

the separation of DNA components and pyrimidine photoproducts in the partition mode.

EXPERIMENTAL

Chemicals

Ammonium formate and calcium chloride were obtained from Eastman Kodak (Rochester, NY, U.S.A.) and Merck (Darmstadt, Germany), respectively. Alkaline phophatase, micrococcal nuclease, nuclease P_1, RNAse A and $tARN^{Met}$ were provided by Boehringer (Mannheim, Germany). 2'-Deoxyribonucleosides were purchased from Genofit (Geneva, Switzerland) and thymidine 5'-monophosphate (Na salt) and nucleobases from Sigma (St. Louis, MO, U.S.A.). 8-Oxo-7,8-dihydro-2'deoxyguanosine was synthesized from 2'-deoxyguanosine according to Lin *et al.* [7] and 2'-deoxyadeosine N-1-oxide according to Mouret *et al.* [8].

Synthesis of the two *cis* diastereoisomers of 5,6-dihydroxy-5,6-dihydrothymidine 5'-monophosphate was adapted from Rajagopalan *et al.* [9] with the following modifications suggested by Berger [10]. Briefly, thymidine 5'-monophosphate (Na salt) (1 m*M*) was dissolved in water (10 ml, room temperature), pure bromine (0.1 ml) was added and the solution was stirred for 30 min at room temperature. The excess of bromine was eliminated by a continuous flow of air throughout the solution. Substitution of bromine was carried out by overnigh treatment with NH_4HCO_3 (0.1 g per 50 ml) (37°C).

After quantitative dephosphorylation with alkaline phosphatase (1 h, 37°C, 5 units, pH 8.5, 0.2 *M*, in NH_4HCO_3), thymidine glycol diastereoisomers were purified and characterized according to Cadet *et al.* [11]. The *cis-syn*-cyclobutadithymine (Thy<>Thy) and 5-hydroxy-6-4'-(5'-methylpyrimidin-2'-one)-5,6-dihydrothymine were generated by far-UV irradiation of thymine in frozen aqueous solution [12].

Biopolymers

The following deoxyribonucleic acids were used: *E. coli*, salmon testes, phage X 174, phage lambda hind III fragments, calf thymus $tARN^{Met}$ and poly-dA (Boehringer, Mannheim, Germany).

Purification and enzymatic digestion of DNA

Dry seeds of *Lactuca sativa* (500 mg) precooled in dry nitrogen were disrupted by mechanical grinding in a porcelain mortar and suspended in a ready-made lysis buffer (10 ml) (Applied Biosystems, Foster City, CA, U.S.A.). After thawing for at least 45 min, the lysate was centrifuged at 5000 *g* for 30 min at room temperature in order to eliminate the cellulosic residues. The brownish supernatant was deproteinized by reaction with proteinase K (100 μg/ml, 2 h, 65°C) with occasional shaking. The DNA and RNA pool was precipitated overnight at −20°C by adding 0.5 volume of 7.5 *M* ammonium acetate and 1 volume of 2-propanol in ten siliconized Eppendorf tubes (2 ml). The major part of the hydrolysed peptides and phenolic compounds was eliminated by centrifugation at 10^4 *g* for 1 h at 0°C. The resulting brownish precipitate was rinsed with 70% ethanol. Without excessive drying, the pellets were resuspended in distilled water. Prepurification was carried out on a small bed of Fractogel HW 55F (1 cm high, 1 cm diameter) equilibrated with distilled water before RNAse treatment [13].

Digestions of DNA into 5′-nucleotides or 3′-nucleotides were achieved with nuclease PI [14] and with a mixture of micrococcal nuclease and spleen phosphodiesterase [15], respectively.

Size-exclusion chromatography (SEC)

Fractogel HW 55F was packed in a Superformance glass column (300 mm × 10 or 16 mm I.D., as specified) (Merck). The columns were packed at a flow-rate of 2 ml/min until the level of gel remained constant in the prefilling column. Molecular weight operating ranges for HW 55F are between 10^3 and 10^5 dalton.

High-performance liquid chromatography (HPLC)

A stainless-steel column (600 × 7.5 mm I.D.) prefilled with TSK G 1000 PW was supplied by LKB (Bromma, Sweden). The chromatographic solvents [0.1 *M* ammonium formate (pH 6.5) or water] were degassed by filtration on a Millipore filter (HAWP, 0.45 μm; Millipore, Bedford, MA, U.S.A.). Samples were injected into the chromatographic system with a Rheodyne Model 7125 injector equipped with a 0.5-ml loop. Delivery of the solvents was achieved using a Merck L 6200 pump (fast size-exclusion chromatography) or a Waters Assoc. Model 501 pump with a flow-rate of 1.0 ml/min.

RESULTS

Chromatographic purification of nucleic acids and polynucleotides on the Fractogel HW 55F column

DNAs of different masses ($> 10^5$ dalton) are excluded in the void volume (V_0) and easily separated from RNA hydrolysate or smaller molecules (10^2–10^3 dalton), which are eluted with higher retention times (Fig. 1). An interesting application is the purification of nucleic acids extracted from dry seeds of *Lactuca sativa*, provided that the detergent is eliminated before the chromatographic run as it coelutes as a macromolecule with DNA in the void volume [16]. Further, Fractogel HW 55F is useful for removing polymerized phenolic compounds [17].

Separation of nucleic acids components

Enzymatic digestion of DNA is generally preferred to acidic hydrolysis because it may provide some insight into the stereochemical structure of the hydroxyl-mediated oxidative adducts [5]. As expected, unhydrolysed DNA is excluded in the void volume before nucleotides, for which the capacity factors (k') remain almost identical regardless of the position of the remaining phosphate (3′- or 5′-).

The nucleotide pool may be dephosphorylated and the resulting 2′-deoxyribonucleosides are further separated on the same column (Fig. 2, Table I). 2′-Deoxycytidine and thymidine partially overlap on Fractogel HW 55F (Fig. 2, Table I) and on TSK G 1000 PW (Table I). Acidic hydrolysis gives rise to nucleobases with concomitant degradation of the polynucleotide chain [18]. A complete separation of the nucleobases was only achieved by liquid chromatography on a TSK G 1000 PW column (Fig. 5, Table I). It should be noted that a faster separation is obtained with a Fractogel HW 55F that permits the separation only of adenine and guanine.

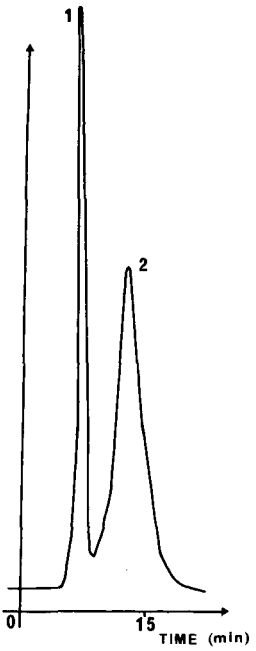

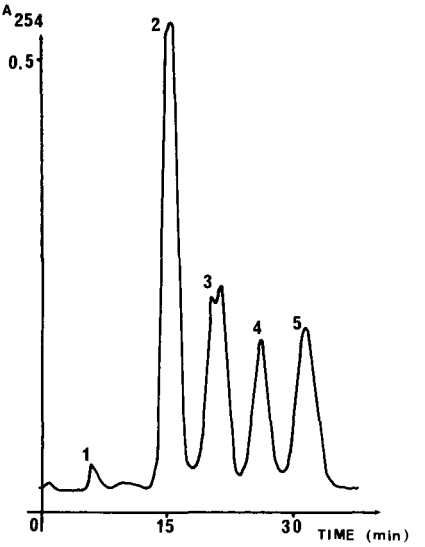

Fig. 1. SEC of (1) DNA and (2) RNA (from *Lactuca sativa*). Column, Fractogel HW 55F (30 × 1 cm I.D.); eluent, 0.1 *M* ammonium formate (pH 6.5); flow-rate, 1.0 ml/min; detection, 254 nm.

Fig. 2. SEC of Salmon testes (1) DNA and into (2) P_1 hydrolysate, (3) 2′-deoxycytidine and thymidine, (4) 2′-deoxyguanosine and (5) 2′-deoxyadenosine. Chromatographic conditions as in Fig. 1.

It is worth noting that TSK G 1000 PW easily discriminates nucleobases from the corresponding 2′-deoxyribonucleosides (Table I).

Separation of radiation- and photoinduced decomposition products of DNA components

Radiation-induced decomposition of nucleosides. The four *cis* and *trans* diastereoisomers of 5,6-dihydroxy-5,6-dihydrothymidine have long been recognized as the most important hydroxyl radical-mediated decomposition products of thymidine [11]. These compounds may be produced by gamma irradiation of DNA in aqueous solutions [19] or by reactive species arising from the reduction of hydrogen peroxide by transition metals (Fe^{2+}, etc.) (Fenton reaction) [20].

Thymidine glycols, which coeluted as a single peak, have a lower retention time than thymidine (Fig. 3, Table I). Another important hydroxyl radical oxidation product of 2′-deoxyguanosine, 8-oxo-7,8-dihydro-2′-deoxyguanosine [21], coelutes with the unmodified nucleoside.

Conversely, 2′-deoxyadenosine N^1-oxide, obtained from 2′-deoxyadenosine in hydrogen peroxide oxidation from a non-Fenton radical pathway [8], was completely separated from its parent compound (Fig. 4).

Photoinduced decomposition products. cis-syn-Cyclobutadipyrimidines, pyrimidine (6–4) pyrimidone photoadducts and 5,6-dihydro-5-(α-thyminyl)thymine, the

TABLE I

CAPACITY FACTORS (k') OF NORMAL AND MODIFIED NUCLEIC ACID CONSTITUENTS

Compound	k'	
	HW 55F	TSK G 1000 PW
$tRNA^{Met}$ and phenolic compounds	0.47	–
Deoxyribonucleoside 3′-monophosphates	1.66	–
Deoxyribonucleoside 5′-monophosphates	1.36	–
2′-Deoxyadenosine	4.21	15.10
2′-Deoxycytidine	2.42	4.50
2′-Deoxyguanosine	3.30	16.75
Thymidine	2.40	6.25
(+)*trans*(5*R*,6*R*),(−)*trans*(5*S*,6*S*), (+)*cis*(5*S*,6*R*),*cis*(−)(5*R*,6*S*)-5,6-Dihydroxy-5,6-dihydrothymidine	1.46	–
(−)*cis*(5*R*,6*S*)- and (+)*cis*(5S,6*R*)-5,6-Dihydroxy-5,6-dihydrothymidine-5′-monophosphate	1.50	–
Adenine	2.61	16.03
Cytosine	2.42	4.25
Guanine	2.31	14.50
Uracil	2.40	7.00
Thymine	2.41	7.00
2′-Deoxyadenosine N^1-oxide	2.01	–
8-Oxo-7,8-dihydro-2′-deoxyadenosine	3.35	–
cis-5,6-Dihydroxy-5,6-dihydrothymine	1.60	3.25
5-Hydroxy-6-4′-(5′-methylpyrimidin-2′-one)-5,6-dihydrothymine	–	8.50
5,6-Dihydro-5-(α-thyminyl)thymine	–	9.00
5-Hydroxy-5-methylbarbituric acid	1.55	–
5,6-Dihydrothymine	1.55	–
cis-syn-Thy<>Thy, Thy<>Ura, Ura<>Ura	1.21	15.50

so-called "spore photoproduct", constitute the three main classes of DNA pyrimidine dimeric far-ultraviolet photoproducts [22].

The three *cis-syn* isomers of DNA cyclobutadipyrimidine involving thymine dimers (Thy<>Thy), thymine–uracil dimer (Thy<>Ura) or uracil dimers (Ura<>Ura) are eluted in a single peak on a TSK G 1000 PW column (Fig. 5, Table I).

The other dimeric products of thymine, *i.e.*, 5-hydroxy-6-4′-(5′-methylpyridine-2′-one)-5,6-dihydrothymine and 5,6-dihydro-5-(α-thyminyl)thymine, which have one of the two pyrimidines still unsaturated, exhibit higher retention times (Fig. 5, Table I).

DISCUSSION

SEC is generally carried out for purification and/or separation of DNAs of different size [23–28]. Fractogel HW 55F allows the separation of biopolymers in the range 10^3–10^5 dalton (SEC mechanism) and the separation of low-molecular-mass compounds ($<10^3$ dalton) in the partition mode. All biopolymers ($>10^5$ dalton) are eluted in a single peak (void volume, V_0).

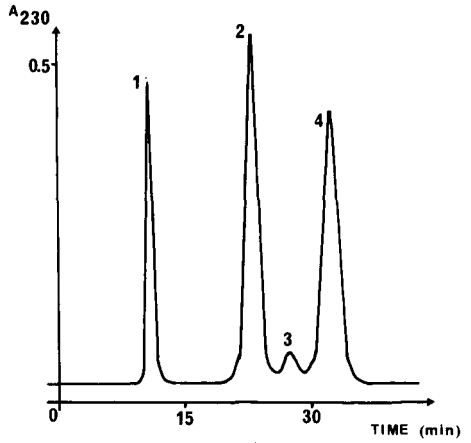

Fig. 3. SEC of (1) phage λ hind III fragments, (2) (+)*cis*(5*S*,6*R*)- and (−)*cis*(5*R*,6*S*)-diastereoisomers of 5,6-dihydroxy-5,6-dihydrothymidine 5′-monophosphate, (3) (+)*cis*(5*S*,6*R*)-, (−)*cis*(5*R*,6*S*)-, (−)*trans*-(5*S*,6*S*)- and (+)*trans*(5*R*,6*R*)-diastereoisomers of 5,6-dihydroxy-5-6-dihydrothymidine and (4) thymidine. Chromatographic conditions as in Fig. 1, except for the column (30 × 1.6 cm I.D.).

Liquid chromatography in the partition mode with TSK G 1000 PW is limited to low-molecular-mass products (up to 10^3 dalton). Fast SEC on Fractogel HW 55F was particularly useful for the clean-up of DNA to remove undesirable polymerized phenolic compounds which always coprecipitated with the nucleic pool from the crude cell lysate.

The group separation of the nucleic acid components [29–32] has received attention in the past. However, it should be noted that only a few papers have reported

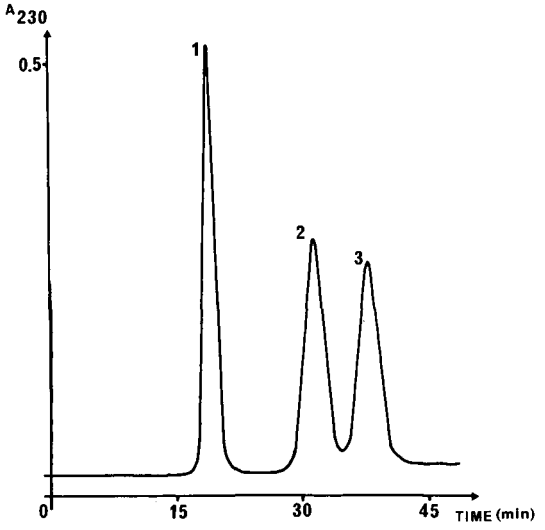

Fig. 4. SEC of (1) 2′-deoxyadenosine N^1-oxide, (2) 2′-deoxyadenosine and (3) adenine. Chromatographic conditions as in Fig. 2.

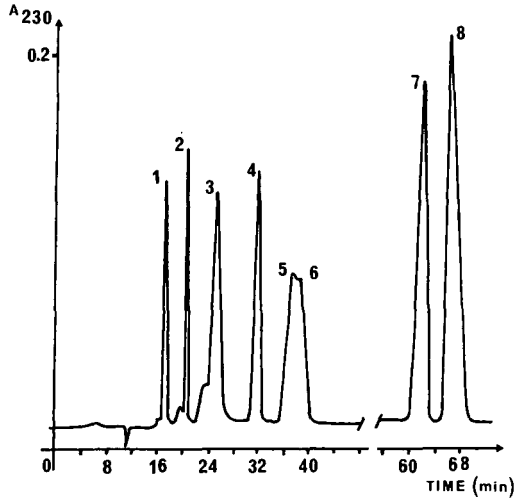

Fig. 5. HPLC of photoinduced decomposition products of nucleobases. Column, TSK G 1000 P (30 × 0.75 cm I.D.); eluent, water; flow-rate, 1.0 ml/min; detection, 230 nm. (1) *cis*-5,6-dihydroxy-5,6-dihydrothymine; (2) cytosine; (3) *cys-syn*-Thy < > Thy, *cis-syn*-Ura < > Thy, *cis-syn*-Ura < > Ura; (4) uracil + thymine; (5) 5-hydroxy-6-4-(5′-methylpyrimidin-2′-one)-5,6-dihydrothymine; (6) 5-dihydro-5-(α-thyminyl)thymine; (7) guanine; (8) adenine.

chromatographic systems that permit the separation of DNA from its digestion products [33–35].

The matrix of these gels can be roughly described as a copolymer of polyacrylamide and poly(vinyl alcohol) the hydrophilicity of which can be attributed to hydroxyl groups (0.5–1 mequiv./ml) and to carboxylic groups (0.001–0.02 mequiv./ml) for TSK HW 55F according to the supplier's information.

In a previous study [29], the chromatographic behaviour of purine and pyrimidine compounds was explained in terms of charge effects. With a gel of the same type, Aoyagi *et al.* [36] assumed that the elution order of DNA compounds is governed by hydrophobic properties. In agreement with Wada [37] and, more recently, with Noguchi *et al.* [38], the fast elution properties of deoxyribonucleotides can be explained by a repulsive interaction between the carboxylic groups of the matrix and the free anionic groups of 2′-deoxyribonucleotides.

The chromatographic behaviour of 2′-deoxyadenosine N^1-oxide may be accounted for in terms of "ion-repulsion" interactions, taking into account the apparent negative charge in the oxygen atom of the N-oxide: $N^+ \rightarrow O^-$ [39]. Weak hydrophobic interactions exist between the polyvinyl structure of the gel matrix and the aromatic ring of purine and pyrimidine compounds [37]. This explains the higher retention of purine nucleobases with respect to the corresponding pyrimidine components (Table I).

Further confirmation of the involvement of weak hydrophobic interactions in the retention mechanism of purine and pyrimidine components was provided by the chromatographic behaviour of the three *cis-syn*-cylobutadipyrimidines involving Thy < > Thy, Thy < > Ura and Ura < > Ura, which exhibit similar capacity factors on the TSK G 1000 PW column (Fig. 5, Table I). This contrasts with the efficient

separation of these compounds on an octadecylsilyl silica gel column in the reversed-phase mode [40], for which the order of elution Ura < > Ura, Ura < > Thy and Thy < > Thy is directly related to the presence of one or two methyl groups. This confirms the lack of any strong hydrophobic interactions of the TSK G 1000 PW matrix with the methyl groups of Thy < > Ura and Thy < > Thy.

Solvophobicity of the (6–4) thymine photoadduct and "spore photoproduct" may explain their longer retention times. This is due to the interactions of the unsaturated pyrimidine ring of the photoproducts with the hydrophobic part of the matrix.

CONCLUSION

SEC is an efficient method for purifying DNAs with molecular masses above those limiting the exclusion limit of the fractionation range (*i.e.*, $> 10^5$ dalton for TSK HW 55F). TSK HW 55F gel columns used with a volatile solvent (0.1 *M* ammonium formate, pH 6.5) may separate DNAs from their constituents in a single chromatographic run.

Low-molecular-mass nucleic acid components can be separated on Fractogel TSK HW 55F and on TSK G 1000 PW in a non-exclusion mode. The separation is governed by a balance between "ionic repulsion" interactions which are predominant for anionic compounds and weak hydrophobic affinities developed through aromatic solutes and the polyvinyl structure of the matrix. An interesting application of the TSK G 1000 PW column in the partition mode is the ability to separate pyrimidine photoproducts by classes. This will allow the separation of groups of particular compounds from a complex mixture which will be further resolved by using another appropriate chromatographic system, such as reversed-phase HPLC [12,40].

ACKNOWLEDGEMENTS

This work was supported in part by grants from the Centre National d'Études Spatiales (89/130J) and l'Oréal.

REFERENCES

1 W. Szybalski, *Methods Enzymol.*, 12 (1968) 33.
2 R. C. Ogden and D. A. Adams, *Methods Enzymol.*, 152 (1987) 61.
3 O. Mikes, *High-Performance Liquid Chromatography of Biopolymers and Biooligomers (Journal of Chromatography Library*, Vol. 41B), Elsevier Amsterdam, 1988, p. B177.
4 A. F. Fucciarelli, B. J. Wegher, E. Gajewsiki, M. Dizdaroglu and W. F. Blakely, *Radiat. Res.*, 119 (1989) 219.
5 G. Teebor, A. Cummings, K. Frenkel, A. Shaw, L. Voituriez and J. Cadet, *Free Rad. Res. Commun.*, 2 (1987) 303.
6 D. M. Wallace, *Methods Enzymol.*, 152 (1987) 41.
7 T. S. Lin, J. C. Cheng, K. Ishigura and A. C. Sartorelli, *J. Med. Chem.*, 28 (1985) 1194.
8 J. F. Mouret, F. Odin, M. Polverelli and J. Cadet, *Chem. Res. Toxicol.*, 3 (1990) 102.
9 R. Rajagopalan, R. J. Melamede, M. F. Laspia, B. F. Erlanger and S. S. Wallace, *Radiat. Res.*, 97 (1984) 499.
10 M. Berger, *Thèse 3ème Cycle*, Université de Grenoble, 1981.
11 J. Cadet, J. Ulrich and R. Téoule, *Tetrahedron*, 31 (1975) 2057.
12 L. Voituriez, C. Voisin, L. S. Kan and J. Cadet, *Book of Abstracts, 10th International Congress of Photobiology, Jerusalem*, 1988, p. 83.

13 J. Marmur, *J. Biol Chem.*, 3 (1960) 208.
14 K. C. Kuo, R. A. McCume and C. W. Gehrke, *Nucleic Acids Res.*, 8 (1980) 4763.
15 K. Randerath, M. V. Reddy and R. C. Gupta, *Proc. Natl. Acad. Sci. U.S.A.*, 78 (1981) 6126.
16 P. F. Rao and T. Takagi, *Anal. Biochem.*, 174 (1988) 251.
17 W. D. Loomis, *Methods Enzymol.*, 31 (1974) 529.
18 R. Téoule, C. Bert and A. Bonicel, *Radiat. Res.*, 72 (1977) 190.
19 S. S. Wallace, *Br. J. Cancer*, 55 Suppl. VIII (1987) 118.
20 M. Kaneko, A. Leadon and T. Ito, *Mutat. Res.*, 207 (1988) 17.
21 H. Kasai and S. Nishimura, *Gann*, 75 (1984) 565.
22 J. Cadet and P. Vigny, in H. Morrison (Editor), *Bioorganic Photochemistry*, Vol. I, Wiley, New York, 1990, p. 1.
23 J. Besson, M. Berger and J. Radisson, *Biochimie*, 57 (1972) 121.
24 Y. Kato, M. Sasaki, T. Hashimoto, T. Murotsu, S. Fukushige and K. Matsubara, *J. Chromatogr.*, 266 (1983) 341.
25 J. M. Schmitter, Y. Mechulam and G. Fayat, *J. Chromatogr.*, 378 (1986) 462.
26 N. Moreau, X. Tabary and F. Le Goffic, *Anal. Biochem.*, 166 (1987) 188.
27 H. Ellengren and T. Lääs, *J. Chromatogr.*, 467 (1989) 217.
28 A. Foriérs, B. Rombaut and A. Boeyé, *J. Chromatogr.*, 498 (1990) 105.
29 J. N. Khym and M. Uziel, *J. Chromatogr.*, 47 (1970) 9.
30 J. X. Khym, *Anal. Biochem.*, 58 (1974) 638.
31 C. D. Lothrop, Jr., and M. Uziel, *Anal. Biochem.*, 109 (1980) 160.
32 R. T. Pon and K. K. Ogilvie, *J. Chromatogr.*, 205 (1981) 202.
33 H. S. Brown and R. Shapiro, *Biochim. Biophys. Acta*, 475 (1977) 241.
34 T. Hatayama and I. M. Goldberg, *Biochemistry*, 19 (1980) 5890.
35 D. J. Cecchini, K. L. Guan and R. W. Giese, *J. Chromatogr.*, 44 (1988) 97.
36 S. Aoyagi, K. Hirayanagi, T. Yoshimura and T. Ishikawa, *J. Chromatogr.*, 252 (1982) 133.
37 H. Wada, *J. Chromatogr.*, 332 (1985) 265.
38 K. Noguchi, Y. Yanaghiara, M. Kasai and N. Hirta, *J. Chromatogr.*, 506 (1990) 145.
39 M. A. Stevens, D. I. Magrath, L. W. Smith and G. B. Brown, *J. Am. Chem. Soc.*, 80 (1958) 2755.
40 J. Cadet, N. E. Gentner, B. Rozga and M. C. Paterson, *J. Chromatogr.*, 280 (1983) 99.

Journal of Chromatography, 539 (1991) 383–391
Elsevier Science Publishers B.V., Amsterdam

CHROM. 22 878

Unfolding of truncated and wild type aspartate aminotransferase studied by size-exclusion chromatography

MARZELL HEROLD*
Hewlett-Packard GmbH, Waldbronn Analytical Division, P.O. Box 1280, W-7517 Waldbronn 2 (Germany)
and
BERND LEISTLER
Abteilung für Biophysikalische Chemie, Biozentrum, Universität Basel, CH-4056 Basle (Switzerland)

ABSTRACT

The reversible unfolding of globular proteins with increasing concentration of guanidinium chloride (GuCl) can be analysed by size-exclusion chromatography, because the hydrodynamic volume of the proteins increases during unfolding. The dimeric enzyme aspartate aminotransferase (AAT) shows an uncoupled dissociation of the identical subunits followed by the unfolding of the monomers. During the monomer unfolding formation of an intermediate is observed. A monomeric mutant of AAT unfolds with a similar shape of the unfolding transition phase, but is less stable, as shown by a shift of the transition mid-point from 1.7 *M* GuCl for the wild type to 1.3 *M* GuCl for the mutant.

INTRODUCTION

It has been demonstrated for many globular proteins that reversible unfolding can be studied by size-exclusion chromatography (SEC). Fundamental work in this field [1,2] showed that the guanidinium chloride (GuCl)-dependent unfolding transition monitored by SEC is the same as the unfolding transition observed by column-independent spectroscopic methods. The hydrodynamic radius, *i.e.*, the Stoke's radius, of proteins clearly increases during denaturation by chaotropic salts such as urea or GuCl. In this study, GuCl was used because it is more chaotropic and comparison with previous GuCl-dependent unfolding studies is possible.

High-performance liquid chromatography (HPLC) is a rapid and powerful method for comparing the conformational stability of site-directed mutants with that of the wild type proteins. Isoenzymes from different organisms can also be easily compared with this method. Moreover, the refolding conditions of proteins which precipitate in "inclusion bodies" during overexpression in the cell can be analysed. Recently, many refolding studies have shown (for a review, see ref. 3) that most globular proteins can be refolded *in vitro*, which is a prerequisite for reproducible stability studies.

The enzyme AAT (aspartate aminotransferase, E.C. 2.6.1.1) from *Escherichia*

0021-9673/91/$03.50

coli has a relative molecular mass of 87 146 (sequence data). It is a dimer consisting of two identical subunits. The crystal structure of the enzyme is known [4,5]. AAT catalyses the reversible transamination of L-amino acids into the corresponding α-keto acids by its covalently bound cofactor pyridoxal 5′-phosphate (PLP). AAT can be reversibly unfolded with GuCl up to protein concentrations of 1 mg/ml [6]. The uncoupled dissociation and unfolding of the dimeric AAT can be analysed by SEC, which is difficult to do by conventional methods. Each subunit of AAT consists of two domains containing no S–S bridges. It has a p*I* value of 4.6. The large domain of AAT, the PLP binding domain (P-domain) [7], was constructed and isolated by site-directed mutagenesis [8]. The P-domain consists of 283 amino acids and has a molecular mass of 32,367 dalton (sequence data). In this paper we compare the stability and GuCl-dependent unfolding of the isolated P-domain with wild type AAT.

EXPERIMENTAL

Materials

All reagents of the purest available grade were purchased from Fluka (Buchs, Switzerland). Water was purified by filtration through an ion-exchange system.

AAT and the mutated protein called "P-domain" were isolated as described previously [6]. The proteins used for column calibration were purchased from Sigma (St. Louis, MO, U.S.A.).

Instrumentation and columns

All experiments were carried out on a Hewlett-Packard (HP) 1050 Ti Series quaternary HPLC pump. To avoid crystallization of salt on the pump pistons, the seal wash option was used with filtered water. A gradient pump was necessary so that the GuCl concentration could be changed automatically by mixing two different solvents. The samples were injected with an HP 1050 Ti Series autosampler and the signals were measured with an HP 1050 Series multiple wavelength detector. The data were transferred from the detector via an HP Series 35900 analog–digital converter to an HP HPLC ChemStation Series 9000. The column used was a TSK 3000 SWXL (300 × 7.5 mm I.D.) packed with 5-μm particles (Tosoh, Yamaguchi, Japan).

Buffers and chromatographic conditions

AAT and P-domain were stored at concentrations of 1.3 and 0.7 mg/ml, respectively, in the following buffer: 10 m*M* HEPES [4-(2-hydroxyethyl)piperazine-1-ethanesulphonic acid] (pH 7.4)–5 m*M* DTE (dithioerythritol)–1 m*M* EDTA (ethylenediaminetetraacetate)–10 μ*M* PLP (100 μ*M* PLP for the P-domain)–1 m*M* 2-oxoglutarate. PLP was added to ensure that the enzymes were always saturated with the coenzyme. The size-exclusion column was calibrated with the following proteins of known molecular mass: thyroglobulin (660 000), aldolase (160 000), AAT (87 000), bovine serum albumin (67 000), ovalbumin (45 000) and RNase A (13 700). The flow-rate was 0.5 ml/min.

Solvent A used for the calibration was 10 *M* HEPES (pH 7.0)–1 m*M* DTE–1 m*M* EDTA–300 m*M* NaCl. For the unfolding studies solvent B contained the same components plus 6 *M* GuCl. All experiments were carried out at room temperature (23 ± 2°C). The absorbance of the eluate was monitored at 230 and 280 nm, band width 8 nm, and a reference wavelength of 550 nm, band width 100 nm.

Fluorescence unfolding studies

Fluorescence measurements were carried out with an SLM 8000 single-photon counting recording fluorimeter. For equilibrium studies the protein was preincubated in solvent A containing the different concentrations of GuCl for at least 3 h. The measurements were performed at 20°C. All solutions were sterilized by filtration directly before use. The measured protein fluorescence spectra were corrected for the small apparent fluorescence of the solutions of GuCl in solvent A. The shift of the protein fluorescence emission maximum (excitation at 280 nm) was monitored depending on the GuCl concentration.

RESULTS AND DISCUSSION

Unfolding of AAT

In each analysis, 26 μg (20 μl) of native AAT were injected onto a TSK 3000 SWXL column which was equilibrated with different GuCl concentrations by mixing solvents A and B. The procedure was automated with the following step gradient from 0 to 6 *M* GuCl: *X*% increase of solvent B every 50 min with automatic injection of protein 20 min after changing %B. Each chromatogram was measured at least three times. The relative standard deviation of the elution volume was 1%.

At 0 *M* GuCl AAT had a retention volume of 8.45 ml, which is consistent with an apparent molecular mass of 86 000. This demonstrates that AAT is in the dimer conformation. With increasing GuCl concentration the retention volume of the protein increased owing to the dissociation of AAT into monomers. The retention volume at 0.7 *M* GuCl was 9.3 ml (see Figs. 1 and 2) which gives an apparent molecular

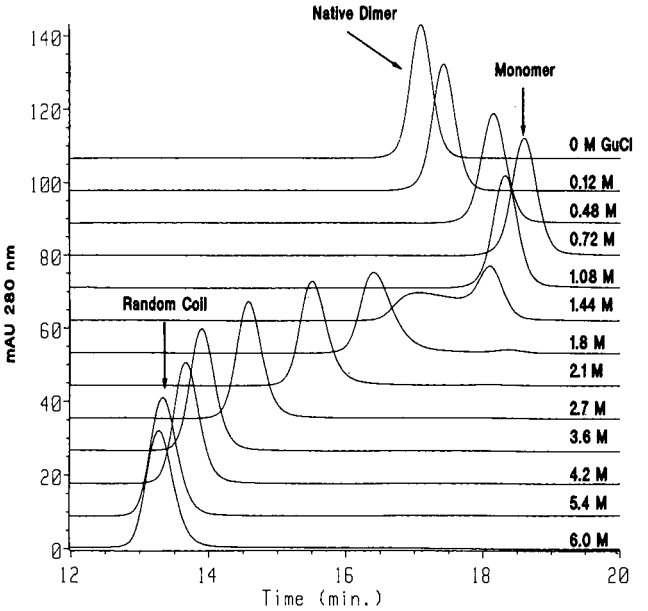

Fig. 1. Elution profiles of holo-AAT at the indicated concentrations of GuCl. Flow-rate, 0.5 ml/min; detection, 280 nm; injection, 20 μl (26 μg) automatically every 20 min after changing the concentration of B.

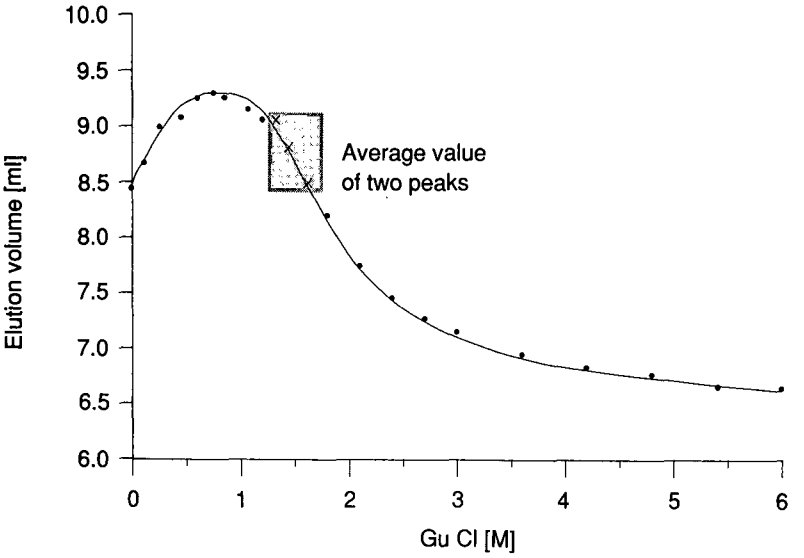

Fig. 2. Change in elution volume of holo-AAT as a function of GuCl concentration. ×, Average value of the retention volume and peak area if two peaks were observed.

mass of 48 000. The true molecular mass of the subunit is 43 573. The apparent molecular mass indicates that the subunits are in a globular conformation, although they are not as compact as in the dimer conformation. The dissociation of the enzyme at 0.7 *M* GuCl into monomers of slightly relaxed globular conformation has been confirmed independently by analytical ultracentrifugation [6].

Further increase in the GuCl concentration beyond 1.2 *M* led to a gradual decrease in elution volume, which is due to the increase in the hydrodynamic volume during the unfolding of the monomers. The transition phase between 1.2 and 3.5 *M* GuCl does not fit to a two-state process and has an overall transition mid-point at 1.7 *M* GuCl (Fig. 2). At concentrations higher than 3.5 *M* GuCl, the change in elution volume is almost linear, indicating that the protein is in the random coil state. The reason for the further decrease in the elution volume is not completely clear. Because it has been observed with all proteins studied so far [2,9,10], this effect seems to be due only to the high GuCl concentration. Even proteins being folded or unfolded over the whole concentration range of GuCl and the small molecule vitamin B_{12} displayed a continuous small decrease in the elution volume with increasing GuCl concentration [9]. Therefore, it is evident that the linear part of the elution volume decrease is not due to a conformational change of the protein. The increase in the GuCl concentration results in an increase in viscosity and might inhibit the diffusion of the molecules into the pores. Shalongo *et al.* [9] assumed a short-time binding of the protein to the column matrix which is diminished with increasing denaturant concentrations. A Superose 12 column (Pharmacia) also showed this effect [6].

In the first part of the monomer unfolding transition, two peaks at 1.44 *M* GuCl were observed simultaneously (see Fig. 1), which indicates the transiently accumulated "structured monomers". The GuCl concentration range with two peaks observed at

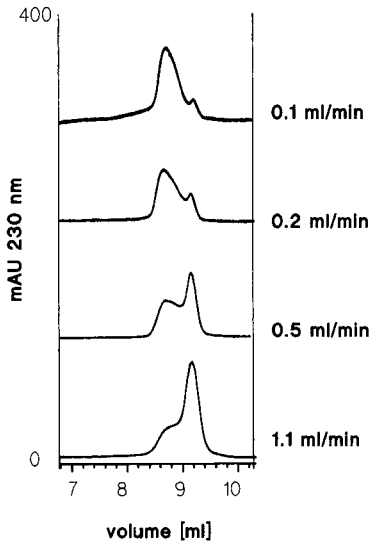

Fig. 3. Elution profiles of AAT in 1.44 *M* GuCl at four flow-rates.

a flow-rate of 0.5 ml/min is shadowed in the unfolding curve in Fig. 2. The formation of the intermediate is relatively slow at room temperature; during the retention time of 18 min only about 50% intermediate is formed. In order to obtain more information about the rate of the intermediate formation, the runs at 1.44 *M* GuCl were repeated with different flow-rates. At the fastest flow-rate of 1.1 ml/min, a small amount of intermediate is formed (*ca.* 15%). In contrast, at the very slow flow-rate of 0.1 ml/min the intermediate is formed to the extent of 90% during 87 min (see Fig. 3). The data were used for a rough estimation of the rate constant of intermediate formation, which gave a value of about $1.1 \cdot 10^{-3}$ s^{-1}.

This strategy can always be used to determine the rate constants of a change of protein conformation provided that the species with different conformations can be separated on the column and that the process is in the time range of the retention time of the column. Generally this requires HPLC size-exclusion columns with a high pressure resistance to allow short retention times and a high separation performance, which is the case with the TSK 3000 SWXL column. A further possibility of detecting folding intermediates is to slow the rate of intermediate formation by decreasing the column temperature.

Unfolding of the P-domain

The conformational stability of mutant proteins compared with the wild type is always of great interest. The AAT subunit consists of two domains. The larger one, the coenzyme binding domain, is compactly folded [7] and binds the coenzyme PLP even in the absence of the truncated small domain [8]. Two questions are of interest concerning the isolated mutated protein: first, is the isolated P-domain still a dimer, and second, how stable is the P-domain compared with the wild type?

The retention volume of 9.6 ml (Fig. 4) clearly indicates that the P-domain is

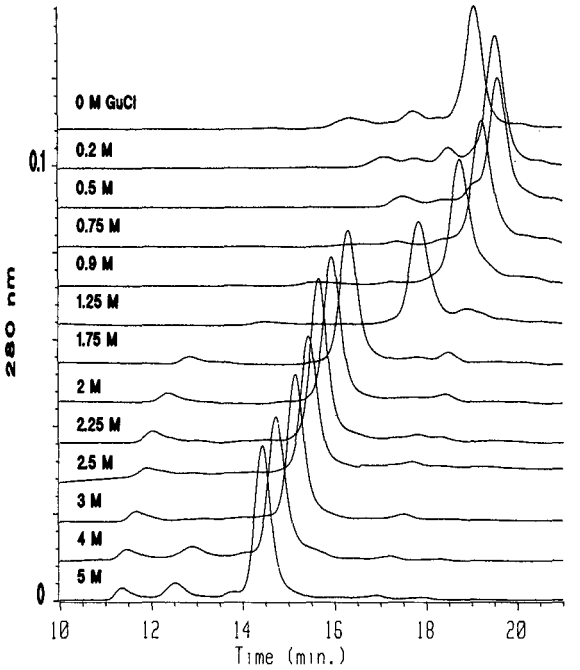

Fig. 4. Elution profiles of P-domain at the indicated concentrations of GuCl. Flow-rate, 0.5 ml/min; detection, 280 nm; injection, 20 μl (14 μg) automatically every 20 min after changing the concentration of GuCl in solvent B.

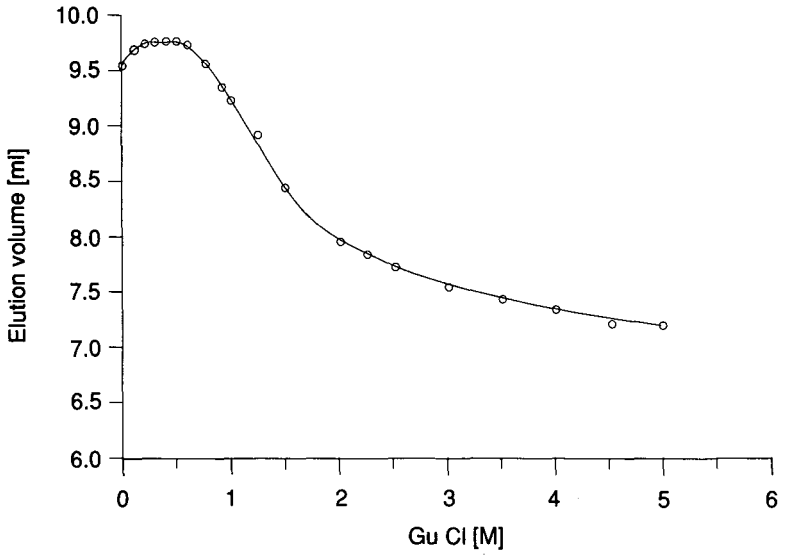

Fig. 5. Change in elution volume of P-domain as a function of GuCl concentration.

monomeric. The apparent molecular mass is 33 500 dalton, which is close to the true value of 32 367 dalton (sequence data). The retention volume of the P-domain increases slightly on adding 0.3 *M* GuCl (see Figs. 4 and 5), suggesting increasing compactness. It is known that the salt concentration in the elution buffer can influence the elution volume of proteins owing to the change in their "viscosity radius" [11]. The explanation given [11] was that the surrounding counter-ion layer of proteins in buffer becomes negligibly small at high ionic strength. Therefore, the elution volume of many proteins increases slightly with increasing salt concentration.

To evaluate the influence of the salt concentration in solvent A, the unfolding experiment shown in Fig. 5 was repeated in the presence of 0.1 *M* instead of 0.3 *M* NaCl (data not shown). Also under these conditions the elution volume increases up to 0.3 *M* GuCl and then decreases with the same unfolding transition phase starting at concentrations higher than 0.5 *M* GuCl. Unfolding was completed at about 3.5 *M* GuCl. The transition mid-point was at 1.3 *M* GuCl, as shown by the normalized curve in Fig. 6. The curve shows the relative change in elution volume; the conformation-independent decrease in the elution volume due to the increase in the salt was subtracted graphically (see als legend of Fig. 6). The measurements repeated at a flow-rate of 0.9 ml/min gave the same transition curve, demonstrating that the experiments were carried out at the thermodynamic equilibrium.

To rule out a column dependent influence on the unfolding curve, the unfolding was additionally monitored by the GuCl-dependent change of the protein fluorescence emission maximum (Fig. 6). The red shift of the fluorescence emission maximum monitors the exposure of the buried tryptophan residues to the solvent during the unfolding of the proteins [12]. Both methods displayed an identical unfolding transition mid-point, whereas the fluorescence method was not able to detect the first conformational change of the protein. This is a further example of the accurate determination of the unfolding transition of a protein by SEC.

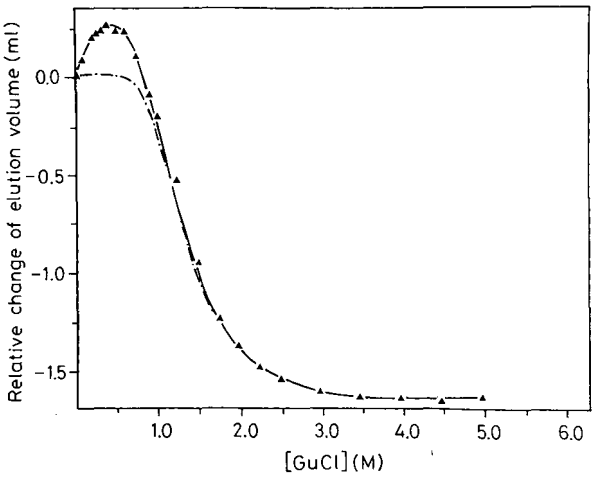

Fig. 6. Normalized unfolding curve of the P-domain. The curve was normalized by extrapolating the linear change in elution volume above 3.5 *M* GuCl to zero GuCl concentration. The relative change in elution volume is the apparent deviation from this baseline. Normalized change in elution volume (▲) compared with the change of the fluorescence emission maximum (– · –, excitation at 280 nm).

Comparison of the stability of AAT and P-domain

The unfolding transition curve measured in the presence of increasing concentrations of a strong denaturant aspect is a measure of the conformational stability of the protein [13]. The unfolding curves revealed by GuCl-dependent SEC can therefore be used to compare the stabilities of related proteins. The P-domain is monomeric under all conditions tested. The small increase in the elution volume of the P-domain at concentrations up to 0.3 *M* GuCl may be due to a conformational change of the protein. This effect has to be confirmed by an independent method. The main unfolding phase is characterized by a strong increase in the hydrodynamic radius between 0.5 and 3.5 *M* GuCl (see Figs. 5 and 6). The transition phase does not fit to a two-phase process, indicating that unfolding of the P-domain is not a simple two-state mechanism. The shape of the unfolding curve looks very similar to the second phase of the unfolding of wild type AAT (the unfolding of the monomers; compare Figs. 2 and 5), indicating that the unfolding of AAT monomers is mainly due to the unfolding of the large PLP-binding domain. The main difference is the shift of the overall transition mid-point from 1.7 *M* (AAT) to 1.3 *M* GuCl (P-domain), demonstrating the lower stability of the isolated P-domain.

Both unfolding curves were confirmed with column-independent spectroscopic methods (ref. 6 and Fig. 6), demonstrating that the SEC unfolding curves show the equilibrium state.

CONCLUSIONS

Protein folding studies with SEC are fast and easy if automated inject and mixing of two solvents are available. Thermodynamic studies do not depend on the type of SEC column. However, for kinetic studies, a column with a high pressure resistance and low elution volume is recommended to facilitate the resolution of time-dependent processes. The following properties of the HPLC system are prerequisites for reproducible results: (i) the pump should work reliably at low pressure and with viscous solutions; (ii) the system should be resistant to corrosion for maximum reliability with very high salt concentrations; a seal washing feature is recommended; and (iii) a gradient system is necessary to allow precise automatic changes of the salt concentration.

ACKNOWLEDGEMENTS

We appreciate critical comments from Gerard Rozing, Heinz Götz, Ginny Curtis and Kasper Kirschner and thank Miriam Hannert for the preparation of the drawings. The work of B. L. was supported by the Swiss National Science Foundation, grant No. 31.25711.88.

REFERENCES

1 S. Endo, Y. Saito and A. Wada, *Anal. Biochem.*, 131 (1983) 108.
2 Y. Saito and A. Wada, *Biopolymers*, 22 (1983) 2123.
3 R. Jaenicke, *Prog. Biophys. Mol. Biol.*, 49 (1987) 117.
4 G. C. Ford, G. Eichele and J. N. Jansonius, *Proc. Natl. Acad. Sci. U.S.A.*, 77 (1980) 2559.
5 J. Jaeger, E. Köhler, P. Tucker, U. Sauder, Z. Housley-Markovic, I. Fotheringham, M. Edwards, M. Hunter, K. Kirschner and J. N. Jansonius, *J. Mol. Biol.*, 209 (1989) 499.

6 M. Herold and K. Kirschner, *Biochemistry*, 29 (1990) 1907.
7 J. N. Jansonius and M. G. Vincent, in F. A. Jurnak and A. McPherson (Editors), *Biological Macromolecules and Assemblies*, Vol. 3, Wiley, New York, 1987, pp. 187–285.
8 M. Herold, B. Leistler, A. Hage, K. Luger and K. Kirschner, in preparation.
9 W. Shalongo, M. V. Jagannadham, C. Flynn and E. Stellwagen, *Biochemistry*, 28 (1989) 4820.
10 M. Herold, *Application Note*, Publ. No. 12-5952-1428, Hewlett-Packard, Waldbronn, 1990.
11 M. Potschka, *J. Chromatogr.*, 441 (1988) 239.
12 J. W. Teipel and D. E. Koshland, Jr., *Biochemistry*, 10 (1971) 798.
13 C. N. Pace, *Methods Enzymol.*, 131 (1986) 266.

Journal of Chromatography, 539 (1991) 393–403
Elsevier Science Publishers B.V., Amsterdam

CHROM. 22 879

Isolation and characterization of two different molecular forms of basic fibroblast growth factor extracted from human placental tissue

SYLVIE UHLRICH*, JÉRÔME TIOLLIER, MICHEL TARDY and JEAN-LOUIS TAYOT
IMEDEX, Z.I. Les Troques, B.P. 38, 69630 Chaponost (France)

ABSTRACT

Basic fibroblast growth factor (bFGF) was purified to homogeneity from human placental tissue on a semi-large scale. Placental bFGF consists of two proteins of apparent molecular masses 16 000 and 18 000 dalton, as determined by sodium dodecyl sulphate polyacrylamide gel electrophoresis under non-reducing conditions. Microsequence analysis showed that both proteins have the same N-terminal sequence Pro–Ala–Leu–Pro–Glu–Asp–Gly–Gly–Ser–Gly–Ala–Phe..., which is identical with that of (1–146) bFGF extracted from human brain. After reduction by dithiothreitol or mercaptoethanol, placental bFGF appears as a single protein of 16 000 dalton. The reduced protein displays the same ability to stimulate the proliferation of CCL39 fibroblasts as the non-reduced doublet. These data indicate that bFGF extracted from placental tissue consists of two proteins with different apparent molecular masses which do not differ in their N-terminal sequence but in their oxidation state.

INTRODUCTION

Basic fibroblast growth factor (bFGF) is a heparin-binding polypeptide mitogen for a wide variety of mesodermal and neuroectodermal cells [1,2]. It was first isolated from bovine pituitary as a single-chain 16 500-dalton protein composed of 146 amino acids [3]. A number of N-terminal modified forms of bFGF have been identified, depending on the source and the method of isolation: bFGF extracted from bovine brain, retina and human brain under acidic conditions had 146 amino acids [4–6] whereas extraction of bovine kidney, adrenal, corpus luteum and testis [7–10] under acidic conditions yielded a truncated form of bFGF lacking the first fifteen amino acids. N-Terminal extended forms of bFGF have been described: an eight amino acid extension on extraction of human prostate under basic conditions [11] and a thirteen amino acid extension on extraction of human placenta after brief acidification [12]. A 25 000-dalton form has also been purified from guinea pig brain [13] and a 22 000-dalton immunoreactive form has been isolated from rat brain [14]. These observations indicate that bFGF consists of different molecular forms. These forms may be naturally occurring processed forms or may be generated by proteases released during the purification procedure.

Elucidation of the molecular heterogeneity of bFGF was also done by studying

0021-9673/91/$03.50

the role of the four cysteines contained in bFGF. By using site-directed mutagenesis, Arakawa *et al.* [15] demonstrated that the analogue protein deprived of all four cysteines exhibited mitogenic activity on NIH 3T3 cells which was indistinguishable from natural sequence protein. In a same manner, Seno *et al.* [16] showed that selective substitution of cysteine residue 69 or 87 by serine did not affect the heparin-binding ability of the protein but reduced its heterogeneity, recognized as several peaks of bFGF eluted from a heparin affinity column.

We report here for the first time the molecular heterogeneity of naturally occurring bFGF due to different oxidation states. Whereas all variations in apparent molecular mass of extracted bFGF which have been described up to now could be attributed to N-terminal variations, we show here that bFGF extracted from placental tissue under acidic conditions consists of a doublet of proteins which display the same N-terminal sequence but differ from each other in their oxidation state.

EXPERIMENTAL

Purification of placental bFGF

Placentas were collected at delivery and immediately frozen at −20°C. Pools of 500–600 placentas were mechanically ground into small pieces and then stirred, until completely thawed, in an 8% (v/v) ethanol–water solution. Placental blood was separated from the tissue on a press. The placental tissue pulp underwent further acid extraction at pH 3.2 at 4°C for 30 min. The acid extract was separated from the residual placental pulp on a press, neutralized and precipitated with 15% ethanol. The supernatant was recovered by centrifugation, concentrated by ultrafiltration and finally diafiltered against 0.1 *M* sodium phosphate (pH 6.0) with 10 000-dalton cut-off membranes. One litre of final placental tissue crude extract corresponded to *ca.* 15 kg of placental tissue pulp. The extract (198 g of proteins) was then applied to a 30 × 10 cm I.D. column of CM-Trisacryl (IBF Biotechnics, Villeneuve la Garenne, France) and eluted with the above-mentioned buffer until the absorbance at 280 nm dropped to the baseline at 2.0 a.u.f.s. The unretained fraction was discarded. The CM-Trisacryl column was eluted with 0.1 *M* sodium phosphate (pH 6.0) containing 0.15 *M* NaCl and then with 0.6 *M* NaCl buffer. The 0.15 *M* NaCl eluate showed of three successive absorbance peaks, denoted CM-1, CM-2 and CM-3. Fractions CM-2 and CM-3 contained most bFGF and were further purified on heparin–Sepharose (Pharmacia, Uppsala, Sweden). Each fraction was adjusted to 0.1 *M* sodium phosphate–0.65 *M* NaCl (pH 7.2) and pumped onto a heparin–Sepharose column (11 × 9 mm I.D.) that had previously been equilibrated with 6.5 m*M* Na_2HPO_4–1.5 m*M* KH_2PO_4–2.7 m*M* KCl–0.65 *M* NaCl (pH 7.2). The heparin–Sepharose column was washed with the same buffer until the absorbance at 206 nm dropped to the baseline at 0.5 a.u.f.s. and then eluted with the same buffer containing successively 1 and 2 *M* NaCl. Both 2 *M* NaCl eluates obtained from the CM-2 and CM-3 fractions were analysed and further stored at −70°C.

Protein determination

Protein concentrations were determined with the Bio-Rad Protein Assay (Bio-Rad Labs., Richmond, CA, U.S.A.) using human albumin (Pasteur Merieux Serums et Vaccins, Lyon, France) as a standard.

Analytical sodium dodecyl sulphate polyacrylamide gel electrophoresis (SDS-PAGE)

Proteins were analysed by SDS-PAGE following standard techniques [17] in the presence or absence of 2% (v/v) mercaptoethanol in 1-mm thick 20% acrylamide gels stained with silver nitrate [18]. About 1 μg of each sample was desalted on a PD10 column (Pharmacia) and lyophilized before SDS-PAGE. Molecular mass standards (Boehringer, Mannheim, Germany) were α_2-macroglobulin (170 000), phosphorylase B (97 400), glutamate dehydrogenase (55 400), lactate dehydrogenase (36 500), trypsin inhibitor (21 500), cytochrome *c* (12 500) and aprotinin (6500 dalton).

Preparative SDS-PAGE

Proteins (typically 5–10 μg per lane) were loaded on the same SDS-polyacrylamide gels as for analytical purposes (see above). After electrophoresis, the gels were dipped for a few seconds in water and then reversibly stained by gentle rocking in 250 ml of 0.3 *M* $CuCl_2$ solution for 5 min at room temperature [19]. The gels were then washed in water to remove excess of reagent. The protein bands appeared as negatively stained areas. Each band of the bFGF doublet (namely 16K and 18K, where K = kilodalton) was excised from the gel. Copper stain was eliminated by incubation in three changes (10 min each) of 0.25 *M* EDTA–0.25 *M* Tris–HCl (pH 9.0). Proteins were then eluted from the gels by vigorous rocking for 72 h at 4°C in 20 m*M* Tris–HCl–0.15 *M* glycine–0.01% SDS. The recovery was between 10 and 20%.

Reversed-phase high-performance liquid chromatography (HPLC)

A Waters Model 600 HPLC system was used, coupled with a Waters 490 programmable multi-wavelength detector (Millipore–Waters, Milford, MA, U.S.A.). Samples were loaded onto a C_4 reversed-phase HPLC column (Vydac 214TP54) (250 × 4.6 mm I.D.) equilibrated with 10% acetonitrile–0.05% trifluoroacetic acid at a flow-rate of 1.0 ml/min. The column was washed with 30 ml of this solvent and bound proteins were eluted with a 60-ml gradient of 10–50% acetonitrile–0.05% trifluoroacetic acid. Proteins were detected by monitoring the absorbance at 215 nm. Fractions of 1 ml were collected. For 16K and 18K chromatography after elution from SDS-polyacrylamide gels, samples were submitted to a first run as described. The main peak was collected, lyophilized, resuspended in 20 m*M* Tris–0.15 *M* glycine–0.01% SDS and rechromatographed under the same conditions before sequencing.

Protein sequence analysis

Protein sequence analysis was carried out at the Laboratoire Central d'Analyses (CNRS, Solaise, France) on a Model 470A gas-phase sequencer (Applied Biosystems, Foster City, CA, U.S.A.) connected "on-line" with a Model 120A phenylthiohydantoin amino acid analyser (Applied Biosystems).

Growth factor assays

The biological characterization of growth factor activities was performed by proliferation assays on bovine corneal endothelial cells and CCL39 fibroblasts. Corneal endothelial cells (EC) were isolated from bovine eye corneal endothelium by trypsinization and scraping. Once cultures had been established, EC were grown and maintained in culture flasks using Minimum Essential Medium (MEM) containing 6% foetal calf serum (FCS) and 100 μg/ml of crude placental extract. CCL39

fibroblasts (ATCC, Rockville, MD, U.S.A.) were subcultivated in MacCoy's medium supplemented with 20% FCS.

For both types of cells, proliferation assays were performed in 24-well plates (Falcon), in serum-free medium ($DMEM/F_{12}$) supplemented with insulin, transferrin, albumin and selenite and with increasing amounts of bFGF fractions to be tested. For EC, 10 000 cells were seeded at day 0 (D0) and stimulation with bFGF fractions were performed at D0, D1, D2, D3 and D4. Medium changes occurred at D2 and D4 and the total number of cells was determined after trypsinisation at D7. For CCL39 fibroblasts, 50 000 cells per well were seeded at D0. Stimulation with bFGF fractions was performed at D0, D1, D2 and D3. The medium was changed at D2 and the final total number of cells was determined at D4.

Reduction of bFGF

A 30-μg sample of bFGF was adjusted in 0.1 *M* Tris (pH 8)–1.5 m*M* EDTA–10 m*M* dithiothreitol and incubated for 1.5 h at 37°C. Reduced sulphydryl groups were then blocked with 20 m*M* iodoacetamide for 30 min at 37°C. Samples were then either desalted against water for SDS-PAGE or desalted against PBS–0.02% Tween 20 and assayed for biological activity.

RESULTS

Purification of placental bFGF

Placental tissue was processed after separation of the placental blood on a press. The extraction of placental tissue at pH 3.2 yielded a final placental extract which contained *ca.* 2.6 g of proteins per kilogram of tissue. When applied to a CM-Trisacryl in 0.1 *M* phosphate at pH 6.0, 90–95% of the proteins were recovered in the unretained fraction. bFGF was bound to the gel and eluted with 0.15 *M* NaCl. The 0.15 *M* NaCl eluate showed of three successive absorbance peaks (namely CM-1–3) (Fig. 1). After a second chromatography on heparin–Sepharose, only fractions CM-2 and CM-3 appeared to contain bFGF, which was eluted from heparin–Sepharose by stepwise elution at 2 *M* NaCl. The final bFGF fractions obtained from either CM-2 or CM-3 (namely HS-CM-2 and HS-CM-3), were analysed by SDS-PAGE (Fig. 2) under non-reducing conditions and consisted of two proteins of *ca.* 16K and 18K. The recovery was quantitative with a yield of purification of 15 μg of bFGF per kilogram of placental tissue.

The biological activity of placental bFGF was characterized on endothelial cells (Fig. 3): both bFGF fractions HS-CM-2 and HS-CM-3 stimulated the proliferation of bovine corneal endothelial cells. The ED_{50} (concentration of proteins necessary to induce half-maximum stimulation) was equivalent for both fractions and *ca.* 0.5 ng/ml. Cell growth depended on the concentration of bFGF in the medium and reached a plateau at 20 ng/ml.

Further characterization of placental bFGF

Separation of 16K and 18K proteins. We tried to separate the 16K and 18K proteins contained in the bFGF fraction by reversed-phase HPLC with an acetonitrile gradient, but both proteins coeluted in the same peak at 35% acetonitrile. However, both proteins could be separated by SDS-PAGE. The bFGF fraction was applied to an

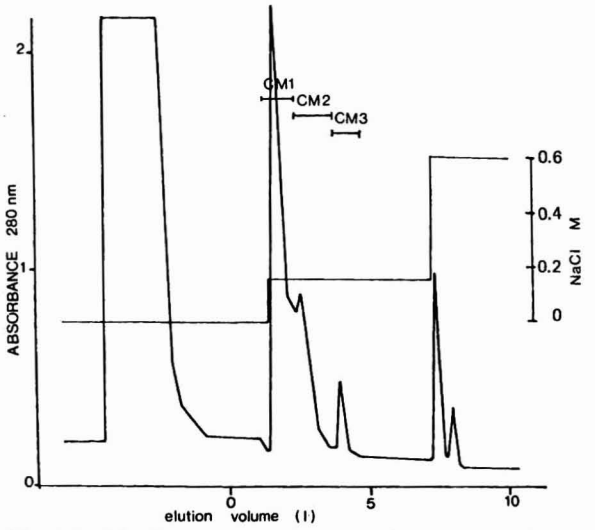

Fig. 1. Purification of crude acid placental extract by cation-exchange chromatography on CM-Trisacryl (30 × 10 cm I.D.) in 0.1 *M* sodium phosphate (pH 6.0). Stepwise elution with NaCl (0.15 and 0.6 *M*); flow-rate, 1.4 l/h.

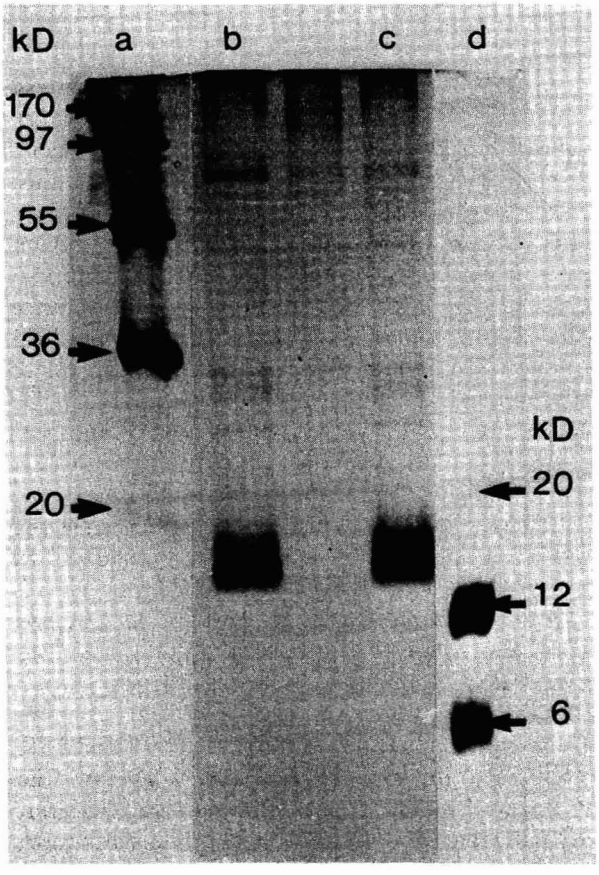

Fig. 2. SDS-PAGE (20%) under non-reducing conditions. Lanes a–d = molecular mass standards; b = placental bFGF purified from CM-2 eluate (HS-CM-2); c = placental bFGF purified from CM-3 eluate (HS-CM-3). kD = Kilodalton.

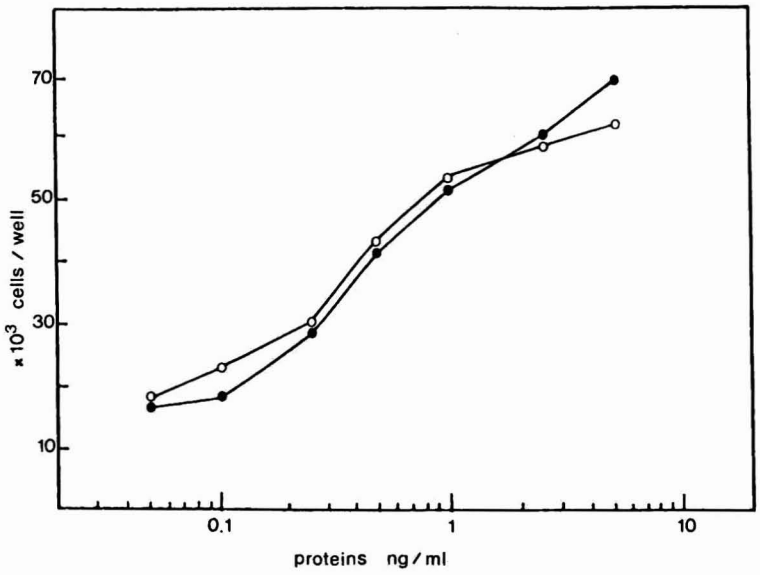

Fig. 3. Biological activity of placental bFGF HS-CM-2 (●) and HS-CM-3 (○) eluate on proliferation of bovine corneal endothelial cells. 10 000 cells at day 0; stimulation with bFGF fractions at day 1, 2, 3 and 4; medium changes at day 2 and 4; determination of total number of cells at day 7.

SDS-PAGE (20%) gel. The bands were reversibly stained with copper chloride, cut out from the gel and eluted by incubation in Tris–glycine buffer. The two proteins were further chromatographed by reversed-phase HPLC. Each protein eluted as a sharp peak at 44% acetonitrile (Fig. 4). SDS-PAGE of each HPLC eluate (Fig. 5) showed that the main peak consisted of the homogeneous protein, but the presence of dimeric (Fig. 5, lanes d and j) and oligomeric structures (Fig. 5, lanes e–f and k–l) was detected in the tail of the peak. This observation could be made for both 16K and 18K, indicating that both proteins are able to make aggregates (either by covalent or non-covalent bonds) under the physico-chemical conditions of reversed-phase HPLC elution. The amino-terminal sequence analysis of 16K and 18K showed that both proteins have the same sequence, Pro–Ala–Leu–Pro–Glu–Asp–Gly–Gly–Ser–Gly–Ala–Phe–Pro–Pro–Gly–His–Phe–Lys–, which is identical with that of (1–146) bFGF extracted from human brain (Table I). Moreover, for both proteins, microsequence analysis showed the presence of degraded polypeptides lacking the last amino acid (Pro) and the last four amino acids (Pro–Ala–Leu–Pro).

Effect of reducing agents on 16K and 18K proteins. The placental bFGF fraction, which consists of a 16K–18K doublet, was submitted to reduction by dithiothreitol followed by iodoacetamide alkylation. SDS-PAGE of the reduced fraction (Fig. 6, lane d) showed a single band at 16 000 dalton. Moreover, the direct analysis of the bFGF fraction in the presence of mercaptoethanol confirmed that the 18K bFGF form is transformed into the 16K bFGF form by reduction (Fig. 6, lane c). The biological activity of placental bFGF was also determined after reductive alkylation on CCL39 fibroblasts. As shown in Fig. 7, the bFGF fraction was equally active after

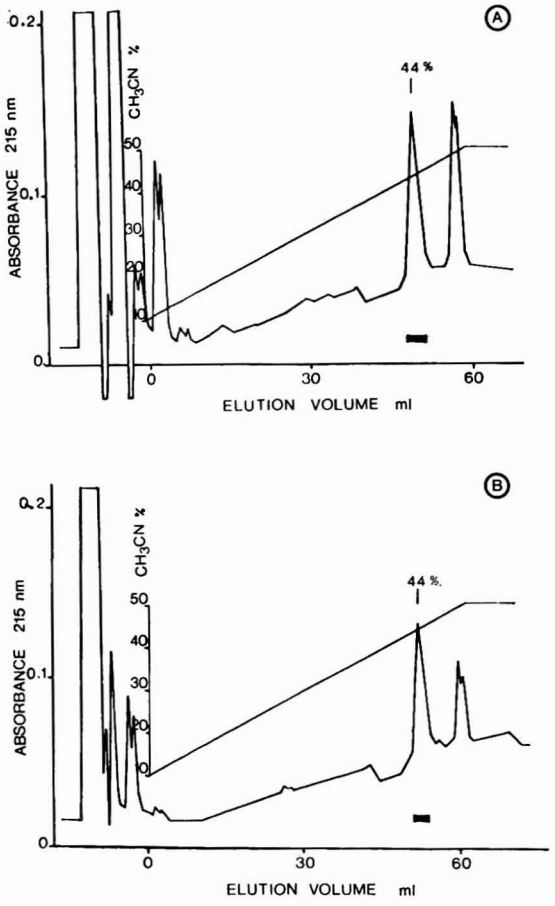

Fig. 4. Purification of 16K and 18K placental bFGF by reversed-phase HPLC on a Vydac C_4 column (250 × 4.6 mm I.D.). Flow-rate, 1.0 ml/min; 60-min gradient elution from 10 to 50% acetonitrile in water–0.05% trifluoroacetic acid. Elution profiles of (A) 16K and (B) 18K protein.

and before reduction, ED_{50} values ranging between 0.7 and 1 ng/ml as determined from four different experiments.

DISCUSSION

After extracting placental tissue by brief exposure to an acidic pH, we purified placental bFGF with two chromatographic steps involving cation-exchange chromatography followed by affinity chromatography on immobilized heparin. The resulting bFGF fraction consists of two proteins of apparent molecular masses 16K and 18K, as determined by SDS-PAGE under non-reducing conditions. Two molecular forms of bFGF have already been described in human placenta: the classical (1–146) bFGF identical with human brain bFGF [20] with a molecular mass of 16 400 dalton and a thirteen amino acid N-terminally extended form [12] with a molecular mass of

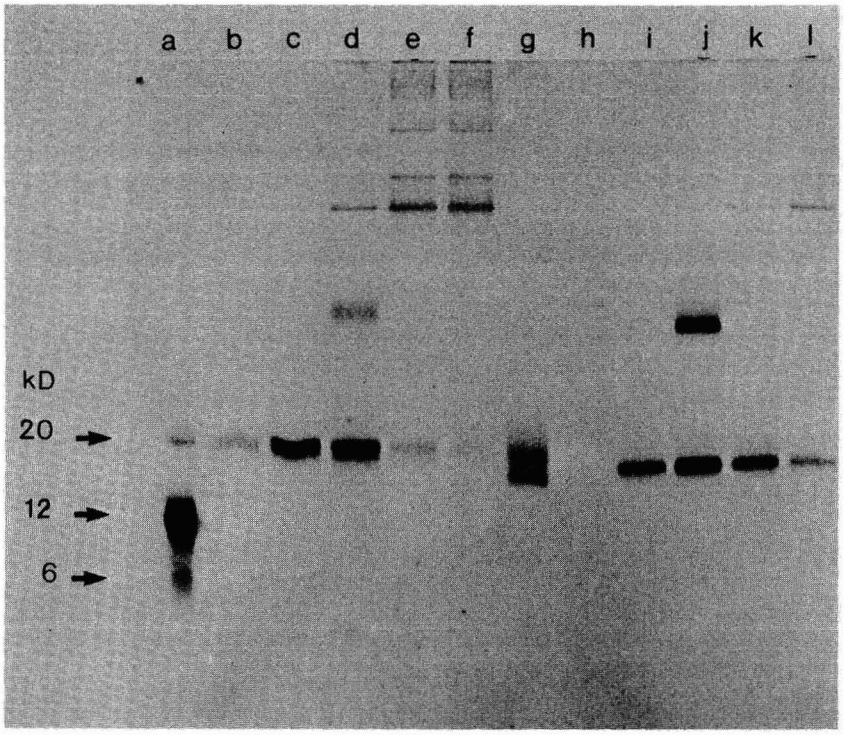

Fig. 5. SDS-PAGE (20%) under non-reducing conditions. Lanes: a = molecular mass standards; b = beginning of 18K peak on HPLC; c = 18K HPLC peak; d,e,f = tail of 18K HPLC peak; g = placental bFGF; i = 16K HPLC peak; j,k,l = tail of 16K HPLC peak. kD = Kilodalton.

17 500 dalton. However, in our case, N-terminal amino acid sequence analysis of the 16K and 18K proteins revealed that both proteins have the same N-terminal sequence, which is identical with that of brain (1–146) bFGF. Moreover, we showed that the 16K–18K doublet appears as a single 16K protein after reductive alkylation or by SDS-PAGE under reducing conditions. (1–146) bFGF contains four cysteines at positions 25, 69, 87 and 92, among which only residues 25 and 92 are conserved through the whole FGF family [21]. By site-directed mutagenesis and replacement of cysteine with serine residues, it was shown that substitution of cysteine residues at positions 69 and 87 did not affect the biological activity and heparin-binding ability of bFGF [16]. Moreover, in contrast to the natural sequence form, SDS-PAGE of the serine-69, 87 analogue under non-reducing conditions revealed little dimer formation [22]. Our data show that placental bFGF is equally active before and after reductive alkylation, indicating that the 18K protein displays the same biological activity as the 16K reduced form. Reversed-phase HPLC of each protein revealed the presence of dimers and oligomers in both instances, which disappeared on analysis in the presence of reducing agent (data not shown). These observations suggest that the 16K and 18K proteins differ from each other only in their oxidation state. The observation that they are both able to form intermolecular bonds supports the hypothesis that both proteins

TABLE I

AMINO-TERMINAL SEQUENCE ANALYSIS OF BOTH PLACENTAL bFGF MOLECULAR FORMS

Cycle	PTH-amino acid	bFGF 16K yield (pmol)	bFGF 18K yield (pmol)	Cycle	PTH-amino acid	bFGF 16K yield (pmol)	bFGF 18K yield (pmol)
1	Pro	42	22	11	Ala	10	4
2	Ala	18	7	12	Phe	10	4
3	Leu	16	6	13	Pro	6	4
4	Pro	15	8	14	Pro	5	1
5	Glu	15	5	15	Gly	4	?
6	Asp	10	4	16	His	3	2
7	Gly	3	4	17	Phe	6	2
8	Gly	7	0, 5	18	Lys	4	2
9	Ser	n.d.[a]	n.d.[a]	19	Asp	3	
10	Gly	7	2	20	Pro	2	

[a] n.d. = Not determined.

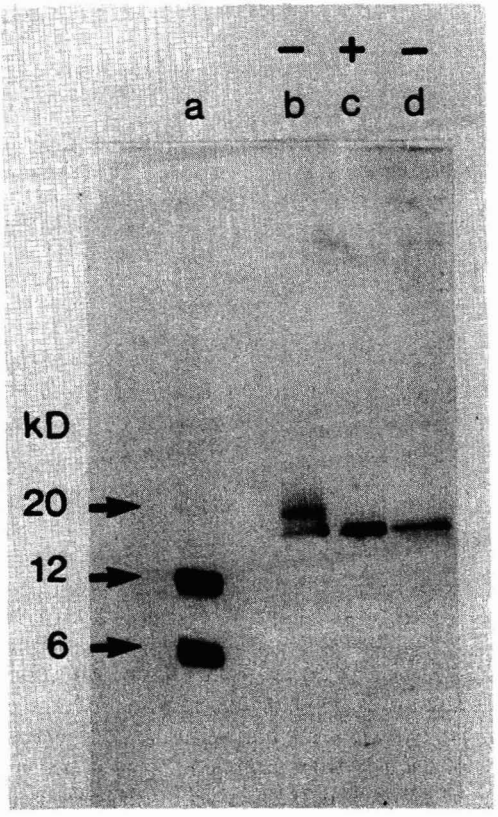

Fig. 6. SDS-PAGE (20%) in the presence (+) or absence (−) of mercaptoethanol. Lanes: a = molecular mass standards; b,c = native placental bFGF; d = placental bFGF after reductive alkylation (dithiothreitol + iodoacetamide). kD = Kilodalton.

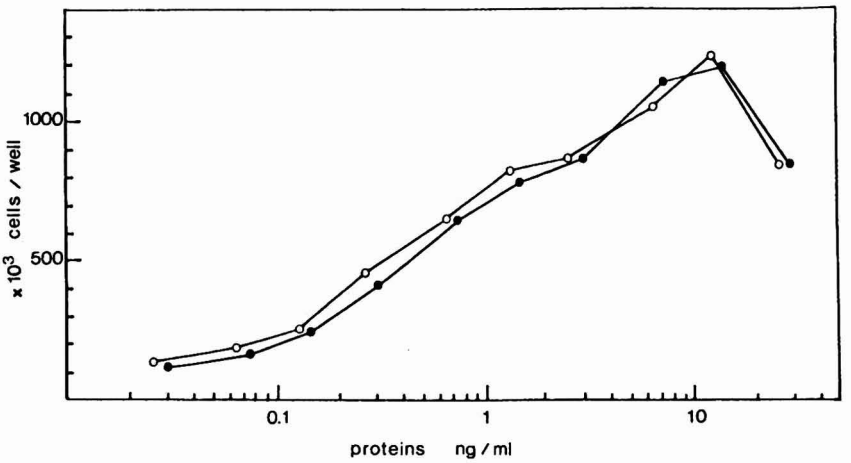

Fig. 7. Biological activity of placental bFGF native (●) or after reduction by dithiothreitol (○) on proliferation of CCL39 fibroblasts. 50 000 cells at day 0; stimulation with bFGF fractions at day 0, 1, 2 and 3; medium changes at day 2 and 4; determination of total number of cells at day 7.

contain free sulphydryl groups, the 16K protein containing all four cysteines free whereas the 18K protein contains at least one disulphide bridge. Moreover, the full biological potential of the 16K reduced form is consistent with the findings of Arakawa *et al.* [15], who showed that human bFGF analogue in which all four cysteines have been replaced with serine exhibited mitogenic activity on NIH 3T3 cell which was indistinguishable from the natural sequence molecule.

ACKNOWLEDGEMENTS

The authors thank Marielle Barthoux, Ginette Bouchut, Marie-Pierre Freychet and Marc Morel for excellent technical assistance and Isabelle Mercier for typing the manuscript.

REFERENCES

1 D. Gospodarowicz and J. S. Moran, *Annu. Rev. Biochem.*, 45 (1976) 531.
2 A. Baird, F. Esch, P. Normede, N. Ueno, N. Ling, P. Bohlen, S. Y. Ying, W. B. Wehrenberg and R. Guillemin, *Recent Prog. Horm. Res.*, 42 (1986) 143.
3 F. Esch, A. Baird, N. Ling, N. Ueno, F. Hill, L. Denoroy, R. Klepper, D. Gospodarowicz, P. Bohlen and R. Guillemin, *Proc. Natl. Acad. Sci. U.S.A.*, 82 (1985) 6507.
4 D. Gospodarowicz, J. Cheng, G. M. Lui, A. Baird and P. Bohlen, *Proc. Natl. Acad. Sci. U.S.A.*, 81 (1984) 6963.
5 A. Baird, F. Esch, D. Gospodarowicz and R. Guillemin, *Biochemistry*, 24 (1985) 7856.
6 P. Bohlen, F. Esch, A. Baird, K. L. Jones and D. Gospodarowicz *FEBS Lett.*, 185 (1985) 177.
7 A. Baird, F. Esch, P. Bohlen, N. Ling and D. Gospodarowicz, *Regul. Pept.*, 12 (1985) 201.
8 D. Gospodarowicz, A. Baird, J. Cheng, G. M. Lui, F. Esch and P. Bohlen, *Endocrinology*, 118 (1986) 82.
9 D. Gospodarowicz, J. Cheng, G. M. Lui, A. Baird, F. Esch and P. Bohlen, *Endocrinology*, 117 (1985) 2383.

10 N. Ueno, A. Baird, F. Esch, N. Ling and R. Guillemin, *Mol. Cell. Endocrinol.*, 49 (1987) 189.
11 M. T. Story, F. Esch, S. Shimasaki, J. Sasse, S. C. Jacobs and R. K. Lawson, *Biochem. Biophys. Res. Commun.*, 142 (1987) 702.
12 A. Sommer, M. T. Brewer, R. C. Thompson, D. Moscatelli, M. Presta and D. B. Rifkin, *Biochem. Biophys. Res. Commun.*, 144 (1987) 543.
13 A. Sommer, D. Moscatelli and D. B. Rifkin, *Biochem. Biophys. Res. Commun.*, 160 (1989) 1267.
14 M. Presta, M. Rusnati, J. A. M. Maier and G. Ragnotti, *Biochem. Biophys. Res. Commun.*, 155 (1988) 1161.
15 T. Arakawa, Y. R. Hsu, S. G. Schiffer, L. B. Tsai, C. Curless and G. M. Fox, *Biochem. Biophys. Res. Commun.*, 161 (1989) 335.
16 M. Seno, R. Sasada, M. Iwane, K. Sudo, T. Kurokawa, K. Ito and K. Igarashi, *Biochem. Biophys. Res. Commun.*, 151 (1988) 701.
17 U. K. Laemmli, *Nature (London)*, 227 (1970) 680.
18 W. Wray, T. Boulikas, V. P. Wray and R. Hancock, *Anal. Biochem.*, 118 (1981) 197.
19 C. Lee, A. Levin and D. Branton, *Anal. Biochem.*, 166 (1987) 308.
20 D. Gospodarowicz, J. Cheng, G. M. Lui, D. K. Fujii, A. Baird and P. Bohlen, *Biochem. Biophys. Res. Commun.*, 12 (1985) 554.
21 T. Yoshida, K. Miyagawa, H. Odagiri, H. Sakamoto, P. F. R. Little, M. Terada and T. Sugimura, *Proc. Natl. Acad. Sci. U.S.A.*, 84 (1987) 7305.
22 G. M. Fox, S. G. Schiffer, M. F. Rohde, L. B. Tsai, A. R. Banks and T. Arakawa, *J. Biol. Chem.*, 263 (1988) 18452.

Journal of Chromatography, 539 (1991) 405–416
Elsevier Science Publishers B.V., Amsterdam

CHROM. 22 885

High-performance anion-exchange chromatographic study of desialylated human α_1-acid glycoprotein variants

Development of a fractionation method for the protein slow variants

FRANÇOISE HERVE*, JEAN-CLAUDE DUCHE, NATHALIE SPORTES and JEAN-PAUL TILLEMENT

Service Hospitalo-Universitaire de Pharmacologie de Paris XII, Centre Hospitalier Intercommunal de Créteil, 40 Avenue de Verdun, 94010 Créteil Cedex (France)

ABSTRACT

The three main desialylated variants (F1, S and A) of human α_1-acid glycoprotein (AAG), a serum acute-phase reactant, were analysed by high-performance anion-exchange chromatography in order to determine their optimum separation conditions. The analysis consisted of three steps, as follows: (1) A desialylated commercial AAG was separated into one "fast"- and one "slow"-migrating fraction by preparative isoelectrofocusing. The "fast" and "slow" fractions were shown to contain the F1 variant and a mixture of the S and A variants, respectively. (2) The pH titration curves of these two fractions were then measured by strong anion-exchange chromatography with several buffer systems of increasing pH. From the data obtained, it was not possible to select the optimum conditions to separate the "fast" variant F1 from the "slow" variants A and S. However, the S and A variants were shown to ionize very differently. (3) The specific fractionation of the S and A variants was therefore carried out by anion-exchange chromatography under operating conditions based on the data obtained from the study of their pH titration curves. This was performed both with the "slow"-migrating fraction obtained by preparative isoelectrofocusing of commercial AAG and with an AAG (containing only variants S and A) purified from an individual serum on immobilized Cibacron Blue F3G-A. Identification of the fractionated proteins was achieved by analytical isoelectrofocusing.

INTRODUCTION

α_1-Acid glycoprotein (AAG), or orosomucoid, is an acute-phase reactant whose serum concentration increases in association with inflammatory states (for a review, see ref. 1). Its physiological function is still unknown but it is thought to act as a transport protein for basic drugs such as antidepressant drugs, neuroleptics and β-blockers, and also plays a role in immunoregulation (for a review, see ref. 1).

It has been well documented that AAG, which has a high carbohydrate content and a large number of sialyl residues, is very heterogeneous, consisting of subpopulations of different size, charge [2] and lectin-binding behaviour [3].

0021-9673/91/$03.50

One extensively studied case of the heterogeneity of AAG is the existence, after desialylation of the protein, of three main variants, distinguished by their electrophoretic migration in analytical isoelectrofocusing (IEF) as one "fast" and two "slow" bands [4], corresponding to the F1 and to the S and A variants, respectively. These variants differ in that numerous amino acids are substituted in the peptide chain [5]. This microheterogeneity is genetically determined and, depending on the relative concentrations of the variants in desialylated serum, three main phenotypes are observed for AAG in a general population: F1 S/A, F1/A and S/A, with expected frequencies of 47.9, 35.1 and 16.4%, respectively [4].

Elucidation of this heterogeneity, especially in the light of the possibility of functional differences between AAG variants, has recently been attempted. Commercial human AAG containing the three variants was fractionated after its desialylation, into a "fast" (F-AAG) and a "slow" AAG (S-AAG) by a preparative IEF technique [6,7]. The F- and S-AAG were shown to contain the F1 and a mixture of the S and A variants, respectively. Comparison of their drug-binding properties showed that S-AAG exhibits a higher binding capacity ($n \cdot k$, where n is the number of binding sites and k is the intrinsic affinity constant) than F-AAG for most of the drugs tested [6,7]. It was also proposed that only one of the two S-AAG variants was responsible for the high-affinity binding site. However, it was impossible to determine which variant, S or A, is involved, as they cannot be fractionated electrophoretically without denaturation, and because commercial AAG is a mixture of the phenotypes and contains equal proportions of the A and S variants.

Using high-performance ion-exchange chromatography (HPIEC), we studied the pH titration curves of the AAG variants in order to optimize their separation by this method. The results enabled us to develop an HPIEC method for the fractionation of S-AAG into its two charge variants and this fractionation was compared with the electrophoretic heterogeneity of S-AAG as shown by analytical IEF. The HPIEC methodology was also applied to the fractionation of an AAG purified in the laboratory from an individual serum of phenotype S/A by chromatography on immobilized Cibacron Blue F3G-A [8].

EXPERIMENTAL

Materials

Human serum containing AAG with the S/A phenotype (S/A-AAG) was obtained from a healthy donor and was frozen until use.

Materials were obtained from the following sources: human AAG (from Cohn fraction VI), *Clostridium perfringens* neuraminidase type X, Norite A charcoal and 1,3-bis[tris(hydroxymethyl)methylamino]propane (Bis–Tris-propane) were from Sigma (St. Louis, MO, U.S.A.), bovine serum albumin (grade A) from Calbiochem (San Diego, CA, U.S.A.), Cibacron Blue F3G-A from Fluka (Buchs, Switzerland), Sephadex G-100, DEAE-Sephadex, Mono Q HR 5/5 prepacked column, gradient gels PAA 4/30, low-molecular-mass marker protein kit, immobiline (pK 4.6 and pK 9.3), Gelbond PAG films, acrylamide and N,N′-methylenebisacrylamide from Pharmacia–LKB (Uppsala, Sweden), Coomassie Brilliant Blue R 250, urea and 2-mercaptoethanol from Merck (Darmstadt, Germany) and YM 10 membrane filter and Centricon 10 microconcentrator from Amicon (Danvers, MA, U.S.A.). All other reagents were of grade A or analytical-reagent grade and were purchased from local suppliers.

Purification of the S/A-AAG on immobilized Cibacron Blue F3G-A

The covalent coupling of Cibacron Blue F3G-A to Sephadex G-100 was performed according to Böhme *et al.* [9], with 0.85 g of dye per gram of dry gel at 80°C, in order to obtain maximum dye substitution. The determination of the amount of dye covalently bound to the matrix was carried out according to Chambers [10]. The S/A-AAG was purified from the serum essentially by the one-step chromatographic procedure on immobilized Cibacron Blue F3G-A described by Birkenmeier and Kopperschläger [8] in 10 m*M* sodium phosphate buffer (pH 5.8) and at 4°C. The purified protein was concentrated on a YM 10 membrane filter and dialysed against deionized water.

Charcoal treatment and desialylation of AAG

Before use, the pure S/A-AAG preparation and the commercial AAG were delipidated by charcoal treatment at pH 3.0 according to Evenson and Deutsch [11] and then lyophilized. Both proteins were then desialylated with neuraminidase as described by Eap *et al.* [6], dialysed against deionized water and lyophilized.

Prior to analytical IEF, the human whole serum used in the chromatographic procedure on immobilized Cibacron Blue was desialylated with neuraminidase as described by Eap *et al.* [4].

Spectrophotometry and protein assay

Absorbance determinations or spectral scans were performed on a Beckman Model DU-3 single-path recording spectrophotometer. Total protein concentrations were determined by the method of Lowry *et al.* [12] with bovine serum albumin (grade A) as a standard. The specific assay of AAG was carried out by an immunonephelometric method using a Beckman assay kit and instrument.

Electrophoretic techniques

The purity of the S/A-AAG preparation was checked by sodium dodecyl sulphate–polyacrylamide gel electrophoresis (SDS-PAGE) [13] using a Pharmacia GE 2-4/LS vertical gel electrophoresis apparatus. Analytical and preparative IEF were performed using an LKB 2117 Multiphor II electrophoresis apparatus.

Separation of the S- and F-AAG from the desialylated commercial AAG was performed by a preparative IEF technique in an immobilized pH 4.4–5.4 polyacrylamide gel gradient [6,7]. The separated F- and S-AAG were detected in strips of the gel by trichloroacetic acid fixation and Coomassie Brilliant Blue staining. The protein in each band was recovered from the remainder of the gel by electrophoretic elution into DEAE-Sephadex. After recovery from Sephadex, the two fractions were dialysed extensively against deionized water and lyophilized.

Analytical IEF of the desialylated AAG variants and AAG phenotyping of the desialylated whole serum were performed essentially as described by Eap and Baumann [14] in an immobilized pH 4.4–5.4 polyacrylamide gel gradient with 8 *M* urea and 2% (v/v) 2-mercaptoethanol. Detection of the variants was made by immunoblotting with two antibody steps [14] or by staining with Coomassie Brilliant Blue. The analytical IEF of the desialylated proteins also permitted the determination of the extent of desialylation. The relative proportion of each protein band in the gels was determined by scanning with an LKB 2202 Ultroscan laser densitometer.

High-performance ion-exchange chromatography (HPIEC)

HPIEC was performed on a Waters Assoc. liquid chromatography system equipped with two Model 6000-A pumps and a Model 660 solvent programmer capable of generating a gradient or step elution profile. Sample injections were carried out with a Waters Assoc. Model U6K injector and chromatograms were recorded by monitoring the absorbance of the eluent at 280 nm using a single-path UV monitor (Cecil Instruments, Cambridge, U.K.) fitted with a 10-mm path-length flow cell. The absorbance units full-scale (a.u.f.s.) were set between 0.02 and 0.5 as appropriate. Fractions were collected with a Gilson Model 203 fraction collector. The HPIEC system was operated at room temperature.

HPIEC of the desialylated AAGs was carried out using a Pharmacia Mono Q strong anion-exchange column (50 × 5 mm I.D.; 10 μm particle size).

In initial experiments, the pH titration curves of the AAG variants were determined using buffer systems of pH 7.0–10.0 (adjusted with 1 *M* hydrochloric acid), with the starting and final buffers containing 6.25 m*M* Bis–Tris-propane and with 0.15 or 0.35 *M* sodium chloride in the final buffer. The F- and S-AAG, obtained by the preparative IEF technique, were chromatographed with each buffer system.

Fractionation of the S-AAG and of the S/A-AAG preparation was carried out on the same anion-exchange column. The starting and final buffers were 6.25 m*M* Bis–Tris-propane chloride adjusted to pH 9.75 with 1 *M* hydrochloric acid, with the final buffer containing 0.15 *M* sodium chloride. A preprogrammed linear gradient was used for the chromatography and the appropriate peak fractions were collected, concentrated and re-equilibrated in deionized water or start buffer, using Centricon 10 microconcentrators, prior to their study by analytical IEF or their rechromatography.

RESULTS AND DISCUSSION

Purification of AAG from an individual serum on immobilized Cibacron Blue F3G-A

Measurement of the absorption spectrum of the Cibacron Blue F3G-A used showed a broad peak at 595–630 nm and the calculated molar absorptivity was 10.3 $l \cdot mmol^{-1}\ cm^{-1}$. This was compared with a value of 13.6 $l \cdot mmol^{-1}\ cm^{-1}$ obtained by Thompson and Stellwagen [15] using especially purified Cibacron Blue F3G-A, and a purity of 75.7% was calculated for the dye sample used in our experiments. This value was used to correct the values obtained for dye release in subsequent experiments.

Under the experimental coupling conditions used, a maximum of 150 μg of dye covalently bound per milligram of dry Cibacron Blue–Sephadex was found by hydrolysis of the substituted gel in 6 *M* hydrochloric acid [10]. This loading density is less than that used by Birkenmeier and Kopperschläger [8] in their chromatographic purification procedure for human AAG. Nevertheless, when the individual serum, dialysed against 10 m*M* sodium phosphate buffer (pH 5.8), was applied to the Cibacron Blue–Sephadex column, the only constituent detected in the breakthrough fraction was AAG. Fig. 1 shows the elution pattern obtained by chromatography of the individual serum and the presence of two peaks can be observed, a major peak and a minor "retarded" peak. Each peak was separately concentrated on an Amicon YM 10 membrane filter. The total protein concentration and the specific AAG concentration were determined in each peak and identical results were obtained with

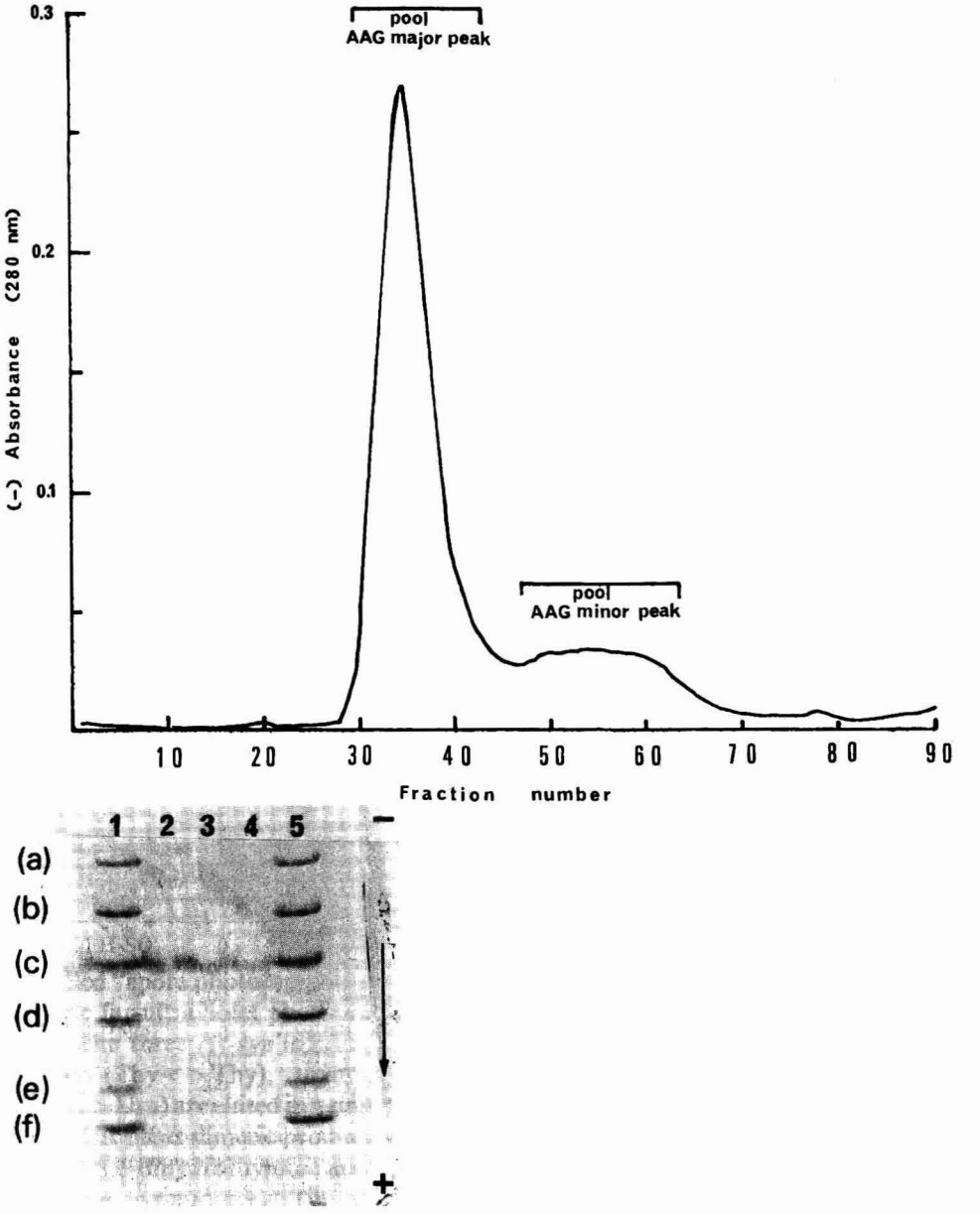

Fig. 1. Elution of AAG by chromatography of a single human serum sample on Cibacron Blue F3G-A–Sephadex G-100 gel at pH 5.8. The dye substitution in the gel was 150 μg of dye per mg of Sephadex. A 50-ml volume of the human serum was dialysed against 10 m*M* sodium phosphate buffer (pH 5.8) and applied to the gel column (50 × 5 cm I.D.) equilibrated with the same buffer at 4°C. The unbound protein was eluted in 10 m*M* sodium phosphate buffer (pH 5.8). The flow-rate was 50 ml/h and fractions of 6.8 ml were collected. The absorbance of each fraction was determined spectrophotometrically at 280 nm. The major and minor peaks of AAG were pooled separately as indicated and concentrated prior to their subjection to SDS-polyacrylamide gel electrophoresis. Inset: SDS-PAGE of the pooled fraction of AAG. Lanes: 1 and 5 = molecular mass (dalton) markers [(a) phosphorylase *b* (94 000), (b) albumin (67 000), (c) ovalbumin (43 000), (d) carbonic anhydrase (30 000), (e) trypsin inhibitor (20 000) and (f) α-lactalbumin (14 000)]; 2 = standard commercial AAG (5 μg); 3 = AAG major peak (5 μg); 4 = AAG minor peak (5 μg).

both assays. The major and minor peaks were shown to contain 88 and 12%, respectively, of the total amount of AAG purified on immobilized Cibacron Blue F3G-A. SDS-PAGE showed that the two peaks seemed to be composed of at least 90% pure AAG because, in both peaks, a single protein band was detected (Fig. 1, inset) and a molecular mass of 44 000 dalton was calculated, identical with that of a standard commercial AAG.

A similar fractionation of "native" AAG into more than one peak has already been described by Gianazza and Arnaud [16] during the chromatography of plasma proteins on commercially available immobilized Cibacron Blue (Affi-gel Blue). The origin of the existence of more than one peak for AAG in dye-affinity chromatography could be due to differences in the sugar chains of the protein sub-populations (for instance, the existence of partially desialylated "old" forms of AAG, physiologically present in the serum). This minor peak requires further study.

The major AAG peak corresponded to 70–75% of the total serum AAG as determined by immunospecific assays of the serum and the chromatographic peak. Hence the chromatography of the serum (50 ml) yielded 18 mg of AAG from a total amount of 25 mg of AAG.

This purified AAG (major peak) was dialysed against deionized water and delipidated. It was then desialylated with neuraminidase and subjected to analytical IEF on an immobilized pH 4.4–5.4 polyacrylamide gel gradient with 8 *M* urea and 2% (v/v) mercaptoethanol. The S/A-AAG was found to contain only the "slow" variants A and S (Fig. 2). This result agreed with the AAG phenotyping of the serum used (not shown). Several faint, more anodic bands were also observed after staining with Coomassie Brilliant Blue (Fig. 2), indicating the presence of a small proportion (less than 5%) of incompletely desialylated protein. The relative proportions of each variant in the S/A-AAG were 63 and 37% for the S and A variants, respectively, as found by scanning. These values agree with the relative proportions of the S and A variants in desialylated whole serum (60 and 40%, respectively).

Separation of S-AAG and F-AAG from desialylated commercial AAG by preparative IEF

The preparative IEF of commercial AAG, previously desialylated with neuraminidase, on an immobilized pH 4.4–5.4 polyacrylamide gel gradient allowed the separation of a "slow" S-AAG from a "fast" F-AAG [6,7]. The respective electrophoretic patterns of the F- and S-AAG, and that of the desialylated unfractionated commercial AAG, obtained by analytical IEF in the presence of 8 *M* urea and 2% (v/v) 2-mercaptoethanol are shown in Fig. 2. It can be seen that, whereas the F-AAG is homogeneous and contains only the F1 variant, the S-AAG is heterogeneous and is composed of the two A and S variants. The relative proportions of the F1, S and A variants in the commercial AAG were 32, 38 and 32%, respectively, as found by scanning. The relative proportions of the "slow" S and A variants were 50% each in the S-AAG and are in accordance with those found with the unfractionated protein.

Chromatographic pH titration curves of the desialylated AAG variants

In the ion-exchange chromatography of proteins, there is a correlation between the ionic strength needed for elution and the net charge of the protein. As the protein charge, and consequently the ionic strength at which it will be eluted, varies with pH,

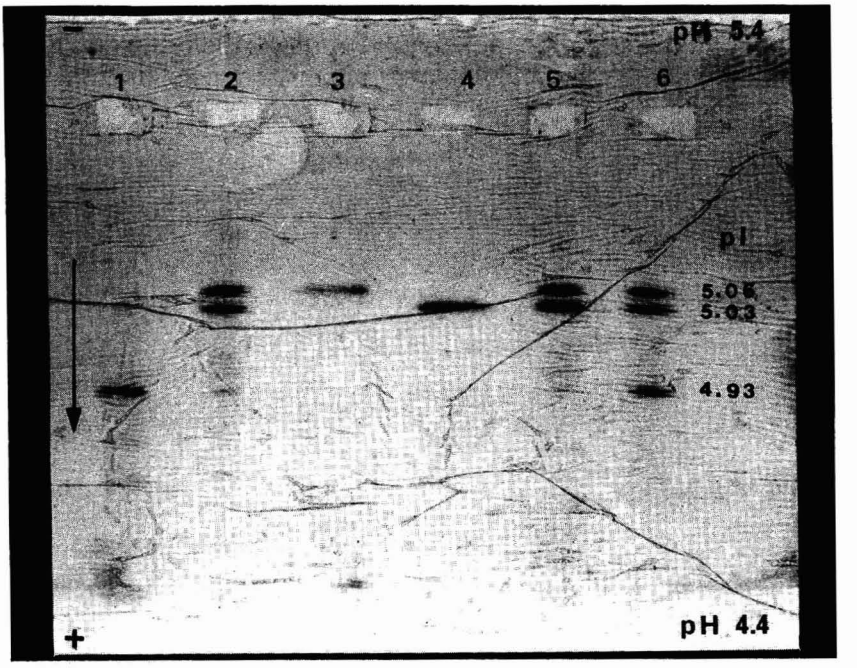

Fig. 2. Electrophoretic patterns of the different desialylated AAG samples on immobilized pH 4.4–5.4 polyacrylamide (4.85%, w/v) gel gradient with 8 *M* urea and 2% (v/v) 2-mercaptoethanol. Detection of the desialylated variants in the gel after fixation of the proteins in 11.5% (w/v) trichloroacetic acid and 3.5% (w/v) sulphosalicylic acid and staining with a 0.115% (w/v) Coomassie Brilliant Blue R 250 solution. Tracks: 1 = F-AAG isolated from desialylated commercial AAG by preparative IEF (20 μg); 2 = S-AAG isolated from desialylated commercial AAG by preparative IEF (20 μg); 3 = peak 2 (variant A) fractionated by HPIEC from S/A-AAG or S-AAG (20 μg); 4 = peak 1 (variant S) fractionated by HPIEC from S/A-AAG or S-AAG (20 μg); 5 = S/A-AAG purified on immobilized Cibacron Blue F3G-A (20 μg); 6 = desialylated commercial AAG (20 μg). The pH scale and the approximate isoionic point (p*I*) value for each variant are indicated.

titration curves are of great interest for predicting the elution pattern over a range of pH. The titration curves of F- and S-AAG were therefore determined separately by strong anion-exchange chromatography with buffer systems of different pH values, ranging from 7.0 to 10.0, to find the pH at which their titration curves are furthest apart and thus their separation will be optimum. The resolution of each buffer system was compared by plotting pH *versus* the amount of sodium chloride needed for elution (Fig. 3). The amounts of sodium chloride were deduced from the elution volume for the major peaks of interest. It can be seen that all the desialylated variants had a low negative charge because, even at pH 10, they eluted at a relatively low ionic strength. S-AAG began to be fractionated at pH 8.5 and, at higher pH, two well differentiated pH titration curves were observed, the lower curve corresponding to the titration of the A variant and the upper curve to that of the S variant.

The pH titration curve of F-AAG shows that, at lower pH, the "fast" variant F1 seems to be slightly more negatively charged than the "slow" variants. This result

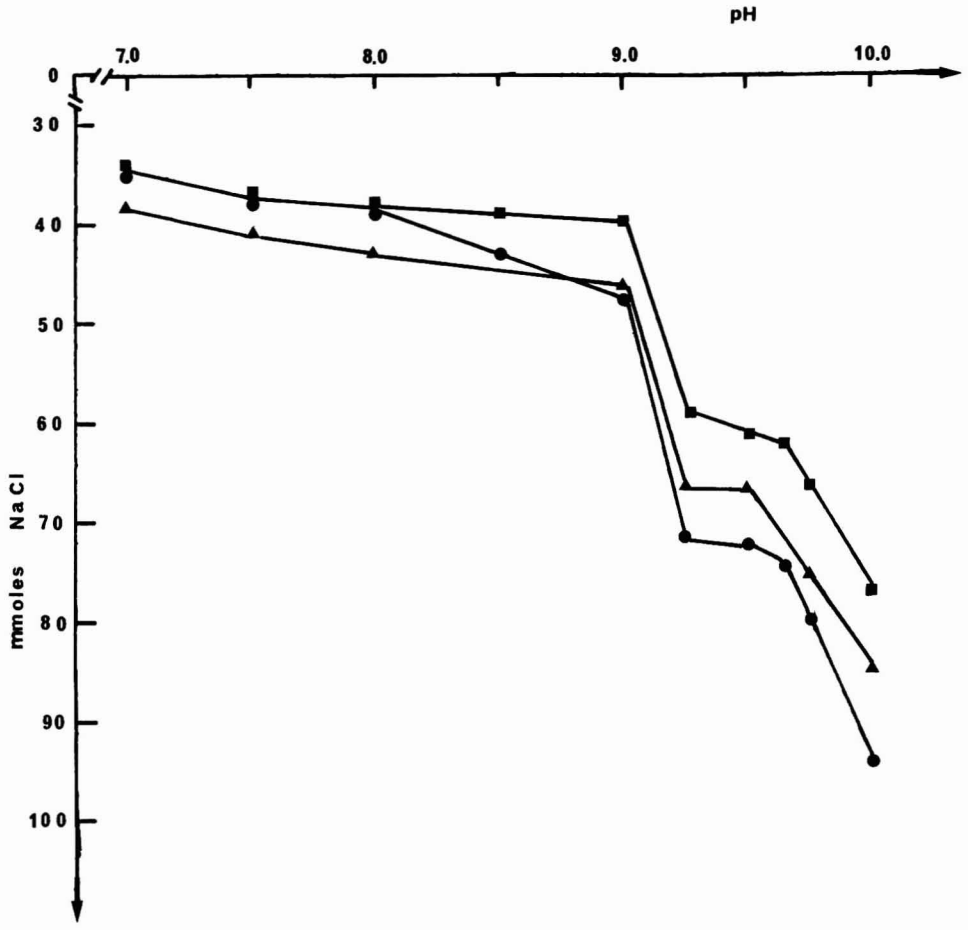

Fig. 3. pH titration curves for the desialylated AAG variants. The pH titration curves of the variants (▲) F1, (■) S and (●) A were determined in 6.25 m*M* Bis–Tris-propane (starting and final) buffer systems, with different pH values ranging from 7.0 to 10.0, adjusted with 1 *M* hydrochloric acid. The final buffer contained 0.15 or 0.35 *M* sodium chloride. The F- and S-AAG (100–200 μg), purified by preparative IEF, were run on a prepacked Mono Q HR 5/5 column with a 20-min gradient time. The flow-rate was 1.0 ml/min and the a.u.f.s. was set to 0.05–0.2. The pH was plotted *versus* millimoles of sodium chloride, which were deduced from the elution volume of each major peak of interest.

agrees with the more anodic migration of the F1 variant in IEF electrophoresis. It can also be seen that, over the pH range considered, the titration curve of the F1 variant parallels that of the S variant. Consequently, at pH 9.0, the titration curve of the F1 variant falls between the upper (S) and the lower (A) titration curves.

Analysis of the pH titration curves of the AAG variants showed that these curves present different inflexion points. Three different inflexion points can be observed in Fig. 3, at pH 8–8.5, 9 and 9.5–9.75. The sharp drops at pH 9 and pH 9.5–9.75 are similar for the three titration curves, indicating that the AAG variants may not differ

greatly in their contents of amino acids ionizing at these pH values. However, the inflexion between pH 8 and 8.5 with variant A was not found with the F1 and S variants. The pH at which this change occurs could correspond to the ionization of a cysteine residue, present in variant A but not in variants F1 and S.

These data agree with the differences between the primary structures of the variants. Human AAG is encoded by two different genes [17], thus explaining the multiple amino acid substitutions found in the primary sequence of AAG [5]. Genetic studies at the protein level in population [4] have shown that variants F1 and S are encoded by two different alleles of the same gene, and would differ only by few (five) amino acids, thus explaining their very similar pH titration curves. Variant A is encoded by the other gene and would differ from the other two variants by more amino acids (at least 22). Examination of the possible amino acid substitutions described for AAG [5] shows that only eight of them would be significant from an ionization point of view and, as most of these involve arginine residues which would not be negatively charged at pH values lower than 10, it becomes obvious why the pH titration curves of the three variants are similar. Given these data, it has not been possible to find optimum conditions for the separation of the "fast" F1 variant from the "slow" S and A variants by strong anion-exchange chromatography. Nevertheless, the specific change in the pH titration curve of the A variant between pH 8 and 8.5 could correspond to the titration of the lone cysteine residue at position 149, which could be substituted by arginine residues in the F1 and S variant molecules. Therefore, the major difference between the titration curves for the S and A variants could be used to optimize their fractionation.

Fractionation of S-AAG and of the pure S/A-AAG preparation

We applied the resolving power of HPIEC to the resolution of S-AAG and S/A-AAG variants. It was found that fractionation of the two proteins at pH 9.75 on the strong anion-exchange column resolves two major peaks, 1 and 2, corresponding to the "slow" variants S and A (Fig. 4). This pH was used, rather than pH 10, because the proteins lost structural integrity at pH 10.5.

Integration showed that these peaks comprised *ca.* 50% each for the total S-AAG and 62.5 and 37.5%, respectively, for the S/A-AAG. The relative proportion of peak 2 in S/A-AAG is less than that in S-AAG. This seems to be due to the fact that, whereas S/A-AAG was purified from an individual serum containing a genetically determined proportion of each variant, S-AAG was prepared from a standard commercial protein which corresponds to a mixture of AAGs of different phenotypes.

The elution diagram also showed the presence of a minor "retarded" peak, which seems to correspond to an incompletely desialylated protein (faint anodic band in Fig. 2, track 3), thus explaining its delayed elution from the anion-exchange column.

Peaks 1 and 2 were isolated and rechromatography showed that they are genuine peaks with different elution volumes (Fig. 5). Characterization of peaks 1 and 2 by analytical IEF (Fig. 2) shows they are essentially pure: peak 1 comigrates with the S variant and peak 2 with the A variant. The elution volumes needed to elute the variant S in peak 1 and the variant A in peak 2 are in accordance with their respective pH titration curves.

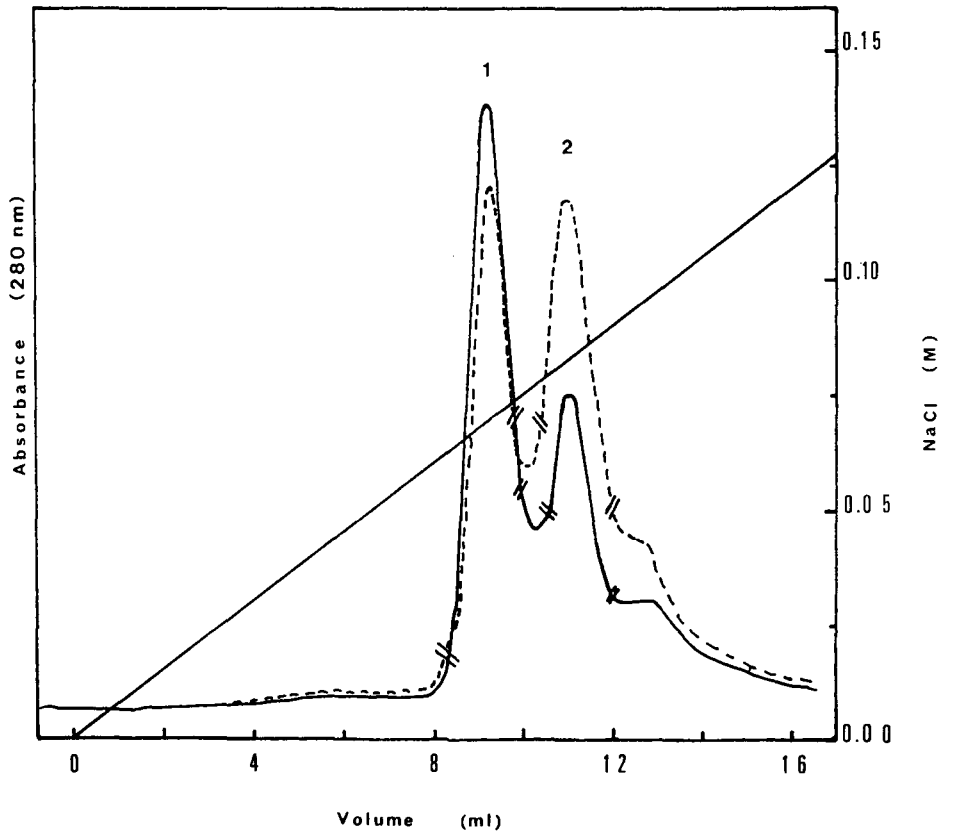

Fig. 4. HPIEC fractionation of S- or S/A-AAG on a prepacked Mono Q HR 5/5 column. S-AAG (dashed line) was isolated by preparative IEF of commercial AAG and S/A-AAG (solid line) was purified from the individual serum by chromatography on immobilized Cibacron Blue F3G-A. The starting buffer was 6.25 m*M* Bis–Tris-propane (pH 9.75) and final buffer was starting buffer containing 0.15 *M* sodium chloride; flow-rate, 1.0 ml/min; a.u.f.s., 0.5. Peaks 1 and 2 were collected as indicated by hatch marks in the elution profile.

CONCLUSION

This method allows the simple and rapid purification of large amounts of the "slow" variants of desialylated AAG. As these variants appear to be the more interesting with respect to drug binding [6,7], this purification method would greatly aid the study of their individual drug-binding properties.

Depending on the phenotype (F1/A or S/A or F1 S/A) of AAG preparations from individuals, the HPIEC method described here could be used to separate the S from the A variant and the preparative IEF technique could be used to separate the F1 from the A variant, but both techniques are required for the F1 S/A phenotype and commercial mixtures.

It was also found that the one-step chromatographic procedure on immobilized

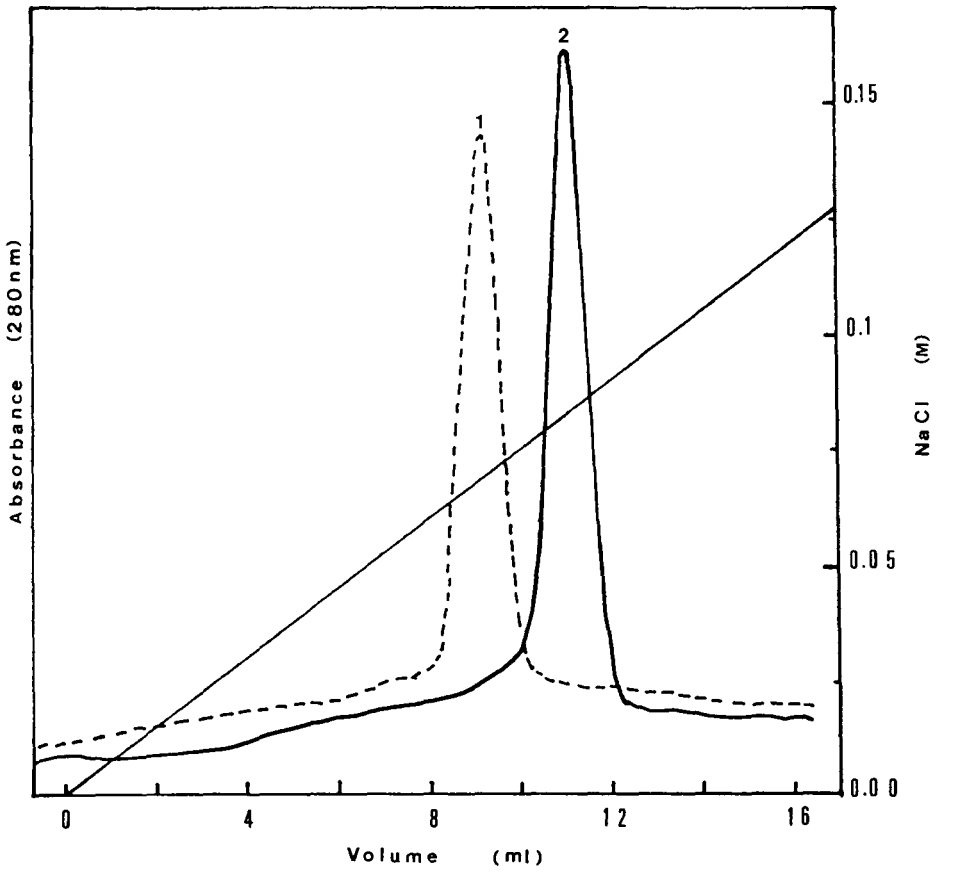

Fig. 5. HPIEC re-injection of peaks 1 (dashed line) and 2 (solid line) isolated from S/A-AAG in Fig. 4. Starting and final buffers and flow-rate as in Fig. 4; a.u.f.s., 0.1 and 0.05 for peaks 1 and 2, respectively. Prior to their injection, the proteins were re-equilibrated in starting buffer on a Centricon 10 microconcentrator.

Cibacron Blue F3G-A [8] is a valuable tool for purifying a "native" AAG with high yield from an individual serum. This procedure could be useful for comparing the drug-binding properties of individual "native" proteins corresponding to the different AAG phenotypes.

ACKNOWLEDGEMENTS

This research was supported in part by research grants from the Institut National de la Santé et de la Recherche Médicale (C.R.E. No. 872014), Réseau de Pharmacologie Clinique (Ministère de la Santé) and Ministère de la Recherche et de l'Enseignement Supérieur (No. 87C0320). The authors are indebted to M. Erdei for expert technical assistance.

REFERENCES

1 J. M. H. Kremer, J. Wilting and L. M. H. Janssen, *Pharmacol. Rev.*, 40 (1988) 1.
2 D. Tinguely, P. Baumann and J. Schöpf, *J. Chromatogr.*, 229 (1982) 319.
3 J. Agneray, in P. Baumann, C. B. Eap, W. E. Müller and J. P. Tillement (Editors), *Alpha$_1$-Acid Glycoprotein: Genetics, Biochemistry, Physiological Functions and Pharmacology*, Alan R. Liss, New York, 1989, p. 47.
4 C. B. Eap, C. Cuendet and P. Baumann, *Hum. Genet.*, 80 (1988) 183.
5 K. Schmid, in F. W. Putnam (Editor), *The Plasma Proteins, Structure, Function and Genetic Control*, Vol. I, Academic Press, New York, 2nd ed., 1975, p. 183.
6 C. B. Eap, C. Cuendet and P. Baumann, *Naunyn Schmiedeberg's Arch. Pharmacol.*, 337 (1988) 220.
7 C. B. Eap, C. Cuendet and P. Baumann, *J. Pharm. Pharmacol.*, 40 (1988) 767.
8 G. Birkenmeier and G. Kopperschläger, *J. Chromatogr.*, 235 (1982) 237.
9 H. J. Böhme, G. Kopperschläger, J. Schulz and E. Hofmann, *J. Chromatogr.*, 69 (1972) 209.
10 G. K. Chambers, *Anal. Biochem.*, 83 (1977) 551.
11 M. A. Evenson and H. F. Deutsch, *Clin. Chim. Acta*, 89 (1978) 341.
12 O. H. Lowry, N. J. Rosebrough, A. L. Farr and R. J. Randall, *J. Biol. Chem.*, 193 (1951) 265.
13 *Polyacrylamide Gel Electrophoresis Laboratory Techniques*, Pharmacia, Uppsala, 1980, p. 25.
14 C. B. Eap and P. Baumann, *Electrophoresis*, 9 (1988) 650.
15 S. T. Thompson and E. Stellwagen, *Proc. Natl. Acad. Sci. U.S.A.*, 73 (1976) 361.
16 E. Gianazza and P. Arnaud, *Biochem. J.*, 203 (1982) 637.
17 L. Dente, M. G. Pizza, A. Metspalu and R. Cortese, *EMBO J.*, 6 (1987) 2289.

Journal of Chromatography, 539 (1991) 417–424
Elsevier Science Publishers B.V., Amsterdam

CHROM. 22 892

Affinity chromatography of fibroblast growth factors on coated silica supports grafted with heparin

M. A. JACQUOT-DOURGES, F. L. ZHOU, D. MULLER* and J. JOZEFONVICZ
L.R.M. CNRS URA 502, Université Paris-Nord, Avenue J. B. Clément, 93430 Villetaneuse (France)

ABSTRACT

Dextran-coated silica beads are excellent supports for affinity chromatography of proteins. They can be easily grafted using conventional coupling methods with different active ligands, such as heparin. Fibroblast growth factors develop specific interactions with heparin through well-defined amino acids sequences. The heparin–dextran coated silica phases exhibit an affinity for these growth factors. Under our experimental conditions, the basic form can be absorbed on the solid support at a moderate salt concentration (0.5 *M* sodium chloride) and can be selectively desorbed by increasing the ionic strength of the eluent. The purification performances of such phases are compaired to those obtained on the heparin grafted soft gels. Because of their mechanical properties, the dextran-coated silica supports were also used in high-performance affinity chromatography to purify fibroblast growth factors from a bovine brain crude extract.

INTRODUCTION

Growth factors, known as fibroblast growth factors (FGF) [1] or heparin binding growth factors [2], are implicated in the growth of different types of cells, particularly fibroblasts and endothelial cells [3,4]. Among their biological activities, angiogenic and wound-healing properties are known and have been studied in order to use fibroblast growth factors in therapy [4,5].

Fibroblast growth factors are able to develop specific interactions with heparin through well defined amino acid sequences and the two forms of FGF, acidic FGF (aFGF) and basic FGF (bFGF), are generally purified by affinity chromatography on heparin-grafted soft gels.

In a previous paper [6], we demonstrated that polystyrene resins can be functionalized in order to obtain a specific affinity for fibroblast growth factors. These synthetic supports can also be used for the purification of FGF by affinity chromatography [7].

However, coated silica supports are excellent stationary phases for the high-performance affinity chromatography (HPAC) of proteins [8]. The passivation of native silica can be achieved by covering the inorganic surface with a layer of a hydrophilic polymer (agarose) substituted with a calculated amount of positively charged diethylaminoethyl (DEAE) functions. Thus the non-specific adsorption of

0021-9673/91/$03.50

proteins is minimized. Because of their polymeric coating, these supports can easily be grafted with functional derivatives, in particular with heparin, using conventional coupling methods. These affinity phases possess the mechanical properties of the starting silica and the hydrophilicity of the coating polysaccharide [9] and they can be used with low-pressure or high-performance liquid chromatographic (HPLC) elution conditions in order to separate or purify fibroblast growth factors. The chromatographic performances of these new affinity supports can be compared with the results observed under the same elution conditions on the conventional heparin–Sepharose affinity phase [10].

EXPERIMENTAL

Growth factors

Crude extracts and radiolabelled fibroblast growth factors were obtained as described previously [11]. Briefly, crude extract is prepared from a bovine brain by ammonium sulphate fractionation (the active fraction was found to be between 20 and 60%) at 4°C, followed by dialysis against acetic acid and phosphate buffer solutions. The sample is then centrifuged (20 000 *g*, 30 min, 4°C) and the ionic strength of the supernatant containing aFGF and bFGF is adjusted to 0.65 *M* NaCl. Acidic and basic fibroblast growth factors are purified from bovine brain crude extract by affinity chromatography on heparin–Sepharose support, and are radiolabelled with 125-iodine using the chloramine T method [6].

All reagents were of analytical-reagent grade and all solutions and buffers were prepared with doubly distilled water, which was degassed and filtered through a 0.22-μm membrane.

Heparin–silica supports

The silica-based (Hep–SiA) supports are prepared in two stages as described previously [9]. Agarose Indubiose A37 HAA, kindly provided by IBF Biotechnics (Villeneuve la Garenne, France), are modified by a controlled substitution with 2-diethylaminoethyl hydrochloride (Janssen Chemica, Pantin, France). First, silica beads X015 M (porosity 1250 Å, particle size 40–100 μm) from IBF Biotechnics are impregnated with a concentrated solution of DEAE-polysaccharide and the polymer coating is cross-linked in order to prevent leakage of the polymeric layer and to obtain a polymeric coverage of 4.5 g per 100 g of dry support. In the second step, heparin (101 I.U./mg), supplied by Institut Choay (Paris, France), is coupled using 1,1′-carbonyldiimidazole (CDI) as activating agent [10]. The yield of the coupling is 68%, corresponding to 34 mg of heparin per 1 g of support.

Low-pressure affinity chromatography

Two columns (30 × 11.4 mm I.D.) are packed, one with 4 ml of heparin–Sepharose (Pharmacia) and the other with 4 ml of heparin–dextran-coated silica phase in phosphate buffer solution (PBS) adjusted to 0.5 *M* NaCl (pH 7.4). This salt concentration (0.5 *M* NaCl) was chosen because aFGF could be retained by the support with a lower salt concentration and other proteins could be desorbed simultaneously by the salt gradient. Similarly, it is impossible to obtain pure aFGF by affinity chromatography on the heparin–Sepharose support if the initial salt concen-

tration of the eluent is lower than 0.5 *M*. A 5-ml sample of crude bovine brain extract mixed with radiolabelled FGFs (10^6 cpm) is injected into the columns. The non-adsorbed compounds are eliminated by washing with 150 ml of 10 m*M* PBS–3 m*M* KCl–0.5 *M* NaCl, pH 7.4). Next, the adsorbed proteins are desorbed using a salt gradient from 0.5 to 2.5 *M* NaCl (150 ml) at a flow-rate of 24 ml/h at room temperature. The absorbance at 280 nm and the ionic strength of the eluent are measured using an A111 UV detector (Gilson, Villiers le Bel, France) and an ion and pH detector (IBF Biotechnics), respectively. The amount of eluted radiolabeled fibroblast growth factor is determined using a gamma counter.

High-performance affinity chromatography

The HPLC apparatus is a Merck–Hitachi 655 A-12 system from Labs. Merck-Clevenot (Nogent sur Marne, France). A stainless-steel column (70 × 7 mm I.D.) is packed using a slurry method with 2.6 ml of heparin–silica phase in phosphate buffer solution (pH 7.4) adjusted to 0.5 *M* NaCl. A 5-ml aliquot of crude bovine brain extract is injected onto the column and the non-adsorbed compounds are eluted with the initial buffer (10 m*M* PBS–0.5 *M* NaCl, pH 7.4) at a flow-rate of 1.0 ml/min. The adsorbed proteins are then eluted by a linear salt gradient from 0.5 to 2 *M* NaCl in 0.01 *M* PBS (pH 7.4). The elution is followed using a variable-wavelength UV monitor at 280 nm. The eluted fractions are collected and characterized.

Characterization of eluted fractions

The collected fractions from low-pressure or HPLAC runs are dialysed, concentrated and analysed by sodium dodecyl sulphate polyacrylamide gel electrophoresis (SDS-PAGE) (20% acrylamide) according to Laemmli [12], using a Pharmacia Phast System (Pharmacia–LKB, Uppsala, Sweden). Proteins are revealed by silver staining [13].

Fractions are also tested for mitogenic activity on Chinese hamster lung fibroblasts (CCL39, American Type Culture Collection) by reinitiation of DNA synthesis as described previously [6].

RESULTS AND DISCUSSION

The heparin–silica supports interact with fibroblast growth factors in solution. The mixture of crude extract and radiolabelled aFGF and bFGF is eluted on heparin–silica (Fig. 1) and heparin–Sepharose (Fig. 2) in a low-pressure affinity chromatography procedure. The elution profiles of radiolabelled FGFs indicate that they are mainly retained by the solid phases at lower ionic strength and desorbed by the salt gradient.

The rates of radiolabelled FGFs reversibly adsorbed on the two supports are presented in Table I. The comparison with heparin–Sepharose support shows that, under our experimental conditions, bFGF exhibits a similar behaviour on both supports (Table I). However, under the same conditions aFGF is not well retained on the silica phases. It is also important to note that both fibroblast growth factors, when they are adsorbed on the affinity phases, are more easily desorbed from the heparin–silica supports by the salt gradient, probably indicating a smaller contribution of ionic interactions in the affinity mechanism on this support. A similar effect has

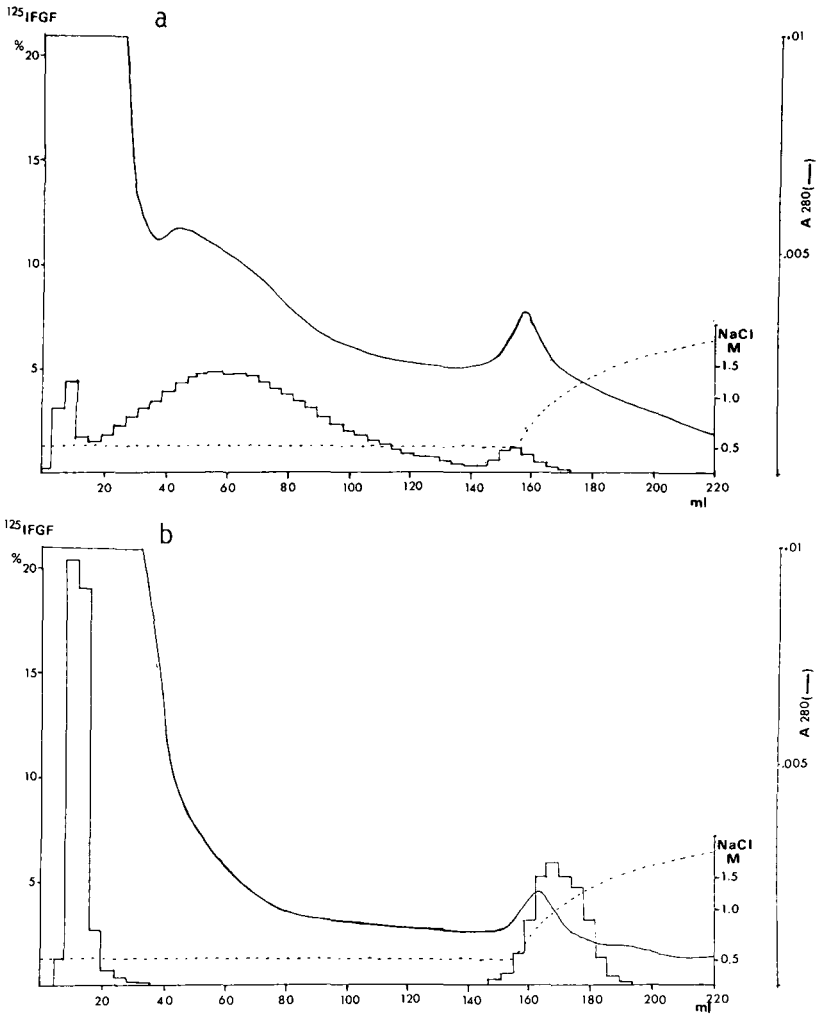

Fig. 1. Low-pressure chromatographic assay of bovine brain crude extract (5 ml) containing radiolabelled aFGF (a) or bFGF (b) on heparin–agarose-coated silica support.

been described for bFGF eluted from heparin affinity HPLC supports [14]. This weaker affinity is probably the reason for the low adsorption of aFGF under our initial eluting conditions (0.01 *M* PBS–0.5 *M* NaCl). Nevertheless, a complete comparison between the two types of affinity supports is difficult because of the non-equivalence of the biological activities of the grafted heparin. First, heparin fixed on commercial Sepharose support is presumably different from the heparin grafted on our silica phases: the molecular mass, the specific anticoagulant activity and the distribution of sugar groups along the network are probably different. Moreover, the coupling of the polysaccharide also depends on the grafting reactions. The macromolecular chain can

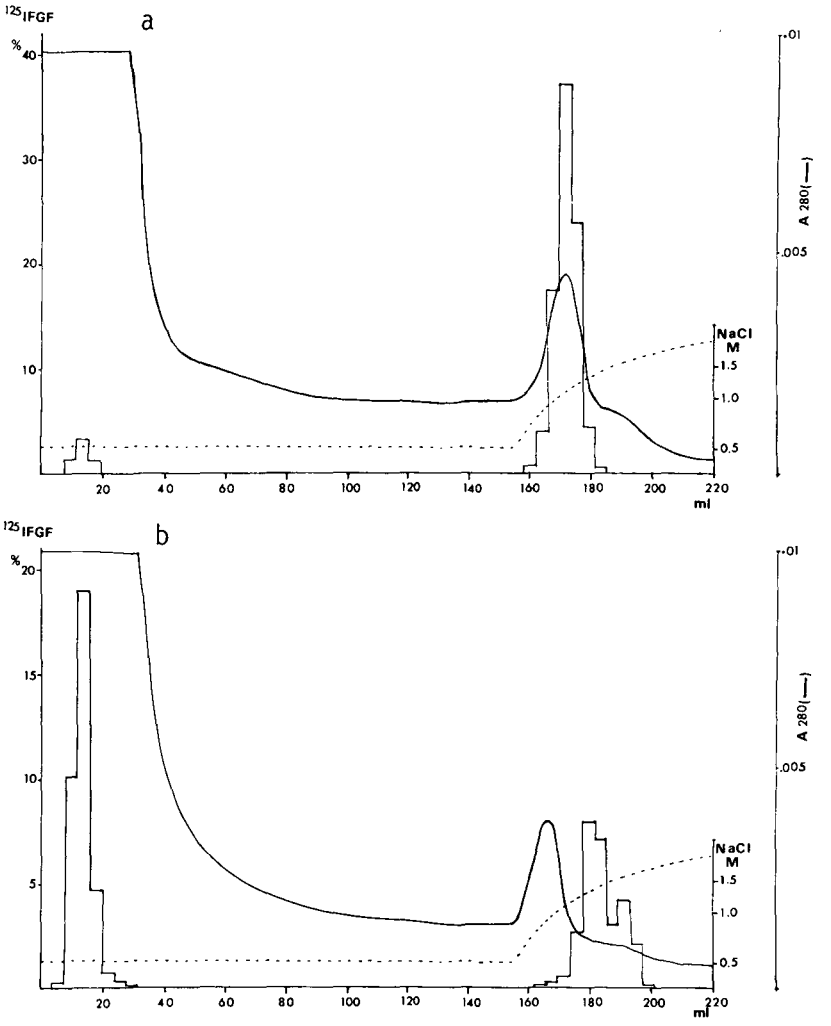

Fig. 2. Low-pressure chromatographic assay of bovine brain crude extract (5 ml) containing radiolabeled aFGF (a) or bFGF (b) on heparin–Sepharose support.

be attached to the Sepharose or agarose structure in different ways with different covalent bonds and consequently the active sequence of heparin is not necessary accessible to aFGF. It is reasonable to assume that the affinity for aFGF could be reinforced by grafting more active heparin fractions.

The HPLAC elution profile of bovine brain crude extract on silica-based resins is presented in Fig. 3. Under our experimental conditions, the proteins are mainly eluted in the washing buffer. When the ionic strength of the eluent is increased, a small amount of proteins (15 μg) is desorbed in a large peak (fraction F). The presence of aFGF and bFGF in this eluted peak is revealed by SDS-PAGE. It should be noted that many other proteins are simultaneously eluted and they can disturb the adsorption

TABLE I

ADSORPTION CONDITIONS OF GROWTH FACTORS ON ACTIVE SUPPORTS

Resin[a]	FGF	NA (%)[b]	RA (%)[b]	NaCl (*M*)[c]
Hep–Seph	aFGF	1	89	1.0
Hep–Seph	bFGF	36	29	1.5
Hep–SiA	aFGF	86	9	0.8
Hep–SiA	bFGF	46	31	1.2

[a] Hep–Seph = heparin–Sepharose support; Hep–SiA = heparin–agarose-coated silica support.

[b] NA (%) = percentage of FGF washed under the initial conditions; RA (%) = percentage of FGF retained and desorbed by the gradient,

[c] NaCl concentration of the gradient corresponding to the maximum of the eluted peak.

process. However, these fractions also stimulate the cellular growth of fibroblast CCL39 (Fig. 4). The stimulation unit of these fractions, which is the concentration needed to obtain 50% of the maximum stimulation, is weaker (2 ng/ml) than those observed under the same conditions with pure aFGF (10 ng/l) and bFGF (3.8 ng/ml). As observed, the eluted fractions obtained from the crude extract are more effective; this could be explained by a smaller deactivation of fibroblast growth factors during the chromatography owing to a faster separation process. This purification procedure is efficient for bFGF but the initial conditions of elution have to be optimized with aFGF. It is also possible to increase the affinity of the heparin-grafted support for aFGF by modifying the coupling method. Moreover, the mechanical properties of the silica phases allow the use of higher flow-rate leading to faster purification.

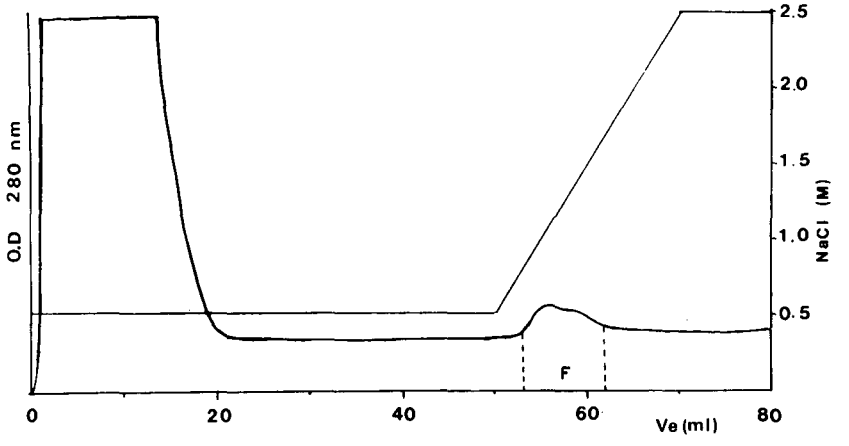

Fig. 3. HPLC of crude bovine brain extract (9 ml) on heparin–agarose-coated silica support.

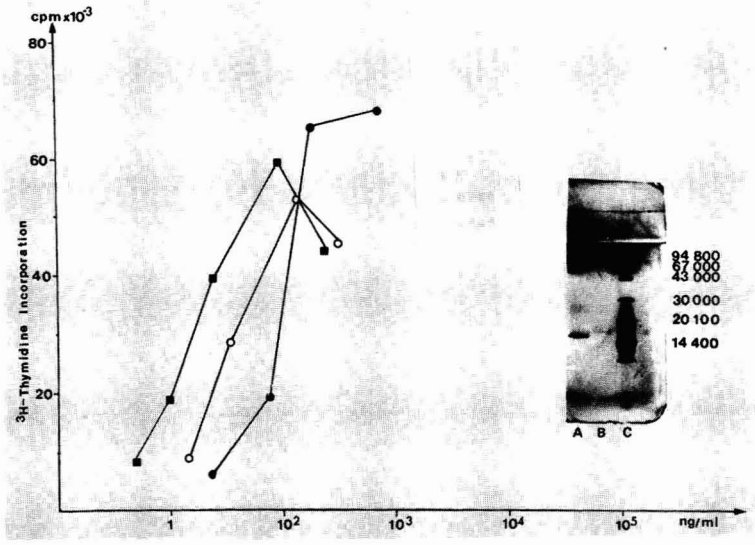

Fig. 4. Effect of (●) aFGF, (○) bFGF and (■) eluted fraction F on the incorporation of [^{3}H]thymidine on CCL39 fibroblast. Inset: SDS-PAGE of (B) bFGF eluted from heparin–Sepharose and of (A) fraction F eluted from heparin–dextran-coated silica; (C) molecular mass markers.

CONCLUSION

The affinity of fibroblast growth factors for heparin is used in chromatography for the purification of these factors. These growth factors are generally purified on heparin–Sepharose support under low-pressure elution conditions. The purification of fibroblast growth factors can be also achieved on agarose-coated silica supports grafted with heparin directly from a bovine brain crude extract. The stimulating effect of eluted fractions on fibroblast growth shows that an important amount of fibroblast growth factor is retained and desorbed from the affinity stationary phase. In fact, the elution of radiolabelled pure FGF demonstrates that on both supports the basic form (bFGF) is strongly adsorbed at low ionic strength and selectively desorbed by the salt gradient. In contrast, aFGF seems to exhibit a weaker affinity for the heparin–agarose coated silica support. Under our initial elution conditions, this growth factor is mainly unretained and eluted by the washing eluent. In order to improve the affinity of aFGF for the heparin–agarose-coated silica support with minimum adsorption of other proteins, the initial conditions of the separation have to be optimized. However, the mechanical properties of such silica-based affinity phases are excellent, they allow fast separations and the purification procedure of fibroblast growth factors can easily be scaled up.

ACKNOWLEDGEMENTS

The authors thank D. Barritault and co-workers for their assistance and for the gift of fibroblast growth factors. This work was supported by the Association

Nationale pour la Valorisation de la Recherche (ANVAR) and Sanofi Recherche, Centre Choay (Gentilly, France).

REFERENCES

1 D. Gospodarowicz, *Methods Enzymol.*, 147 (1987) 106.
2 R. R. Lobb, J. W. Harper and J. W. Fett, *Anal. Biochem.*, 154 (1986) 1.
3 D. Gospodarowicz, N. Ferrara, L. Schweigerer and G. Neufeld, *Endocrine Rev.*, 8 (1987) 95.
4 A. Baird and P. A. Walicke, *Br. Med. Bull.*, 45 (1989) 438.
5 J. Van Brunt and A. Klausner, *Biotechnology*, 6 (1988) 25.
6 M. A. Jacquot-Dourges, D. Gulino, J. Courty, J. Badet, D. Barritault and J. Jozefonvicz, *J. Chromatogr.*, 526 (1990) 35.
7 M. A. Jacquot-Dourges, D. Muller, D. Barritault and J. Jozefonvicz, *J. Chromatogr.*, 510 (1990) 141.
8 F. L. Zhou, D. Muller, X. Santarelli and J. Jozefonvicz, *J. Chromatogr.*, 476 (1989) 195.
9 X. Santarelli, D. Muller and J. Josefonvicz, *J. Chromatogr.*, 443 (1989) 55.
10 F. L. Zhou, D. Muller and J. Jozefonvicz, *J. Chromatogr.*, 510 (1990) 71.
11 J. Courty, C. Loret, M. Moenner, B. Chevalier, O. Lagente, Y. Courtois and D. Barritault, *Biochimie*, 67 (1985) 265.
12 U. K. Laemmli, *Nature (London)*, 277 (1970) 680.
13 J. Henskeshoven and R. Dernick, *Electrophoresis*, 6 (1985) 103.
14 M. Iwane, T. Kurokawa, R. Sasada, M. Seno, S. Nakagawa and K. Garashi, *Biochem. Biophys. Res. Commun.*, 146 (1987) 470.

Journal of Chromatography, 539 (1991) 425–432
Elsevier Science Publishers B.V., Amsterdam

CHROM. 22 902

Immobilized Fe^{3+} affinity chromatographic isolation of phosphopeptides

P. SCANFF*, M. YVON and J. P. PELISSIER
Station de Recherches Laitières, INRA, Domaine de Vilvert, 78350 Jouy en Josas (France)

ABSTRACT

Immobilized Fe^{3+} affinity chromatography is suggested as a means of concentrating phosphopeptides that are present in too low a proportion in a complex mixture to be purified by a single-step method. A high-performance liquid chromatographic system and a chelating Superose HR 10/2 column were used. The chromatographic conditions were optimized using a tryptic hydrolysate of whole casein. The unbound fractions did not contain any phosphorylated peptide. All caseinophosphopeptides were retained. Only four other strongly basic peptides were also retained. The quantitative accuracy of the method was evaluated. This method allowed the isolation of phosphopeptides in gastric effluents of calves fed with milk.

INTRODUCTION

Casein phosphopeptides (CPPs) display the interesting property of being able to form soluble complexes with di- or trivalent metal ions [1,2]. This has led to speculation that CPPs might have a physiological role and could enhance calcium intestinal solubilization and absorption. Naito and co-workers [3,4] reported the occurrence of such phosphopeptides in the distal small intestine of rats during the course of the luminal digestion of a diet containing caseins. Moreover, the amount of soluble calcium in the distal small intestine was higher with caseins than with other dietary proteins [5]. In 1986, Sato *et al.* [6] demonstrated that CPPs enhanced both Ca^{2+} intraluminal solubilization and absorption. Gerber and Jost [7] reported an increase in the calcium bioavailability with CPPs with *in vitro* cultured embryonic rat bone. In contrast, Pointillart and Gueguen [8] demonstrated *in vivo* that calcium absorption and bone parameters of pigs fed CPP-enriched diets were not modified. This Ca^{2+} solubilizing effect of CPPs on its absorption is still much debated. Moreover, the way in which they are introduced to the intestine could also be a determining factor. Hence it would be interesting to know how and when they are released from the stomach after a meal.

The identification of such peptides in the digestive tract is relatively difficult because they are mixed with a number of other peptides and consequently are found in too low a proportion to be purified by a single-step method. Meisel and Frister [9] enriched the CPP fraction of intestinal chyme by affinity chromatography using iron(III) ions immobilized on a chelating Sepharose 6B (Pharmacia–LKB, Uppsala,

0021-9673/91/$03.50

Sweden) column according to the method described by Andersson and Porath [10]. This allowed them to show the occurrence of a phosphopeptide in the chyme from the small intestine of minipigs (Göttinger Miniaturschweine) after ingestion of a casein diet. However, their chromatographic method is time consuming.

In order to study the kinetics of gastric emptying of CPPs in calves fed milk, we developed a faster immobilized metal affinity chromatographic (IMAC) method to concentrate phosphopeptides using a fast protein liquid chromatographic (FPLC) system and a chelating Superose HR 10/2 column (Pharmacia–LKB). The separation of each phosphopeptide was performed in a second step by high-performance liquid chromatography (HPLC) on a C_{18} reversed-phase column. In order to adjust the chromatographic conditions we used a tryptic hydrolysate of bovine whole casein.

EXPERIMENTAL

Chemicals

All buffers were prepared with deionized water purified with a Milli-Q system (Millipore, Bedford, MA, U.S.A.). Sodium acetate, sodium dihydrogenphosphate and iron(III) chloride were purchased from Prolabo (Paris, France). Trifluoroacetic acid (TFA) was purchased from Pierce (Rockford, IL, U.S.A.) and acetonitrile from Baker (Deventer, The Netherlands). All mobile phases were deaerated with helium.

Preparation of samples

The chromatographic conditions were adjusted using a casein tryptic hydrolysate. This hydrolysate was obtained by incubating a 1% casein solution in phosphate buffer (0.1 *M*, pH 7.4) with trypsin (Sigma, St. Louis, MO, U.S.A.) for 24 h at 37°C. The enzyme/substrate (E/S) ratio was 1:100 by weight. The reaction was stopped by adding HCl to a final pH of 2.0.

Gastric effluents of preruminant calves fed bovine raw skim milk were collected over 7 h after the meal, fractions being taken during 10-min intervals for the first 30 min and then at 30-min intervals. To each sample trichloroacetic acid was immediately added to a final concentration of 12% to stop the enzyme action. After centrifugation, the pellet was resuspended in water and solubilized by increasing the pH to 7.0. An aliquot of this solution was brought to pH 5.0 and centrifuged. The supernatant (100 μl) was applied to the affinity column.

Preparative chromatography

The preparative step of phosphopeptide recovery was carried out with an FPLC system consisting of an LCC 500 controller, two pumps and a chelating Superose HR 10/2 column (2 × 1 cm I.D.). The absorbance was monitored at 220 nm. The chelating ligand of the column is iminodiacetate covalently bound to a Superose 12 matrix. Iron(III) ions were immobilized on this support to give a group-specific sorbent for phosphorylated amino acid side-chains. Iron(III) ions were loaded by applying a 20-m*M* iron(III) chloride solution in water at a flow-rate of 1.0 ml/min until the metal appeared in the eluate. After washing off the unbound metal with water, the column was equilibrated with a loading buffer.

The chelating Superose column was run at 37°C. It was first equilibrated with 10 ml of 20 m*M* sodium acetate buffer (A) adjusted to pH 5.0 at 1.0 ml/min. The tryptic

hydrolysate was then applied and the column was washed with 10 ml of buffer A. The elution was carried out with 10 ml of 100 m*M* sodium dihydrogenphosphate in A at the same flow-rate for 10 min. The column was then re-equilibrated with buffer A for further use.

Analytical chromatography

Analytical chromatography of the chelating chromatographic fractions was carried out with a Waters Assoc. HPLC system on a 10-μm Nucleosil C_{18} column (250 × 4.6 mm I.D.) (SFCC, Neuilly-Plaisance, France). The absorbance was monitored at 220 nm. The column was equilibrated in solvent A (0.115% TFA) and elution was effected with a linear gradient from 0 to 100% solvent B (0.1% TFA–60% acetonitrile). The column and solvents were kept at 40°C. The elution rate was 1.0 ml/min.

Peptide identification

The HPLC fractions were collected and dried with a Speed-Vac evaporator (Savant, France). The peptides were identified from their amino acid composition. These were determined after acid hydrolysis (110°C, 24 h, 5.7 *M* HCl, under vacuum) using the method of Spackman *et al.* [11] with a Biotronik LC 5000 analyser.

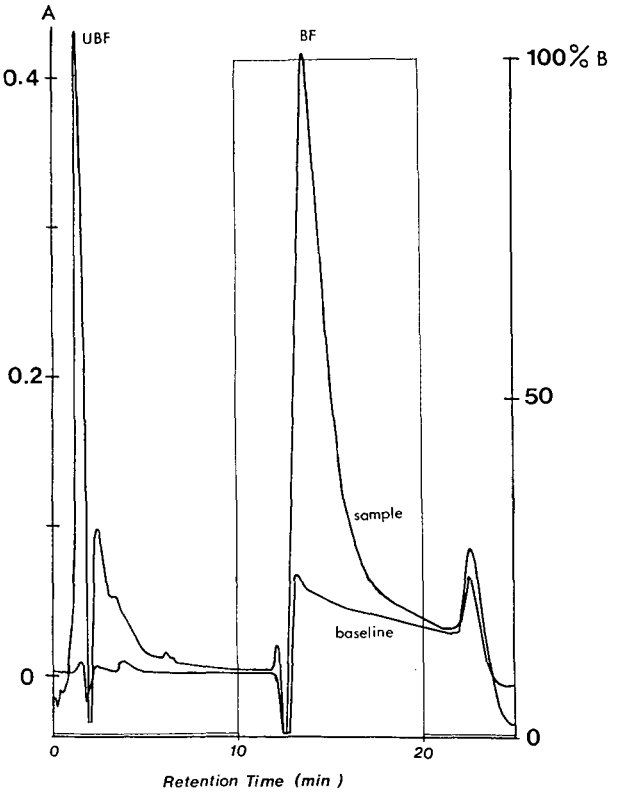

Fig. 1. Preparative affinity chromatography of a tryptic digest of whole casein on Fe^{3+}-chelating Superose HR 10/2. Temperature, 37°C; flow-rate, 1.0 ml/min; detection, UV (220 nm). Eluents: A = 20 m*M* sodium acetate (pH 5.0); B = A + 100 m*M* sodium dihydrogenphosphate.

RESULTS

Fig. 1 shows the IMAC pattern of the tryptic hydrolysate of whole casein. The first peak corresponds to the unbound material and the second peak to the retained material.

The whole casein tryptic hydrolysate (CTH) and the unbound (UBF) and bound (BF) fractions were analysed on the reversed-phase column under exactly the same conditions. The elution patterns are superimposed in Fig. 2. The UBF did not contain any phosphorylated peptide. The peptides of the BF were collected (Fig. 3) and identified by their amino acid composition (Table I). Nine peptides containing phosphoserine residues were found, of which seven could be identified. The amino acid composition of the other two (indicated with asterisks in Fig. 3) did not permit their identification. Peaks 1–4 corresponded to non-phosphorylated small peptides (four or five residues) which contained one His residue.

The quantitative response of the method was tested in each step. In the analytical step (reversed-phase HPLC), the relationship between peak area and amount of phosphopeptides injected was linear up to 10 nmol. In the affinity step the peak area of the BF was also directly proportional to the amount injected up to 1.75 mg of

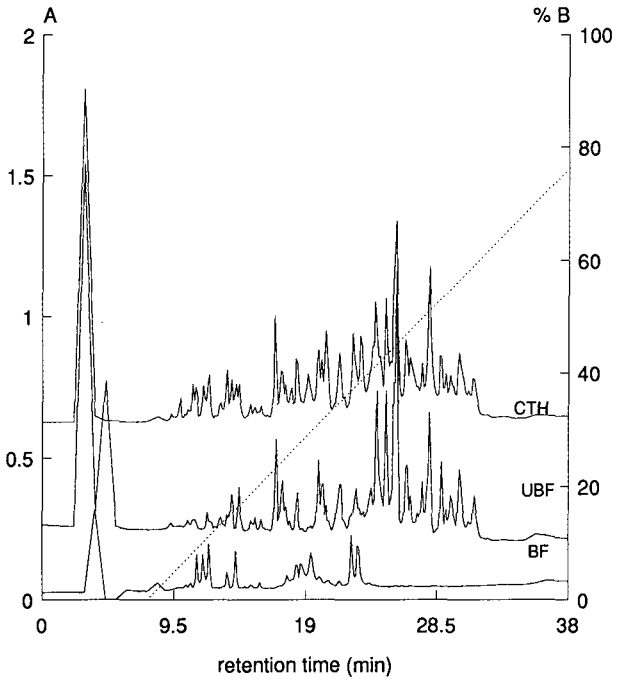

Fig. 2. Superimposition of the chromatograms of the tryptic digest (CTH), the bound fraction (BF) and the unbound fraction (UBF) on an Fe^{3+} affinity column. Column, C_{18} Nucleosil (10 μm); temperature, 40°C; flow-rate, 1.0 ml/min; detection, UV (220 nm). Eluents: A = 0.115% TFA; B = 0.1% TFA–60% acetonitrile. The dotted line indicates the %B gradient.

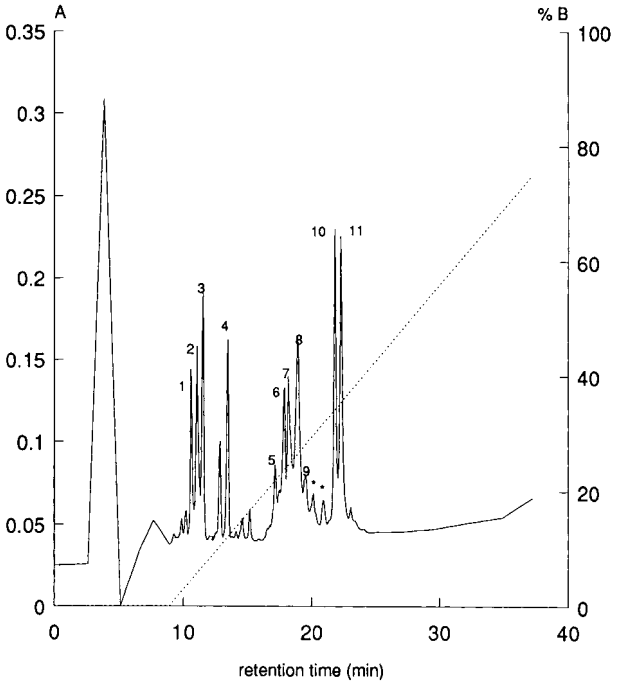

Fig. 3. Analytical RP chromatography of the BF. Conditions as in Fig. 2. For amino acid composition of the peaks 1–11 see Table I.

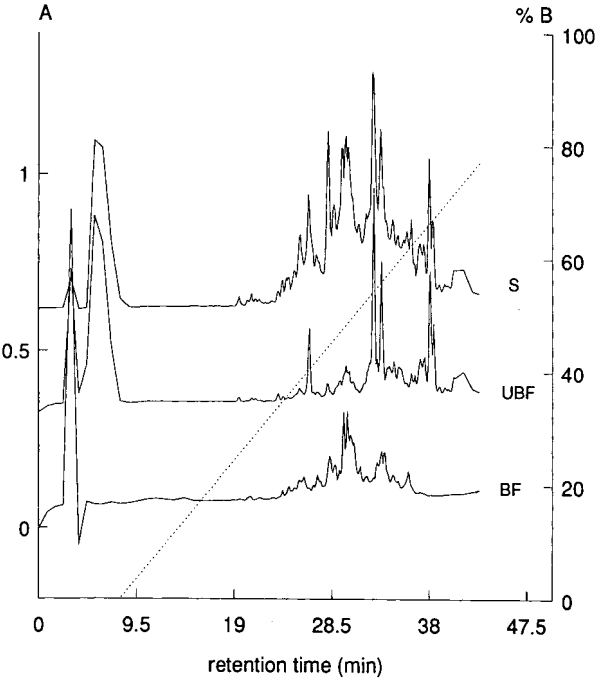

Fig. 4. Superimposition of the chromatograms of a gastric effluent (S), the bound fraction (BF) and the unbound fraction (UBF) on an Fe^{3+} affinity column. The amounts injected for the three chromatograms were different. Conditions as in Fig. 2 except for the gradient. The dotted line indicates the %B gradient.

TABLE I

AMINO ACID COMPOSITION (in mol/mol) OF THE PEPTIDES NUMBERED IN FIG. 3

The theoretical composition of the identified peptide is given in parentheses. Ide. = Identification; Phos. = phosphate.

Amino acid	Peak No.										
	1	2	3	4	5	6	7	8	9	19	11
Asx	–	–	–	–	1.54(2)	1.78(2)	1.23(1)	2.40(3)	3.40(4)	1.40(1)	1.15(1)
Thr	–	–	–	–	0.75(1)	0.80(1)	–	1.05(1)	0.92(1)	0.21(0)	0.91(1)
Ser	–	–	–	0.87(1)	1.20(1)	3.40(5)	4.10(5)	2.20(2)	2.60(3)	1.14(1)	4.91(5)
Glx	0.85(1)	1.06(1)	–	–	9.50(9)	7.89(8)	6.76(7)	4.80(4)	7.34(5)	4.20(4)	6.68(7)
Pro	–	–	0.95(1)	–	–	–	0.91(1)	–	–	2.02(2)	1.09(1)
Gly	0.30(0)	–	–	–	–	1.82(1)	–	0.63(1)	0.74(1)	–	1.26(1)
Ala	–	–	–	–	0.38(0)	2.21(3)	0.91(1)	0.80(1)	1.04(1)	1.00(1)	–
Cys	–	–	–	–	–	–	–	–	–	–	–
Val	–	–	–	–	–	1.43(2)	0.87(2)	0.40(0)	1.12(1)	1.30(2)	1.33(2)
Met	–	–	–	0.56(1)	–	–	0.87(1)	0.75(1)	1.02(1)	–	–
Ile	–	0.82(1)	0.85(1)	–	–	0.94(1)	1.32(2)	1.70(2)	1.60(2)	0.66(1)	1.31(2)
Leu	–	–	–	0.84(1)	0.68(1)	–	–	–	0.78(1)	1.09(1)	2.70(2)
Tyr	0.54(1)	–	–	–	–	0.48(1)	–	–	–	0.69(1)	–
Phe	–	–	–	–	0.56(1)	–	–	–	–	–	–
His	0.95(1)	1.02(1)	1.04(1)	0.90(1)	–	–	–	–	–	–	–
Lys	1.00(1)	1.00(1)	1.00(1)	1.00(1)	1.00(1)	1.00(1)	1.00(1)	1.00(1)	1.00(1)	1.15(1)	–
Arg	–	–	–	–	–	–	–	–	–	0.88(1)	1.71(2)
Ide.	77–80 α_{s_2}	80–84 α_{s_1}	4–7 α_{s_1}	120–124 α_{s_1}	33–48 β	46–70 α_{s_2}	59–79 α_{s_1}	43–58 α_{s_1}	37–58 α_{s_1}	104–119 α_{s_1}	1–25 β
Phos.	0	0	0	0	1	3	5	2	2	1	4

phosphopeptide. However, during this step the recovery was not the same for all the tested phosphopeptides, *i.e.*, 65% for peptides 6, 7 and 8 and 80% for peptide 11.

This method was then applied to gastric effluents of calves fed bovine raw skim milk. The three chromatograms of the sample (S), the BF and UBF are superimposed in Fig. 4. A group of three peptides was particularly retained on the chelating Superose column. They were eluted at a retention time of 30 min on the C_{18} column. The amino acid compositions of these peptides are similar and correspond approximately to the sequence 110–145 from α_{s_1}-casein. Their N- and C-terminal residues have to be cidentified in order to establish the exact sequence of these peptides.

DISCUSSION

This study demonstrated that a chelating Superose gel loaded with Fe^{3+} can be employed successfully to concentrate phosphopeptides from a mixture in which they are present in too low a proportion to be purified by a single-step method. This technique has the advantage of being faster than that used by Meisel and Frister [9], only 30 min, including the equilibration time, being required. Only one run on each of the two chromatographic systems is necessary to collect enough peptide for identification. The column can be used immediately after a run since regeneration is not necessary. No modification of retention was observed after repeated separations.

Chromatographic conditions were chosen according to the conditions described previously [10]. Phosphoserine was strongly retained at pH 3.1 or 5.0 and recovered from the Fe^{3+} column with 20 m*M* phosphate. The loading was therefore performed at pH 5.0. Some peptides were not desorbed by 50 m*M* sodium dihydrogenphosphate in sodium acetate (pH 5.0). The phosphate concentration was too low and 100 m*M* phosphate was necessary for complete desorption. A gradient of phosphate concentration gave a poor separation. Desorption with EDTA was possible but the column had to be reloaded with iron(III) ions between each run.

All peptides were eluted independently of their phosphate content and their strength of binding on the column and the analytical step in the reversed-phase mode allows their separation. Eleven phosphopeptides were theoretically present in the tryptic hydrolysate. Seven phosphopeptides were identified: all phosphopeptides from α_{s_1}- and β-caseins were found and one phosphopeptide from α_{s_2}-casein was also identified. Two others phosphopeptides were found but have not been completely identified. One of them was probably the phosphopeptide NH_2-terminus of α_{s_2}-casein, but it was not pure. Two small phosphopeptides (twelve and thirteen residues) were not found, probably because the proportion in the mixture was too small and their absorbance at 220 nm too low.

The observed recoveries vary with the phosphopeptides. The phosphate content of the peptides might be responsible for these differences, as Muszynska *et al.* [12] showed with IDA–Fe^{3+} gel that the strength of binding was dependent on the phosphate content: peptide 11 (80% recovery) contains four phosphate groups whereas peptide 7 contains five phosphate groups and was obtained with 65% recovery. The recoveries for peptides 6 and 8, containing three and two phosphate groups, respectively, were the same as for peptide 7. Because of these differences in recovery, an internal standard of each peptide to be analysed must be used in quantitative assays.

The IMAC step provides a good enrichment of the phosphopeptide fraction. Phosphopeptides represented 12% by number of the peptides present in the casein tryptic hydrolysate. In the enriched fraction, they were predominant. Moreover, they were eluted later than the non-phosphorylated peptides in HPLC. This made their purification easier.

The non-phosphorylated peptides retained on the Chelating Superose column were small peptides containing one His and one Lys residue. Some tests were performed by adding 10 or 20 m*M* imidazole (Kodak, Rochester, NY, U.S.A.) to the loading buffer (the pH being readjusted to 5.0 with acetic acid). No change was observed and His-containing peptides and phosphopeptides were always retained on the chelating Superose gel. This result shows that binding is not due to coordination via histidine. Other tests were also made by adding 100 m*M* NaCl sodium chloride to the loading buffer. His-containing peptides were not retained on the chelating Superose but the retention of some phosphopeptides slightly decreased. These observations could be consistent with electrostatic interactions. His- and Lys-containing peptides (strongly basic) could interact with the iminodiacetate groups of the chelating Superose. Binding of phosphopeptides probably occurs via the oxygen of the phosphate group by coordination with Fe^{3+}. Secondary, electrostatic interactions can also occur and explain the different recoveries of the phosphopeptides.

The proposed method could be optimized by coupling the two columns via a six-way valve as described by Rybacek *et al.* [13]. Some tests were made using the chelating Superose column and a pepRPC column (Pharmacia–LKB), but the major problem was the different pressure resistances of the two gels and consequently the columns cannot be used in series.

The method described is suitable for concentrating phosphopeptides from complex mixtures and for identifying them in gastric effluents of animals. It is therefore now possible to study the kinetics of the gastric emptying of phosphopeptides.

REFERENCES

1 R. Oesterberg, *Thesis*, University of Uppsala Almqvist & Wiksell, Stockholm, 1963.
2 W. Manson and J. Cannon, *J. Dairy Res.*, 45 (1978) 59.
3 H. Naito, A. Kawakami and T. Imamura, *Agric. Biol. Chem.*, 36 (1972) 409.
4 H. Naito and H. Suzuki, *Agric. Biol. Chem.*, 38 (1974) 1543.
5 Y. S. Lee, T. Noguchi and H. Naito, *Agric. Biol. Chem.*, 43 (1979) 2009.
6 R. Sato, T. Noguchi and H. Naito, *J. Nutr. Sci. Vitaminol.*, 32 (1986) 67.
7 H. G. Gerber and R. Jost, *Calif. Tissue Int.*, 38 (1986) 350.
8 A. Pointillart and L. Gueguen, *Reprod. Nutr. Dev.*, 29 (1989) 477.
9 H. Meisel and H. Frister, *Biol. Chem. Hoppe-Seyler*, 369 (1988) 1275.
10 L. Andersson and J. Porath, *Anal. Biochem.*, 154 (1986) 250.
11 D. H. Spackman, W. H. Stein and S. Moore, *Anal. Chem.*, 30 (1958) 1190.
12 G. Muszynska, L. Andersson and J. Porath, *Biochemistry*, 25 (1986) 6850.
13 L. Rybacek, M. D'Andrea and J. Tarnowski, *J. Chromatogr. Sci.*, 397 (1987) 355.

Journal of Chromatography, 539 (1991) 433–441
Elsevier Science Publishers B.V., Amsterdam

CHROM. 22 903

High-performance liquid chromatographic analysis of the unusual pathway of oxidation of L-arginine to citrulline and nitric oxide in mammalian cells

B. CHENAIS, A. YAPO, M. LEPOIVRE and J. P. TENU*
CNRS URA 1116, Batiment 432, Université Paris-Sud, 91405 Orsay Cedex (France)

ABSTRACT

A very unusual pathway of the oxidation of L-arginine to citrulline and nitric oxide has been discovered recently in cytotoxic macrophages. In an attempt to detect molecules generated through this metabolic pathway, a fast radio high-performance liquid chromatographic method was developed to analyse the whole set of radiolabelled L-arginine-derived metabolites produced by mammalian cells after appropriate induction. A new intermediate which might be N^G-hydroxy-L-arginine was found.

INTRODUCTION

It has recently been shown that mammalian cells can synthesize the highly reactive nitric oxide molecule (NO•), which was then identified as an important mediator in cellular communication [1]. NO• biosynthesis has been demonstrated in, for example, cytotoxic macrophages [2] and stimulated endothelial cells [3]. The nitrogen atom of NO• is derived from one of the two guanidino nitrogens of L-arginine via an unusual metabolic route. A proposed scheme, still speculative, is shown in Fig. 1. Citrulline and nitrite/nitrate, the oxidation products of NO•, are the stable products of the pathway [4]. In addition to macrophages and endothelial cells various cell lines, including the EMT6 [5] and TA3 murine adenocarcinomas [6], can generate these L-arginine-derived molecules after induction with appropriate cytokines such as interferon-γ [5]. The triggering of the NO•-generating pathway is associated with antiproliferative effects [5]. It has been involved, for instance, as an effector of the extracellular antiproliferative function exerted by cytotoxic macrophages against tumour cells [7,8].

The L-arginine: NO• synthase activity responsible for the NO•-generating pathway has been found in 150 000 *g* cytosolic supernatants isolated from cytotoxic macrophages. It is activated by Mg^{2+} or Ca^{2+}, requires L-arginine, NADPH and tetrahydrobiopterin (BH_4) as cofactors [8,9] and is specifically inhibited by N^G-monomethyl-L-arginine (L-NMMA) [7,10,11] (Fig. 1).

In an attempt to detect molecules generated through this metabolic pathway and to investigate their role, we have developed a fast radio high-performance liquid

0021-9673/91/$03.50

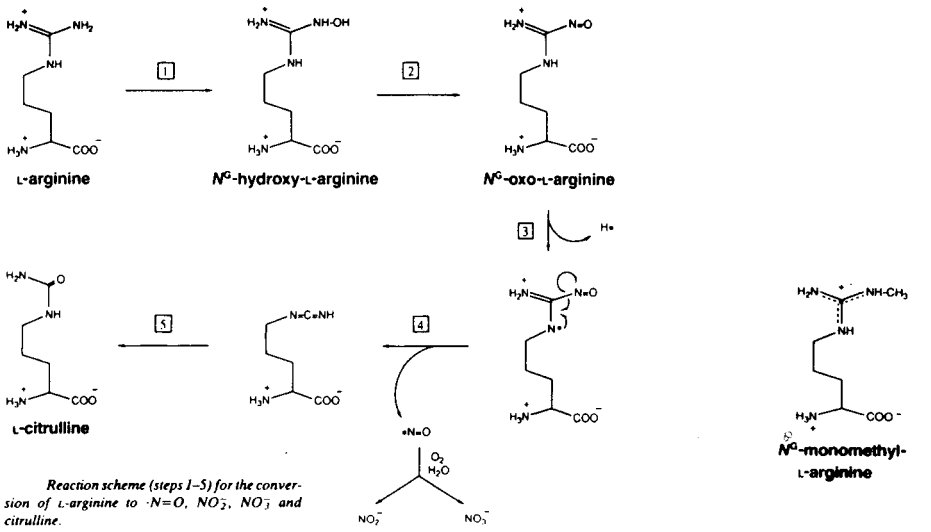

Fig. 1. Proposed scheme for the NO·-citrulline-generating pathway, according to Marletta [1].

chromatographic (HPLC) method to analyse the whole set of radiolabelled L-arginine-derived metabolites produced by suitable mammalian cells after appropriate induction.

EXPERIMENTAL

Chemicals and cytokines

N^G-Monomethyl-L-arginine (L-NMMA) was obtained from Calbiochem (La Jolla, CA, U.S.A.), 6-(*R,S*)-5,6,7,8-tetrahydro-L-biopterin from Serva (Heidelberg, Germany), L-arginine and 4-(2-hydroxyethyl)-1-piperazineethanesulphonic acid (HEPES) from Merck (Darmstadt, Germany), dithioerythritol (DTE) from Sigma (St. Louis, MO, U.S.A.) and lipopolysaccharide (LPS) from *Salmonella enteritidis* from Difco (Detroit, MI, U.S.A.). L-[U-^{14}C]Arginine (11.1 GBq/mmol), L-[guanidino-^{14}C]arginine (1.85 GBq/mmol), DL-[1-^{14}C]ornithine (1.72 GBq/mmol) and [^{14}C]urea (2.2 GBq/mmol) were purhased from CEA (Saclay, France) and L-[ureido-^{14}C]citrulline (2.0 GBq/mmol) from NEN (Boston, MA, U.S.A.). Human recombinant tumour necrosis factor-alpha (TNF-α) and murine recombinant gamma interferon (IFN-γ), kindly provided by Dr. G. M. Adolf (Vienna, Austria), were from Gennentech (San Francisco, CA, U.S.A.). RPMI 1640 medium (containing 1.45 m*M* L-arginine) was obtained from Gibco (Cergy-Pontoise, France).

HPLC analysis of arginine metabolism

We chose a strong cation exchanger (sulphonate) linked to silica particles, *viz.*, a Zorbax 300 SCX column (250 × 4.6 mm I.D.) (Société Française Chromato Colonne, Neuilly Plaisance, France). The HPLC device included a Waters Assoc. Model 600 multi-solvent delivery system and the detector was a Berthold 506 C-1

radioactivity monitor connected to Epson PC AX microcomputer running under the Berthold HPLC program version 9.6. The following elution conditons were used: flow-rate, 1.0 ml/min; 0–7 min, isocratic, 0.02 *M* sodium citrate (pH 2.2); 7–17 min, linear gradient to 0.1 *M* sodium citrate (pH 3.0); 17–27 min, linear gradient to 0.2 *M* sodium citrate (pH 3.0); 27–35 min, isocratic, 0.2 *M* sodium citrate (pH 3.0).

Cell lines

The hydroxyurea-resistant TA3 M2 clone was obtained as described previously [12]. The EMT6 cell line is a murine mammary adenocarcinoma from BALB/c mice, kindly provided by Dr. G. Lopez-Berenstein (Tumor Institute, Houston, TX, U.S.A.).

TA3 M2 cytosolic extracts

These were prepared as described previously [6]. Briefly, TA3 M2 cells were treated for 24 h with appropriate additives. Lysates were centrifuged for 20 min at 4°C in a Beckman TL-100.2 rotor at 150.000 *g*. The supernatant was rapidly frozen in liquid nitrogen and stored at −80°C.

Determination of L-Arginine: NO˙ synthase activity

The following reagents were incubated in a final volume of 90 μl: 100 m*M* HEPES (pH 7.6), 15 m*M* magnesium acetate, 10 m*M* DTE, 130 μ*M* NADPH, 500 μ*M* BH_4, 8 kBq L-[guanidino-^{14}C]arginine (1.85 GBq/mmol) and the indicated concentrations of L-arginine to which appropriate amounts of cell extract were added. Where indicated, L-NMMA was used at a final concentration of 2.2 m*M*. Samples were incubated for 50 min at 30°C and then heated at 90°C for 2 min. Precipitates were pelleted and 200 μl of 0.02 *M* sodium citrate (pH 2.2) were added to the supernatant, which was filtered through a YM-10 ultrafiltration membrane (M_r cut-off 10 000; Amicon, Danvers, MA, U.S.A.). A 50-μl aliquot of the filtrate was loaded onto the analytical column.

Analysis of EMT6 culture medium

EMT6 cell monolayers were obtained as described previously [5]. The medium was washed out and replaced with 1 ml of fresh medium RPMI 1640 supplemented with IFN-γ and LPS if the cells were to be induced. In some experiments, L-NMMA (2.2 m*M*) was added. Radiolabelled precursors were then added: 100 kBq of L-[U^{14}C]arginine (11.1 GBq/mmol) or 80 kBq of L-[guanidino-^{14}C]arginine (1.85 kBq/mmol) or 37 kBq of L-[ureido-^{14}C]citrulline (2.0 GBq/mmol). Supernatants were collected after 18 h and kept frozen at −80°C until anaysis. They were diluted with the starting elution buffer and processed in the same way as TA3 M2 cytosilic extracts: 50–100-μl samples were injected.

RESULTS

The low pH of the buffers (2.2–3.0) was chosen taking into account the p*K* values of the α-carboxyl groups of amino acids to control partly their ionization state (ornithine 2.0, arginine 2,2 citrulline 2.4). Typical retention times for authentic markers were urea 3.8 min, citrulline 11.5 min, ornithine 21 min and arginine 31 min (Fig. 2).

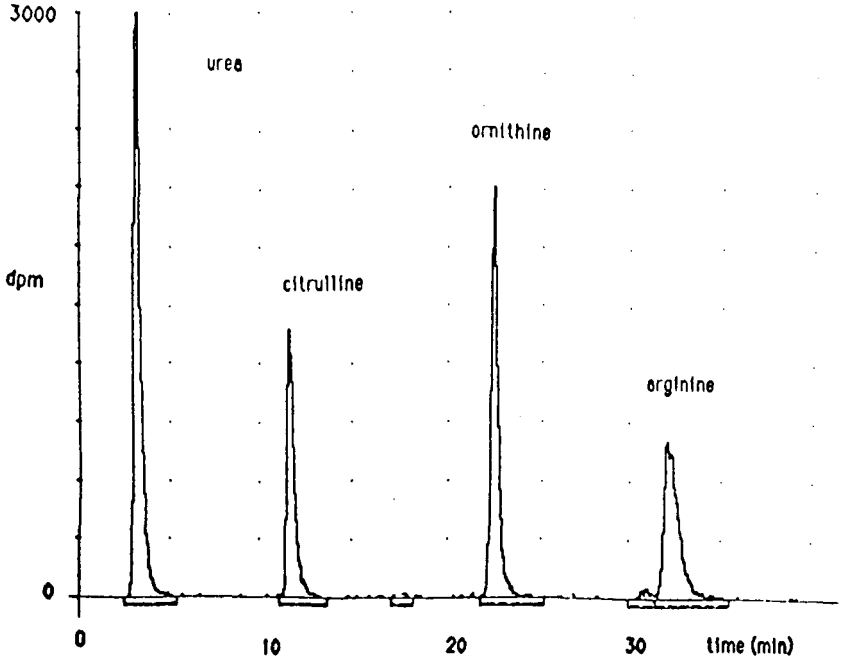

Fig. 2. Chromatogram of radiolabelled amino acid standards. Column: strong cation exchanger on silica, Zorbax 300 SCX (250 × 4.6 mm I.D.). Elution as follows: 0–7 min, isocratic with 0.02 *M* sodium citrate (pH 2.2), 7–17 min, linear gradient to 0.1 *M* sodium citrate (pH 3.0) 17–27 min, linear gradient to 0.2 *M* sodium citrate (pH 3.0); 27–35 min, isocratic with 0.2 *M* sodium citrate (pH 3.0). Flow-rate: 1.0 ml/min.

An intermediate of the NO˙-generating pathway found in induced EMT6 cells culture supernatants

Induced EMT6 cells were obtained by incubation overnight with IFN-γ (40 U/ml) and LPS (100 ng/ml). We first used L-[U-^{14}C]arginine as a precursor in order to label as many metabolites as possible. An extra metabolite refered to as X was found in the culture medium, eluting between ornithine and arginine. This compound and citrulline were not observed in the culture medium of untreated EMT6 cells (Fig. 3). The formation of this metabolite and of citrulline was inhibited by L-NMMA, a specific inhibitor of the NO˙-generating pathway (Fig. 4). We then used L-[guanidino-^{14}C]arginine to obtain more information about compound X, as shown in Fig. 5. Ornithine disappeared, as expected, but compound X and citrulline were still detected. Hence X is not involved in the urea cycle. We also observed a new derivative (retention time *ca.* 15 min) which also did not belong to the urea cycle and might be an intermediate in the creatine biosynthetic pathway. The [X]/[citrulline] concentration ratio was about 0.2 with both types of labelling (Fig. 5).

The metabolite X, closely related to the production of citrulline, did not seem to be a degradation product of citrulline. When induced EMT6 cells were incubated in the presence of L-[ureido-^{14}C]citrulline, a small amount of arginine was generated through the urea cycle and a trace amount of X. Its concentration was more closely related to

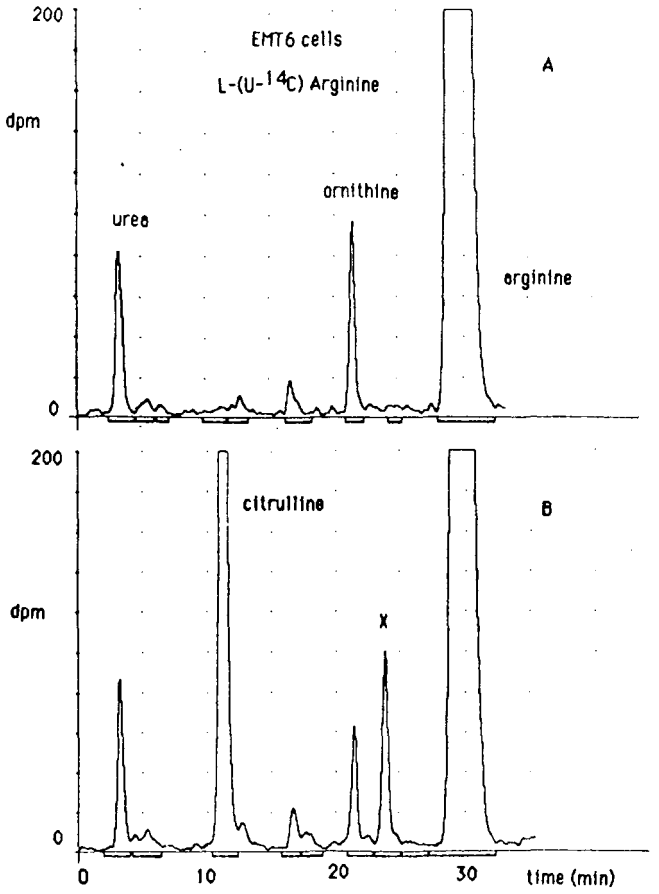

Fig. 3. HPLC analysis of untreated and induced EMT6 cell culture media. L-[U-^{14}C]Arginine: 100 kBq/ml. (A) EMT6 monolayers in 35-mm dishes (Nunclon) were incubated in 1 ml of RPMI 1640 medium for 18 h. (B) induced EMT6 cells were incubated for 18 h in 1 ml of RPMI 1640 supplemented with IFN-γ (40 U/ml) and LPS 100 ng/ml).

the concentration of arginine produced than to that of added citrulline. Moreover, the production of X and not that of arginine was again inhibited by L-NMMA (Fig. 6). It must be pointed out that X was not found in cell lysates. This metabolite was also demonstrated in cytosols of induced TA3 M2 cells supplemented with cofactors of the NO$^{\bullet}$-generating pathway (BH4, NADPH).

The NO$^{\bullet}$-generating pathway was induced in TA3 M2 cells by incubation for 24 h with IFN-γ (40 U/ml), TNF-α (150 U/ml) and LPS (10 μg/ml). When cytosols of induced cells were supplemented with BH_4 and NADPH, in the presence of L-[guanidino-^{14}C]arginine, the NO$^{\bullet}$-generating pathway was triggered and citrulline and metabolite X were generated. They were not detected in induced cells in the absence of cofactors or in non-induced cytosols even in the presence of cofactors. The production of citrulline and of metabolite X by induced cytosols was also here

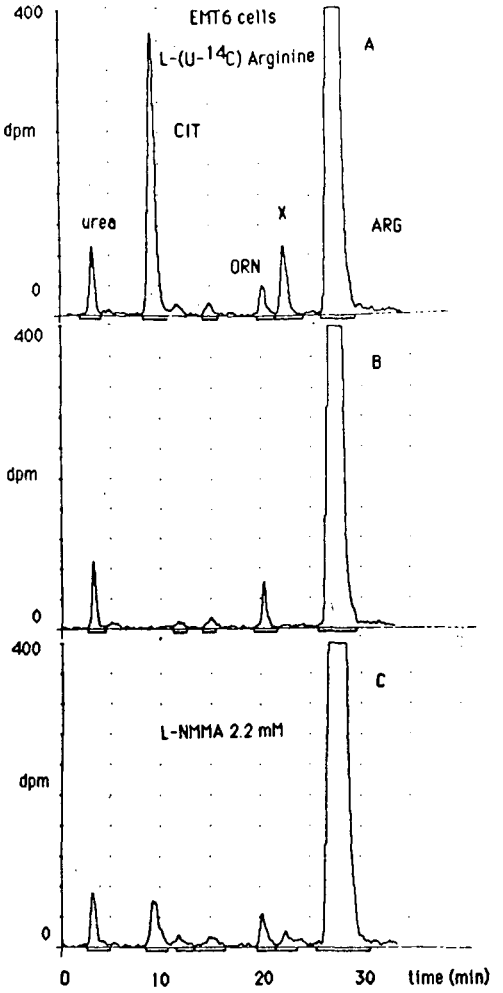

Fig. 4. Effect of L-NMMA on the production of L-arginine-derived metabolites by induced EMT6 cells in the culture medium. Cells were cultivated as described in Fig. 3. (A) EMT6-induced cells; (B) untrated EMT6 cells; (C) EMT6-induced cells cultivated in the presence of 2.2 m*M* L-NMMA.

inhibited by L-NMMA. The generation of the metabolite referred to as "creatine derivative" was also found in cytosols of TA3 M2 cells to the same extent regardless of whether the cells had been induced or not; this was not inhibited by L-NMMA (Fig. 7). The dependence of the formation of citrulline and X on arginine concentration was studied and we again found a nearly constant [X]/[citrulline] concentration ratio, which was close to 0.2. We failed to observe compound X in either lysates or supernatants of cytotoxic macrophages, although we could easily detect the production of citrulline.

The metabolite X was not very stable even when kept frozen at −80°C. It was

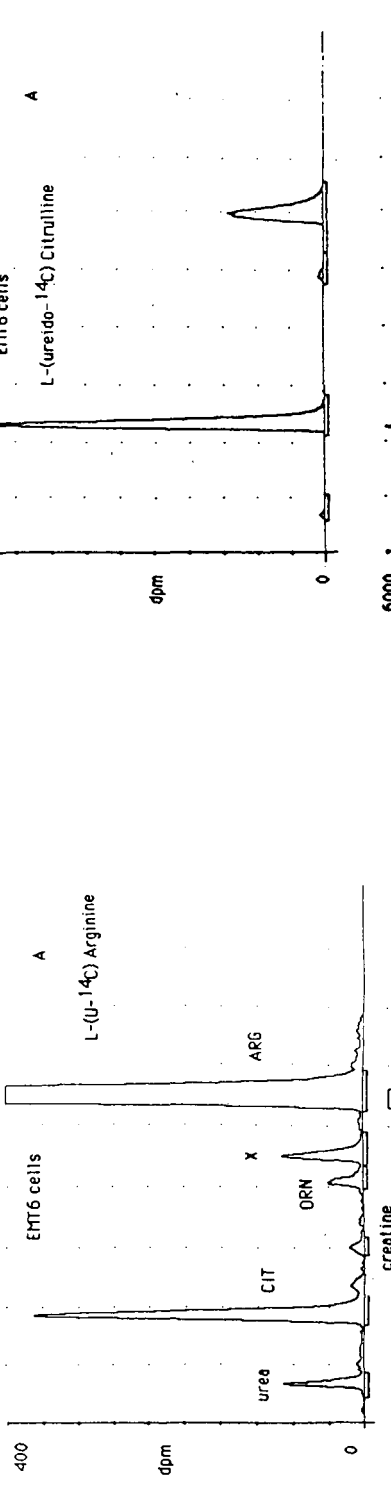

Fig. 5. Comparison of radiolabelled L-arginine-derived metabolites generated in induced EMT6 cell culture media in the presence of (A) L-[U-^{14}C]arginine or (B) L-[guanidino-^{14}C]arginine.

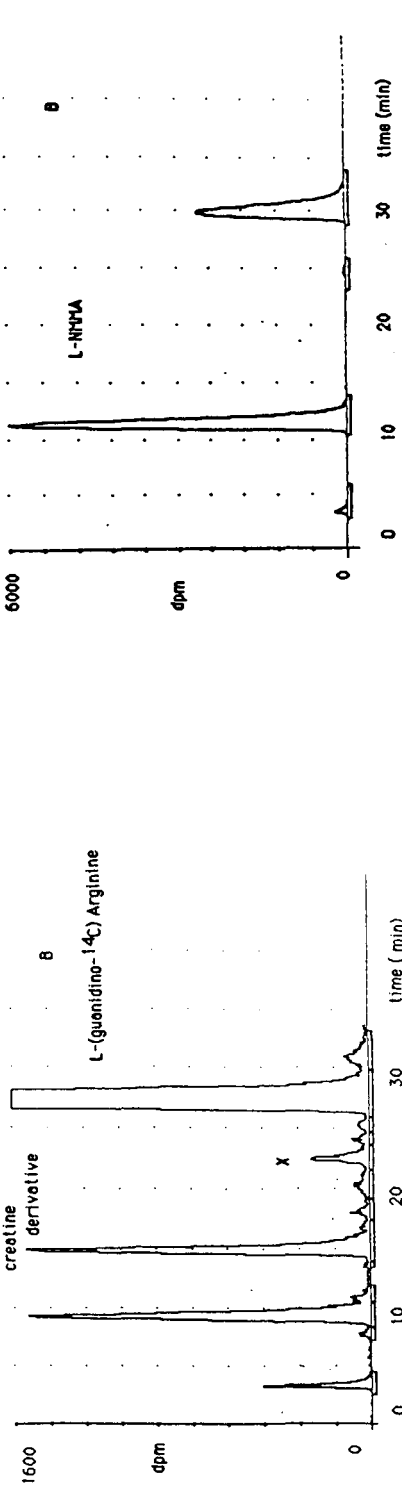

Fig. 6. Radiolabelled L-[ureido-^{14}C]citrulline-derived metabolites generated in induced EMT6 cell culture media. Added radiolabelled citrulline: 37 kBq. (A) in the absence of L-NMMA; (B) in the presence of 2.2 m*M* L-NMMA.

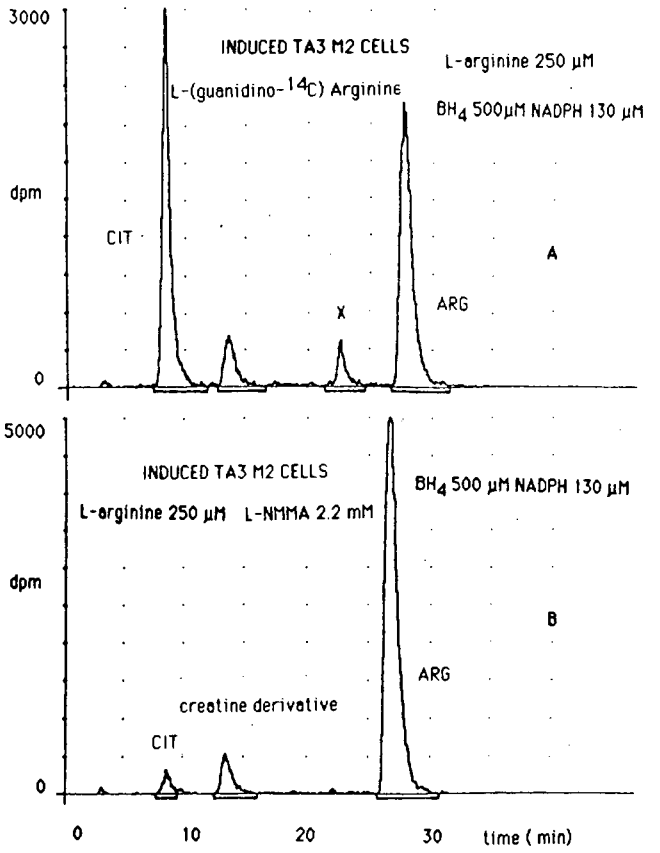

Fig. 7. HPLC analysis of cytosolic extracts from induced TA3 M2 cells. (A) In the absence of L-NMMA; (B) in the presence of 2.2 m*M* L-NMMA. Cytosolic extracts from induced cells were processed as indicated under Experimental in the presence of cofactors of the NO˙-generating pathway (NADPH, BH_4) and of 8 kBq of L-[guanidino-^{14}C]arginine.

first transformed into a less basic compound. It was very labile at alkaline pH, leading to urea as a detectable product when L-[guanidino-^{14}C]arginine was used.

DISCUSSION

We have found in culture media or cytosols of cells, in which the NO˙-generating pathway has been induced, a metabolite, X, generated at the same time as citrulline (inhibition by L-NMMA, triggering by BH_4). Metabolite X, unlike citrulline, was not found in cytotoxic macrophages, probably because of the intense metabolism of these cells (*e.g.*, very active arginase) and the lability of X. An additional product from L-arginine metabolism was found and is possibly linked to the creatine pathway. More information on this could be obtained by incubating the cells with [^{3}H]glycine (a precursor).

Metabolite X is eluted between ornithine and arginine and is therefore more

basic than ornithine and less so than arginine. It may be assumed that N^G-hydroxyarginine or N^G-oxoarginine would be less basic than arginine because of the loss of resonance energy which stabilizes the guanidinium cation. Thus, taking into account the chromatographic properties of X and the location of its radiolabelling (guanidino-^{14}C), it may be hypothesized that X is probably either N^G-hydroxyarginine or N^G-oxoarginine, the intermediates which have been postulated (Fig. 1). We are currently trying to obtain large amounts of the compound to check this hypothesis by mass spectrometry.

The metabolites of the NO•-generating pathway (NO•, N^G-hydroxyarginine) might be direct inhibitors of a key enzyme of DNA synthesis ribonucleotide reductase. This would explain the antiproliferative effects obtained through the induction of the NO•-generating pathway [6].

REFERENCES

1 M. A. Marletta, *Trends Biochem. Sci.*, 14 (1989) 489.
2 D. J. Stuehr and M. A. Marletta, *Proc. Natl. Acad. Sci. U.S.A.*, 82 (1985) 7739.
3 R. M. J. Palmer, A. G. Ferridge and S. Moncada, *Nature (London)*, 327 (1987) 524.
4 M. A. Marletta, P. S. Yoon, R. Iengar, C. D. Leaf and J. S. Wishnok, *Biochemistry* 27 (1988) 8706.
5 M. Lepoivre, H. Boudbid and J. F. Petit, *Cancer Res.*, 49 (1989) 1970.
6 M. Lepoivre, B. Chenais, A. Yapo. G. Lemaire, L. Thelander and J. P. Tenu, *J. Biol. Chem.*, 265 (1990) 14 143.
7 J. B. Hibbs, Jr., Z. Vavrin and R. R. Taintor, *J. Immunol.*, 138 (1987) 550.
8 J. B. Hibbs, Jr., R. R. Taintor and Z. Vavrin, *Science*, 235 (1987) 473.
9 M. A. Tayeh and M. A. Marletta, *J. Biol. Chem.*, 264 (1989) 19654.
10 N. S. Kwon, C. F. Nathan and D. J. Stuehr, *J. Biol. Chem.*, 264 (1989) 20496.
11 S. Moncada, R. M. J. Palmer and E. A. Higgs, *Biochem. Pharmacol.*, 38 (1989) 1709.
12 S. Eriksson, A. Graslund, S. Skog, L. Thelander and B. Tribukait, *J. Biol. Chem.*, 260 (1984) 9114.

Journal of Chromatography, 539 (1991) 443–448
Elsevier Science Publishers B.V., Amsterdam

CHROM. 22 904

Simple equilibrium dialysis–high-performance liquid chromatographic method for the *in vitro* assessment of 5-methoxypsoralen bound to human albumin

S. MAKKI*

*Laboratoires de *Chimie Analytique et de Dermatologie et Biologie Cutanée, Faculté de Médecine et Pharmacie, Place St. Jacques, 25030 Besançon Cedex (France)*

P. MURET

Laboratoires de Dermatologie et Biologie Cutanée et de Pharmacologie, Faculté de Médecine et Pharmacie, Place St. Jacques, 25030 Besançon Cedex (France)

A. RENAUD

Laboratoire de Pharmacologie, Faculté de Médecine et Pharmacie, Place St. Jacques, 25030 Besançon Cedex (France)

P. AGACHE

Laboratoire de Dermatologie et Biologie Cutanée, Faculté de Médecine et Pharmacie, Place St. Jacques, 25030 Besançon Cedex (France)

and

P. MAGNIN

Laboratoire de Pharmacologie, Faculté de Médecine et Pharmacie, Place St. Jacques, 25030 Besançon Cedex (France)

ABSTRACT

Increasingly used in therapeutics, 5-methoxypsoralen (5-MOP), a linear furocoumarin, associated with UVA irradiation (PUVA), is now an established treatment for skin diseases such as vitiligo, mycosis funcoides and particularly psoriasis. Succesful PUVA therapy depends on a sufficiently high peak 5-MOP plasma concentration coinciding with the UVA irradiation. However, as with most drugs, only the free plasma fraction is able to enter the target cells and has a pharmacological effect.

In this work, the binding of 5-MOP to human albumin was studied *in vitro*, using a dialysis chamber. Bound and free 5-MOP fractions were quantified by a modification of Stolk's high-performance liquid chromatographic method. Dialysis was performed at 37°C and pH 7.4 for 2 h, against a 4% albumin solution in phosphate buffer. The 5-MOP concentrations used were from $5 \cdot 10^{-5}$ to $5 \cdot 10^{-2}$ g/l in $1 \cdot 10^{-1}$ g/l steps. The 5-MOP bound strongly to human albumin in an unsaturable way. The mean 5-MOP binding to albumin was 95.3%. These results are in accordance with those published by Artuc *et al.* and not with those of Veronese *et al.*, who found a lower saturable fixation (91%). These two research groups used tritiated 5-MOP. The technique used in this work is simple and inexpensive. It can be employed easily *in vivo*, *e.g.*, for the assessment of 5-MOP free fractions in different therapeutic conditions.

0021-9673/91/$03.50

INTRODUCTION

The psoralens, linear furocoumarins, are increasingly used in therapeutics. The psoralens employed in dermatology are 8-methoxypsoralen (8-MOP), 5-methoxypsoralen (5-MOP) and trimethylpsoralen (TMP). The PUVA therapy, association of psoralens (P) with ultraviolet radiation (UVA) is one of the main treatments for psoriasis and vitiligo. 5-MOP (Fig. 1), the last to be introduced in this therapy, is the least studied, especially regarding its binding to serum albumin, the principal carrier of the molecule to the skin.

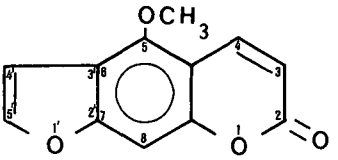

Fig. 1. 5-Methoxypsoralen (5-MOP).

Artuc *et al.* [1] and Veronese *et al.* [2] studied the relationship between 5-MOP and albumin. They used radiolabelled 5-MOP to determine its fixation to human albumin. However, their results concerning the saturation of the binding of 5-MOP to the albumin were contradictory.

In this paper, we present a simple method which employs equilibrium dialysis for the study of 5-MOP fixed to human albumin and the detection of the remaining non-linked, free drug. The determination of these fractions was carried out by high-performance liquid chromatography (HPLC). No radiolabelled 5-MOP was employed. Our results are in agreement with those reported by Artuc *et al.* [1].

EXPERIMENTAL

Equilibrium dialysis

The binding of 5-MOP was accomplished with a Dianorm apparatus [3]. The drug was placed in one half of each cell and the human albumin in the other half. The two halves were separated by a semi-permeable cellulose membrane (Diachema). The experiments were carried out under the following conditions: 37°C, pH 7.4, phosphate buffer (0.2 *M*) and incubation for 2 h with constant rotation at 20 rpm.

Extraction procedure

Sample volumes of 0.5 ml were withdrawn at different time intervals (0, 0.25, 0.50, 1, 2 and 18 h) from the two sides (halves) of the cells: the free 5-MOP from the first half of the cell and the free and bound 5-MOP from the second half. Each sample was extracted with 5 ml of heptane–methylene chloride (4:1, v/v). The mixture was stirred for 5 min and centrifuged at 1700 *g* for about 7 min. The organic layer was transferred to a test-tube and evaporated to dryness on a water-bath at 50°C under a stream of nitrogen [4].

HPLC

HPLC separations were carried out with a Merck–Hitachi Model 655A-11 instrument. The method was based on Stolk's technique [4], with some modifications. To increase the sensitivity, a spectrofluorimeter (excitation at 312 nm, emission at 490 nm [5]) was used instead of a UV detector. The mobile phase was methanol–water (60:40, v/v). The column was LiChrospher 100 RP-8 (5 μm) in LiChrocart 125-4 (Merck, Darmstadt, Germany). After having established the calibration graph with solutions of known concentrations, psoralens, extracted from phosphate buffer, were injected into the HPLC system.

Calibration graph

Basic solutions were prepared with 200 μg/ml of 5-MOP and 8-MOP in ethanol. The calibration graph was obtained by adding 25, 50, 75, 100, 300 and 600 ng/ml of 5-MOP and 200 ng/ml of 8-MOP to six human serum samples of 1 ml each, free of drug. 8-MOP was used as an internal standard. The calibration graph was a plot of peak-height ratios (5-MOP/8-MOP) *versus* 5-MOP concentrations in different samples.

RESULTS AND DISCUSSION

Determination of free (F) and bound (B) 5-MOP at different times

Table I shows the concentrations of F- and B-5-MOP as a function of time. It is noticeable that by the second hour (Fig. 2), an equilibrium between the two halves of the cell was obtained with equal concentrations of F-5-MOP and stabilization of 5-MOP bound to human albumin. The standard deviations are small. This demonstrates little variation and good reproducibility. The concentration of 5-MOP used for this study was 196 ng/ml. The free active fraction of 5-MOP was 8 ng/ml (about 5%) and there was no change in this value between 2 h and 18 h.

Assessment F- and B-5-MOP in relation to increasing concentrations

Table II shows that at a concentration of 50 ng/ml, the proportion of the 5-MOP bound to albumin was small. From 200 to $5 \cdot 10^4$ ng/ml the binding of 5-MOP to

TABLE I

DETERMINATION OF FREE (F) AND BOUND (B) 5-MOP AS A FUNCTION OF TIME

Each value represents the average of three dialyses. All samples were analysed twice by HPLC.

Time (h)	5-MOP (ng/ml)		
	Free (F)	Bound + free (B + F)	Bound (B), calculated
0	196	–	–
0.25	63.8 ± 0.8	85.8 ± 0.6	22.4 ± 1.6
0.50	27.7 ± 0.8	138.8 ± 2.0	111.2 ± 2.0
1	14.0 ± 1.4	152.7 ± 0.1	138.0 ± 0.5
2	8.0 ± 1.3	173.0 ± 0.1	165.0 ± 0.7
18	7.8 ± 1.2	170.8 ± 1.0	162.8 ± 1.0

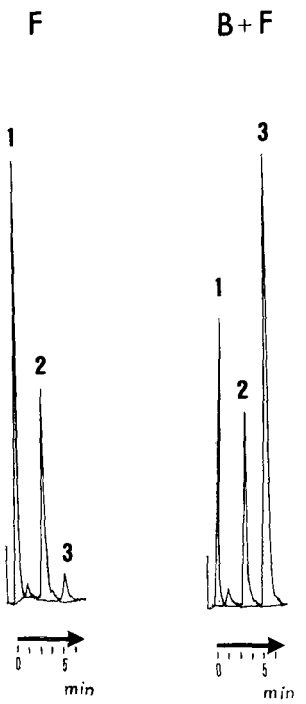

Fig. 2. Chromatograms of psoralens, detected for the determination of free 5-MOP (F-, peak 3) and bound and free 5-MOP (B + F-, peak 3) at equilibrium (2 h). Peaks: 1 = solvent (ethanol); 2 = 8-MOP (internal standard); 3 = 5-MOP.

albumin was stabilized at about 95% and B-5-MOP/F-5-MOP ratio remained constant (20.00 $\pm$ 0.36). The lower binding ability at low concentrations of 5-MOP could be due to fixation on a first type of receptor on the albumin molecule, quickly saturated, and hidden by the very large binding ability of a second receptor. Such a phenomenon has been described for some drugs bound to albumin in an unsaturable way such as weak acids [6].

TABLE II

ASSESSMENT OF F- AND B-5-MOP IN RELATION TO INCREASING CONCENTRATION

Concentration (ng/ml)	F (ng/ml)	B + F	B (ng/ml)	B/F	% of B
50	4.1	41	36.9	9	90
200	8.1	173.2	165.1	20.38	95.3
$1 \cdot 10^3$	40.3	851.4	811.1	20.12	95.2
$1 \cdot 10^4$	435.2	9438.6	9003.4	20.68	95.4
$5 \cdot 10^4$	2230.6	47 320.7	45 090.1	20.21	95.2

DISCUSSION

The aim of this work was to devise a simple technique for the *in vitro* determination of 5-MOP bound to human albumin. This would be of help in assessing the free 5-MOP concentration, which is the fraction responsible for the therapeutic effect.

The binding to human serum albumin of 8-MOP, the most commonly employed psoralen in PUVA therapy [7], has been evaluated by several investigations using liquid scintillation counting, and showed saturable binding [8–11]. For 5-MOP only a few studies are available, in which radio-labelled psoralen was used. Whereas Artuc *et al.* [1] found an unsaturable binding of 5-MOP to human albumin in the 5 ng/ml–230 μg/ml, Veronese *et al.* [2] reported saturable binding using a more limited range of concentration (30 ng/ml–30 μg/ml) (Table III). However, in the latter work, there was only a trend towards a saturation process visible at higher concentrations.

TABLE III

SUMMARY OF METHODS AND RESULTS

Step	Parameter	Artuc *et al.* [1]	Veronese *et al.* [2]	This work
Dialysis equilibrium	Time (h)	36–50	14	2
	Temperature (°C)	4	37	37
	Apparatus	Rotating	Agitated	Rotating
	Buffer	0.1 *M* phosphate (pH 7.2)	0.05 *M* phosphate (pH 7.4)	0.2 *M* phosphate (pH 7.4)
5-MOP determination	–	Liquid scintillation counting	Liquid scintillation counting	HPLC
Results	Binding (%)	98–99	91	95.3
	Saturation	Non-saturable	Saturable	Non-saturable
	Concentration range	5 ng/ml–230 μg/ml	30 ng/ml–30 μg/ml	50 ng/ml–50 μg/ml

The method proposed here is simple and rapid and does not require labelled drug. In 1984, Prognon [5] used this technique to study 3-carbethoxypsoralen fixation to albumin. Using this method, the *in vivo* fixation of psoralens on albumin can be assessed in clinical practice. This is of major importance as the strong correlation observed between 5-MOP plasma concentration and PUVA therapy efficiency [7] may be related only to the free 5-MOP concentration. Investigations of the influence of low- and high-fat meals on the fixation of 5-MOP to human albumin are in progress.

ACKNOWLEDGEMENTS

The authors thank Mr. G. Pannetton (Iconographie, Faculté de Médecine et de Pharmacie, Besançon) for technical assistance and Bergaderm Laboratories (Paris) for providing the chemicals.

REFERENCES

1 M. Artuc, G. Stuettgen, W. Schalla, H. Schaffer and J. Gazith, *Br. J. Dermatol.*, 101 (1979) 669.
2 F. M. Veronese, R. Bevilaequa, O. Schiavon and G. Rodighiero, *Farmaco, Ed. Sci.*, 34 (1979) 716.
3 M. Lecomte, R. Zini, P. d'Athis and J. P. Tillement, *Eur. J. Drug Metab. Pharmacokinet.*, 1 (1979) 23.
4 L. M. Stolk, *Pharm. Weekbl.*, 2 (1980) 281.
5 P. Prognon, *Thèse Série E*, No. 194, Université Paris Sud, Paris, 1984.
6 R. Zini, P. d'Athis, J. Barre and J. P. Tillement, *Biochem. Pharmacol.*, 28 (1979) 2661.
7 E. Andrew, A. Nilsen, P. Thune and I. Wilk, *Clin. Exp. Dermatol.*, 6 (1981) 591.
8 F. M. Veronese, R. Bevilacqua, O. Schiavon and G. Rodighiero, *Farmaco, Ed. Sci.*, 33 (1978) 667.
9 R. Bevilacqua, C. A. Benassi, O. Schiavon and F. M. Veronese, *Farmaco, Ed. Sci.*, 36 (1981) 598.
10 O. Schiavon, C. A. Benassi and F. M. Veronese, *Farmaco, Ed. Sci.*, 39 (1984) 109.
11 M. Pibonin, R. Zini, P. Nguyen, A. Renouard and J. P. Tillement, *Br. J. Dermatol.*, 117 (1987) 207.

Journal of Chromatography, 539 (1991) 449–453
Elsevier Science Publishers B.V., Amsterdam

CHROM. 22 906

Scaling up in isolation of medium-size uraemic toxins

PHILIPPE M. GALLICE* and AIMÉ D. CREVAT
Laboratoire de Biophysique, Faculté de Pharmacie, 27 Boulevard Jean Moulin, 13385 Marseille Cedex 5 (France)
and
YVON F. BERLAND
Centre d'Hémodialyse, Hôpital Sainte-Marguerite, Boulevard de Sainte Marguerite, Marseille (France)

ABSTRACT

Plasmatic accumulation of uraemic toxins in the middle molecular mass range has been reported to be associated with several pathologies observed in uraemic patients. The very low concentration of these toxins in uraemic body fluids makes classical chromatography techniques inadequate in isolating sufficient amounts of these endogenous substances, thus precluding their identification. A scaling up of gel permeation and ion-exchange chromatographies was therefore developed. This considerably increased the amount of uraemic toxins isolated, thus allowing the study of their chemical nature and facilitating understanding of their biological activities.

INTRODUCTION

Uraemic haemodialysed patients classically develop several associated disorders such as uraemic neuropathy and disturbances of ionic metabolism (Na^+, Ca^{2+}, etc.). These pathologies are commonly attributed to plasmatic accumulation of endogenous substances in the molecular mass range 200–2000, the so-called uraemic middle molecules (UMM) [1].

In previous papers [2,3] we demonstrated that UMM, isolated by successive gel permeation and anion-exchange chromatography, exhibit some biological effects correlated with several pathologies such as neuropathy and Na^+ metabolism disorders which are associated with end-stage renal failure treated by haemodialysis.

However the concentrations of these toxins in uraemic body fluids are very low. Hence the standard chromatographic technique described previously [4] is inadequate for isolating sufficient amounts of these active molecules, thus precluding their identification and a better understanding of their biological activities. We therefore scaled up the standard chromatographic process to increase the amounts of UMM isolated. In this paper we report the UMM separations obtained using scale-up and standard chromatographic conditions simultaneously for comparison.

0021-9673/91/$03.50

EXPERIMENTAL

Biological samples

Ultrafiltrates of plasma from uraemic patients (UF) were obtained at the beginning of dialysis by applying a negative pressure (400 mmHg) in the dialyser compartment before the dialysis fluid was run through the dialyser. Samples were stored at −20°C until use.

Gel permeation chromatography (GPC)

Preparative scale. A 100-ml volume of UF was separated on a glass column (900 × 50 mm I.D.) packed with Sephadex G-15. The column was eluted with Tris–HCl buffer (10^{-2} *M*, pH 8.6) at a flow-rate of 296 ml h^{-1} (linear velocity 15.07 cm h^{-1}). The absorbance was monitored at 254 nm and the eluate was collected in 9-ml aliquots.

Standard conditions. A 20-ml volume of UF was chromatographed on a 900 × 26 mm I.D. column of Sephadex G-15 eluted with Tris buffer at a flow-rate of 80 ml h^{-1}.

Ion-exchange chromatography (IEC)

Preparative scale. A UMM sample (corresponding to 400 ml of UF) was injected onto a glass column (230 × 26 mm I.D.) packed with DEAE-Sephadex A-25 and equilibrated with Tris–HCl buffer (10^{-2} *M*, pH 8.6) at a flow-rate of 275 ml h^{-1}.

The column was eluted for 60 min with the same buffer, followed by a 12-h exponential gradient of NaCl at the same flow-rate. At any time the NaCl concentration was

$$C_t = C_f[1 - \exp(-Qt/V)]$$

where C_t represents the NaCl concentration at time t, C_f the final NaCl concentration (0.13 *M*), Q the flow-rate and V the volume of the gradient mixing chamber (1000 ml). The absorbance was monitored continuously at 254 nm and aliquots (13 ml) were collected.

Standard IEC. A UMM sample from 40 ml of UF was separated using a 23 cm × 8 mm I.D. column (DEAE-Sephadex A-25) equilibrated with Tris–HCl buffer at a flow-rate of 26 ml h^{-1}. Elution was carried out with an exponential gradient of NaCl (0–0.15 *M*) using a 125-ml mixing volume chamber.

RESULTS

Fig. 1 shows typical elution profiles of 100 ml and 20 ml of UF separated by GPC (Sephadex G-15) according to preparative (top) and standard (bottom) conditions, respectively. The elution profiles obtained with the preparative procedure and standard chromatographic method(s) were identical. Thus, GPC provided 8–10 fractions. Peak 2 is observed in uraemic but not in normal plasma ultrafiltrates [4]. The apparent molecular mass of the peak is about 1000 dalton, hence this compound falls in the molecular mass range of the so-called "uraemic middle molecules" [5], which have been suggested to be connected with various uraemic disorders [1,6,7]. Thus peak

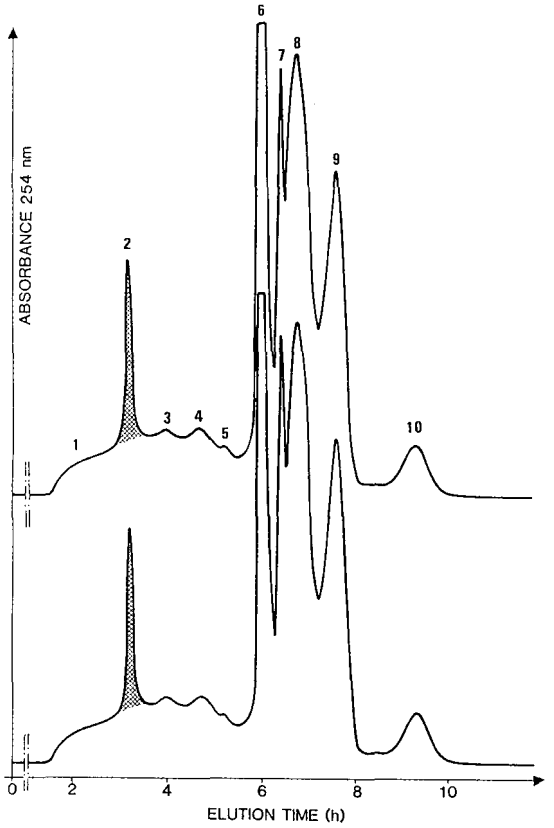

Fig. 1. Typical GPC of uraemic plasmatic ultrafiltrates: scale up (top) and standard procedures (bottom). The hatched fraction represents the elution of UMM (peak 2). For peaks, see Results section.

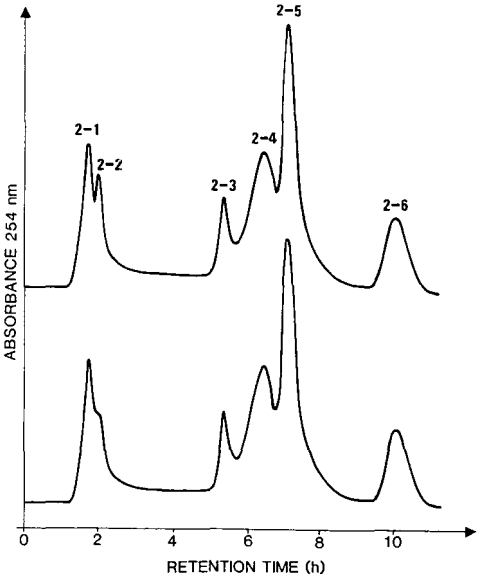

Fig. 2. Typical IEC elution profiles of crude UMM (peak 2): scale up (top) and standard procedures (bottom).

2 was called "crude UMM". It contains compounds which have been reported to be toxic [2,3]. IEC separation was therefore performed on this peak.

Fig. 2 represents IEC separations of crude UMM (peak 2). As in GPC, the chromatograms obtained were identical. IEC allows the separation of peak 2 into six fractions numbered in order of elution 2-1, ..., 2-6. The method of peak labelling is based on the decimal system, where 1, 2, 3, etc., refer to the primary peaks obtained with GPC. Next, sub-peaks obtained in the subsequent separation of peak 2 by IEC are designed in order of elution: 2-1, 2-2, 2-3, etc. This numbering system follows previously established nomenclature [8].

DISCUSSION

Separation of UMM by the standard technique using two successive chromatographic steps is an efficient method but it does not allow the isolation of sufficient amounts of compounds. Therefore, in order to obtain a greater amount of these substances, we scaled up the GPC and IEC procedures.

For GPC an increase in productivity was achieved by increasing the column diameter (from 26 mm to 50 mm), which increased the stationary phase volume (from 478 to 1767 ml) and allowed the separation of an increased sample volume (from 20 to 100 ml). In order to preserve the chromatographic resolution and the separation time, the flow-rate was increased (from 80 to 296 ml h^{-1}) to obtain a constant linear velocity of eluent (15.07 cm h^{-1}).

The comparative results obtained (Fig. 1) show that scaling up in GPC allows a five-fold increase in sample volume treated per chromatographic run.

For the scaling up in IEC, the column size was adapted to the sample volume treated. To select an appropriate column, we used the equation

$$S.F. = \frac{(I.D._2)^2 \times L_2}{(I.D._1)^2 \times L_1}$$

where $S.F.$ is the scale factor for separation, $I.D._2$ is the I.D. of the preparative column and L_2 is its length, $I.D._1$ is the I.D. of the standard column and L_1 is its length.

To preserve the resolution we maintained the column length ($L_1 = L_2 = 23$ cm). Because the sample volume to be processed per chromatographic run increases from 40 to 400 ml, the $S.F.$ value was 10. Under these conditions, as $I.D._1$ was 8 mm, the calculated $I.D._2$ was about 26 mm. Therefore, the preparative column selected for IEC was 230 × 26 mm I.D. (see Experimental). In addition, to preserve the separation time, we adjusted the flow-rate to 275 ml h^{-1} to maintain a constant linear velocity of 51.8 cm h^{-1}.

As elution was achieved using an increasing exponential NaCl gradient (see Experimental), modification of the flow-rate modified the slope of the gradient. Therefore, in order to preserve a similar gradient curve, we recalculated the other gradient parameters taking into account the new flow-rate. The mixing gradient chamber volume was therefore increased from 125 to 1000 ml and the final NaCl concentration was 0.13 M.

Under these optimized conditions, the separation of UMM (peak 2) by scaling up in IEC is comparable to the separation carried out under the standard conditions

(Fig. 2). Moreover, scaling up makes it possible to process ten times more UMM sample volume per run.

Consequently, this scaling up in the isolation steps of UMM considerably increases the amount of compounds isolated, thus making it possible to study their chemical nature and biological activity.

ACKNOWLEDGEMENTS

The authors are grateful to M. Vidalin and H. Bouteille for skillful technical assistance.

REFERENCES

1 J. Bergström and P. Fürst, in W. Drukker, F. M. Parsons and J. M. Maher (Editors), *Replacement of Renal Function by Dialysis*, Martinus Nijhoff, Boston, MA, 1983, Ch. 19, p. 354.
2 D. Braguer, P. Gallice, J. P. Monti, A. Murisasco and A. Crevat, *Clin. Nephrol.*, 25 (1986) 4.
3 P. Gallice, J. P. Monti, M. Baz, A. Murisasco and A. Crevat, *Clin. Chem.*, 34 (1988) 2044.
4 P. Gallice, N. Fournier, A. Crevat, M. Briot, R. Frayssinet and A. Murisasco, *Kidney Int.*, 23 (1983) 764.
5 A. L. Babb, P. C. Farrell, D. A. Uvelli and B. H. Scribner, *Trans. Am. Soc. Artif. Organs*, 18 (1980) 98.
6 H. Klinkmann, J. Bergström, R. Dzurik and J. L. Funck-Brentano (Editors), *Middle Molecules in Uremia and Other Diseases, Proceedings of Symposium on Present Status and Future Orientation of Middle Molecules in Uremia and Other Diseases, Avignon, France, November 28–29, 1980*, International Society Artificial Organs, Cleveland, OH, 1980, pp. 59–119.
7 S. Ringoir, R. Vanholder and S. G. Massry (Editors), *Uremic Toxins, Proceedings of Ghent Symposium on Uremic Toxins, Ghent, Belgium, October 3–4, 1986*, Plenum Press, New York, 1987.
8 H. Klinkmann, *Artif. Organs*, 4, Suppl. (1980) 188.

Journal of Chromatography, 539 (1991) 455–463
Elsevier Science Publishers B.V., Amsterdam

CHROM. 22 880

Selective extraction of native β-lactoglobulin from whey

EMILIA CHIANCONE* and MAURIZIO GATTONI
CNR Centre of Molecular Biology, Department of Biochemical Sciences, University of Rome "La Sapienza", 00185 Rome (Italy)

ABSTRACT

A method is proposed for the selective extraction from whey of β-lactoglobulin, the major allergenic component of cow milk. It represents an application of subunit exchange chromatography, which exploits the tendency of β-lactoglobulin to undergo reversible association–dissociation equilibria at slightly acidic pH values. Immobilized A and B β-lactoglobulin subunits are capable of interacting in a highly specific and reversible way with the soluble protein and can be used to extract A and B β-lactoglobulin from whey under conditions that favour subunit association. The soluble protein retained by the immobilized protein can be recovered under conditions that promote dissociation into subunits. The subunit exchange column, if coupled to an anion-exchange column, allows the complete deproteinization of whey. All the whey proteins are extracted in their native form and are of high purity; their functional properties are intact even after lyophilization. This important characteristic and the possibility of removing β-lactoglobulin selectively render the proposed method a potentially powerful tool in the processing of whey to produce human food products for specific end-uses such as hypoallergenic milk formulas.

INTRODUCTION

In recent years, the attitude towards whey proteins has changed and they are no longer considered as waste products, but rather as valuable nutrients that can be used by the food industry. However, this use is dependent on, among other factors, the possibility of tailoring whey proteins for specific end-uses and recovering them with intact functional properties [1]. Their use in the baby-food industry, for example, for the production of hypoallergenic infant milk formulas, requires the selective removal of β-lactoglobulin, the major allergenic component of cow milk [2].

β-Lactoglobulin, which represents half of whey proteins, occurs in the form of two genetic variants, A and B, plus a minor variant, C, of different electrophoretic mobility; it is a dimer of relative molecular mass 36 000. At pH < 3.7 and > 5.4, the two main genetic variants dissociate reversibly into single polypeptide chains; the extent of dissociation increases with increasing temperature. Between pH 3.7 and 5.2 in the cold, the native dimeric molecule undergoes a reversible tetramerization which in the A variant is maximum in the pH range 4.40–4.65; the tendency to tetramerize is significantly less marked with the B variant [3–8]. In mixtures of A and B β-lactoglobulin all molecules can aggregate with three types of bonds of different strengths and mixed A–B tetramers are also formed [9].

0021-9673/91/$03.50

The occurrence of association–dissociation phenomena in β-lactoglobulin suggested the application of subunit exchange chromatography for its selective extraction from whey. This is a bioaffinity chromatographic method which exploits the fact that immobilized subunits of polymeric and self-associating proteins retain the capacity to interact in a very specific and reversible way with soluble subunits of the same or of a homologous protein. Hence, under experimental conditions where the soluble protein is in self-association equilibrium, subunits are exchanged between the liquid and the solid phase and part of the protein, that was initially in solution, is bound to the matrix. The amount of matrix-bound polymer thus formed is governed by the law of mass action and depends on several parameters, *i.e.*, on the concentration of immobilized and soluble protein, on the association constants in the liquid and in the solid phase and on the stoichiometry of the association reaction [10–12]. In principle, therefore, one may achieve purification of the polymerizing protein in two steps by changing the state of association in an appropriate way. In the first, the protein is extracted from the medium and bound to the immobilized subunits under conditions that favour polymer formation. In the second step, the specifically bound protein is eluted under conditions that promote dissociation of the polymer into subunits [13–15].

The data reported in this paper show that subunit exchange chromatography can be employed for the selective extraction of A and B β-lactoglobulin from whey. Moreover, the experimental conditions used in the bioaffinity column are such that other whey proteins can be recovered easily in a concentrated from by means of an anion-exchange column. A major advantage of the proposed method is that all the proteins are obtained in their native form and hence are amenable to a variety of uses in the food industry.

EXPERIMENTAL

Chemicals

The different β-lactoglobulins, *i.e.*, the genetic species A and B and their mixture, were crystallized products from Sigma (St. Louis, MO, U.S.A.). Whey was obtained from fresh cow milk (Centrale del Latte, Rome, Italy) after precipitation of casein at pH 4.65. Milk and a sodium acetate buffer of ionic strength, (I) 0.1 M at pH 4.65 were mixed in equal volumes and stirred for 15 min at room temperature while maintaining the pH constant by addition of 1 M acetic acid in small amounts. The precipitated casein was removed by centrifugation for 10 min at 15 000 g in a Sorvall centrifuge and the supernatant (whey) was dialysed against the same acetate buffer. After dialysis, whey was clarified by filtration through a Millipore filter.

Equipment

Gel electrophoresis experiments were performed according to Davis [16]. Sedimentation velocity experiments were carried out in a Spinco Model E ultracentrifuge equipped with an RTIC unit at 52 000 rpm and 10°C; the sedimentation coefficients were corrected to $s_{20,w}$ (sedimentation coefficient corrected to the value it would have in a solvent with the viscosity and density of water at 20°C) by standard procedures.

Protein immobilization

The mixture of A and B β-lactoglobulin was immobilized under different experimental conditions (such as pH of immobilization and coupling time, extent of matrix activation, concentration of added protein). After the coupling step, the matrix was washed with coupling buffer; subsequently, any non-covalently bound protein was removed with a dissociating buffer at acidic pH, namely 0.1 *M* NaCl–HCl at pH 2.0. The concentration of immobilized protein was determined spectrophotometrically by using the specific absorbance ($A_1^{1\%}{}_{cm}$) of 9.6 at 278 mm [5]. The turbidity of the material was minimized with the use of protein-free gel in the reference beam.

Determination of the associating capacity of the immobilized protein

The capacity of immobilized β-lactoglobulin to bind the protein in solution was measured by frontal analysis of the eluate from a thermostated chromatographic column containing *ca.* 5 ml of immobilized protein and equilibrated with associating buffer (0.1 *M* sodium acetate buffer, pH 4.65) at a constant flow-rate of about 10 ml/h. β-Lactoglobulin solutions in the same buffer were percolated through the column until a steady state was reached, *i.e.*, until the absorbance of the effluent was the same as that of the in-flowing solution. The effluent absorbance was monitored at 278 nm with a Gilford 2000 spectrophotometer equipped with a flow cell. The elution volume of the protein, V, was calculated by constructing the equivalent sharp boundary [10]. The column was freed from the retained protein with dissociating buffer, 0.1 *M* NaCl–HCl (pH 2.0), unless stated otherwise. The same buffer was used to measure the void volume of the column, V_0.

RESULTS AND DISCUSSION

Application of subunit exchange chromatography to purified β-lactoglobulin

The effects of the pH of immobilization, extent of matrix activation and concentration of added protein, on the amount of A and B β-lactoglobulin immobilized per millilitre of added gel are shown in Table I. It is worth pointing out that pH values above 7.0 were avoided owing to the slow denaturation processes that take place under these pH conditions [4].

β-Lactoglobulin immobilized under all the conditions given in Table I is stable for several months when kept at pH 4.65 in the presence of 0.2% sodium azide. The

TABLE I

IMMOBILIZATION OF A AND B β-LACTOGLOBULIN ON SEPHAROSE 4B

Coupling reaction carried out using 0.05 *M* phosphate buffer; coupling time, 18 h at 6°C.

Sample No.	pH of immobilization	mg BrCN/ml Sepharose	mg β-lactoglobulin added/ml Sepharose	mg β-lactoglobulin immobilized/ml Sepharose
1	6.0	50	8	1.5
2	6.7	50	8	3.8
3	6.7	100	14	4.8
4	6.7	50	14	4.1

leakage of the protein from the matrix was found to correspond to about 2% of the immobilized material 8 months after the coupling reaction.

The associating capacity of the immobilized samples was measured as described under Experimental. A typical experiment in 0.1 *M* acetate buffer (pH 4.65) at 8°C is shown in Fig. 1. The establishment of a reversible association–dissociation equilibrium between the liquid and the solid phase results in the specific binding of soluble β-lactoglobulin to the immobilized subunits and hence in the retardation of the elution of β-lactoglobulin (V) with respect to an inert protein (V_0). The difference in elution volume, $\Delta V = V - V_0$ (Fig. 1), is related to the amount of protein bound to the matrix under steady-state conditions, $[\bar{Y}]$, by the expression $[\bar{Y}] = \Delta Vc$, where c is the steady-state concentration of the protein in solution. It is useful to define the quantity $[\bar{Y}]/R - X_1$, where $R - X_1$ is the amount of immobilized monomer, which may be called the binding number as its limiting value at infinite concentration of soluble protein equals $n-1$, n being the degree of polymerization [11].

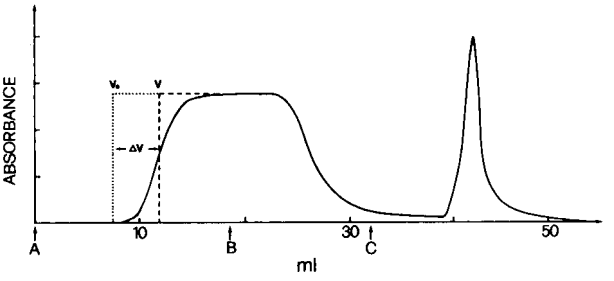

Fig. 1. Elution profile of A and B β-lactoglobulin from a column containing Sepharose-bound A and B β-lactoglobulin. The protein in the solid phase was 4.8 mg/ml of settled gel and the bed volume was 5.0 ml. The column was equilibrated with 0.1 *M* acetate buffer (pH 4.65) at 8°C. Arrows indicate the application of (A) the β-lactoglobulin solution at 2 mg/ml, (B) equilibrating buffer and (C) 0.1 M NaCl–HCl dissociating buffer (pH 2.0). Dashed lines represent the position of the hypersharp front of the boundaries of β-lactoglobulin (V) and of a non-interacting protein (V_0).

β-Lactoglobulin is probably immobilized on the matrix as the monomer of relative molecular mass of 18 kilodalton, as the coupling reaction is expected to shift the association–dissociation equilibrium of the native dimeric species [4,7] towards monomer formation. In line with this expectation, no traces of protein were found in the eluate on extensive washing of the immobilized protein with dissociating buffer after the coupling reaction.

Table II reports the results obtained in experiments of this kind in which solutions of A and B β-lactoglobulin at a concentration of 2 mg/ml in acetate buffer of $I = 0.1$ *M* were allowed to interact with the same protein mixture immobilized under the conditions detailed in Table I. The associating capacity of the Sepharose-bound protein varies as a function of the coupling conditions. In particular, a change in the immobilization pH from 6.7 to 6.0 (samples 1 and 2) and a high extent of matrix activation (samples 3 and 4) decrease the associating capacity of the immobilized protein; in the latter instance the effect is probably due to multi-point attachment to the matrix.

TABLE II

AMOUNT OF β-LACTOGLOBULIN RETAINED ON A COLUMN OF IMMOBILIZED A AND B β-LACTOGLOBULIN

A column (5 ml) was saturated with β-lactoglobulin or whey at a concentration of 2 mg/ml in 0.1 *M* acetate buffer (pH 4.65 or 6.0) at the indicated temperatures; elution with 0.1 *M* NaCl–HCl (pH 2.0).

Solution	Immobilized protein[a]	mg bound β-lactoglobulin/mg immobilized protein[b]		
		8°C		23°C, pH 6.0
		pH 4.65	pH 6.0	
A and B β-lactoglobulin	1	0.13	–	–
	2	0.30	0.23	–
	3	0.22	0.32	–
	4	0.44	0.36	–
Whey	2	0.31	0.21	–
	3	0.19	0.37	0.23[c]
	4	0.53	–	0.41[c]

[a] Samples have the same numbering as in Table I.
[b] Amount of protein recovered after application of dissociating buffer.
[c] Protein eluted with 0.2 *M* acetate buffer (pH 3.6).

As mentioned above, the law of mass action requires the value of $[\bar{Y}]$, and therefore the elution volume V, to depend on the concentations of soluble and immobilized protein and on the association constants in solution and on the solid phase. The dependence of V and $[\bar{Y}]/R-X_t$ on the steady-state concentration of soluble protein was measured for sample 4 and is depicted in Figs. 2 and 3, respectively. Fig. 2 shows the significant increase in elution volume when the concentration of soluble protein is low (<2 mg/ml), a typical feature of subunit exchange chromatography. Fig. 3 shows that the data are consistent with a dimerization constant of 250 dl/g both in solution and on the solid phase. It also shows that at high protein concentrations (above 4 mg/ml), although dimer formation is still predominant, higher polymers are formed. In line with these findings, sedimentation velocity experiments carried out with the same A and B β-lactoglobulin mixture at a protein concentration of 5 mg/ml yielded a single peak with $s_{20,w} = 2.9$S, a value which corresponds to the weight-average relative molecular mass (34 kilodalton) calculated with the dimerization constant given above using a partial specific volume $\bar{V} = 0.750$ and $f/f_0 = 1.2$.

Selective extraction of β-lactoglobulin from whey

The high capacity and affinity of immobilized A and B β-lactoglobulin for the protein in solution can be exploited for its selective extraction from whey. Whey, in the associating buffer 0.1 *M* acetate (pH 4.65), was percolated through a column of immobilized A and B β-lactoglobulin equilibrated with the same buffer in sufficient volume to ensure the establishment of a steady state (Fig. 4, top). The elution pattern shows two distinct sigmoidal profiles: the first (at V_0) corresponds to the elution of all

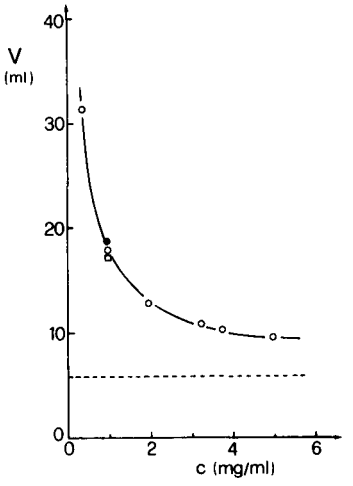

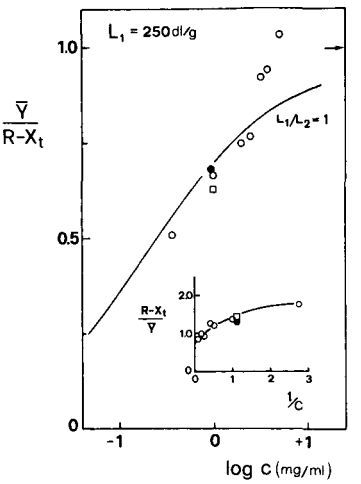

Fig. 2. Elution volume of A and B β-lactoglobulin from a column containing Sepharose-bound A and B β-lactoglobulin as a function of protein concentration in solution. ○ = Mixture of both genetic variants; ● = variant A; □ = variant B. The protein in the solid phase was 4.1 mg/ml and the bed volume 5.0 ml. The column was equilibrated with 0.1 *M* acetate buffer (pH 4.65) at 8°C. The dashed line represents the elution volume (V_0) of a non-interacting protein.

Fig. 3. Binding of A and B β-lactoglobulin in solution to a column containing Sepharose-bound A and B β-lactoglobulin as a function of the protein concentration in solution. The ordinates correspond to the binding number, *i.e.*, to the amount of soluble protein bound under steady-state conditions to the matrix, $\bar{Y}$, divided by the amount of immobilized monomer, $R - X_t$. The continuous curve was calculated according to eqns. 5 and 6 in ref. 10. Experimental conditions and symbols as in Fig. 2.

inert whey proteins and the second to the elution of β-lactoglobulin. After clearing the column with the equilibrating acetate buffer, the specifically bound protein was eluted by application of the dissociating buffer. The amount of eluted protein closely corresponds to that expected on the basis of the amount of whey applied to the column. The inset in Fig. 4 shows the quality of the separation achieved. Table II summarizes the results obtained with the samples described in Table I.

Fig. 4 (bottom) shows an experiment carried out at 20°C and pH 6.0. These conditions were tested because they allow complete deproteinization of whey to be achieved simply by applying the inert proteins that are eluted in the void volume of the subunit affinity column onto an ion-exchange column (see below). The elution profile is very similar to that obtained at pH 4.65, indicating that the subunit affinity column is efficient also at higher pH. In this experiment elution of the specifically bound β-lactoglobulin was attempted at pH 3.6, where the matrix is more stable than at pH 2.0; the recovery of the protein corresponds to about 80% of the column capacity.

Deproteinization of whey

Complete deproteinization of whey can be obtained easily by associating a DEAE-cellulose column [4,17,18] to the subunit exchange column. To this end, whey in 0.1 *M* acetate buffer (pH 6.0) was percolated through the column containing

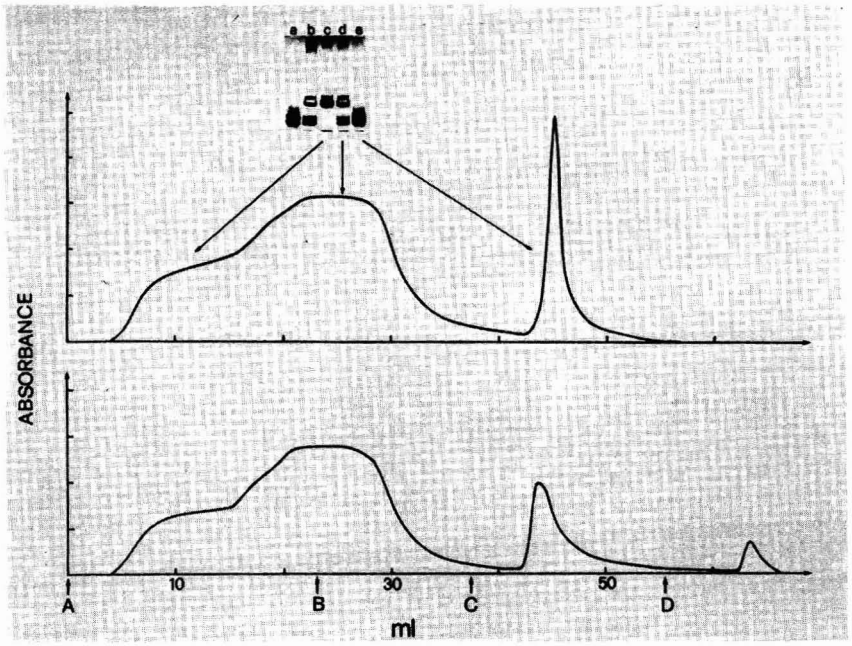

Fig. 4. Selective extraction of A and B β-lactoglobulin from whey with a column containing Sepharose-bound A and B β-lactoglobulin. The protein in the solid phase was 4.1 mg/ml and the bed volume was 5 ml. Bottom: the column was equilibrated with 0.1 *M* acetate buffer (pH 6.0) at 23°C. (A) Application of whey at 2 mg/ml in the same buffer; (B) application of equilibrating buffer; (C) application 0.2 *M* acetate dissociating buffer (pH 3.6); (D) application 0.1 *M* NaCl–HCl dissociating buffer (pH 2.0). Top: the column was equilibrated with 0.1 *M* acetate buffer (pH 4.65) at 8°C. Application of whey at 2 mg/ml in the same buffer, application of equilibrating buffer, application of 0.1 *M* NaCl–HCl dissociating buffer (pH 2.0) as indicated for the bottom part by A, B and C, respectively. The inset shows the polyacrylamide gel electrophoresis patterns [16] of (a) commercial A and B β-lactoglobulin, (b) the whey solution applied and (c–e) the fractions indicated on the elution profile.

immobilized β-lactoglobulin and equilibrated in the same buffer. The inert proteins that elute in the void volume were diluted with an equal volume of distilled water and applied to a DE-52 column equilibrated with the same buffer, *i.e.*, 0.05 *M* sodium acetate (pH 6.0). All the whey proteins bind to the column and can be eluted either all at the same time with 0.1 *M* acetate buffer (pH 4.65) containing 0.2 *M* NaCl, or in a differential way by applying an ionic strength gradient [4,17,18]. The gel electrophoretic patterns in Fig. 5 show the different fractions isolated in the various stages of the procedure. All the proteins obtained can be lyophilized and maintain their functional and physico-chemical properties, in particular their solubility, intact after rehydration.

CONCLUSIONS

The proposed use of a subunit affinity column containing immobilized A and B β-lactoglobulin offers the possibility of extracting both variants selectively from whey, thus permitting the use of the remaining whey proteins for the preparation of

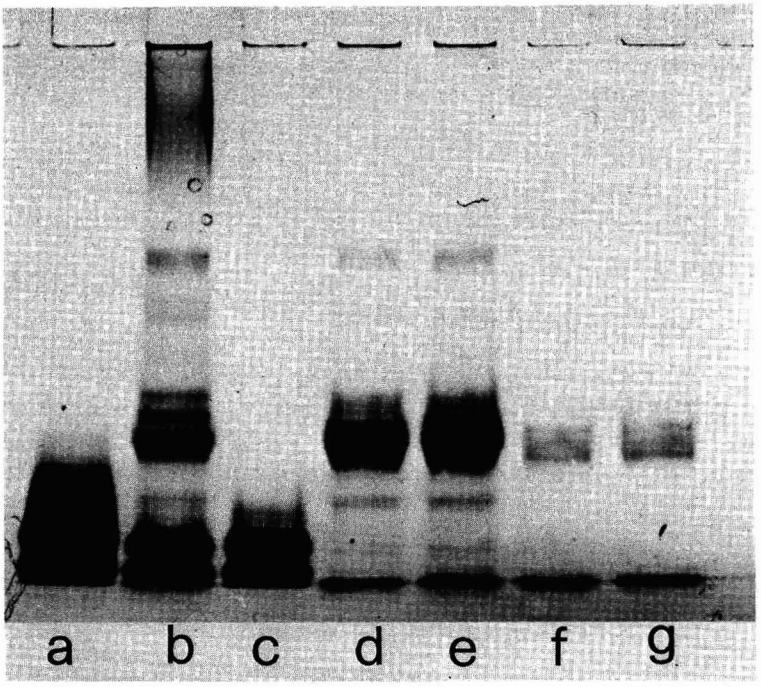

Fig. 5. Polyacrylamide gel electrophoresis patterns of whey proteins purified by the combined use of subunit-exchange and ion-exchange chromatography. (a) Commercial A and B β-lactoglobulin; (b) whey; (c) A and B β-lactoglobulin purified by subunit-exchange chromatography; (d–g) protein fractions eluted from a DEAE-cellulose column as described in the text.

special diet food, *e.g.*, hypoallergenic infant milk formulas. The combined use of the bioaffinity column with a DEAE column allows the complete deproteinization of whey and the recovery of the remaining whey protein in a concentrated form. A further advantage of the proposed method is that all the proteins can be lyophilized and are fully soluble and functional after rehydration.

Immobilized β-lactoglobulin can also be used to extract the protein directly from milk [19].

ACKNOWLEDGEMENTS

This work was supported in part by the CNR Target Project on Biotechnology and Bioinstrumentation.

REFERENCES

1 K. R. Marshall, in K. K. Fox (Editor), *Developments of Dairy Chemistry*, Applied Science Publ., Barking, 1982, p. 339.
2 L. M. J. Heppel, A. J. Cant and P. J. Kilshaw, *Br. J. Nutr.*, 29 (1984) 51.
3 K. A. Piez, E. W. Davie, T. E. Folk and J. A. Gladner, *J. Biol. Chem.*, 236 (1861) 2912.

4 H. A. McKenzie, in H. A. McKenzie (Editor), *Milk Protein Chemistry and Molecular Biology*, Vol. II, Academic Press, New York, 1971, p. 257.
5 R. Townend, L. Weinberger and S. N. Timasheff, *J. Am. Chem. Soc.*, 82 (1960) 3175.
6 S. N. Timasheff and R. Townend, *J. Am. Chem. Soc.*, 83 (1961) 470.
7 H. A. McKenzie and W. H. Sawyer, *Nature (London)*, 214 (1967) 1101.
8 H. E. Swaisgood, in P. F. Fox (Editor), *Developments of Dairy Chemistry*, Applied Science Publ., Barking, 1982, p. 1.
9 T. F. Kumosinski and S. N. Timasheff, *J. Am. Chem. Soc.*, 88 (1966) 5635.
10 E. Antonini, M. R. Rossi Fanelli and E. Chiancone, in H. Sund and G. Blauer (Editors), *Protein–Ligand Interactions*, Walter de Gruyter, Berlin, 1975, p. 45.
11 E. Chiancone, M. Gattoni and E. Antonini, in I. M. Chaiken, M. Wilchek and I. Parikh (Editors), *Affinity Chromatography and Biological Recognition*, Academic Press, Orlando, FL, 1983, p. 103.
12 E. Chiancone and M. Gattoni, *Methods Enzymol.*, 135 (1987) 487.
13 G. Carrea, P. Pasta and E. Antonini, *Biotechnol. Bioeng.*, 27 (1985) 704.
14 S. Shuder, J. B. Wittenberg, B. Haseltine and B. A. Wittenberg, *Anal. Biochem.*, 92 (1979) 473.
15 J. Bode and K. G. Wagner, *Biochim. Biophys. Res. Commun.*, 62 (1975) 868.
16 B. J. Davis, *Ann. N.Y. Acad. Sci.*, 121 (1964) 404.
17 M. L. Groves, *Biochim. Biophys. Acta*, 100 (1965) 154.
18 F. Cervone, J. D. Brito, G. Di Prisco, F. Garofano, L. Norona, S. Traniello and R. Zito, *Biochim. Biophys. Acta*, 295 (1973) 555.
19 E. Chiancone and M. Gattoni, *Ital. Pat.*, No. 47785 A/87; *Eur. Pat.*, No. 88830115.7 (1990); *U.S. Pat. Appl.*, No. 07/173.384 (under consideration).

Journal of Chromatography, 539 (1991) 465–473
Elsevier Science Publishers B.V., Amsterdam

CHROM. 22 881

Purification and characterization of recombinant tropomyosins

CONCHITA FERRAZ, JOANNES SRI WIDADA and JEAN-PIERRE LIAUTARD*
CRBM du CNRS, INSERM U-249, Route de Mende, B.P. 5051, 34033 Montpellier Cedex (France)

ABSTRACT

The cloning of a cDNA coding for the skeletal human β-tropomyosin in the bacterial expression vector pKK233-2 is reported. Deletion mutants were also constructed. pCF-T1088 was obtained by elimination of exon 9 and pCF-T1089 was built by deleting 2/3 of the first exon. The recombinant tropomyosins were synthesized in *E. coli* after induction by IPTG. The mutant proteins were characterized by western blot using antibodies raised against native tropomyosin. The amount of the human protein synthesized in *E. coli* varies with each mutant, suggesting the involvement of the structure of the protein or of the mRNA on the synthesis or the stability of the recombinant protein. After precipitation of most of the bacterial proteins at 100°C, purification was achieved by high-performance liquid chromatography (HPLC) using TSK-DEAE, hydroxyapatite and reversed-phase columns. The chromatographic behaviour of the mutants were compared. Characterization of the mutated tropomyosins was achieved by tryptic digestion and analysis of the peptide composition by reversed-phase HPLC. A computer program for predicting the retention times of the peptides generated was written. It is shown that it is possible to identify the mutations solely by comparing the chromatogram of the tryptic digest with the profile obtained by computer simulation.

INTRODUCTION

Tropomyosin is a major muscular protein involved in the regulation of muscle contraction by Ca^{2+} [1]. The mechanisms of this regulation are still a matter of debate [1]. Muscle tropomyosin is a two-stranded elongated molecule, having virtually 100% α-helix conformation. It winds along the long-pitch grooves of the F-actin helix. This rod-like fibrillar molecule is considered to be a good model to investigate the nature of protein stability and particularly to understand the respective roles of hydrogen bonds and inter-helix interactions in the formation of the tertiary structure of proteins [2].

Tropomyosin genes from different species and different tissues have already been cloned (for reviews see Colote *et al.* [3] and Sri Widada *et al.* [4]). Muscle tropomyosin gene is constituted of nine exons, three of which arise from alternative splicing. Using an evolutionary approach, we have shown that the alternatively spliced exons are conserved, suggesting an important role in the function of these parts of the molecule. Tropomyosin presents numerous elementary functions such as troponin binding, head-to-tail interactions or actin binding. None of them is defined at the molecular level [1].

0021-9673/91/$03.50

To understand the function of tropomyosin better, it is therefore necessary to dissect the mechanisms that it involves at the submolecular level. Protein engineering permits such an approach. We have cloned and expressed in *E. coli* the human skeletal muscle β-tropomyosin. Two deletion mutants were performed, expressed in *E. coli* and purified using high-performance liquid chromatography (HPLC). In this paper we describe the purification behaviours of these proteins and compare their chromatographic patterns. Tryptic digests were analysed by reversed-phase HPLC. We show that a computer simulation can be used to identify the resulting peptides and thus rapidly characterize the mutants.

EXPERIMENTAL

Materials

HPLC analyses were performed with a Gilson (Paris, France) apparatus. Absorbances at 280 and 220 nm were monitored with a Holochrom spectrophotometer (Gilson).

A DEAE-TSK column (150 × 21.5 mm I.D.) and a TSK column (60 × 21.5 cm I.D.) for gel permeation were obtained from LKB (Uppsala, Sweden). A hydroxyapatite column (Hypatite-C) (100 × 12.5 mm I.D.) was purchased from SFCC (Paris, France). The column containing RP-18 (5-μm spherical particles) (130 × 4.0 mm I.D.) was obtained from Brownlee Labs. (Santa Clara, CA, U.S.A.).

Open chromatography was carried out on an HA-Ultrogel column from IBF (France). Acetonitrile (Chromasol Gradient) was purchased from SDS (Peypin, France).

Recombinant DNA constructions

Construction of the expression vector containing β-skeletal tropomyosin has been described previously [5]. Briefly, the human tropomyosin clone exhibiting an NcoI site at its start codon was inserted into the NcoI site of the PKK 233-2, thus under the control of isopropyl thiogalactoside (IPTG)-inducible trc promoter. This construction produces a complete unfusioned tropomyosin TM1 [5]. A deletion mutant lacking the last 31 amino acids of the C-terminus (TM [C31]) was obtained by taking advantage of a Cla I restriction site at this position. Another deletion mutant of 21 amino acids of the N-terminus (TM [N21]) was obtained after cutting with FnuDII restriction enzyme and addition of initiation codon. TM1, TM[C31] and TM[N21] were produced respectively in HB101, HB101 and JM109 bacteria strains.

Production and extraction of tropomyosin mutants

E. coli containing the different vectors were grown in 20 l of culture medium in a fermenter under controlled conditions. Recombinant protein synthesis was induced by IPTG. Bacteria were centrifuged and then disrupted in a French press, and the supernatant was heated in a boiling water-bath for 5 min. The mixture was centrifuged for 15 min at 10 000 *g*. Tropomyosin present in the supernatant was concentrated by ammonium sulphate fractionation. After precipitation of the nucleic acids at 35% saturation (209 g/l) of ammonium sulphate, β-tropomyosin was precipitated at 60% saturation (addition of a further 164 g/l). The pellet was resuspended and dialysed against buffer D [20 m*M* Tris–HCl (pH 7.5)–0.5 m*M* dithiothreitol (DTT)].

HPLC on DEAE-TSK column

A 250-mg sample of protein in buffer D was applied to the DEAE-TSK column. Elution was performed by increasing the salt concentration to 0.6 *M* ammonium acetate in buffer D with an increase of 10 m*M*/min using a flow-rate of 4.0 ml/min. Absorbance was measured at 220 and 280 nm.

Chromatography on hydroxyapatite column

We employed either open-column chromatography using HA-Ultrogel or HPLC using Hypatite-C. Proteins eluted from the DEAE-TSK column were adjusted to 1 *M* NaCl and 1 m*M* phosphate (pH 7.0)–0.5 m*M* DTT. Proteins were adsorbed on HA-Ultrogel (100 ml) equilibrated with the same buffer. Elution was performed at 100 ml/h with a 400-ml linear gradient from 1 to 300 m*M* phosphate (pH 7) containing 1 *M* NaCl and 0.5 m*M* DTT. Alternatively, the mixture was deposited on a 100 × 12.5 mm I.D. HPLC column containing hydroxyapatite. Elution was performed at 1.0 ml/min using a gradient of the following solutions: solution A, 10 m*M* NaH_2PO_4 (pH 6.9)–0.2 *M* sodium acetate–0.5 m*M* DTT; and solution B, 300 m*M* NaH_2PO_4–0.2 *M* sodium acetate–0.5 m*M* DTT.

Simulation of tryptic digestion pattern and chromatogram

We have written a program that simulates the tryptic digestion pattern of a protein. The retention of peptides on the reversed-phase column was calculated using the algorithm of Meek [6] as modified by Guo *et al.* [7] It nevertheless appears that the correlation between the calculated retention times and the experimental results is good when the peptides are composed of more than six amino acids.

Digestion of 0.2 mg of protein in 0.1 *M* Tris–HCl (pH 8.1) was performed with 10 μg of trypsin (TPCK-treated) (Sigma) for 2 h at 37°C. Reversed-phase chromatography was performed on a C_{18} column using an acetonitrile gradient (1% /min) containing 0.1% trifluoroacetic acid.

Other methods

Immunoblot analysis. Sodium dodecyl sulphate polyacrylamide gel electrophoresis (SDS-PAGE) was performed essentially as described by Laemmli [8], using 12.5% acrylamide. Proteins were transferred from SDS polyacrylamide slab gels to nitrocellulose (Schleicher & Schüll) using a Bio-Rad transfer apparatus in the presence of 0.02% SDS. The nitrocellulose sheets were blocked with 8% dry milk in phosphate-buffered saline (PBS). The nitrocellulose was incubated with anti-tropomyosin antibodies raised against chicken gizzard tropomyosin diluted at 1:100 in PBS supplemented with 5% bovine serum albumin (BSA). The antibody was revealed using a protein A–peroxidase system containing 0.06% of chloronaphthol.

Protein sequence determination. The sequence of the NH_2 terminus was determined with 120 pmol of protein using an Applied Biosystems Model 470A gas-phase sequencer coupled with a Model 12A phenylthiohydantoin analyser.

Amino acid composition. The purified protein was hydrolysed by heating at 110°C in 5.7 *M* hydrochloric acid for 24 h. Composition was determined in a Beckman 7300 system.

RESULTS

Preparation and concentration of recombinant tropomyosins

The same purification scheme was used for the three recombinant tropomyosins, *i.e.*, TM1, TM[C31] and TM[N21]. The heat precipitation step is very interesting because a large amount of material can easily be processed. Most of the bacterial proteins were precipitated whereas the three tropomyosin mutants remained in the supernatant. We did not note any loss of recombinant protein in this step. As tropomyosin is denatured at temperatures above 50°C [9], the solubilization is due to a very rapid and efficient renaturation. The fact that the mutated proteins were resistant to heat treatment implies that the spatial structure is at least partially conserved. Analysis of the purified mutants by circular dichroism confirmed this fact (data not shown).

Although most of the bacterial proteins were removed by heat treatment, the nucleic acid still remained in the supernatant. Some of them were removed by precipitation with 30% ammonium sulphate. Tropomyosin was then precipitated by increasing the ammonium sulphate concentration to 60%. In this step the recovery was generally greater than 90%.

Chromatography on DEAE-TSK

Proteins concentrated by ammonium sulphate precipitation were dialysed against buffer D and quantified using the Bradford reaction. A 250-mg sample of proteins was chromatographed on the DEAE-TSK column as described under Experimental. The chromatogram of each mutant is presented in Fig. 1.

The chromatographic profile is very reproducible for a given preparation. The yield in this step was *ca.* 60%. Nevertheless, the efficiency of the heat precipitation of bacterial proteins varied with the amount of the extract. A better yield was achieved with a smaller amount. The yield of the engineered proteins also depended on the bacterial strain used. Finally, the amount produced varied from one mutant to another.

Fig. 1 shows that mutant TM[C31] was eluted earlier than the other two. This behaviour is in agreement with the number of charges contained within the molecules. TM[C31] possesses only 21 negative charges whereas TM1 and TM[N21] have 26 and 28 negative charges, respectively. Although TM[N21] eluted slightly (but reproducibly) earlier than TM1, this difference is not very important, probably owing to the high number of charges (53 positive and 81 negative charges for TM1 and 43 positive and 69 negative charges for TM[N21]). However, this result also implies that the charges are mainly located at the surface of the molecule. This, in turn, is in good agreement with the spatial model proposed by Phillips *et al.* [10].

Chromatography on hydroxyapatite

Tropomyosin is known to bind Ca^{2+}. We therefore used hydroxyapatite for further purification. Fig. 2 shows the results obtained with the three mutants. The resolution of the column is not as good as with DEAE-TSK. However, because tropomyosin eluted at the end of the gradient (300 m*M* phosphate), it is generally electrophoretically pure after this step. The fact that the three mutants eluted at the same concentration of phosphate strongly suggests that the calcium binding site on the tropomyosin is situated in the middle of the molecule and is not removed from the mutants.

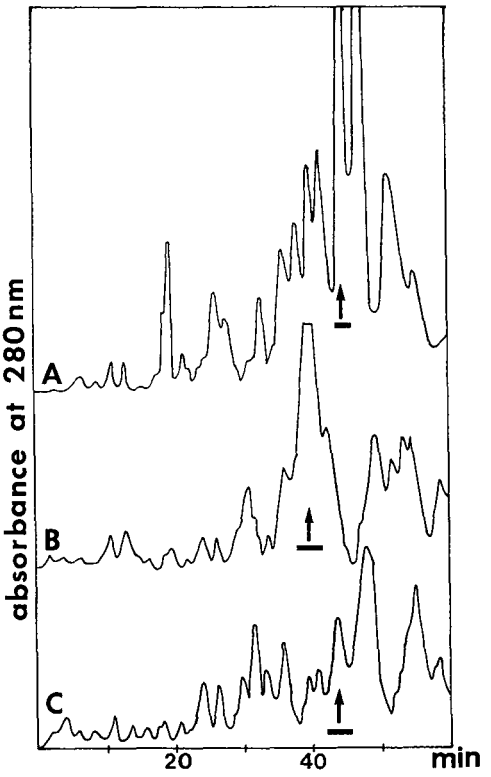

Fig. 1. Chromatographic profile on TSK-DEAE obtained for the three mutants of tropomyosin. Proteins were extracted from *E. coli* containing expression plasmids, heat treated and fractionated by ammonium sulphate precipitation as described. Protein mixtures (250 mg) containing (A) complete tropomyosin (TM1), (B) deletion mutants TM[C31] or (C) TM[N21] (see text) were chromatographed on a TSK-DEAE column as described. Eluted fractions were analysed by SDS-PAGE. The localization of the tropomyosin mutants is shown by bars and the maxima are indicated with arrows.

A further purification was sometimes needed. This was done by gel permeation on a TSK-G300 column. However, the recovery was very low and we carried out this procedure no often than was strictly necessary. We also tried reversed-phase chromatography but the resolution for large molecules was very poor. We performed instead a p*I* precipitation at pH 4.1 to remove the remaining contaminants.

Tryptic digestion analysis

One major problem in site-directed mutagenesis lies in the way one has to control whether the protein produced in *E. coli* is the one desired. As no selective pressure is exerted on this kind of protein, the possibility of mutation or deletion is very high. This makes the control of its sequence essential. To perform this task we used the tryptic digest analysis by taking advantage of the possibility of predicting the elution time of peptides using the algorithm of Meek [6] and the coefficient of Guo *et al.* [7].

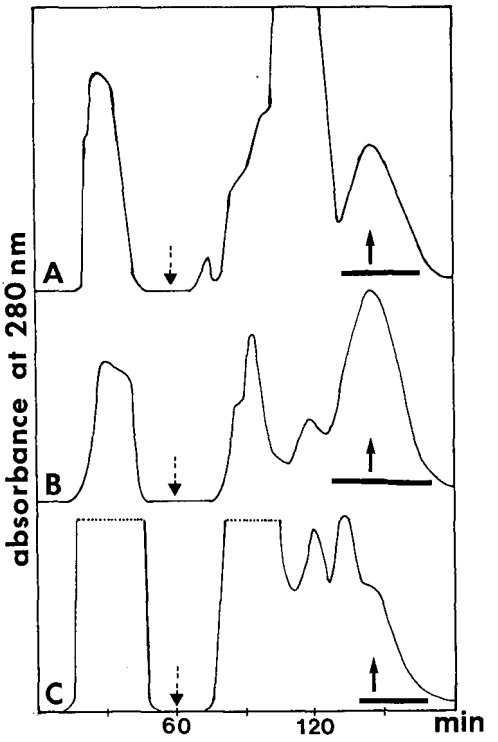

Fig. 2. Hydroxyapatite purification. Fractions from the DEAE-TSK chromatography containing tropomyosin were pooled and purified on hydroxyapatite as described. The eluted fractions were then analysed by SDS-PAGE. The position of the tropomyosin mutants is shown by bars (the broken arows indicate the start of gradient. Chromatograms of (A) TM1; (B) TM[C31] and (C) TM[N21].

Fig. 3 shows the analysis of tryptic digest by reversed-phase HPLC and compares the pattern obtained with that predicted by computer simulation. The presence of tyrosine or phenylalanine in a peptide was monitored by the absorbance at 280 nm and is indicated by black spots in the computer simulation (Fig. 3, A1, B1, C1). First, agreement between the experimental result and the simulation was good for long peptides. This allowed the identification of the peptides that were lost in the TM[C31] mutant. They are missing in the chromatogram of TM[C31] shown in Fig. 3B (these peptides are indicated by black triangles in Fig. 3A, on the chromatogram of TM1). This result clearly demonstrates that the TM[C31] mutant is correct. The case of the TM[N21] mutant was more difficult to resolve by this method. Peptides arising from the deleted region are very small because of the high content of lysine and cannot be identified accurately. Only a new peptide arising from the NH_2-terminus is characteristic of this mutant, and is shown by the black diamond in Fig. 3C.

Further biochemical characterization

Further analyses were carried out to confirm the reality of each mutation. First, the purity and the antigenicity of the protein were checked by western blot analysis.

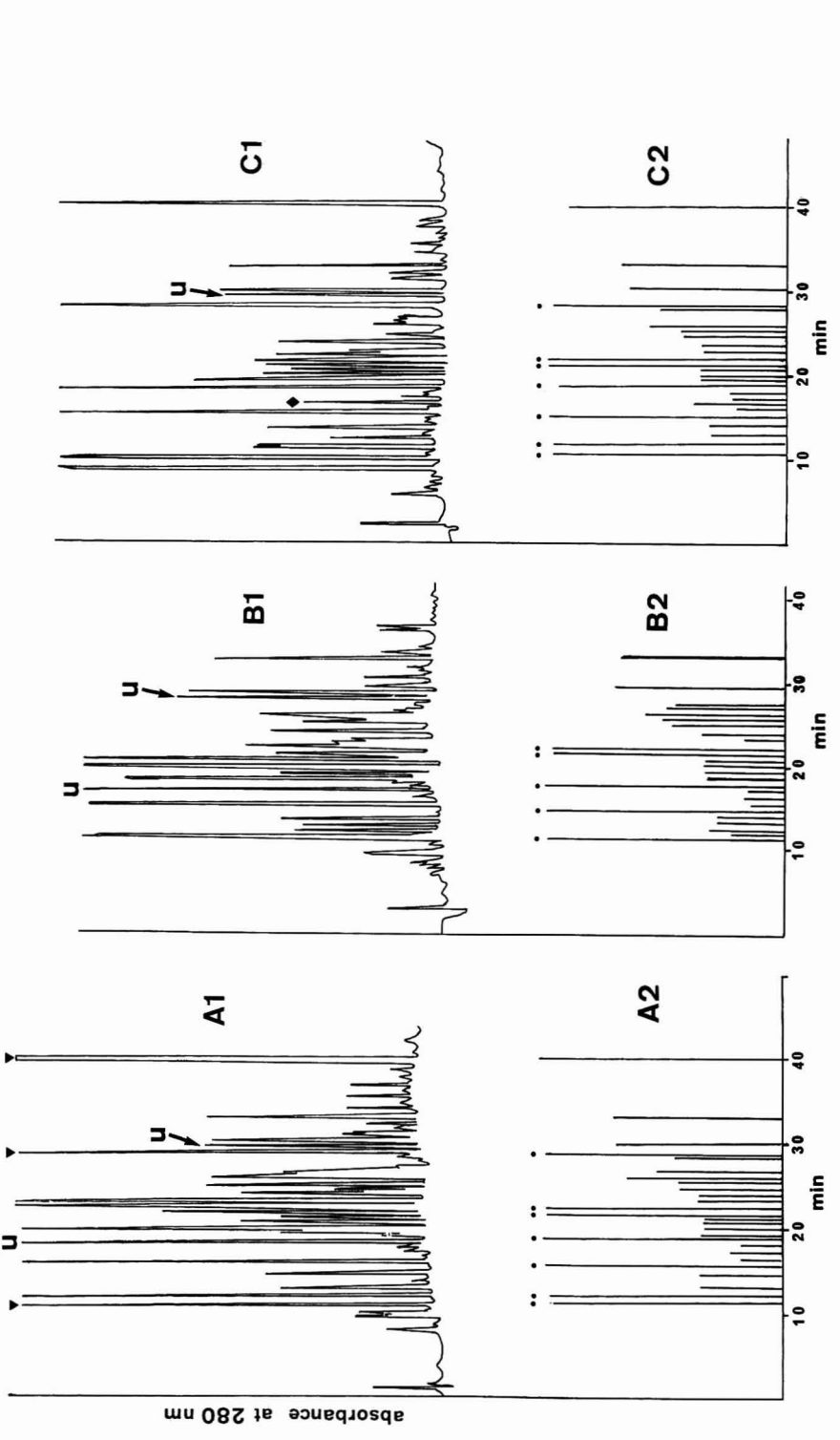

Fig. 3. Comparison of chromatographic behaviours and computer simulation of tryptic digests. After complete purification, as controlled by SDS-PAGE, the tropomyosin mutants were digested by trypsin and the tryptic digests were then chromatographed, as described. The elution profiles (A1, B1, C1 for TM1, TM[C31], TM[N21], respectively) are given in parallel with the results of computer simulation (A2, B2, C2). Peptides not found in TM[C31] deletion mutant are indicated by black triangles on the chromatogram of TM1 (A1) and a new peptide arising from TM[N21] is indicated by a black diamond (C1). On the simulation scheme, the peptides containing a tyrosine or a phenylalanine are indicated by black circles. U represents unidentified major peptides.

The results are shown in Fig. 4. Amino acid analysis was also performed, although the results were difficult to interpret because the sensitivity of the method is very low. However, the amino acid composition coincided with the theoretical results (result not shown). We also sequenced the NH_2-terminus. This is particularly important for the TM[N21] mutant. The results in Table I clearly confirm that the purified protein actually exhibits the desired mutation. The extra alanine at the N-terminus of TM[N21] is due to the cloning procedure. Further, it must be pointed out that methionine was removed only from the TM[N21] mutant. This is due to the size of the amino acid immediately adjacent to the methionine initiator. Methionine is removed by the bacteria if this amino acid is small, as with the TM[21] mutant.

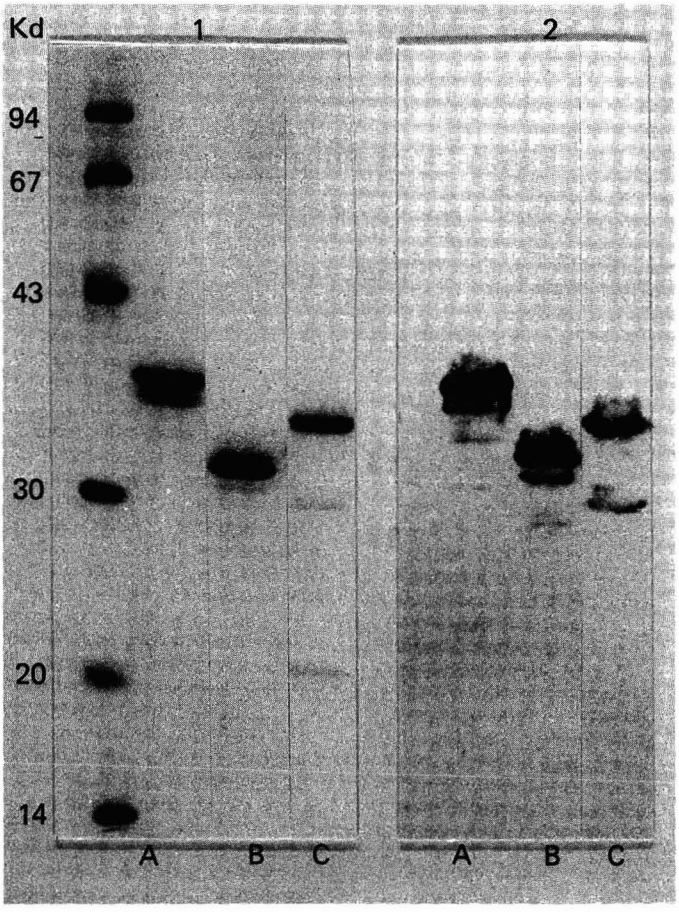

Fig. 4. Purity and antigenicity of proteins. The purified tropomyosin mutants were analysed by SDS-PAGE (1) and controlled by western blotting (2). TM1 is shown as track A, TM[C31] as track B and TM[N21] as track C.

TABLE I

SEQUENCE OF THE NH_2-TERMINUS OF THE PROTEINS

The NH_2 sequences were determined as described under Experimental. The sequence of TM1 and TM[C31] is identical with the N-terminus sequence of genuine tropomyosin. In contrast, as expected, TM[N21] exhibits the sequence of the tropomyosin devoid of the first N-terminal 20 amino acids. Single-letter code used for amino acids; Ac = Acetyl.

Protein	Sequence
Genuine β-tropomyosin	Ac- MDAIKKKMQMLKLDKENAID RAEQAEADKKQAE-
TM1	MDAIKKKMQMLKLDKE-
TM[C31]	MDAIKKKMQMLKLDKE-
TM[N21]	AAEQAEADKKQAE-

CONCLUSION

We have shown that recombinant tropomyosins can be rapidly purified using HPLC. Although the purification was performed at room temperature, very little degradation was observed, probably owing to the very rapid separation. The spatial structure of tropomyosin was conserved. This is worth noting because mutant proteins are often less stable than native proteins. The mutant proteins moreover retained their activity in the regulation of muscle contraction (to be published elsewhere). We have also shown that the use of simulation of tryptic digestion analysis is a powerful tool for rapidly controlling the preparation of proteins. One drawback of this method is that the identification of small peptides is very difficult.

ACKNOWLEDGEMENTS

We are indebted to J. Derancourt for performing the sequencing of the mutants. This work was supported by the Association Française contre les Myopathies and the Association pour la Recherche contre le Cancer (ARC).

REFERENCES

1 P. C. Leavis and J. Gergely, *CRC Crit. Rev. Biochem.*, 16 (1984) 235.
2 S. Pothekin and P. L. Privalov, *J. Mol. Biol.*, 159 (1982) 519.
3 S. Colote, J. Sri Widada, C. Ferraz, F. Bonhomme, J. Marti and J. P. Liautard, *J. Mol. Evol.*, 27 (1988) 228.
4 J. Sri Widada, C. Ferraz, S. Colote, J. P. Liautard and J. Marti, in B. A. F. Rousset (Editor), *Cellular and Molecular Biology of Muscle Development*, Alan R. Liss, New York, 1989, pp. 503–512.
5 C. Ferraz, J. Sri Widada, J. Derancourt and J. P. Liautard, *Biochimie*, 71 (1989) 307.
6 J. Meek, *Proc. Natl. Acad Sci. U.S.A.*, 77 (1980) 1632.
7 D. Guo, C. Mant, A. Taneja, R. Parker and R. J. Hodges, *J. Chromatogr.*, 359 (1986) 499.
8 U. K. Laemli, *Nature (London)*, 227 (1970) 680.
9 D. Betteridge and S. S. Lehrer, *J. Mol. Biol.*, 167 (1983) 481.
10 G. N. Phillips, J. P. Fillers and C. Cohen, *J. Mol. Biol.*, 192 (1986) 11.

Journal of Chromatography, 539 (1991) 475–484
Elsevier Science Publishers B.V., Amsterdam

CHROM. 22 882

Isolation and purification of cat albumin from cat serum by copper ion affinity chromatography: further analysis of its primary structure

J. P. DANDEU* and J. RABILLON
Unité d'Immuno-Allergie, Institut Pasteur, 28 Rue du Dr. Roux, 75015 Paris (France)
J. L. GUILLAUME and L. CAMOIN
Laboratoire d'Immuno-pharmacologie Moleculaire, Institut Cochin de Genetique Moleculaire, 22 rue Méchin, 75014 Paris (France)
and
M. LUX and B. DAVID
Unité d'Immuno-Allergie, Institut Pasteur, 28 Rue du Dr. Roux, 75015 Paris (France)

ABSTRACT

Proteins, regardless of their origin, have to be highly purified, particularly from the immunochemical point of view, if they are to be used to study their allergenicity. It is shown that cat albumin, a highly potent allergen for cat-sensitive humans, can be isolated and purified from cat serum using immobilized metal ion affinity chromatography (copper ions) instead of a salting-out process or precipitation with alcohol, techniques generally used for the preparation of serum proteins. During the process described, immunoglobulins are concomitantly isolated in a relatively pure form. Cat albumin amino acid composition and sequence were analysed after an ultimate purification by ion-exchange chromatography. The highest homology (>80%) was found with the rat serum albumin.

INTRODUCTION

Previous studies have shown that several allergens [1–3] may be extracted from cat pelts. One of them is the major feline allergen Fel dI [4] and the others, to which cat-sensitive patients are less frequently sensitive, are albumin [2,3,5] and immunoglobulins [5,6]. Nevertheless, cat albumin is a very potent allergen, hence a highly purified form is obviously useful. Pure allergens are needed either for diagnosis or for therapy of hypersensitivity.

A better knowledge of the allergen structures could lead to a better understanding of their allergenic potency. The purpose of this work was to prepare a highly purified cat albumin, to analyse its primary structure and to compare it with other mammalian albumins for which cross-reactions have been reported either *versus* rabbit IgG antibodies or *versus* human IgE antibodies [5,7].

The cat serum albumin (CSA) purification process described here is essentially

0021-9673/91/$03.50

based on immobilized metal ion affinity chromatography (IMAC). We chose IMAC taking in account the previous observations by other workers during human serum protein fractionation [8,9], who stated that the adsorption capacity of the metal chelates for serum proteins, particularly for albumin, decreased in the order Cu > Zn > Ni > Mn [10]. We examined a Cu^{2+} charged chelating Sepharose fast flow gel packed in a glass column, the ligand-exchange principle being involved in the elution process.

EXPERIMENTAL

Materials

Cat sera were a kind gift from Dr. Prel, a veterinary clinician.

Rabbit IgG antibodies against cat serum were purchased from Sigma (St. Louis, MO, U.S.A.).

As standard references for cat serum proteins, cat albumin (Cohn fraction V) and cat immunoglobulins were purchased from Sigma.

Immobilized metal ion affinity chromatography

IMAC was performed on a cross-linked agarose gel to which imminodiacetate was coupled, *i.e.*, chelating Sepharose fast flow from Pharmacia (Uppsala, Sweden). After being washed according to the manufacturer's suggestions, the gel was packed in an HR 10/10 column and charged until saturation with copper ions from 0.5% (w/v) copper(II) chloride solution. After thorough rinsing with water to eliminate unbound copper ions, the column was washed again with a solution containing 1 m*M* imidazole and 1 *M* sodium chloride buffered with 0.02 *M* sodium phosphate buffer (pH 7.0). Saturation with imidazole was performed by injecting 30 ml of 10 m*M* imidazole dissolved in the same salt-buffered solution.

A pre- and a post-column packed with the chelating gel without metal ions were incorporated in the system to remove any free metal ions that might interfere with the chelating process; the columns used were of the HR 5/5 type.

After loading the cat serum sample onto the column, elution was performed in three steps: first an isocratic run, then either a linear concentration gradient of imidazole followed by a plateau at 100% solution B, or stepwise elution with different solutions of increasing imidazole concentration. The compositions of the solutions were as follows: solution A, 1 m*M* imidazole in 1 *M* NaCl buffered with 0.02 *M* sodium phosphate (pH 7.0) (see above); solution B, 20, 40 or 50 m*M* imidazole in 1 *M* NaCl buffered with 0.02 *M* sodium phosphate (pH 7.0).

The whole process was controlled by a fast protein liquid chromatography system (FPLC) (Pharmacia).

Chromatofocusing

A Mono P column of the HR 5/20 type (Pharmacia) was used after being equilibrated with 0.025 *M* sodium acetate buffer (pH 5.58). The protein of interest was dissolved in the same buffer and loaded onto the column. Elution was effected with a Servalytes 2–4 solution at 40% (Serva, Heidelberg, Germany), diluted with water to 0.2% and adjusted to pH 2.05 with 1 *M* hydrochloric acid. The pH gradient was recorded using a pH monitor (Pharmacia).

Anion-exchange chromatography

A Mono Q column of the HR 10/10 type (Pharmacia) was previously equilibrated with 0.03 *M* NaCl solution, buffered with a 0.02 *M* Tris–HCl (pH 8.00) (solution).

Protein sample dissolved in solution A was loaded onto the column. Elution began with an isocratic run with solution A, followed by a linear concentration gradient of NaCl from 0.03 to 1 *M* (50% solution B). Solution B consisted of 2 *M* NaCl solution buffered with 0.02 *M* Tris–HCl (pH 8.00). The third run was a plateau at 100% B to desorb all the strongly bound material. Thereafter, the Mono Q column can be washed and equilibrated with solution A to make it ready for the next separation process.

Sodium dodecyl sulphate polyacrylamide gel electrophoresis (SDS-PAGE)

Analyses were performed with a PHAST apparatus using PHAST gels 8–25 (Pharmacia) according to the manufacturer's instructions.

Amino acid analysis

The amino acid composition was determined with a Beckman 7300 amino acid analyser after acid hydrolysis. Hydrolysis was performed in the vapour phase with 6 *M* hydrochloric acid containing 0.1% phenol for 24 h at 110°C *in vacuo* [11].

Micro-sequencing

Proteins were sequenced on a Model 470 A gas-phase protein sequencer (Applied Biosystems, Roissy, France). Phenylthiohydantoin (PTH) derivatives of amino acids were separated and identified by on-line reversed-phase high-performance liquid chromatography with a Model 120 A-PTH analyser (Applied Biosystems) added to prevent wash-out and to improve the initial yields [12].

An exhaustive search of homology cases was performed on the PSEQIP database.

Crossed immunoelectrophoresis methods

To follow the purification steps of the cat serum albumin (CSA), crossed immunoelectrophoresis (CIE) methods were used as previously described [13], using rabbit IgG raised against the whole cat serum (Sigma). Each fraction obtained by chromatographic techniques was tested by crossed line rocket immunoelectrophoresis (CLRIE), *i.e.*, the intermediate gel of a crossed line immunoelectrophoresis (CLIE) was lengthened on the right-hand part, allowing a rocket-line experiment (RLIE) to be performed, leading to an easy identification of each antigen [14].

RESULTS

Immobilized metal ion affinity chromatography

A 1-ml volume of cat serum was loaded onto a copper column, prepared as described under Experimental. For identification purposes this method was named copper chelate chromatography (CCC).

In a first series of experiments we applied, after an isocratic run of 40 min with solution A (1 m*M* imidazole), a linear concentration gradient of imidazole from 1 to 20

m*M*. Two peaks were eluted at 6 and 8 m*M*, the strongly bound material being eluted during the last run at 100% B, *i.e.*, 20 m*M* imidazole. The last peak was broad with pronounced tailing. We therefore increased the imidazole concentration up to 50 m*M* and a sharper peak without tailing was obtained. Finally, the complete process was defined as a stepwise elution at 0, 12, 16 and 100% B (Fig. 1).

Fractions of 1 ml were collected and pooled according to the recorded elution scheme, dialysed against neutral distilled water and freeze-dried.

Using cat albumin and immunoglobulins from Sigma chromatographed under the same conditions, we were able to identify peak Cu3 as probably being cat albumin and Cu4 as essentially being cat immunoglobulins.

Chromatofocusing

In order to compare the degree of purity of cat albumin from a Cohn fraction V (Sigma) and that of cat albumin prepared by IMAC (fraction Cu3), we performed a chromatofocusing as described under Experimental on the two protein batches at the same concentration, *i.e.*, 20 mg/ml, of 200 μl were loaded onto the column.

Fig. 2 shows that cat albumin obtained by copper chelate chromatography (CSA-CCC) is as pure as that obtained by the Cohn method. It should be noted that the last peaks on the chromatogram correspond to ampholytes in the pH 2 zone, which absorb in the UV region at 280 nm.

SDS-PAGE

Homogeneity of the cat albumin Cu3 was compared with that of Cohn fraction V (Sigma) by SDS-PAGE in an 8–25% gradient gel (PHAST gel). Fig. 3 shows that Cu3 is at least as pure as the Cohn fraction.

Anion-exchange chromatography

Considering the results obtained either by chromatofocusing or by SDS-PAGE, and also those obtained by immunochemical analysis, we concluded that some other unidentified proteins contaminate cat albumin preparations whatever the purification

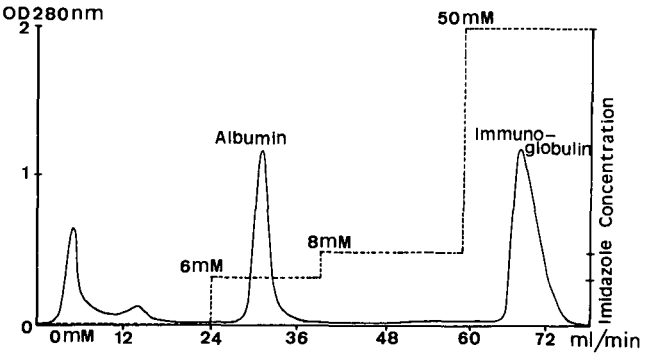

Fig. 1. Copper chelate chromatography. Column, HR 10/10 packed with chelating Sepharose fast flow (Pharmacia), charged with Cu^{2+}, washed with 1 m*M* imidazole in 1 *M* NaCl solution buffered with 0.02 *M* sodium phosphate buffer (pH 7.0), saturated with 10 m*M* imidazole in the same buffered salt solution. A 1-ml volume of cat serum, previously dialysed against 1 m*M* imidazole, was loaded onto the column. Stepwise elution was performed at a flow-rate of 1.0 ml/min.

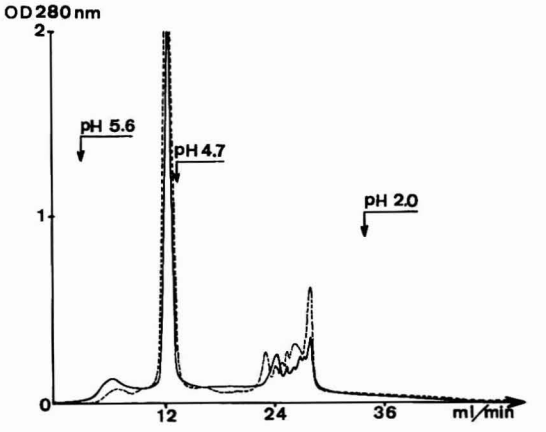

Fig. 2. Chromatofocusing with a Mono P HR 5/20 column equilibrated with 0.025 *M* sodium acetate buffer (pH 5.58). A 200-μl aliquot (4 mg of CSA) was loaded onto the column. Elution was performed at a flow-rate of 1.0 ml/min with a Servalytes 2–4 solution (Serva) at 0.2% adjusted to pH 2.05. The pH gradient was recorded using a pH monitor (Pharmacia). Solid curve, CSA-CCC; dashed curve, CSA Cohn fraction V.

process used. To eliminate these contaminants from the CSA-CCC, anion-exchange chromatography was carried out on Cu3. A 20-mg amount of lyophilized Cu3, solubilized in 1 ml of solution A (0.03 *M* NaCl), was loaded on the Mono Q column previously equilibrated with the same buffered salt solution. After a short isocratic elution during which no material was eluted, a linear concentration gradient of NaCl was applied, which gave five elution peaks (Fig. 4). Fractions from four of them, the quantitatively most important, *i.e.*, P2, P3, P4 and P5 were pooled, then dialysed against neutral water and freeze-dried.

Analyses were performed by SDS-PAGE and CLRIE, the results of which are shown in Figs. 3 and 5, respectively. P4 appears as a highly pure cat albumin preparation, while P5, found to be pure in CLRIE, contains two components, as shown by SDS-PAGE, with M_r 67 and 90 kilodalton, respectively.

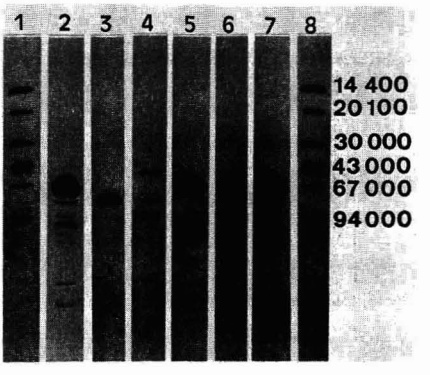

Fig. 3. SDS-PAGE using PHAST gels 8–25 on a PHAST apparatus (Pharmacia). Lanes 1 and 8, standard protein markers; lane 2, cat albumin CCC, 1.20 μg; lane 3, fraction P2, 0.40 μg; lane 4, fraction P3, 0.35 μg; lane 5, fraction P4, 0.64 μg; lane 6, fraction P5, 1.65 μg; lane 7, cat albumin (Sigma), 1.20 μg.

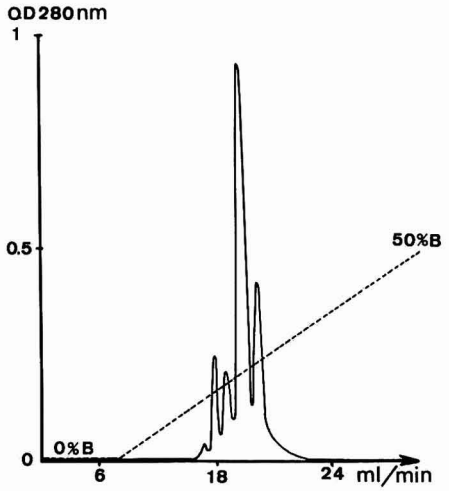

Fig. 4. Anion-exchange chromatography on Mono Q HR 10/10 column equilibrated with 0.03 *M* NaCl solution buffered with 0.02 *M* Tris–HCl (pH 8.00) (solution A). Elution was performed at a flow-rate of 1.0 ml/min with a linear concentration gradient of NaCl from 0.03 to 1 *M* (50% solution B). Solution B consisted of 2 *M* NaCl solution buffered with 0.02 *M* Tris–HCl (pH 8.00). A 1-ml volume of CSA-CCC (20 mg) was loaded onto the column.

Immunochemical analyses

The above results on the immunochemical purity of the different fractions obtained in the purification of cat albumin from cat serum were obtained using the method described under Experimental (Fig. 5). Rabbit IgG raised against whole cat serum was used in a CLIE, the LIE part was lengthened on the righ-hand part and rockets were included which allowed the proteins of interest to be identified commercially available preparations were used to identify albumin and immunoglobulins.

From an immunological point of view, albumin from fraction Cu3 seems to be less contaminated than the Cohn fraction V and P4, the most homogeneous cat albumin that we prepared, appears to be totally free from contaminants, at least under the conditions of this experiment, *i.e.*, antigen concentrations as indicated in Fig. 5 and using rabbit IgG antibodies.

Amino acid analysis

As Cu3P4 could be considered as a highly pure cat albumin, its amino acid composition was determined (Table I) and it showed differences in comparison with three other serum albumin amino acid compositions cited in the literature [15], *e.g.*, glycine is twice as concentrated and tryptophan seems to be absent.

Sequencing of the N-terminal peptide

The amino acid sequence of a 30-residue N-terminal peptide was determined and homologies were investigated (Table II).

The highest homologies were observed with RSA (83%), then with BSA (80%)

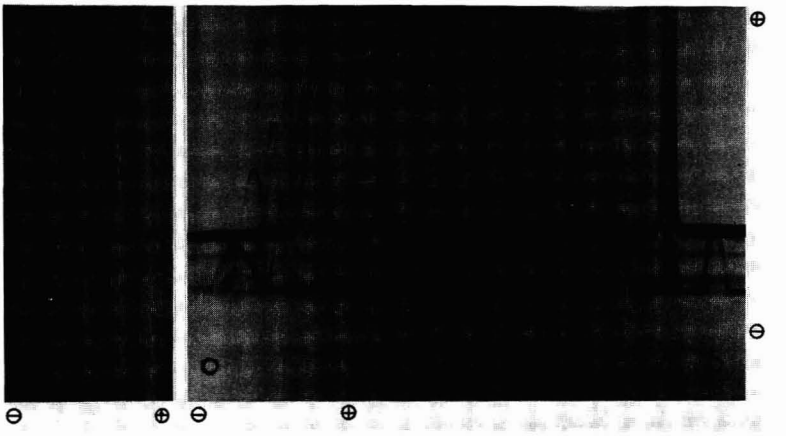

Fig. 5. CIE and CLRIE performed as described. The antibody containing agarose gel was poured in two parts; the upper part contained 1.5 μl/cm^2 of antibodies and the lower past 0.5 μl/cm^2. The amount of each "antigen" deposited was as follows. In the first dimension either in the CIE or in the CLRIE experiments, 10 μl of 1:50 diluted cat serum were submitted to zone electrophoresis. The intermediate gel, in the CLRIE, contained a dilution of the same cat serum enriched with cat IgG (Sigma). For the RLIE, the antigens were as follows: 1, Cu3 (partially purified CSA), 54 μg in 10 μl; 2, Cu3P2, 13 μg in 10 μl; 3, Cu3P3, 10 μg in 10 μl; 4, Cu3P4, 100 μg in 10 μl; 5, Cu3P5, 50 μg in 10 μl; 6, Cu4, 60 μg in 10 μl; 7, whole cat serum (protein equivalent), 58 μg in 5 μl; 8, cat immunoglobulins (Cohn fraction V, Sigma), 5 μg in 10 μl.

TABLE I

AMINO ACID COMPOSITION OF FOUR SERUM ALBUMINS

Amino acid	CSA[a]	BSA [15][b]	HSA [15][b]	RSA [15][b]
Asx	7.7	7.0	6.1	5.5
Asn	nd	2.2	2.9	3.4
Thr	4.8	5.8	4.8	5.6
Ser	6.0	4.8	4.1	4.1
Glx	15.3	10.1	10.6	9.7
Gln	nd	3.4	3.4	4.3
Pro	5.3	4.8	4.1	5.1
Gly	5.3	2.7	2.0	2.9
Ala	10.7	7.9	10.6	10.4
Cys	nd	6.0	6.0	6.0
Val	7.5	6.2	7.0	6.0
Met	1.2	0.7	1.0	1.0
Ile	1.4	2.4	1.3	2.2
Leu	10.5	10.5	10.4	9.6
Tyr	3.2	3.2	3.0	3.6
Phe	5.8	4.6	5.3	4.4
His	3.0	2.9	2.7	2.5
Lys	8.1	10.1	10.0	9.0
Arg	4.2	4.4	4.1	4.1
Try	–	0.3	0.1	0.1
Σ(mol-%)	100.0			

[a] nd = Not detected.
[b] Calculated from the amino acid sequences.

TABLE II

CAT SERUM ALBUMIN HOMOLOGIES (N-TERMINUS): N-TERMINUS COMPARISONS

COMMON RESIDUES [a]

BSA[1]	D	T	H	K	S	E	I	A	H	R	F	K	D	L	G	E	E	H	F	K	G	L	V	L	I	A	F	S	Q	Y
HSA[2,3]	D	A	H	K	S	E	V	A	H	R	F	K	D	L	G	E	E	N	F	K	A	L	V	L	I	A	F	A	Q	Y
RSA[4]	E	A	H	K	S	E	I	A	H	R	F	K	D	L	G	E	Q	H	F	K	G	L	V	L	I	A	F	S	Q	Y
CSA	E	A	H	Q	S	E	I	A	H	R	F	N	D	L	G	E	E	H	F	R	G	L	V	L	V	A	F	S	Q	Y

HOMOLOGOUS RESIDUES TO THOSE OF CSA[a]

BSA[1]	D	T	H	K	S	E	I	A	H	R	F	K	D	L	G	E	E	H	F	K	G	L	V	L	I	A	F	S	Q	Y
HSA[2,3]	D	A	H	K	S	E	V	A	H	R	F	K	D	L	G	E	E	N	F	K	A	L	V	L	I	A	F	A	Q	Y
RSA[4]	E	A	H	K	S	E	I	A	H	R	F	K	D	L	G	E	Q	H	F	K	G	L	V	L	I	A	F	S	Q	Y
CSA	E	A	H	Q	S	E	I	A	H	R	F	N	D	L	G	E	E	H	F	R	G	L	V	L	V	A	F	S	Q	Y

[a] 1 = Albusbovin, serum albumin precursor, bovine (bos taurus) [16]; 2 = Albushuman, serum albumin precursor, human (homo sapiens) [17]; 3 = Base8, preproalbumin human serum [18]; 4 = Albusrat, serum albumin precursor, rat (rattus norvegicus) [19].

and HSA (70%). For the RSA, three lysine residues are changed into glutamine, asparagine and arginine in positions 4, 12 and 20, respectively. The isoleucine in position 25 was replaced by a valine residue and glutamine in position 17 by a glutamic acid residue. The residues at position 28 in HSA and CSA are different.

DISCUSSION

Although cat albumin was stated to be a less important allergen than the major feline allergen Fel dI [2], it remains a protein of interest for the human patients sensitive to this albumin [7].

Identifying structures of allergenic molecules responsible for IgE antibody synthesis induction, apart their specific epitopes, is a difficult task and requires the availability of allergenic molecules of the highest degree of purity.

Sometimes, cloning of an allergenic protein as Der pI, a major allergen from *Dermatophagoides pteronyssinus* mite, is possible [20]. Otherwise, a major allergen such as Fel dI, the major feline allergen, can be purified either by using monoclonal antibody immunosorbent [21] or metal chelate chromatography [14].

Some proteins, such as albumins and immunoglobulins, have been obtained in a relatively pure form by a salting-out procedure, precipitation with alcohol or gel permeation. In order to improve their purification, we tried to use IMAC, a suitable chromatographic process for the large-scale fractionation and purification of proteins. IMAC has certainly already been used for serum protein fractionation [7,22] but, to our knowledge, copper chelate chromatography with a ligand-exchange process has never been used to isolate and purify cat serum albumin. Only human albumin was purified from a Cohn fraction on immobilized nickel by Andersson *et al.* [23].

IMAC, a method for protein fractionation, was developed about 15 years ago

[10]. It was essentially based on metal and amino acid interactions first described by Gurd and Wilcox [24], *i.e.*, histidine and cysteine, which have an electron donor atom in their side-chains, form fairly stable complexes with copper and zinc ions in nearly neutral aqueous solutions. That imidazole side-chains of histidine residues play the role of a ligand for divalent metal ions such as Cu^{2+} was further studied for HSA by Peters [15], since it was previously stated by Hearon [25] that exposed imidazole and thiol groups of the proteins, more particularly albumins, were involved in the protein–metal ions interactions. Subsequently a hydrophilic gel such as Sepharose, a cross-linked agarose, activated by a chelating agent (immunodiacetate) charged with metal ions, was shown to be a selective adsorbent for cysteine- and histidine-containing proteins [10]; although a relationship between the number of transition metal ions bound and the number of imidazole side-chains has never been clearly demonstrated [26], their chromatographic behaviour could be governed by the surface number of imidazole and/or thiol groups [9]. Consequently, and as it has been shown that the adsorption capacity of the metal chelate for serum proteins decreased in the order Cu > Zn > Ni > Mn [10], we chose copper chelate chromatography for the isolation and purification of cat serum albumin.

It is known that proteins can be eluted from IDA–M^{2+} columns (M = metal) at nearly neutral pH by a competing electron donor solute such as imidazole, which forms a stable metal complex with IDA–M^{2+}. However, the copper chelate gel has to be previously saturated with imidazole before an increasing concentration gradient of imidazole can be applied to the column [27].

The results reported show that cat serum loaded on a copper ion-charged chelating Sepharose fast flow column can be fractionated into four fractions, one of them relatively strongly bound to the IDA-Cu^{2+} containing a highly pure albumin, purer than a Cohn fraction V (Sigma), as judged by chromatofocusing, SDS-PAGE and immunochemical methods. Nevertheless, as we wished to analyse further structures of this potent allergen at chemical and immunological levels, we further purified this CSA preparation by anion-exchange chromatography. The resulting CSA was shown to be suitable for amino acid analysis and sequencing, and we therefore undertook an exhaustive search for homologies. It seemed that the CSA amino acid sequence, at least for the amino-terminal peptide, displayed only some small differences and showed the highest homology first with the rat serum albumin (83%), second with the bovine serum albumin (80%) and then the human serum albumin (70%).

If the primary structure of a protein is not totally responsible for its antigenic and/or allergenic potency, it is an important part of the constitution of its epitopes. It may be assumed that proteins having a high level of homologies in their amino acid sequence, even if the three-dimensional structures of homologous proteins are generally better conserved than primary ones, could display very important cross-reactions when tested against polyclonal and monoclonal antibodies, whatever their origin, *e.g.*, rabbit or human. It was recently shown that dog albumin and CSA cross-react with human IgE antibodies from cat-sensitive sera [7]; hence it would be interesting to analyse their homologies and also to test cross-reactions between RSA and CSA against the same IgE antibodies. This is currently under study.

REFERENCES

1 J. L. Ohman, Jr., F. C. Lowell and K. J. Bloch, *J. Allergy Clin. Immunol.*, 52 (1973) 31.
2 J. L. Ohman, Jr., F. C. Lowell and K. J. Bloch, *J. Immunol.*, 113 (1974) 1668.
3 M. C. Anderson and H. Baer, *J. Immunol.*, 127 (1981) 972.
4 K. Leitermann and J. L. Ohman, Jr., *J. Allergy Clin. Immunol.*, 74 (1984) 147.
5 H. Lowenstein, P. Lind and B. Weeke, *Allergy*, 40 (1985) 430.
6 J. L. Ohman and B. Sundin, *Clin. Rev. Allergy*, 5 (1987) 37.
7 Y. Boutin, J. Hebert, E. R. Vrancker and W. Mourad, *Clin. Exp. Immunol.*, 77 (1989) 440.
8 J. Porath and B. Olin, *Biochemistry*, 22 (1983) 1621.
9 J. Porath, *J. Chromatogr.*, 443 (1988) 3.
10 J. Porath, J. Carlsson, I. Olsson and G. Belfrage, *Nature (London)*, 258 (1975) 598.
11 S. Moore and W. H. Stein, *J. Biol. Chem.*, 176 (1948) 367.
12 G. E. Tarr, J. F. Beecher, M. Bell and D. McKean, *Anal. Biochem.*, 84 (1978) 622.
13 N. H. Axelsen, J. Kroll and B. Weeke, *Scand. J. Immunol.*, 2, Suppl. 1 (1973) 47.
14 J.-P. Dandeu, J. Rabillon, M.-J. Beltrand, M. Lux and B. David, *J. Chromatogr.*, 512 (1990) 177.
15 T. Peters, Jr., *Adv. Protein Chem.*, 37 (1985) 161.
16 R. T. A. MacGillivray, D. W. Chung and E. W. Davie, *Eur. J. Biochem.*, 98 (1979) 477.
17 R. M. Lawn, J. Adelman, S. C. Bock, A. E. Franke, C. M. Houck, R. C. Najarian, P. H. Seeburg and K. L. Wion, *Nucleic Acid Res.*, 9 (1981) 6103.
18 T. D. Sargent, M. Yang and J. Bonner, *Proc. Natl. Acad. Sci. U.S.A.*, 78 (1981) 243.
19 A. Dugaiczyk, S. W. Law and O. E. Dennison, *Proc. Natl. Acad. Sci. U.S.A.*, 79 (1982) 71.
20 K. Y. Chua, G. A. Stewart, W. R. Thomas, R. J. Simpson, R. J. Dilworth, T. M. Plozza and K. J. Turner, *J. Exp. Med.*, 167 (1988) 175.
21 M. D. Chapman, R. C. Aalberse, M. J. Brown and T. A. E. Platts-Mills, *J. Immunol.*, 140 (1988) 812.
22 H. Hanson and L. Kagedal, *J. Chromatogr.*, 215 (1981) 333.
23 L. Andersson, E. Sulkowski and J. Porath, *J. Chromatogr.*, 421 (1987) 141.
24 F. R. N. Gurd and P. E. Wilcox, *Adv. Protein Chem.*, 11 (1956) 311.
25 A. J. Z. Hearon, *J. Natl. Cancer Inst.*, 9 (1948) 1.
26 U. Kragh-Hensen, *Pharmacol. Rev.*, 33 (1981) 17.
27 E. Sulkowski, *Trends Biotechnol.*, 3 (1985) 1.

Journal of Chromatography, 539 (1991) 485–492
Elsevier Science Publishers B.V., Amsterdam

CHROM. 22 883

Purification of a hybrid plasminogen activator protein

JANET DEISTUNG*, DEIRDRE M. FORDE, JAMES P. O'CONNELL, KAREN A. PROUDFOOT, DIANE EATON, FRANCIS WILLENBROCK, ROSALINE O. KINGABY, BERNADETTE HUGHES, SAROJANI ANGAL, CATH CATTERALL, SANDY CARNE and JOHN SPENCER EMTAGE

Celltech Limited, 216 Bath Road, Slough, Berks. SL1 4EN (U.K.)

ABSTRACT

Recombinant DNA technology has been employed to produce a hybrid gene in which the kringle and serine protease domains of tissue plasminogen activator are linked to the heavy-chain Fd region of a fibrin-specific antibody. The hybrid gene is co-expressed with antibody light chains. This communication describes a purification procedure for the hybrid protein, involving affinity and ion-exchange chromatography. The purified hybrid protein has been used *in vivo* and *in vitro* clot lysis experiments and has been shown to be effective at clot dissolution.

INTRODUCTION

It is well known that the presence of blood clots in blood vessels can be life threatening and can lead to acute cardiovascular diseases. A particular class of agents which could be used to treat such diseases are plasminogen activators. These agents act by converting plasminogen to plasmin, which then acts on the firbrin in blood clots, causing it to break down and be dissolved (see Fig. 1). There are three well known plasminogen activators, these being streptokinase, urokinase and tissue plasminogen activator (t-PA); only t-PA will be discussed in this communication. Recombinant t-PA has been marketed by Genentech under the name of "Activase" as a thrombolytic for clinical use. The unique property of t-PA is its ability to selectively activate plasminogen bound to fibrin which minimises systemic fibrinolysis. However, it is impossible to differentiate between fibrin in the thrombus or the heamostatic plug and hence its use may cause undesired bleeding. t-PA has a relatively short half life of approximately 6 min [1], and therefore treatment requires large and lengthy doses to maintain biological effect.

Although t-PA is being used as a thrombolytic it would be desirable to improve its half-life and its specificity or to produce a novel molecule having thrombolytic properties, but having an improved half-life and specificity as compared to t-PA. In order to achieve this end, recombinant DNA technology has been employed to produce novel plasminogen activators. Various approaches include: domain shuffling, *i.e.*, deleting domains from existing plasminogen activators or combining different

0021-9673/91/$03.50

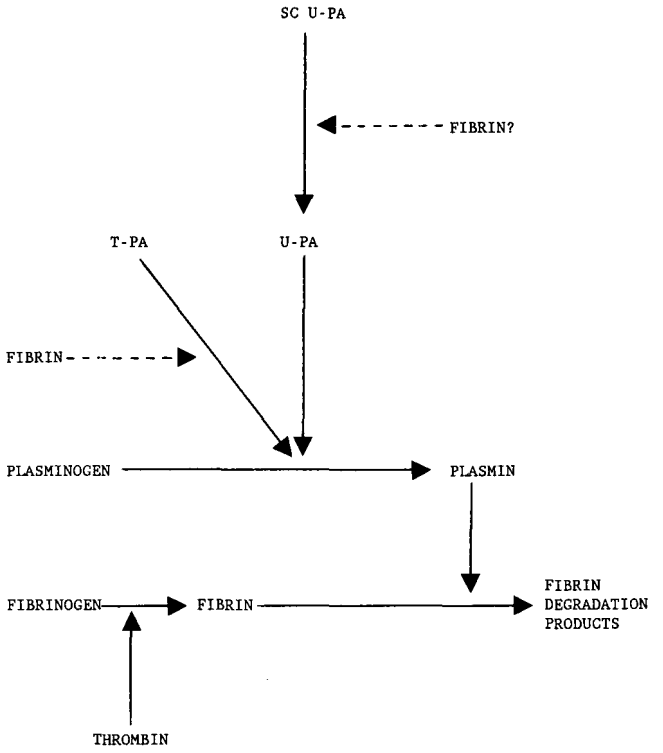

Fig. 1. A schematic representation of the fibrinolytic system. ——— = Major fibrinolytic pathways; – – – = site of cofactor action; SC U-PA = single chain urokinase; U-PA = urokinase; T-PA = tissue plasminogen activator.

domains from different activators [2]; linking a plasminogen activator to a molecule with high fibrin binding activity [3,4] or producing an antibody/plasminogen activator molecule using a monoclonal antibody having a specificity for fibrin [5]. Our approach has involved the use of recombinant DNA technology to combine the clot dissolution properties of a plasminogen activator with the fibrin specificity of an antibody in the form of a hybrid molecule (see Fig. 2). This communication is primarily concerned with the development of a purification procedure for such a hybrid protein.

MATERIALS AND METHODS

Recombinant DNA techniques and cell culture

Methods used for the production of expression vectors and to transfect cell lines were as described by Maniatis *et al.* [6] and Bebbington and Hentschel [7]. A Chinese hamster ovary cell line was established and cultured at 100-l scale using Airlift Fermenter (ALF) technology as described by Rhodes and Birch [8]. Fermenter harvests containing hybrid protein were clarified by continuous centrifugation and concentrated 10-fold by ultrafiltration.

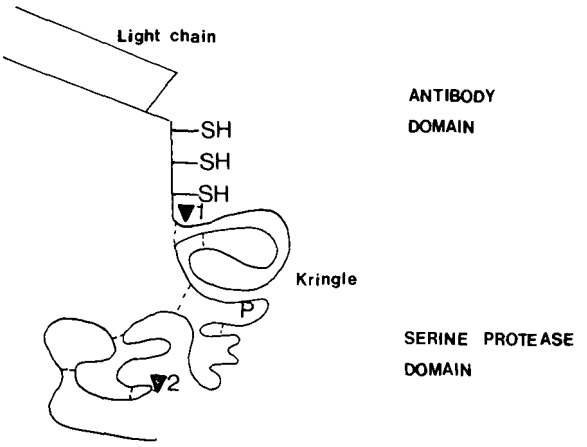

Fig. 2. Diagrammatic representation of the hybrid molecule. The molecule has two domains —the antibody domain and the serine protease domain of t-PA. The molecule has two potential glycosylation sites (▼) which are situated in the serine protease domain. These correspond to Asn 184(1) and Asn 448(2) from the t-PA molecule, the former site is only optionally glycosylated. P indicates the site of plasmin cleavage whereupon the molecule can be cleaved to the two chain form. - - - = Disulphide bridges.

Purification of the protein

Initial purification of the hybrid protein was achieved by the use of a Fibrinogen–Reacti-Gel adduct. Fibrinogen–Reacti-Gel was prepared by coupling fibrinogen (human, Kabi Vitrum) to carbonyldiimidazole (CDI) Reacti-Gel (6 ×) from Pierce according to manufacturers instructions.

Concentrated culture supernatant (2.5 l) was loaded onto the Fibrinogen–Reacti-Gel matrix (100 ml) pre-equilibrated in 50 m*M* sodium phosphate buffer pH 7.4 containing 0.9% (w/v) NaCl; 0.05% (v/v) Tween 80. After loading the matrix was washed with the same buffer containing 50 m*M* ε-aminocaproic acid. Bound hybrid protein was then eluted from the matrix using 0.3 *M* glycine hydrochloride buffer pH 2.5, containing 0.9% (w/v) NaCl and 0.05% (v/v) Tween 80, and immediately adjusted to neutrality using 1 *M* Tris.

The eluate from Fibrinogen–Reacti-Gel™ was diluted two-fold with 50 m*M* sodium phosphate buffer pH 5.5 containing 0.01% Tween 80 and the pH adjusted to 5.5 by the addition of hydrochloric acid and then loaded onto an sulfopropyl Sepharose (S-Sepharose) column (40 ml) pre-equilibrated with 50 m*M* sodium phosphate buffer (pH 5.5) containing 0.01% (v/v) Tween 80. Bound protein was eluted with 50 m*M* sodium phosphate buffer (pH 7.4) containing 0.1 *M* NaCl and 0.01% (v/v) Tween 80. Fractions containing enzymatically active hybrid protein were combined, concentrated as necessary by ultrafiltration and dialysed into final buffer.

Active site titrations

The activity of the protein was measured (using the S2288 chromogenic substrate assay, see Dodd *et al.* [12]) in the presence of an inhibitor, diisopropyl fluorophosphate (DFP), which binds irreversibly to the protein in a 1:1 ratio. A plot of activity against DFP concentration thus yields the activity of the enzyme as the intercept on the

ordinate and the concentration of the enzyme as the intercept on the abscissa. The titration was calibrated using commercially available t-PA (American Diagnostics) of known concentration. Both the standard and hybrid protein were converted to their two chain forms by incubation with plasmin before titration. This ensures that mixtures of single and two chain species are not present in the titration.

In vitro and in vivo clot lysis

In vitro clot lysis by the hybrid protein was tested using fresh human blood labelled with ^{125}I according to the method described by Zamarron *et al.* [9]. The *in vivo* clot lysis was tested using the rabbit jugular vein model using the method described by Collen *et al.* [10].

Miscellaneous

Sodium dodecyl sulphate–polyacrylamide gel electrophoresis (SDS-PAGE) was carried out essentially according to Laemmli [11]. Fibrin zymography and amidolytic activity assays using S2288 chromogenic substrate were carried out as described by Dodd *et al.* [12].

RESULTS AND DISCUSSIONS

Purification of the hybrid protein

The hybrid protein was purified as described in the Materials and Methods section and monitored throughout using the assay systems described previously. Table I shows that 32 mg of purified protein (calculated from S2288 activity assay) was obtained from the process, corresponding to a 39% recovery of activity units. The major loss in recovery for the process occurred upon chromatography using Fibrinogen–Reacti-Gel. This reflects the removal of degraded protein which contributes to the S2288 chromogenic substrate activity of culture supernatants. Analysis of eluates throughout the purification was carried out using SDS-PAGE (reducing and non-reducing) and zymography.

Analysis by zymography is shown in Fig. 3. Strong clearance of the fibrin agar gel was observed at a single spot indicating that most of the enzymic activity was associated with a single species, identified as the hybrid protein by N-terminal sequence analysis. The relative molecular mass (M_r) of this species was determined by

TABLE I

YIELD TABLE FOR THE PURIFICATION OF THE HYBRID PROTEIN

Total yield (mg) obtained from each step in the process was calculated from S2288 activity assay data using a conversion factor of 444 000 IU = 1 mg.

	Total recovery (mg)	Cumulative yield (%)
Culture supernatant (10× concentrate)	92	100 (assumed)
Fibrinogen–Reacti-Gel	39.5	43
S-Sepharose	34.5	37
Dialylsis	32	35

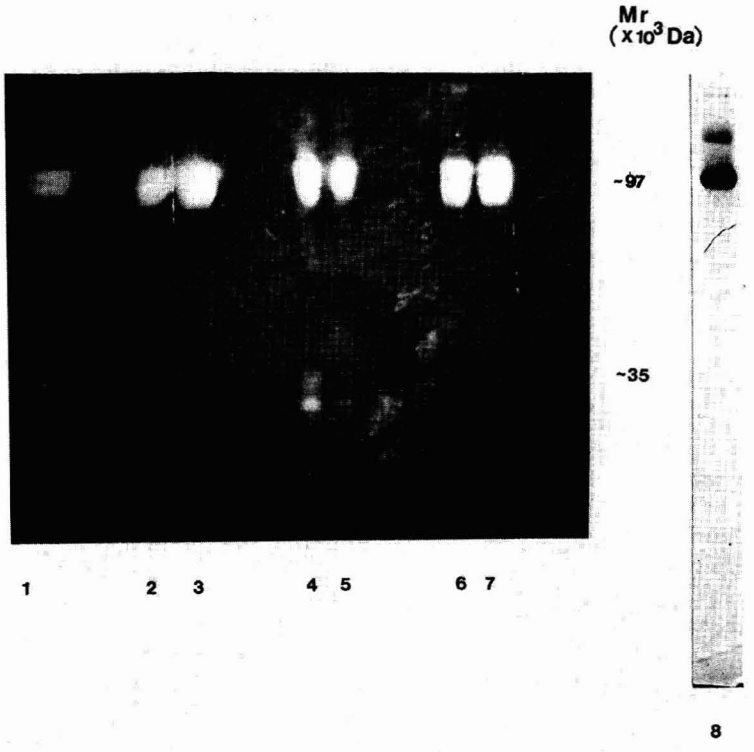

Fig. 3. Analysis of eluates from the purification of the hybrid protein using zymography and SDS-PAGE. Lanes: 1 = culture supernatant (10 × concentrate); 2,3 = eluate from Fibrinogen–Reacti-Gel; 4,5 = eluate from S-Sepharose; 6,7 = final product after dialysis; 8 = final product after analysis by Coomassie blue staining of SDS-PAGE (non-reducing).

Coomassie blue-stained SDS-PAGE (non-reduced) to be approximately 97 000 dalton (Da) and constitutes $\geqslant 90\%$ of total protein as determined by scanning densitometry. Slight clearing of the zymogram was also observed at approximately 35 000 dalton, which is consistent with some cleavage of the serine protease domain of the molecule.

Analysis of eluates across the purification using Coomassie blue staining of SDS-PAGE (reducing) is shown in Fig. 4. From this figure it can be seen that most of the contaminant protein elutes in the flow through from the Fibrinogen–Reacti-Gel step with remainder being eluted from the matrix in the subsequent wash steps. Chromatography using S-Sepharose serves as a final polishing step and remove trace amounts of albumin present after chromatography on Fibrinogen–Reacti-Gel.

Bands for the heavy and light chain moieties of the hybrid protein (M_r 67 000 and 30 000 dalton, respectively) can be observed as well as three additional bands (M_r 40 000, 38 000 and 35 000 dalton) which have been subjected to N-terminal sequence analysis to identify their origin. The 40 000- and 38 000-dalton bands correspond to the molecule without light chain and serine protease domains. The difference in molecular mass is a result of differential glycosylation of glycosylation

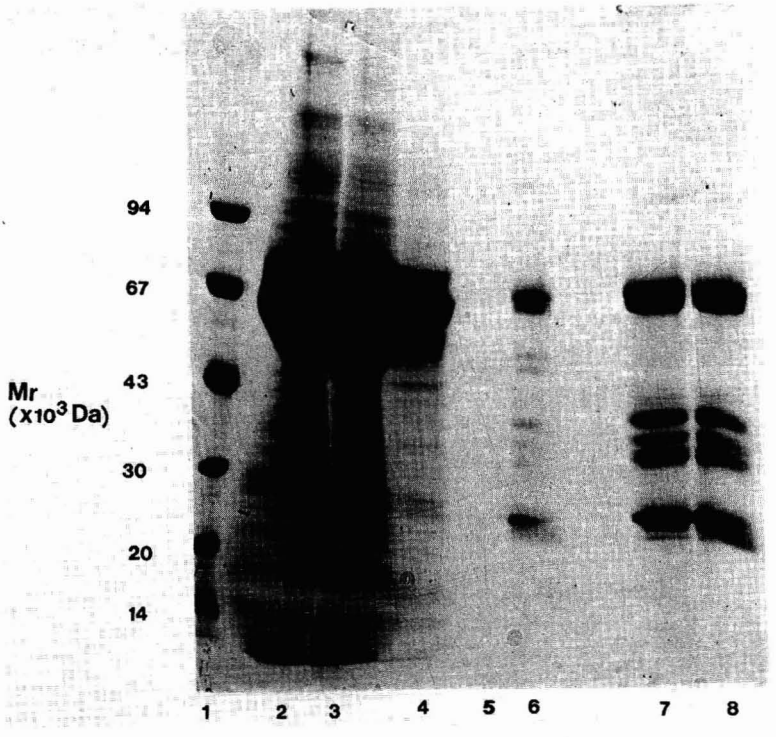

Fig. 4. Analysis of eluates from the purification of the hybrid protein using SDS-PAGE (reducing). Lanes: 1 = molecular mass markers; 2 = culture supernatant; 3 = flow through from Fibrinogen–Reacti-Gel; 4,5 = wash eluates from Fibrinogen–Reacti-Gel; 6 = eluates from Fibrinogen–Reacti-Gel; 7 = eluate from S-Sepharose; 8 = final purified hybrid protein.

site 1 (Fig. 2). The 35 000-dalton band corresponds to cleaved serine protease. The 67 000-dalton band appears as a doublet which is a result of differential glycosylation of the heavy chain moiety. This cleavage is not observed by SDS-PAGE under non-reducing conditions as internal disulphide bonds hold the molecule together (Fig. 2).

Active site titration of purified hybrid protein

Active site titrations of the purified hybrid protein were carried out as described in the Materials and Methods and compared to t-PA. The intrinsic activities of these molecules towards the low-molecular-mass substrate (S2288) were determined. The results of these measurements are shown in Table II. It can be seen from these data that the activity of the hybrid molecule towards the low-molecular-mass substrate S2288 is similar to that of t-PA and appears to be unaffected by the removal of part of the t-PA molecule and addition of the antibody variable region.

Activity of the hybrid protein in vitro

A comparison of *in vitro* clot lysis activity of t-PA and the hybrid protein was

TABLE II

ACTIVITY OF HYBRID PROTEIN TOWARDS ITS LOW-MOLECULAR-WEIGHT SUBSTRATE S2288

This compares the activity of the hybrid protein with that of t-PA towards the low-molecular-mass substrate, Ile–Pro–Arg–pNA (S2288).

Enzyme	Concentration of enzyme (n*M*)	Enzyme activity (AU/min)[a]	Specific activity (AU/min/n*M* enzyme)
t-PA	4.6	8.30	1.8
Whole hybrid	4.3	8.15	1.89

[a] AU = Activity units.

carried out. The hybrid protein and t-PA were present at 500 units/ml in plasma (as determined using the S2288 chromogenic substrate assay). Fig. 5 shows the results of this experiment. From this preliminary study it is apparent that the hybrid protein has comparable clot lysing activity *in vitro* to that of t-PA.

Activity of the hybrid protein in vivo

The results of preliminary experiments giving a local infusion of the hybrid protein via the ipsilateral ear vein (10 ml over a period of 10 min) are shown in

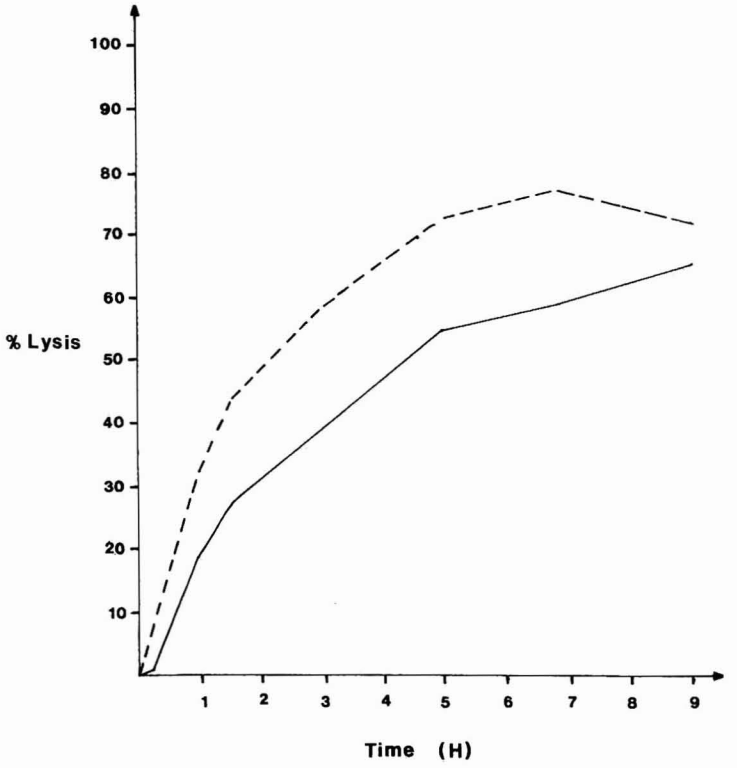

Fig. 5. Activity of the hybrid protein *in vitro*. Activity of the hybrid protein in *in vitro* clot lysis experiments and compared to that of t-PA. - - - = t-PA; ——— = hybrid protein.

TABLE III

ACTIVITY OF THE HYBRID PROTEIN *IN VIVO*

This table compares the activity of the hybrid protein and t-PA *in vivo* at two dose levels (calculated using S2288 assay). Each data point was obtained using a separate rabbit ($n = 3$).

Dose (IU/kg)	% Lysis (t-PA)	% Lysis (hybrid)
50 000	17.53 ± 5.17	20.03 ± 3.52
500 000	50.9 ± 1.85	41.7 ± 8.79

Table III. Lytic activity was compared with that of t-PA. These results indicate that the hybrid protein is thrombolytically active *in vivo* and that its activity is broadly similar to that of t-PA. However, further experiments will be required to fully evaluate the efficacy of the hybrid protein *in vivo*.

CONCLUSIONS

A purification procedure has been described for the hybrid plasminogen activator molecule from Chinese hamster ovary (CHO) culture supernatant, which includes both an affinity chromatography and an ion-exchange chromatography step. The purified material has been obtained with an overall yield of 35% with a purity $\geqslant 90\%$. The hybrid plasminogen activator molecule has been shown to be effective at clot dissolution in both *in vitro* and *in vivo* clot lysis experiments. Further experiments are necessary to fully evaluate this molecule as a potential thrombolytic agent.

ACKNOWLEDGEMENTS

We would like to thank Drs. Nieuwenhuizen and Kluft at the Gaubius Institute for their contribution to the *in vivo* clot lysis experiments. We would also like to thank Dr. E. L. V. Harris for helpful discussions and comments on the manuscript.

REFERENCES

1 M. Verstraete and D. Collen, *Blood*, 67 (1986) 1529.
2 T. J. R. Harris, *Protein Eng.*, 1 (1987) 449.
3 K. C. Robbins and Y. Tanaka, *Biochemistry*, 25 (1986) 3603.
4 K. C. Robbins and I. G. Boreisha, *Biochemistry*, 26 (1987) 4661.
5 J. M. Schnee, M. S. Runge, G. R. Matseuda, N. W. Hudson, J. G. Seidman, E. Haber and T. Quartermous, *Proc. Natl. Acad. Sci. U.S.A.*, 84 (1987) 6904.
6 T. Maniatis, E. F. Fritsch and J. Sambrook, *Molecular Cloning: A Laboratory Manual*, Cold Spring Harbour Laboratory, Cold Spring Harbour, NY, 1982.
7 C. Bebbington and C. Hentschel, in D. M. Glover (Editor), *DNA Cloning*, Vol. 3, American Society for Microbiology, Washington, DC, 1987, p. 163.
8 P. M. Rhodes and J. Birch, *Biotechnology*, 6 (1988) 518.
9 C. Zamarron, H. R. Lijnen and D. Collen, *Throm. Res.*, 35 (1984) 335.
10 D. Collen, J. M. Stassen and H. J. Verstraete, *Clin. Invest.*, 71 (1983) 368.
11 U. K. Laemmli, *Nature (London)*, 227 (1970) 680.
12 I. Dodd, R. Fears and J. H. Robinson, *Throm. Haemostas.*, 55 (1986) 94.

Journal of Chromatography, 539 (1991) 493–500
Elsevier Science Publishers B.V., Amsterdam

CHROM. 22 884

Purification of heparin cofactor II from human plasma

P. TOULON*[a], G. CHADEUF and M. AIACH
Laboratoire d'Hémostase, Hôpital Broussais, Paris (France)

ABSTRACT

Heparin cofactor II (HCII) is an inhibitor of thrombin in human plasma whose activity is enhanced by heparin and dermatan sulphate. HCII was purified to homogeneity from normal human plasma with an overall yield of 7.5%. After treatment with barium chloride, precipitation with 50% saturated ammonium sulphate and dialysis of the resuspended precipitate against 0.02 *M* Tris–HCl (pH 7.4), the sample was chromatographed on a heparin–Sepharose CL 6B affinity column, DEAE-Sepharose CL 6B ion-exchange gel and an AcA 34 gel permeation column. For the final steps, a high-performance liquid chromatographic system was used which included ion-exchange chromatography on a Mono-Q column and gel permeation using a Superose column. The purified protein was homogeneous by sodium dodecyl sulphate–polyacrylamide gel electrophoresis. The specific activity of purified HCII was 12.2 U/mg. The HCII activity was evaluated as antithrombin dermatan sulphate cofactor activity. A specific antiserum against HCII was raised in the rabbit.

INTRODUCTION

Heparin cofactor II (HCII) is a recently described plasma inhibitor of thrombin [1,2], the activity of which is potentiated by heparin and more specifically by dermatan sulphate, another glycosaminoglycan [3]. HCII displays structural and biological similarities with antithrombin III (ATIII) [4,5], the main plasma cofactor of heparin [6]. Nevertheless, whereas ATIII is active towards most of the activated clotting factors [6], HCII is a specific inhibitor of thrombin [1,2,7].

We report here the purification to homogeneity of HCII from human plasma and the production of a specific antiserum against the inhibitor raised in the rabbit.

EXPERIMENTAL

Materials

All reagents were of analytical-reagent grade and were obtained from Merck (Darmstadt, Germany) unless stated otherwise. Heparin–Sepharose CL6B and DEAE-Sepharose CL6B were purchased from Pharmacia (Uppsala, Sweden). The

[a] Present address: Laboratoiree d'Hématologie, Hôpital Cochin, 27 Rue du Faubourg Saint Jacques, F-75674 Paris Cedex 14, France.

0021-9673/91/$03.50

anion-exchange chromatographic Mono-Q column and the gel permeation Superose column were obtained prepacked from Pharmacia. The fast protein liquid chromatography (FPLC) system (Pharmacia) was used. The AcA-34 gel permeation column was obtained from IBF (Villeneuve la Garenne, France).

Collection of plasma

Venous blood was collected from at least 30 healthy individuals in evacuated tubes containing 0.129 *M* trisodium citrate (1:9) (Vacutainer 606608; Beckton Dickinson, Orangeburg, NJ, U.S.A.). Blood samples were immediately centrifuged at 2300 *g* and 3°C for 15 min. Plasma samples were pooled and stored frozen at −70°C until used.

Purification of HCII

The thawed plasma (485 ml) was treated with 1 *M* barium chloride solution (1:10, v/v) with constant magnetic stirring for 15 min at room temperature. After a 10-min centrifugation at 5000 *g*, the precipitate was discarded. All subsequent steps were carried out at 4°C, except the two final steps performed using the FPLC system. The supernatant was treated with 50% saturated ammonium sulphate (final concentration) for 20 min with constant magnetic stirring and centrifuged at 10 000 *g* for 20 min. The precipitate was dissolved in 65 ml of 0.02 *M* Tris–HCl buffer (pH 7.4), dialysed overnight against the same buffer, and the solution was centrifuged at 10 000 *g* for 20 min.

The supernatant was applied to a column (20 × 2.5 cm I.D.) of heparin–Sepharose CL6B equilibrated in 0.02 *M* Tris–HCl (pH 7.4). The column was extensively washed with this buffer until the absorbance of the effluent was zero. The column was eluted with 350 ml of a linear gradient from 0.0 to 0.4 *M* NaCl in 0.02 *M* Tris–HCl (pH 7.4). Fractions of 4.2 ml were collected at a flow-rate of 13 ml/h. Fractions containing more than 1.5 U/ml of dermatan sulphate (DS) cofactor activity were pooled (volume $v = 29.4$ ml) and diluted 1:3 in 0.02 *M* Tris–HCl (pH 7.4) to reduce the ionic strength.

This protein solution was applied to a column (30 × 1.5 cm I.D.) of DEAE-Sepharose equilibrated in 0.02 *M* Tris–HCl (pH 7.4). The column was extensively washed until the absorbance of the effluent was zero and eluted with 150 ml of a linear gradient from 0 to 0.4 *M* NaCl in 0.02 *M* Tris–HCl (pH 7.4). Fractions of 1.5 ml were collected at a flow-rate of 9 ml/h. Fractions containing more than 1.5 U/ml of DS cofactor activity were pooled ($v = 10.5$ ml) and concentrated against polyethylene glycol (PEG) to a final volume of 3 ml.

The solution was applied to a column (80 × 1.5 cm I.D.) of AcA-34 equilibrated with 0.15 *M* NaCl buffered with 0.02 *M* Tris–HCl (pH 7.4). Gel permeation chromatography was carried out in this buffer at a flow-rate of 6 ml/h. Fractions of 1.2 ml were collected. Fractions containing more than 2.0 U/ml DS cofactor activity were pooled ($v = 8.4$ ml).

The final steps were performed using the FPLC system at room temperature. The protein solution was applied to a Mono-Q ion-exchange column equilibrated with 0.02 *M* Tris–HCl (pH 7.4). The elution was carried out using a linear gradient from 0.0 to 0.5 *M* NaCl in 0.02 *M* Tris–HCl (pH 7.4). Fractions of 1.0 ml were collected at a flow-rate of 1.0 ml/min. Fractions containing the peak of DS cofactor activity were

pooled ($v = 3$ ml), concentrated against PEG and applied to a gel permeation (Superose) column equilibrated in 0.02 *M* Tris–HCl (pH 7.4) containing 0.3 *M* NaCl. The chromatography was performed using this buffer and 1.0-ml fractions were collected at a flow-rate of 0.10 ml/min. Fractions containing the peak of DS cofactor activity were pooled ($v = 4$ ml). This preparation was stored frozen at −70°C in aliquots.

Electrophoretic techniques

Sodium dodecyl sulphate–polyacrylamide gel electrophoresis (SDS-PAGE) was performed, according to Laemmli [8], in 7.5% polyacrylamide slab gels containing 0.1% (v/v) SDS. Apparent relative molecular masses (M_r) were obtained by comparison with a mixture of reduced reference proteins (Bio-Rad Labs., Richmond, CA, U.S.A.): β-galactosidase (M_r 116 000 dalton), phosphorylase B (M_r 92 000 dalton), bovine serum albumin (M_r 66 000 dalton), ovalbumin (M_r 45 000 dalton), carbonic anhydrase (M_r 31 000 dalton) and soybean trypsin inhibitor (M_r 22 000 dalton). All gels were stained with Coomassie Brillant Blue R.

Crossed immunoelectrophoresis was performed according to Ganrot [9] in 1% agarose gel containing 1% antisera against HCII.

Determination of proteins

The protein concentrations in the chromatographic fractions were determined by measuring the absorbance at 280 nm [10] in a cell of 1-cm light path. The extinction coefficients at 280 nm ($A^{1\%}_{280}$) used were 10 for a mixture of proteins and 11.7 for purified HCII [2].

HCII activity assay

HCII activity was assayed as antithrombin dermatan sulphate cofactor activity [11].

Production of specific antiserum against HCII

A 50-μg sample of the purified protein mixed with 1 ml of complete Freund's adjuvant was injected subcutaneously into rabbits. The animals received three subsequent injections of 50 μg of HCII mixed with 1 ml of Freund's incomplete adjuvant at 1-week intervals. The rabbits were bled 1 week after the last injection. The blood was allowed to clot at 37°C for 3 h and the serum, obtained by centrifugation at 2300 *g* for 15 min, was stored frozen at −30°C in aliquots.

RESULTS

Purification of HCII

As shown in Fig. 1, the peak of DS cofactor activity was eluted from the heparin–Sepharose column with a mean concentration of 0.18 *M* NaCl in 0.02 *M* Tris–HCl (pH 7.4). The fractions containing more than 1.5 U/ml were pooled, diluted in buffer to reduce the ionic strength and applied to a DEAE-Sepharose column and eluted with a linear gradient from 0 to 0.4 *M* NaCl in 0.02 *M* Tris–HCl (pH 7.4). Fractions containing a DS activity of more than 1.5 U/ml were eluted with a mean sodium concentration of 0.18 *M*, as shown in Fig. 2. These fractions were then pooled,

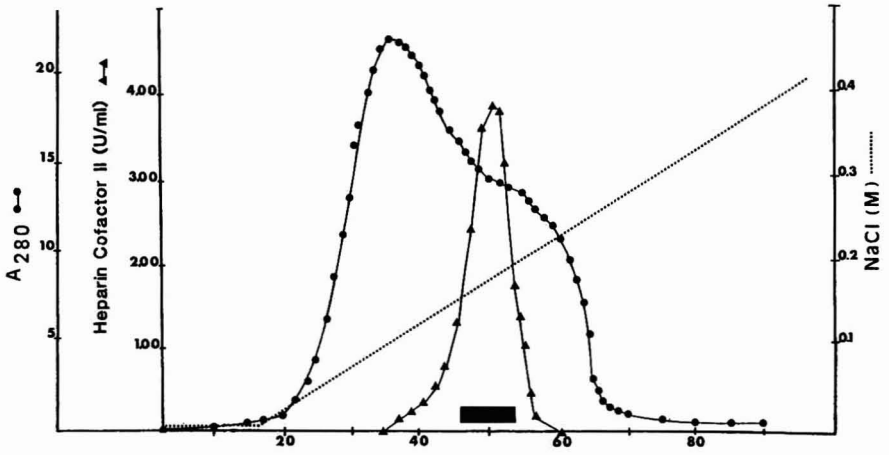

Fig. 1. Elution of HCII activity from heparin–Sepharose. The column (20 × 2.5 cm I.D.) was eluted with a 350-ml linear gradient from 0.0 to 0.4 *M* NaCl in 0.02 *M* Tris–HCl (pH 7.4). Fractions of 4.2 ml were collected at a flow-rate of 13 ml/h. ● = Absorbance at 280 nm; ▲ = HCII cofactor activity evaluated as antithrombin dermatan sulphate cofactor activity. Pooled fractions are indicated by a solid bar.

concentrated against PEG and gel chromatographed on an AcA-34 column. The elution profile is shown in Fig. 3. The DS cofactor activity was eluted with an elution volume of 54.0 ml. This protein solution was then applied to a Mono-Q ion-exchange column connected to the FPLC system. The column was eluted with a linear gradient from 0.0 to 0.5 *M* NaCl in 0.02 *M* Tris–HCl (pH 7.4). As shown in Fig. 4, the peak of DS cofactor activity was eluted with a mean concentration of 0.28 *M* NaCl. The final step consisted of gel permeation using a Superose column. The elution profile is shown in Fig. 5.

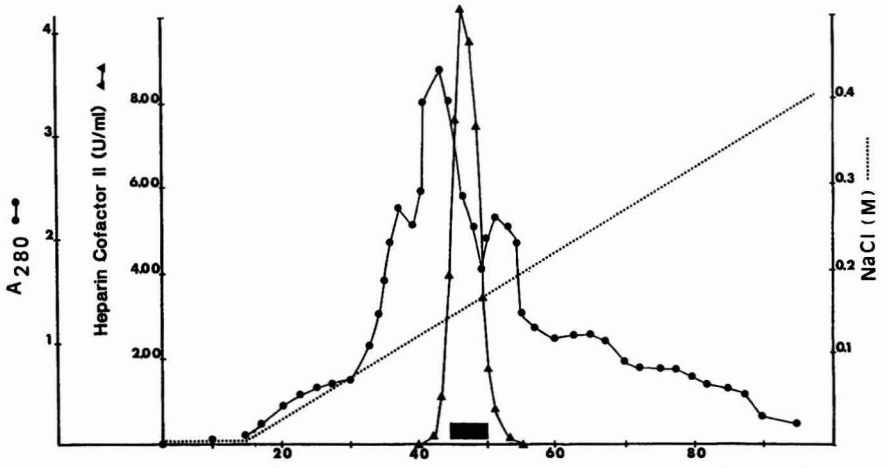

Fig. 2. Elution of HCII activity from DEAE-Sepharose. The column (30 × 1.5 cm I.D.) was eluted with a 150-ml linear gradient from 0.0 to 0.4 *M* NaCl in 0.02 *M* Tris–HCl (pH 7.4). Fractions of 1.5 ml were collected at a flow-rate of 9 ml/h. Symbols as in Fig. 1.

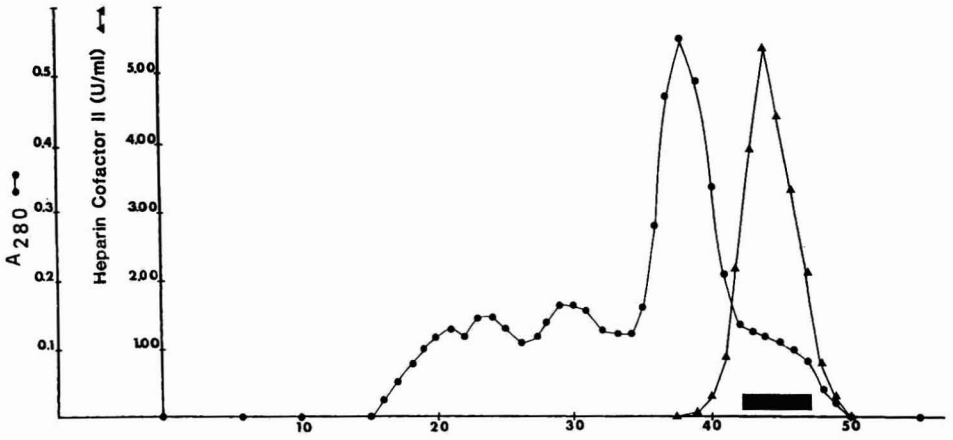

Fig. 3. Gel permeation of HCII activity on AcA 34. The proteins were chromatographed on a column (80 × 1.5 cm I.D.) equilibrated with 0.15 *M* NaCl in 0.02 *M* Tris–HCl (pH 7.4). Fractions of 1.2 ml were collected at a flow-rate of 6 ml/h. Symbols as in Fig. 1.

HCII was purified 760-fold from human plasma with an overall yield of 7.5% (Table I). The final product was homogeneous in SDS-PAGE (Fig. 6). No anti-Xa activity or immunoreactive ATIII could be detected in the protein preparation. Thus the purified HCII preparation was devoid of ATIII. HCII was eluted from the column of heparin–Sepharose (Fig. 1) with a much lower ionic strength (0.18 *M*) than ATIII, which appeared in the effluent at higher saline concentrations (0.80 *M*) (not shown).

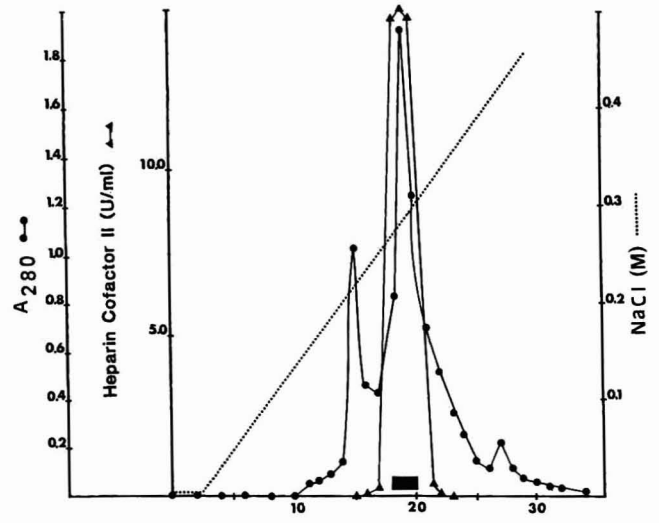

Fig. 4. Elution of HCII activity from a Mono-Q anion-exchange column. The column was eluted with a 35-ml linear gradient from 0.0 to 0.5 *M* NaCl in 0.02 *M* Tris–HCl (pH 7.4). Fractions of 1.0 ml were collected at a flow-rate of 1.0 ml/min. Symbols as in Fig. 1.

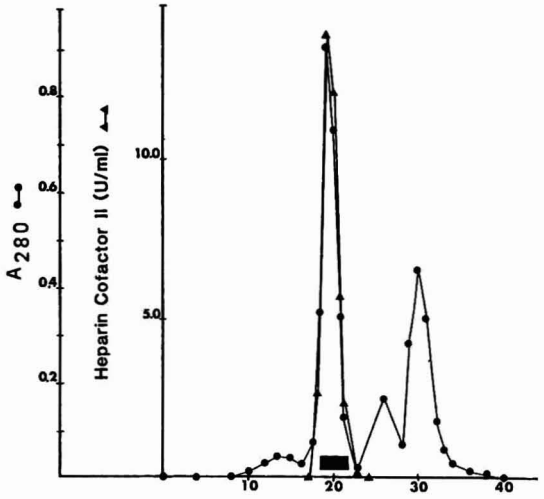

Fig. 5. Gel permeation of heparin cofactor II on a Superose column. The column was eluted with 0.3 *M* NaCl in 0.02 *M* Tris–HCl (pH 7.4). Fractions of 1.0 ml were collected at a flow-rate of 0.10 ml/min. Symbols as in Fig. 1.

Specificity of the antiserum against HCII

The antiserum was found to be monospecific, as evidenced by the single peak pattern of normal human plasma in crossed immunoelectrophoresis (CIE) as shown in Fig. 7. When purified ATIII was submitted to CIE, no immunoreactive protein could be found (not shown).

DISCUSSION

Functionally active heparin cofactor II was purified to homogeneity from human plasma with a recovery of 7.5%. The specific activity of the purified protein

TABLE I

PURIFICATION OF HEPARIN COFACTOR II FROM HUMAN PLASMA

Step	Volume (ml)	Total protein (mg)	Total HCII (U/ml)	Specific activity (U/mg)	Yield (%)	Purification factor
Starting plasma	485	26 389	418.5	0.016	100	1
Barium chloride-treated plasma	495	25 533	413.2	0.016	98.7	1
Ammonium sulphate precipitate	110	5809	176.0	0.030	42.1	1.88
Heparin–Sepharose	29.4	71.3	85.8	1.201	20.5	75.1
DEAE-Sepharose	10.5	12.8	61.5	4.805	14.6	300
AcA-34	8.4	6.8	46.0	6.765	11.0	422
Mono-Q	3	4.1	42.7	10.41	10.2	650
Superose	4	2.57	31.4	12.20	7.5	763

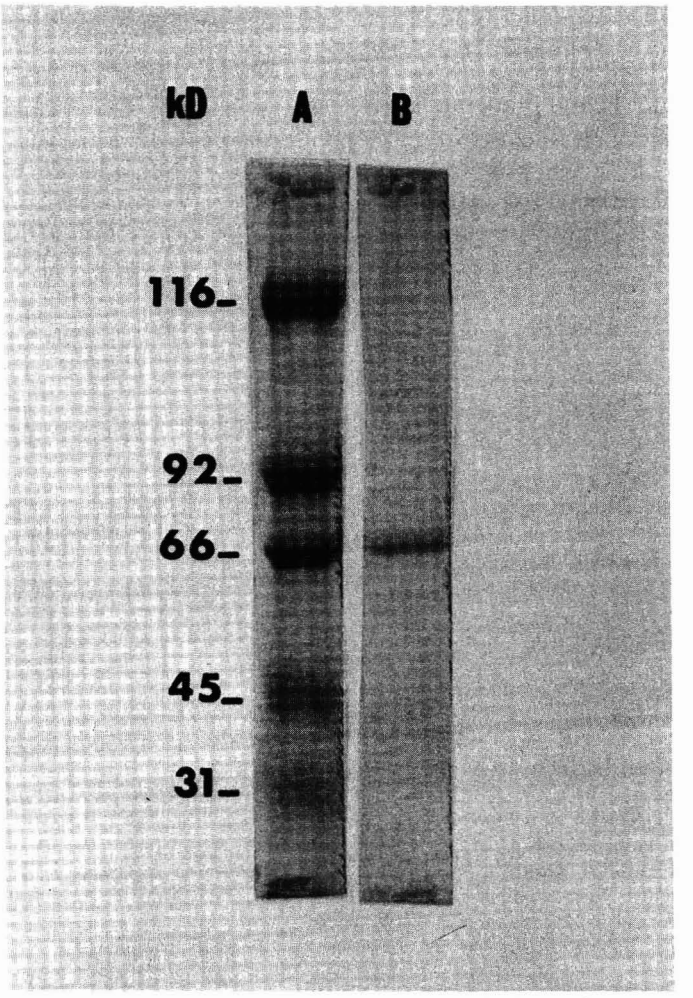

Fig. 6. SDS-PAGE of the final preparation of HCII. The final product was homogeneous and migrated with M_r 66 500 dalton (lane B). The molecular mass standards (M_r in kilodaltons) are in lane A.

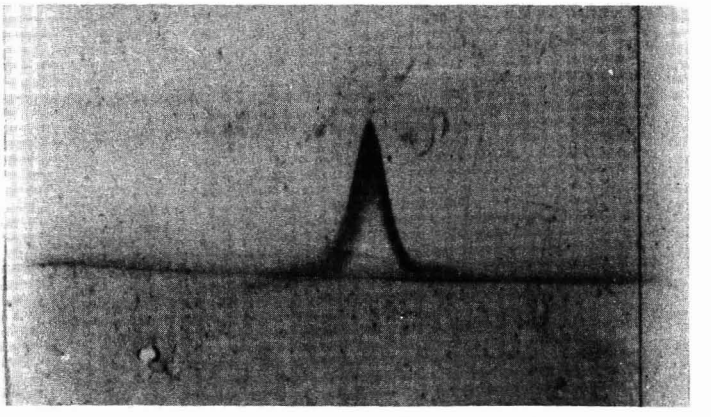

Fig. 7. Crossed immunoelectrophoresis of a plasma sample. The antiserum was used at a concentration of 1% (v/v) in the second dimension. A single peak pattern was found, suggesting the monospecificity of the antiserum.

was 12.2 U/mg. These results are similar to those obtained with previously published purification procedures [2,12–14], which gave purified HCII with a overall yield between 3% [2] and 30% [13].

The physiological role of HCII is still unknown. Even though cases of hereditary HCII deficiency were reported in patients with thrombophilia [15,16], the correlation between HCII deficiency and thrombosis is still controversial [17,18]. In addition to the quantitative deficiencies, a hereditary HCII variant, HCII OSLO (Arg-189–His) was recently found [19] in a clinically asymptomatic subject; the plasma HCII activity, measured as dermatan sulphate cofactor activity, was decreased whereas the HCII antigen concentration was normal. The specific antiserum against HCII, raised in the rabbit, can be a useful tool for the measurement of HCII antigen concentrations in clinical studies.

REFERENCES

1 G. F. Briginshaw and J. N. Shanberge, *Arch. Biochem. Biophys.*, 161 (1974) 683.
2 D. M. Tollefsen, D. W. Majerus and M. K. Blank, *J. Biol. Chem.*, 257 (1982) 2162.
3 D. M. Tollefsen, C. A. Pestka and W. J. Monafo, *J. Biol. Chem.*, 258 (1983) 6713.
4 M. J. Griffith, C. M. Noyes and F. C. Church, *J. Biol. Chem.*, 260 (1985) 2218.
5 M. A. Blinder, J. C. Marasa, C. H. Reynolds, L. L. Deaven and D. M. Tollefsen, *Biochemistry*, 27 (1988) 752.
6 R. D. Rosenberg and P. S. Damus, *J. Biol. Chem.*, 248 (1973) 6490.
7 K. A. Parker and D. M. Tollefsen, *J. Biol. Chem.*, 260 (1985) 3501.
8 U. K. Laemmli, *Nature (London)*, 227 (1970) 680.
9 P. O. Ganrot, *Scand. J. Clin. Lab. Invest.*, 29, Suppl. 124 (1972) 39.
10 J. Babul and E. Stellwagen, *Anal. Biochem.*, 28 (1969) 216.
11 P. Toulon, C. Jacquot, L. Capron, M. O. Frydman, D. Vignon and M. Aiach, *Thromb. Haemostas.*, 57 (1987) 263.
12 R. Yamagishi, M. Niwa, S. I. Kondo, N. Sakuragawa and T. Koide, *Thromb. Res.*, 36 (1984) 633.
13 T. H. Tran, B. Lämmle, B. Zbinden and F. Duckert, *Thromb. Haemostas.*, 55 (1986) 19.
14 F. C. Church, C. M. Noyes and M. J. Griffith., *Proc. Natl. Acad. Sci. U.S.A.*, 82 (1985) 6431.
15 T. H. Tran, G. A. Marbet and F. Duckert, *Lancet*, ii, (1985) 413.
16 P. Sie, D. Dupouy, J. Pichon and B. Boneu, *Lancet*, ii, (1985) 414.
17 R. M. Bertina, I. K. van der Linden, L. Engeser, H. P. Muller and E. J. P. Brommer, *Thromb. Haemostas.*, 57 (1987) 196.
18 P. A. Toulon, J. F. Vitoux, J. N. Fiessinger, Y. Sultan and M. Aiach, *Circulation*, 78, Suppl. II (1987) 326.
19 M. A. Blinder, T. R. Anderson, U. Abildgaard and D. M. Tollefsen, *J. Biol. Chem.*, 264 (1989) 5128.

Journal of Chromatography, 539 (1991) 501–505
Elsevier Science Publishers B.V., Amsterdam

CHROM. 22 895

Purification of cloned trypanosomal calmodulin and preliminary NMR studies

P. J. SWEENEY* and J. M. WALKER
Division of Biological Sciences, Hatfield Polytechnic, College Lane, Hatfield, Hertfordshire AL10 9AB (U.K.)
and
D. G. REID and N. ELSHOURBAGY
Department of Chemistry, SmithKline Beecham Pharmaceuticals Ltd., The Frythe, Welwyn, Hertfordshire AL6 9AR (U.K.)

ABSTRACT

Cloned trypanosomal calmodulin was expressed in *Escherichia coli* and purified to homogeneity using hydrophobic interaction chromatography on phenyl-Sepharose. The purified protein was subjected to NMR analysis which allows detailed changes to be observed when, firstly, calcium, and secondly, the drug calmidazolium bind. These spectral changes are the result of conformational changes in the protein and proximity effects due to the drug.

INTRODUCTION

Calmodulin is a 17 000-dalton, multifunctional, universal regulator of calcium functions, which is present in all eukaryotic cells. The protein detects free calcium and translates changes in calcium concentrations into altered states of metabolism [1]. Calcium-bound calmodulin interacts with and regulates a large number of enzymes, particularly those of nucleotide phosphate transfer and hydrolysis [2].

Calmodulin has been purified to homogeneity from a wide variety of sources, including vertebrates, invertebrates, plants and protozoans [3,4]. The size, abundance, heat stability and ability of the calcium-bound protein to bind drugs and target proteins have provided the basis for a number of isolation procedures [5,6]. NMR studies on human and bovine calmodulins have yielded much information on the conformational transitions associated with calcium binding and drug interactions [7].

We report here the purification of cloned trypanosomal calmodulin using hydrophobic interaction chromatography. Calmodulin is a highly conserved protein. However, the trypanosomal protein contains 22 amino acid substitutions when compared to the human protein. Substitutions at positions 77 and 79 are unique to trypanosomal calmodulin and are in a region thought to be involved in drug and target protein interaction.

0021-9673/91/$03.50

The purpose of these investigations is to study drug interactions with the trypanosomal protein and eventually compare assignments of human and trypanosomal calmodulins with a view to the design of trypanosomal calmodulin-specific drugs. We therefore also report preliminary NMR studies on the trypanosomal protein.

MATERIALS AND METHODS

E. coli strain AR58, containing the cDNA clone of trypanosomal calmodulin inserted into the expression vector pMG/Nco, was cultured in 25 250-ml conical flasks, each containing 100 ml of media, at 30°C, with shaking. The medium was a minimal bacterial medium, containing the following: 5 g/l sodium acetate, 2.5 g/l ammonium chloride, 1.9 g/l disodium hydrogen phosphate, 0.75 g/l potassium dihydrogen phosphate, 0.13 g/l sodium sulphate, 0.05 g/l magnesium sulphate, 0.2 ml LB broth and 0.05 ml trace element solution. When the cultures reached an absorbance of 0.4–0.6 at 550 nm, the flasks were transferred to a 42°C shaking water bath for 2 h to induce expression of calmodulin. The cells were then recovered by centrifugation, washed in 40 m*M* Tris–HCl, pH 7.5, resuspended in 250 ml of 50 m*M* Tris–HCl (pH 7.5), 1 m*M* mercaptoethanol, 1 m*M* EDTA (buffer 1), disrupted by sonication for 6 min, and the solution was clarified by centrifugation at 15 000 g for 15 min.

Calmodulin was purified from the clarified supernatant according to a method based on that described by Gopalakrishna and Anderson [8]. The soluble *E. coli* extract was passed through a phenyl-Sepharose (Pharmacia) column (14 cm × 1.6 cm I.D.), equilibrated with buffer 1, and the unbound fraction collected and made 5 m*M* in $CaCl_2$. It was then applied to a second phenyl-Sepharose column (14 cm × 1.6 cm I.D.), equilibrated with buffer 2 (50 m*M* Tris–HCl, pH 7.5, 1 m*M* mercaptoethanol, 0.1 m*M* $CaCl_2$) and the column washed with 15 column volumes of buffer 2, followed by 3 column volumes of buffer 3 (buffer 2 containing 0.5 *M* NaCl). The bound calmodulin was then eluted by washing the column with buffer 1. This fraction was made 50 m*M* in EDTA to remove calcium and the calcium free protein was then passed through a G-25 Sephadex (Pharmacia) column (45 cm × 1.6 cm I.D.), equilibrated with 100 m*M* ammonium bicarbonate, to remove EDTA, the calmodulin fractions were collected, pooled, freeze-dried and stored at −70°C.

Sodium dodecyl (lauryl) sulphate–polyacrylamide gel electrophoresis (SDS-PAGE) was performed according to the method of Laemmli [9]. N-Terminal sequencing was determined by sample application to an Applied Biosystems 477 pulsed liquid phase sequencer, with a 120A phenylthiohydantoin analyser for detection (Applied Biosystems).

Proton NMR spectra were acquired at 37°C and 360 MHz on a Bruker AM360 spectrometer. A 25-mg sample of trypanosomal calmodulin was dissolved in 0.4 ml ^2H_2O (Aldrich), which was 0.1 *M* and 0.05 *M* with respect to potassium chloride and potassium phosphate and adjusted to pH 7.0. $^{43}CaCl_2$ was used for the calcium titration experiments and calmidazolium was the compound chosen to perform the drug titration experiments. Calmidazolium (R24571) (Roche) was dissolved in deuterated methanol (Aldrich). One thousand scans were collected at each titration point and resolution enhancement was achieved using a convolution difference procedure (LB = 2.5) followed by exponential multiplication (LB = 1).

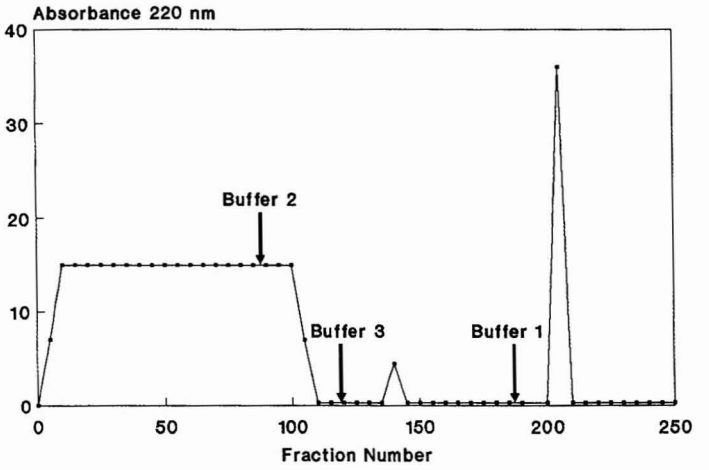

Fig. 1. Phenyl-Sepharose chromatography elution profile for trypanosomal calmodulin (second chromatography, see Results and Discussion).

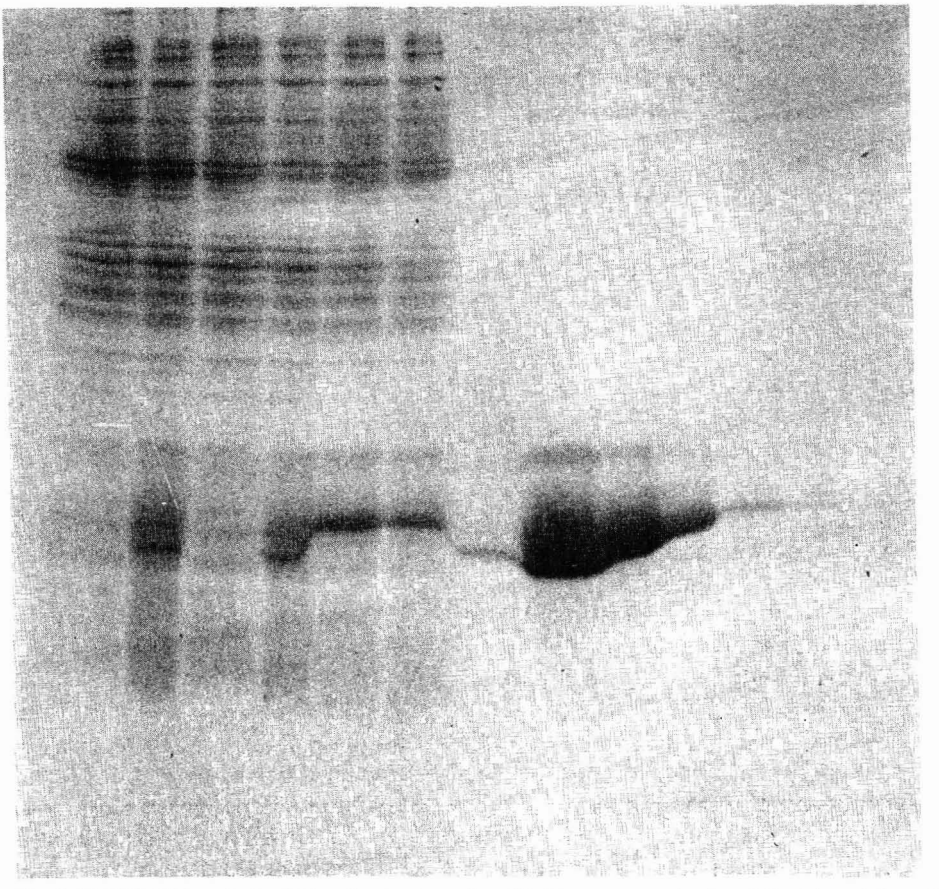

Fig. 2. SDS-PAGE analysis of *E. coli* extracts and purified trypanosomal calmodulin. From left to right, lanes 1,3: *E. coli* extract at point of induction, lanes 2,4: *E. coli* extract 12 h after induction, lanes 5,6: 12-h extracts in 1 m*M* EDTA (showing altered electrophoretic mobility of calmodulin in the absence of calcium), lanes 7–11: purified calmodulin fractions from column.

RESULTS AND DISCUSSION

Calmodulin was purified to homogeneity at a yield of 12–13 mg/l culture. The elution profile is illustrated in Fig. 1. The protein migrated as a single band on SDS-PAGE (Fig. 2) and N-terminal sequencing revealed a single N terminus. The first fifteen residues were identified by sequencing and agreed with the published sequence (single-letter code for amino acids): A–D–Q–L–S–N–E–Q–I–S–E–F–K–E–A.

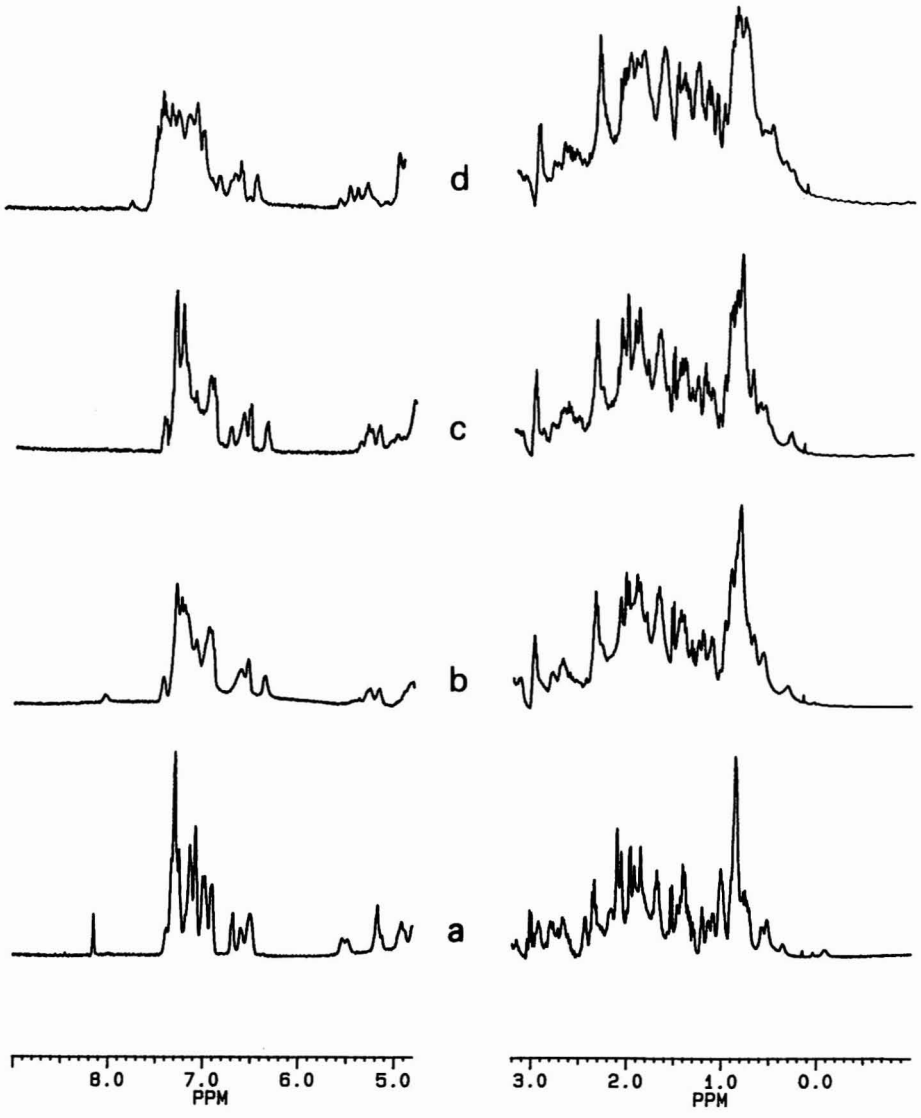

Fig. 3. NMR spectra of aromatic (4.5–9.0 ppm) and aliphatic (−1.0–3.0 ppm) regions of trypanosomal calmodulin. (a) 25 mg of calcium-free calmodulin, (b) 2:1 calcium–calmodulin complex, (c) 4:1 calcium–calmodulin complex, (d) 1:1 calmidazolium–calcium-saturated calmodulin complex.

The binding of calcium takes place in two distinct phases, corresponding to binding the two high-affinity, and the two low-affinity sites, respectively. As reported for bovine calmodulin [10], these two phases are characterized by slow exchange (discrete signals observed for Ca^{2+}-free and Ca^{2+}-bound protein) and fast exchange (time-averaged single resonances observed for both forms of the protein) on the NMR time scale, corresponding to successive occupation of the two high-affinity and two low-affinity sites. As shown in Fig. 3a, b and c, the interaction produces major conformational changes which are reflected in dramatic differences in the proton NMR spectra at each stage of the titration. Further changes accompany drug binding (Fig. 3d), corresponding, firstly, to the appearance of drug signals in the 6.5 to 7.5 ppm spectral region, and, secondly, to chemical shift and line-width changes in signals from the protein. The latter reflect both the effects of the drug on residues close to its binding site, and long range drug-induced conformational changes. The appearance of the aromatic region of trypanosomal calmodulin is very similar to that of the bovine protein, with the exception of the absence of the doublet corresponding to tyrosine, which may be accounted for by the Y-99–F-99 change in the former. However, spectral changes induced by the addition of one equivalent of calmidazolium are quite different from those observed in bovine calmodulin [11], although the compound still binds with high affinity, reflected in the slow exchange nature of most of the changes.

We are currently analysing the nature of the drug binding site by nuclear Overhauser effect experiments, assisted by selective and total deuteration of the protein, to allow drug signals to be observed in isolation, and assigned unambiguously.

REFERENCES

1 C. B. Klee and T. C. Vanaman, *Adv. Protein Chem.*, 35 (1982) 213.
2 P. Harris, in J. R. Jeter, I. L. Cameron, G. M. Madilla and A. M. Zimmerman (Editors), *Cell Cycle Regulation*, Academic Press, New York, 1978, p. 75.
3 Y. M. Lin, *Mol. Cell. Biochem.*, 45 (1982) 101.
4 L. Ruben, C. Egwuagu and C. L. Patton, *Biochim. Biophys. Acta*, 758 (1983) 104.
5 D. L. Newton, M. H. Krinks, J. B. Kaufman, J. Shilaoch and G. B. Klee, *Prep. Biochem.*, 18 (1988) 247.
6 G. A. Jamieson, Jr. and T. C. Vanaman, *Biochem. Biophys. Res. Commun.*, 90 (1979) 1048.
7 J. S. Evans, B. A. Levine, R. J. P. Williams and M. R. Wormald, in P. Cohen and C. B. Klee (Editors), *Molecular Aspects of Cellular Regulation*, Vol. 5, Elsevier, Amsterdam, 1988, p. 57.
8 R. Gopalakrishna and W. B. Anderson, *Biochem. Biophys. Res. Commun.*, 104 (1982) 830.
9 U. K. Laemmli, *Nature (London)*, 277 (1970) 680.
10 K. B. Seamon, *Biochemistry*, 19 (1980) 207.
11 D. G. Reid, L. K. MacLachlan, K. Gajjar, M. Voyle, R. J. King and P. J. England, *J. Biol. Chem.*, 265 (1990) 9744.

Journal of Chromatography, 539 (1991) 507–510
Elsevier Science Publishers B.V., Amsterdam

CHROM. 22 897

Use of dye pseudo-affinity chromatography in the purification of homoserine dehydrogenase

M. COSTA-FERREIRA* and J. C. DUARTE
Biotechnology Unit, National Laboratory for Industrial Engineering and Technology (LNETI/DTIQ), Estrada das Palmeiras, 2745 Queluz de Baixo (Portugal)

ABSTRACT

Homoserine dehydrogenase (E.C. 1.1.1.3) from a mutant strain of *Corynebacterium glutamicum* was purified using the pseudo-specific affinity dye Cibacron Blue F3G-A. The triazine dye was coupled either directly or via 1,4-diaminobutane to Sepharose 4B. Both the recovery and purification factor were significantly higher when the dye was coupled to the gel matrix via the spacer. Using this configuration, a recovery of about 62% was obtained with a purification factor of about 95-fold, achieved in a rapid one-step protocol.

INTRODUCTION

Procedures for the purification of homoserine dehydrogenase (E.C. 1.1.1.3) have been reported for various microorganisms [1–4] but these early procedures suffered from various limitations in that they were time consuming and consisted of several tedious steps. More recently, improved purification scheme have been reported for the *E. coli* enzyme using Sepharose substituted with alkyl chains of varying length [5]. Also, a Green A–agarose dye affinity column has been used as the final step in a purification scheme that involved a total of five steps [6].

Our interest in the improvement of *Corynebacterium glutamicum* strains that over-produce amino acids of the aspartate family [7,8] led us to undertake the purification of this key regulatory enzyme. We report here a simple one-step procedure for the purification of homoserine dehydrogenase using the pseudo-specific triazine dye Cibacron Blue F3G-A. A comparison is made between the purification achieved when the dye was immobilized to Sepharose 4B directly and that obtained when immobilized via 1,4-diaminobutane.

EXPERIMENTAL

Reagents

Sepharose 4B was purchased from Pharmacia (Uppsala, Sweden) and Cibacron Blue F3G-A (Reactive Blue), tresyl chloride, 1,4-diaminobutane and Coomassie

0021-9673/91/$03.50

Brilliant Blue from Sigma (St. Louis, MO, U.S.A.). All other reagents were of analytical-reagent grade.

Immobilization of Cibacron Blue F3G-A

In the absence of the spacer arm, coupling was effected by mixing Cibacron Blue (10 μmol/ml gel) with Sepharose 4B suspended in sodium carbonate, using essentially the procedure described previously [9]. The reaction was allowed to proceed for 2 h at 80°C. In the second aternative, the spacer arm, 1,4-diaminobutane, was added in ten-fold excess to tresyl-activated Sepharose 4B [10] and the coupling was run for 1 h at room temperature. After extensive washing, the gel was mixed with Cibacron Blue as described above except that the reaction was allowed to proceed for 1 h at 40°C.

Extraction of homoserine dehydrogenase from Corynebacterium glutamicum

The *C. glutamicum* mutant was grown as described previously [7]. Cells were harvested in the late log phase by centrifugation. The cell pellet was suspended in 100 m*M* potassium phosphate buffer (pH 7.0)–100 m*M* KCl–1 m*M* dithiothreitol (DTT)–1 m*M* EDTA at 4°C. This cell suspension [4% w/v (wet weight)] was disrupted by ultrasonic homogenization (200 W for 4 min). The homogenate was centrifuged (10 000 *g* for 20 min) and the resultant supernatant filtered (0.22-μm filter; Millipore). The cell-free extract (1 ml) was diluted (1:1) with 100 m*M* Tris–HCl (pH 7.0) containing 100 m*M* KCl, 0.5 m*M* DTT, 0.1 m*M* EDTA and 5 m*M* cysteine and applied immediately to a column (30 × 1 cm I.D.) packed with Sepharose 4B–Cibacron Blue previously equilibrated with the same buffer and washed at a flow-rate of 20 ml/h until the absorbance at 280 nm was less than 0.03. Homoserine dehydrogenase was eluted from the column with three column volumes of 2 m*M* nicotinamide–adenine dinucleotide phosphate, oxidized (NADP) in the same buffer system.

Homoserine dehydrogenase activity [11] and protein concentrations [12] were determined using published procedures.

RESULTS AND DISCUSSION

Homoserine dehydrogenase was eluted from the pseudo-affinity column by forming a stable ternary complex [13] with NADP and the competitive inhibitor cysteine [6]. Homoserine dehydrogenase activity was detected in a single essentially symmetrical peak. No homoserine dehydrogenase activity was detected in the large peak containing unbound protein that appeared in the void volume (results not shown).

The results presented in Table I show that the use of Cibacron Blue coupled to Sepharose 4B via the spacer arm gave a significantly higher recovery than when the dye was coupled directly to the gel matrix. In the latter instance the total enzyme activity was about 62%, suggesting incomplete elution. However, neither increasing the NADP concentration 10-fold nor eluting with up to five column volumes resulted in increased recovery. Despite some loss of activity, the yield nevertheless compares favourably with the 24% yield obtained by other workers [6] who used Green A–agarose as the final stage in a multi-step purification scheme.

When Cibacron blue was coupled to the gel via the spacer arm, a 95-fold purification of homoserine dehydrogenase was obtained in a single step. This

TABLE I

PURIFICATION OF HOMOSERINE DEHYDROGENASE FROM *CORYNEBACTERIUM GLUTAMICUM*

Parameter	Crude extract	Cibacron Blue–Sepharose 4B	
		Without spacer	With spacer
Total protein (mg)	8133	75	53
Total activity (U)	244	93	151
Specific activity (U/mg protein)	0.03	1.24	2.85
Recovery (%)	100	38.1	61.9
Purification (-fold)	1	41	95

purification factor is about double than that obtained in the absence of the spacer arm.

In order to exclude the possibility that the higher yield observed may have resulted from higher dye loading on the dye–spacer–Sepharose matrix, the absorbances at 600 nm of the two matrices were determined after gentle heating. As no significant difference was observed between the two matrices, it appears that the total dye load was the same in both instances (Fig. 1).

The higher yield observed in the presence of the spacer suggests that, as has been reported previously for various enzymes such as alcohol dehydrogenase [9], a spacer arm that renders the ligand more flexible is necessary for correct spatial orientation to

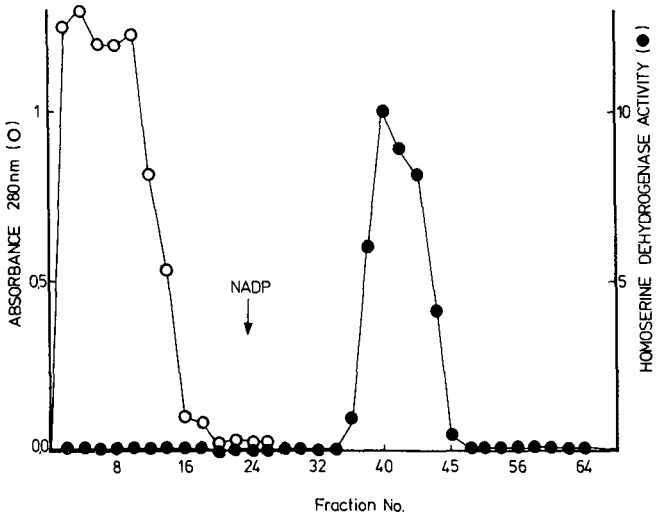

Fig. 1. Dye pseudo-affinity purification of homoserine dehydrogenase. An extract of *C. glutamicum* (244 units of enzyme) was applied to a column of Cibacron Blue F3G-A immobilized onto Sepharose 4B via 1,4-diaminobutane. The homoserine dehydrogenase was eluted with 2 m*M* NADP (as indicated by arrow) in 100 m*M* Tris–HCl (pH 7.0) containing 100 m*M* KCl, 0.5 m*M* DTT, 0.1 m*M* EDTA and 5 m*M* cysteine. Fractions (2 ml) were collected and enzyme activity was assayed as described under Experimental.

homoserine dehydrogenase, whereas in the absence of the spacer steric factors hinder access to the ligand.

Work is in progress to optimize the purification by avoiding problems associated with the use of unpurified dyes [14], studying the effect of using longer spacer arms such as diaminohexane and studying the many other factors that affect purification efficacy.

ACKNOWLEDGEMENTS

We thank Dr. Torbjörn Ling of the Department of Biotechnology, University of Lund, Sweden, for helpful advice on the use of triazine dyes.

REFERENCES

1 N. Guiso and P. Truffa-Bachi, *Eur. J. Biochem.*, 42 (1974) 401.
2 M. Shailaja and M. R. Raghavendra Rao, *Mol. Cell. Biochem.*, 12 (1976) 15.
3 P. Datta, *J. Biol. Chem.*, 245 (1970) 5779.
4 M. Jenkins and V. Woodward, *Biochim. Biophys. Acta*, 212 (1970) 21.
5 L. Broussard, W. Harms and W. Shive, *Anal. Biochem.*, 72 (1976) 16.
6 W. Karsten, J. Hunsley and R. Viola, *Anal. Biochem.*, 147 (1985) 336.
7 M. Costa-Ferreira and J. C. Duarte, *Appl. Biochem. Biotechnol.*, (1991) in press.
8 M. Costa-Ferreira and J. C. Duarte, *Port. Pat. Appl.*, No. 91 207, 1989.
9 B. Mattiasson and T. G. I. Ling, *J. Chromatogr.*, 376 (1986) 235.
10 K. Nilsson and K. Mosbach, *Methods Enzymol.*, 104 (1984) 56.
11 P. Datta and H. Guest, *Methods Enzymol.*, 2 (1970) 703.
12 M. Bradford, *Anal. Biochem.*, 72 (1976) 248.
13 G. Svanas and H. Weiner, *Anal. Biochem.*, 124 (1982) 314.
14 B. Weber, K. Willeford, J. G. Moe and D. Piszkiewicz, *Biochem. Biophys. Res. Commun.*, 86 (1979) 252.

Journal of Chromatography, 539 (1991) 511–516
Elsevier Science Publishers B.V., Amsterdam

CHROM. 22 899

Purification on poly(U)–Sepharose 4B of human breast cancer cell line T-47D DNA polymerases

D. BERNARD* and C. MOYRET
Laboratoire d'Oncologie Moléculaire, Centre Jean Perrin, Place Henri Dunant, B.P. 392, 63011 Clermont-Ferrand Cedex (France)
and
J. C. MAURIZIS
INSERM U 71, Rue Montalembert, 63005 Clermont-Ferrand Cedex (France)

ABSTRACT

The purification of DNA polymerases (RNA-directed DNA polymerases and DNA-directed DNA polymerases) on poly(U)–Sepharose 4B from a breast tumour cell line (T-47D) is reported. The elution of these enzymes was followed in each fraction by activity measurements with the four primer-templates poly(rA)–oligo$(dT)_{12-18}$, poly(dA) oligo$(dT)_{12-18}$, poly(rC)–oligo$(dG)_{12-18}$ and poly(rCm)–oligo $(dG)_{12-18}$. The control of the polymerase purification by chromatography was performed by sodium dodecyl sulphate–polyacrylamide gel electrophoresis of the pooled active enzymatic fractions.

INTRODUCTION

DNA polymerase (RNA-directed DNA and DNA-directed DNA polymerase) activities have been detected in Rous sarcoma [1] and in different human neoplasias, such as leukaemias [2–4] and breast tumours [5].

The DNA polymerases have been purified using glycerol gradient centrifugation [6], a combination of sucrose gradient and ion-exchange column chromatography [7] or extraction of retroviruses with a detergent followed by an oligo$(dT)_{12-18}$–cellulose column and non-dissociating gel electrophoresis [8]. These procedures are cumbersome and their yields are often poor. This paper demonstrates that highly pure DNA polymerase can be readily prepared by a single chromatographic step on a polyuridylic acid [poly(U)]–Sepharose 4B column.

EXPERIMENTAL

Chemical and reagents

Poly(riboadenylic acid)–oligo(deoxythymidylic acid)$_{12-18}$ [poly(rA)–oligo-$(dT)_{12-18}$], poly(deoxyadenylic acid)–oligo(deoxythymidylic acid)$_{12-18}$ [poly(dA)–oligo$(dT)_{12-18}$], poly(ribocytidylic acid)–oligo(deoxyguanylic acid)$_{12-18}$ [poly(rC)–oligo$(dG)_{12-18}$], poly(2′-O-methylribocytidylic acid)–oligo(deoxyguanylic acid)$_{12-18}$-

0021-9673/91/$03.50

[poly(rCm)–oligo(dG)$_{12-18}$] and poly(uridylic acid) [poly(U)]–Sepharose 4B were purchased from Pharmacia (Uppsala, Sweden). Nonidet P 40 (NP 40) and trichloroacetic acid (TCA) were purchased from Sigma (St. Louis, MO, U.S.A.). Deoxy[^{3}H]-methylthymidine 5′-triphosphate ([^{3}H]-dTTP) and deoxy[8-^{3}H]guanosine 5′-triphosphate([^{3}H]-dGTP) were purchased from Amersham International (Amersham, U.K.). Filters were obtained from Millipore (Bedford, MA, U.S.A.) and T_{75} flasks from Corning (Corning, NY, U.S.A.). RPMI 1640 medium was purchased from Gibco Europe (Renfrewshire, U.K.). Foetal calf serum (FCS) and phosphate-buffered saline (PBS) were obtained from Boehringer (Mannheim, Germany).

Cell culture and harvesting

T-47D cell line originated from a pleural effusion of a patient with intraductal and invasive breast carcinoma [9]. Cells were grown in closed plastic T_{75} flasks in growth medium composed of RPMI 1640 buffered with sodium hydrogencarbonate (2 g/l) supplemented with 2 m*M* glutamine, gentamycin (20 μg/ml) and 10% heat-inactived FCS. Cells were grown in a humidified incubator with 5% carbon dioxide at 37°C. Cultures were re-fed every 2–3 days. Culturing (after growth for 1 week) involved trypsin digestion (7.5 mg/ml PBS per flask), to obtain monocellular suspensions, followed by the plating of 3×10^6 cells per flask. Cultures were confluent after 5–6 days (*ca.* 10^7 cells per flask). Ten flasks were used.

Preparation of NP 40 extract

The growth medium was removed from each flask and cells were washed in the flask with PBS. Protein solubilization was performed with 3 ml of 0.5% NP 40 in TBS [150 m*M* NaCl–50 m*M* Tris–0.02% NaN_3 (pH 7.0)] for 15 min at 4°C. The insoluble material was removed by centrifugation at 30 000 *g* for 30 min. The collected extract was used immediately.

Affinity chromatography on poly(U)–Sepharose 4B

The NP 40 extract was poured onto a poly(U)–Sepharose 4B column (10 × 0.9 cm I.D.), previously equilibrated with 2–3 volumes of buffer A [50 m*M* Tris–HCl (pH 7.5)–0.1 *M* EDTA–3 m*M* dithiothreitol–0.02% (v/v) NP 40–10% (v/v) glycerol]. NP 40 extract precycling was performed for DNA–polymerase adsorption on the affinity gel. The enzyme was eluted with a linear gradient from 0 to 0.8 *M* KCl in buffer A at 10 ml/h. Fractions (1.5 ml) were collected with an automatic fraction collector and aliquots (100 μl) were taken and assayed for DNA polymerase activity [10].

Sodium dodecyl sulphate–polyacrylamide gel electrophoresis (SDS-PAGE)

Control of the purification of the DNA polymerases was performed by SDS-PAGE after their elution on poly(U)–Sepharose. Fractions exhibiting an enzymatic activity were pooled, then concentrated by ultrafiltration (Millipore CX 10 immersible ultrafilters, cut-off 10 000 dalton) to a final volume of 500 μl.

A sample of 50 μl was denatured by heating for 2 min at 100°C with addition of 50 μl SDS gel sample buffer [60 m*M* Tris–HCl (pH 6.8)–11.2% glycerol–3% SDS–0.01% bromophenol blue–5% β-mercaptoethanol]. The sample was then analysed on a 12.5% SDS-polyacrylamide gel together with molecular mass standards (phosphorylase *b*, M_r 94 000; bovine serum albumin, M_r 67 000; ovalbumin, M_r 43 000;

carbonic anhydrase, M_r 30 000; soybean trypsin inhibitor, M_r 20 100; α-lactalbumin, M_r 14 400; Pharmacia). Electrophoresis was performed at 20 mA for 3 h. The gel was then fixed in 20% TCA (0.5 h), stained with 0.04% (w/v) Serva Blue W (Serva, Heidelberg, Germany) in water (0.5 h), destained with water (1 h) and 20% glycerol (12 h) and dried on a slab dryer (Protean II; Bio-Rad Labs.) under vacuum.

Assays for DNA–polymerase activity

Before assay with the primer templates poly(rA)–oligo(dT)$_{12\text{-}18}$ and poly-(dA)–oligo(dT)$_{12\text{-}18}$, samples were dialysed for 5 h against buffer B [40 m*M* Tris–HCl (pH 7.8)–60 m*M* KCl–2.2 m*M* dithiothreitol–10 m*M* $MgCl_2$–0.1% Triton X-100]. Before assay with the primer-templates poly(rCm)–oligo(dG)$_{12\text{-}18}$ and poly(rC)–oligo(dG)$_{12\text{-}18}$, samples were dialysed in buffer C, which was buffer B with 0.8 m*M* $MnCl_2$ in place of 10 m*M* $MgCl_2$ [11]. The assay was run to a final volume of 130 μl containing 8 μCi of [^{3}H]-dTTP (specific activity 2.07 TBq/mmol) and 1.6 μg of poly(rA)–oligo(dT)$_{12\text{-}18}$ or poly(dA)–oligo(dT)$_{12\text{-}18}$, or 8 μCi of [^{3}H]-dGTP (specific activity 518 GBq/mmol) with 1.6 μg of poly(rCm)–oligo(dG)$_{12\text{-}18}$ or poly(rC)–oligo(dG)$_{12\text{-}18}$. Aliquots of the solubilized proteins (100 μl) and buffer B or C (14 μl) were then added. Controls were performed in the same reaction medium without a primer-template. Each assay was performed in triplicate. The reaction was conducted for 30 min at 37°C and stopped by precipitation of the polymerized material with a mixture of 5% TCA, 0.05 *M* sodium pyrophosphate and 0.5 *M* HCl (4 ml). Precipitates were collected by filtration on 0.22-μm filters, washed, dried and their radioactivity measured in a liquid scintillation counter (Packard Tri-Carb 4530) after dissolution in Ready Solv MP (Beckman) scintillation medium.

RESULTS AND DISCUSSION

We have demonstrated the purification of DNA polymerases (RNA-directed DNA polymerase and DNA-directed DNA polymerase) on poly(U)–Sepharose 4B (gives a high yield of purified enzyme) in comparison with more conventional methods, such as sucrose gradient centrifugation followed by phosphocellulose [8] or oligo-(dT)$_{12\text{-}18}$–cellulose [12] columns, which are time consuming (and give a limited amount of purified enzyme).

The cellular DNA polymerases can be obtained with poly(U)–Sepharose 4B from different cell sources such as cell lines, surgical biopsies or peripheral blood. The method allows the identification of the DNA polymerases in the eluted fractions using a synthetic primer-template. Ross *et al.* [13] have demonstrated that poly(rA)–oligo-(dT)$_{12\text{-}18}$ was copied by DNA polymerases. Later, it was demonstrated that poly(dA)–oligo(dT)$_{12\text{-}18}$ was copied by DNA–DNA polymerases and RNA–DNA polymerases [14]. Other workers have demonstrated that RNA–DNA polymerase activity was more specific with poly(rC)–oligo(dG)$_{12\text{-}18}$ than with poly(rA)–oligo(dT)$_{12\text{-}18}$ [15]. Gerard *et al.* [7] have demonstrated that poly(rCm)–oligo-(dG)$_{12\text{-}18}$ was highly specific for RNA–DNA polymerases.

In this work, we determined in each fraction the DNA polymerase activities from T-47D cells after chromatography of the extract on poly(U)–Sepharose 4B, with the four primer-templates poly(rA)–oligo(dT)$_{12\text{-}18}$, poly(dA)–oligo(dT)$_{12\text{-}18}$, poly-(rC)–oligo(dG)$_{12\text{-}18}$ and poly(rCm)–oligo(dG)$_{12\text{-}18}$, in order to establish an activity

spectrum allowing enzyme characterization. The reactions were conducted as follows. After incubation of the ^{3}H-labelled nucleotide with primer-template complex, the high-molecular-mass polydeoxyribonucleotides obtained, insoluble in 5% TCA, were separated from the TCA-soluble labelled starting materials by filtration. The incorporated radioactivity was determined by dissolution in a scintillation liquid and counting.

The results for the primer-templates poly(rA)–oligo(dT)$_{12-18}$ and poly(dA)–oligo(dT)$_{12-18}$ are plotted in Fig. 1. Each value corresponds to the arithmetic mean of the three different assays for each eluted fraction. Significant incorporation of [^{3}H]-dTTP into poly(dA)–oligo(dT)$_{12-18}$, corresponding to a DNA–DNA polymerase activity, was measured. Fractions 8–19 were concentrated and submitted to SDS-PAGE as described above. Between fractions 10 and 15 was measured a low incorporation of [^{3}H]-dTTP into poly(rA)–oligo(dT)$_{12-18}$, corresponding to a low specificity of DNA–DNA polymerase against this primer-template, which confirms the findings of Ross *et al.* [13]. Conversely, no incorporation of [^{3}H]-dGTP with the primer-templates poly(rC)–oligo(dG)$_{12-18}$ and poly(rCm)–oligo(dG)$_{12-18}$, which usually corresponds to an RNA- directed DNA polymerase activity, was measured. This result shows the absence of RNA–DNA polymerase in the solubilized proteins from non-stimulated T-47D cells. This enzyme, characteristic of the retroviruses and retrovirus-like particles, was not found because the cells were not stimulated by 17β-estradiol and progesterone, which are necessary for the activation of the retrovirus life cycle [9].

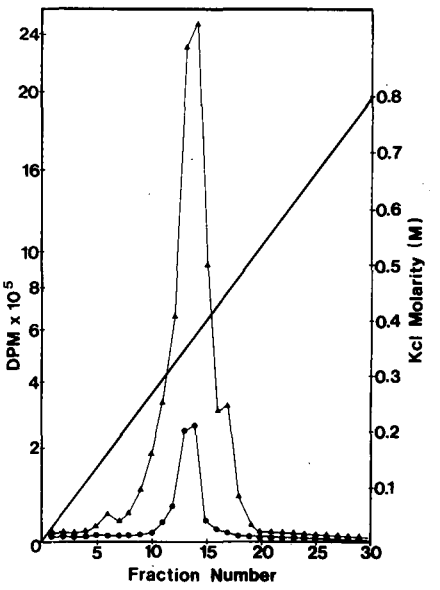

Fig. 1. Elution pattern on poly(U)–Sepharose 4B of DNA polymerases obtained from T-47D tumour cells. Flow-rate, 10 ml/h with a linear gradient of KCl from 0 to 0.8 *M* in buffer A. Aliquots (100 μl) of each 1.5-ml fraction were assayed for incorporation of [^{3}H]-dTTP into (▲) poly(dA)–oligo(dT)$_{12-18}$ and (●) poly(rA)–oligo(dT)$_{12-18}$.

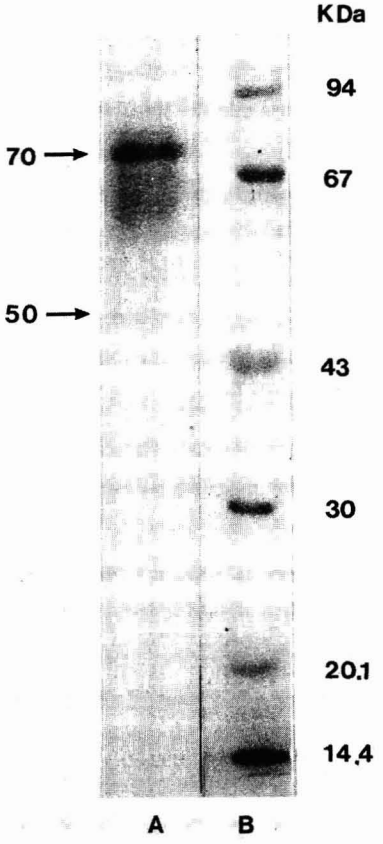

Fig. 2. SDS-PAGE of DNA polymerases after purification on poly(U)–Sepharose 4B (A). Molecular mass standards were phosphorylase *b* (M_r 94 000), bovine serum albumin (M_r 67 000), ovalbumin (M_r 43 000), carbonic anhydrase (M_r 30 000), soybean trypsin inhibitor (M_r 20 100), α-lactalbumin (M_r 14 400) (B). Staining was performed with Serva Blue W. KDa = Kilodalton.

The purification yield on poly(U)–Sepharose of DNA polymerases from 10^8 cells as starting material was about 54% when the incorporation of radioactivity was measured with the primer-template poly(rA)–oligo$(dT)_{12\text{-}18}$ and about 67% when the incorporation of radioactivity was measured with poly(dA)–oligo$(dT)_{12\text{-}18}$. Moreover, the degree of purity of DNA polymerases after purification on poly(U)–Sepharose was demonstrated after SDS-PAGE of pooled active enzymatic fractions. One major band was obtained at 70 000 dalton, and less intense bands between 70 000 and 50 000 dalton (Fig. 2). These results are in agreement with the findings of Hesselwood *et al.* [16] on calf thymus α-DNA polymerase and De Recondo *et al.* [17] on rat liver. Similar results were obtained by Grummt *et al.* [18], who demonstrated that calf thymus α-DNA polymerase was constituted of an association of seven polypeptide chains between 64 000 and 52 000 dalton.

In conclusion, poly(U)–Sepharose 4B chromatography enables DNA poly-

merases (RNA- and DNA-directed DNA polymerases) to be isolated from cell extracts with a good yield and high purity. Their enzymatic activities can be determined in the eluted fractions by measuring the incorporation of [^{3}H]nucleotides in their corresponding primer-templates. In this way, DNA polymerases can be obtained from cells and from retroviruses secreted in the culture medium.

ACKNOWLEDGEMENTS

We thank Lucien Veyssade for the illustrations and Michelle Labonde for typing the manuscript. C. M. was supported by a grant from the Association de la Recherche contre le Cancer Région Grand Centre.

REFERENCES

1 H. Temin and S. Mizutani, *Nature (London)*, 266 (1970) 1211.
2 N. R. Rice, R. M. Stephens, A. Burny and R. V. Gilden, *Virology*, 142 (1985) 357.
3 T. Thompson and H. Fan, *Virus Genes*, 2 (1988) 83.
4 M. T. Boyd, N. McLean and D. G. Oscier, *Lancet, i* (1989) 814.
5 C. F. Moyret, D. J. Bernard, J. C. Maurizis, J. Chassagne, M. de Latour, G. Bétail, R. Plagne and P. Chollet, *In Vivo,* 4 (1990) 101.
6 H. Rainer, K. Moser and E. Deutsch, *Lancet, ii* (1974) 357.
7 G. F. Gerard, P. M. Loewenstein and M. Green, *Nature (London)*, 256 (1975) 140.
8 G. F. Gerard, P M. Loewenstein and M. Green, *Cancer Res.*, 38 (1978) 1008.
9 I. Keydar, L. Chen, S. Karby, R. Weiss, J. Delarea, M. Radu, S. Chaitcik and H. J. Brenner, *Eur. J. Cancer*, 15 (1979) 659.
10 D. P. Grandgenett, *J. Virol.*, 20 (1976) 348.
11 K. Ono, A. Ohashi, A. Yamamoto, A. Matsukage, N. Nishioka, T. Takhashi, C. Nakayama and S. Saneyoshi, *Cell. Mol. Biol.*, 25 (1980) 323.
12 B. I. Gerwin and J. B. Milstien, *Proc. Natl. Acad. Sci. U.S.A.*, 69 (1972) 2599.
13 J. Ross, E. M. Scolnick, G. J. Todaro and S. A. Aaronson, *Nature (London)*, 231 (1971) 163.
14 A. M. Wu and R. C. Gallo, *CRC Crit. Rev. Biochem.*, 3 (1975) 289.
15 P. D. Boyer, in P. D. Boyer (Editor), *The Enzymes*, Vol. 10, Academic Press, London, 3rd ed., 1974, p. 205.
16 I. P. Hesselwood, A. M. Holmes, W. F. Wakeling and I. R. Johnson, *Eur. J. Biochem.*, 84 (1978) 123.
17 A. M. de Recondo, J. A. Lepesant, O. Fichot, L. Grasset, J. M. Rossignol and M. Cazillis, *J. Biol. Chem.*, 248 (1973) 131.
18 F. Grummt, C. Waltfl, H. M. Jantzen, K. Hamprecht, V. Hulscher and C. C. Kuenzle, *Proc. Natl. Acad. Sci. U.S.A.*, 76 (1979) 6081.

Journal of Chromatography, 539 (1991) 517–523
Elsevier Science Publishers B.V., Amsterdam

CHROM. 22 900

Purification of NAD glycohydrolase from *Neurospora crassa* conidia by a polyclonal immunoadsorbent

MARIO PACE*, DARIO AGNELLINI, GUIDO LIPPOLI, PIER GIORGIO PIETTA and PIER LUIGI MAURI

Dipartimento di Scienze e Tecnologie Biomediche, Sez. Chimica Organica, University of Milan, Via G. Celoria 2, 20133 Milan (Italy)

and

SERGIO CINQUANTA

CNR, c/o Ist. Patologia Vegetale, University of Milan, Via G. Celoria 2, 20133 Milan (Italy)

ABSTRACT

NAD glycohydrolase from *Neurospora crassa* conidia was purified by affinity chromatography on a column of polyclonal antibodies bound to an agarose matrix. The procedure was easy, non-denaturating and suitable for repetitive use of the gel. The enzyme obtained appeared homogeneous by sodiumdodecyl sulphate–polyacrylamide gel electrophoresis.

INTRODUCTION

NAD glycohydrolase (NADase, E.C. 3.2.2.5) from *Neurospora crassa* conidia is a hydrolytic enzyme which uses NAD^+ as a substrate, catalysing the reaction

$$NAD^+ + H_2O \xrightarrow{\text{NADase}} \text{nicotinamide} + \text{ADPR} + H^+ \quad (1)$$

NADase is a glycoprotein of 33 000 dalton and was purified by affinity chromatography [1] using a competitive inhibitor, 4-methyl-NAD, bound to a Sepharose-4B gel through a hydrophilic spacer arm. The enzyme possesses hydrophobic characteristics which were used for its immobilization onto propyl–Sepharose [2] and for the isolation of the protein by hydrophobic chromatography [3]. However, both purification methods used show some disadvantages:

(a) 4-methyl-NAD is not a commercial nucleotide and its preparation is a long and cumbersome process;

(b) the crude extract of conidia contains pyrophosphatases and nucleotidases which hydrolyse the ligand and shorten the life of the affinity column;

(c) hydrophobic chromatography can be performed only under well established conditions, *i.e.*, with a propylic residue as a ligand and a gel capacity in the range 0.09–0.17 mmol/g; and

0021-9673/91/$03.50

(d) the elution of the protein from propyl–Sepharose gels can be accomplished only under the conditions that lead to a high percentage of denaturation (6 *M* urea or 1 *M* *n*-propylamine).

For these reasons, we prepared a new column with a polyclonal antibody to NADase bound to an agarose gel and in this paper we report the results obtained for the purification of the enzyme.

EXPERIMENTAL

NAD^+ was purchased from Boehringer (Mannheim, Germany) and adenosine diphosphoribose (ADPR) from Sigma (St. Louis, MO, U.S.A.). Acrylamide, N,N-bis-acrylamide and sodium dodecyl sulphate of electrophoresis grade and Affi-Gel 10 were obtained from Bio-Rad Labs. (Richmond, CA, U.S.A.). All other reagents were of analytical-reagent or high-performance liquid chromatographic (HPLC) grade. A crude extract of NADase was obtained by washing the *Neurospora crassa* conidia with water and centrifuging the suspension at 5000 *g* for 15 min at 2°C.

NADase was previously purified by affinity chromatography [1] in order to obtain polyclonal antibodies.

NAD glycohydrolase activity was assayed by HPLC [4] when the enzyme was in phosphate buffer, or by titrating the hydrogen ions produced in the reaction with 5 m*M* sodium hydroxide through a pH-Stat apparatus (Radiometer) when a dialysed solution was used.

HPLC was carried out on a C_{18} Resolve column (Waters Assoc., Milford, MA, U.SA.) (150 × 4.5 mm I.D.; 5 μm average particle size) with a Corasil precolumn (35 × 3.9 mm I.D.), eluted with 4% (v/v) methanol in 0.1 *M* phosphate buffer (pH 6.2) using a Waters Assoc. apparatus. The instrument consisted of a Model 590 pump equipped with a Model U6K universal injector, a Lambda-Max Model 480 UV detector and a Model 730 data module. The chromatographic assay was accomplished at a flow-rate of 2.0 ml/min and the eluent was monitored by UV absorption at 254 nm (0.05 a.u.f.s.).

One NAD glycohydrolase unit is defined as the amount of enzyme which catalyses the hydrolysis of 1 μmol of NAD^+ per minute at 37°C and pH 7.0.

Preparation of the polyclonal antibodies of NADase

Antisera were obtained in rabbits by a series of 4-weekly injections of NADase, previously purified by affinity chromatography, emulsified with complete Freund's adjuvant and bleeding 1 week after the last injection. Antibodies against NADase from *Neurospora crassa* conidia were purified according to the rivanol method [5], and linked to alkaline phosphatase by means of glutaraldehyde [6] in order to assay their specificity. For extended storage the derivatives were kept frozen in working aliquots and each sample was assayed by enzyme-linked immunosorbent assay (ELISA) using *p*-nitrophenyl phosphate as substrate. The working dilution of each stock solution of enzyme–antibody conjugate in the ELISA assay was 1:100 and the reaction lasted 30 min.

ELISA assay

Each well of a polystyrene plate was filled with 200 μl of antibody solution [1

μg/ml in phosphate buffer (pH 7.5)] and allowed to stand at 4°C for 18 h. After washing three times with phosphate buffer (pH 7.5) containing 0.9% NaCl [phosphate-buffered saline (PBS)] and 0.05% (v/v) Tween-20, 200 μl of NADase (1 μg/ml) in PBS was added to each well and the plate incubated for 1 h at 37°C. The wells were then washed three times with PBS–Tween-20 and 200 μl (5 μg/ml) of antibody, linked to alkaline phosphatase by means of glutaraldehyde, were added to some of the wells. The wells containing no antigen were filled with conjugate as a control and the plate was incubated for 1 h at 37°C. After addition of 200 μl of *p*-nitrophenyl phosphate (1 mg/ml) in 10% diethanolamine (pH 9.8), containing 1 m*M* $MgCl_2$, the plate was incubated at 37°C for 30 min. For each determination, triplicate wells were pooled and the absorbance at 405 nm was measured.

Immobilization of antibodies onto Affi-Gel 10

A 7.5-ml aliquot of the N-hydroxysuccinimide ester of derivatized cross-linked agarose gel beads (Affi-Gel 10) was washed with 23 ml of isopropanol and 23 ml of chilled water, according to the procedure of Ikura *et al.* [7]. To the gel was added 1 ml of 0.1 *M* phosphate buffer (pH 8.0), containing 48 mg of antibodies; after reaction for 4 h with gentle shaking at 4°C, the gel was washed with 23 ml of 0.1 *M* phosphate buffer (pH 8) and 1 ml of 0.1 *M* lysine (pH 8.0) was added. After 1 h at room temperature with shaking, the gel was washed with 10 m*M* Tris–HCl buffer (pH 7.5) containing 0.15 *M* NaCl, 0.1 m*M* dithiothreitol and 1 m*M* EDTA.

Chromatography of NADase on the polyclonal antibody–Affi-Gel 10 column

Five small columns were filled with 1.5 ml of polyclonal antibody conjugated with Affi-Gel 10, and each column was loaded with 3 ml of the extract of *Neurospora crassa* conidia in water (4 mg/ml) according to the following procedure: 1 ml of extract was adsorbed into each gel at a flow-rate of 0.5 ml/min and allowed to rest in the column for 10 min, then the gels were washed with a second portion of 1 ml of extract and after 10 min replaced with the remaining enzyme solution. The eluate from each gel was applied again to the column according to the same procedure.

The gels were then washed with 7 ml of 0.1 *M* phosphate buffer and eluted with the following solutions:

1st gel: 9 ml of 0.1 *M* citrate buffer (pH 2.2) containing 1 *M* NaCl;
2nd gel: 9 ml of 0.1 *M* phosphate buffer containing 0.5% Triton X-100;
3rd gel: 9 ml of 10% dioxane in water (pH 7.0);
4th gel: 9 ml of 10% dioxane in 20 m*M* HCl (pH 2.5);
5th gel: 9 ml of 50% ethylene glycol in 20 m*M* HCl (pH 2.5).

The entire process was carried out at 4°C.

Sodium dodecyl sulphate–polyacrylamide gel electrophoresis (SDS-PAGE) was performed according to the procedure of Weber and Osborn [8] after concentration of the eluate from the immunoadsorbent gel by means of Centricon (Amicon, Danvers, MA, U.S.A.).

RESULTS AND DISCUSSION

Polyclonal antibodies obtained from active and denatured NADase cross-reacted with both types of enzyme and were mixed before their immobilization onto Affi-Gel 10 in order to recognize all the forms of the enzyme.

TABLE I

EFFECT OF VARIOUS SOLUTIONS ON THE CATALYTIC ACTIVITY OF NAD GLYCOHYDROLASE AFTER STORAGE FOR 1 h AT 4°C AND 25°C

The samples in citrate and in Triton X-100–phosphate buffer were assayed by HPLC and the other samples were tested by automatic titration.

Solution	Activity after storage at 4°C	Activity after storage at 25°C
Water	3.25 (100%)	2.5 (100%)
Citrate–NaCl (pH 2.2)	2.0 (61%)	2.75 (110%)
Triton–phosphate (pH 7.0)	3.9 (120%)	2.7 (108%)
Ethylene glycol (pH 2.2)	3.45 (106%)	2.45 (98%)
10% dioxane in water	3.1 (95%)	2.25 (90%)
10% dioxane (pH 2.2)	2.6 (80%)	1.85 (74%)

The total amount of polyclonal antibody obtained was 62.5 mg, as calculated spectrophotometrically by the extinction coefficient 1.4 for 1 mg protein/ml at 280 nm, whereas the amount of antibody bound to Affi-Gel 10 was 5.9 mg/ml of gel (92% yield).

The eluents for the immunoaffinity column were chosen from recommendations in the literature [9–11]. However, before the chromatography of the enzyme, the solutions chosen were tested in order to assess their effect on the NADase activity, after exposure for 1 h at 4 and 25°C. The behaviours of the five solutions described above at both temperatures tested were similar, whereas at alkaline pH (pH 10.5) (data not shown here) the enzyme was completely inactivated. The results are reported in Table I.

After elution of the gels with the solutions described above, NADase activity was assayed in the eluates and in the gels. Table II shows the recovery of the activity for a typical experiment.

The data in Table II show that no enzyme activity was found in the 0.1 *M* citrate–1 *M* NaCl eluate and virtually all NADase remained immobilized in the gel.

TABLE II

NADase ACTIVITY IN THE GELS DETERMINED BY AUTOMATIC TITRATION AFTER EXHAUSTIVE WASHING WITH DOUBLY DISTILLED WATER

The enzyme in the column washing and in the eluate was assayed by HPLC and then checked with the pH-Stat method after dialysis against water.

Eluent	Activity in the gel (units)	Activity in the washings	Activity in the eluate
Citrate–NaCl (pH 2.2)	6.62	0.3	0.0
Triton–phosphate (pH 7.0)	0.28	3.1	2.8
Ethylene glycol (pH 2.2)	1.93	3.5	0.75
10% dioxane in water	2.33	3.75	0.1
10% dioxane (pH 2.2)	2.59	3.82	0.05

TABLE III

NADase ACTIVITY DETERMINED BY AUTOMATIC TITRATION AFTER DIALYSIS OF THE SAMPLES AGAINST WATER

Run No.	NADase activity in the washings (%)	NADase activity in the eluate (%)
1	51	45
2	54	47
3	40	51
4	54	48
5	34	66
6	55	40
7	51	45
8	50	44

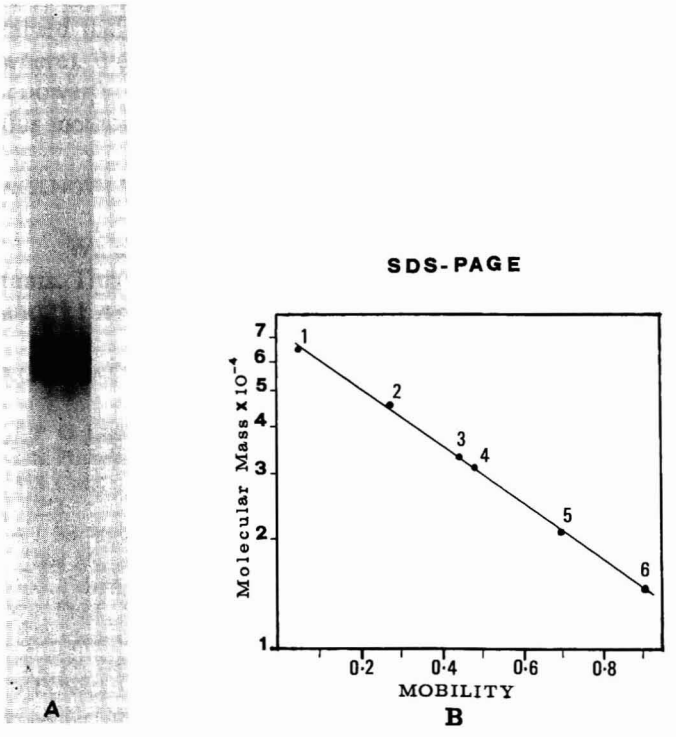

Fig. 1. (A) SDS-PAGE of the eluate with Triton X-100–phosphate buffer (pH 7.0). (B) Mobility of NADase (3) compared with (1) bovine serum albumin (M_r 66 200), (2) ovalbumin (M_r 45 000), (4) carbonic anhydrase (M_r 31 000), (5) soybean trypsin inhibitor (M_r 21 000) and (6) lysozyme (M_r 14 500).

Most of the NADase activity was similarly found in the gels eluted with 10% dioxane both in water and in 20 m*M* HCl and with ethylene glycol in 20 m*M* HCl, whereas their eluates contained only traces of activity. In contrast, the gel eluted with 0.5% Triton X-100 in 0.1 *M* phosphate buffer (pH 7.0) showed a minimum of NADase activity adsorbed, and most of the enzyme was found in the eluate and in the washings with 0.1 *M* phosphate buffer (pH 7.0).

The last column was repeatedly used for a total of eight runs and the results obtained were similar in each instance, as shown in Table III.

The purity of the samples eluted by Triton X-100–phosphate buffer was assessed by SDS-PAGE and by the spectrum of the eluate in the ultraviolet region.

SDS-PAGE showed only one band, corresponding to a protein of about 33 000 dalton (Fig. 1), as determined by comparison with standard proteins.

The UV spectrum showed the characteristic maximum of NADase at 234 nm [12], with a ratio A_{234}/A_{280} of 5.1, while the enzyme purified by affinity chromatography had a ratio of 5.6. The difference may be due to the presence of Triton X-100 in the eluate.

CONCLUSIONS

The purification method for NADase reported here seems to have some advantages over previous procedures. First, the immunoadsorbent can be used many times without a loss of efficiency, as showed in Table III. Moreover, a unique extraction with water of *Neurospora crassa* conidia is sufficient for loading the column, whereas affinity chromatography on 4-methyl-NAD–Sepharose needs at least two kinds of extraction (water and 0.17 *M* KCl) in order to prolong the life of the column [1]. The entire procedure causes no denaturation, in contrast to elution from the hydrophobic gel [3], because it is done under milder conditions. The capacity of the immunoadsorbent gel is not very high, as shown by the ratio of enzyme held by the column to enzyme washed with buffer, when only a few units were loaded onto 1.5 ml of gel (see Table II). On the other hand, the possibility of reusing the gel many times makes it suitable to the purification of larger amounts of NADase. The enzyme eluted with Triton X-100 in phosphate buffer (pH 7.5) is apparently homogeneous by SDS-PAGE and seems to be analogous to that purified by affinity chromatography.

ACKNOWLEDGEMENTS

This work was supported by the CNR Target Project on Biotechnology and Bioinstrumentation.

REFERENCES

1 F. Menegus and M. Pace, *Eur. J. Biochem.*, 113 (1981) 485.
2 M. Pace, D Agnellini, P. G. Pietta, A. Cocilovo and L. Bonizzi, *Prep. Biochem.*, 14 (1984) 349.
3 M. Pace, P. G. Pietta, D. Agnellini and P. L. Mauri, in O. M. Nejissel, R. R. van der Meer and K. Ch. A. M. Luyben (Editor), *Proceedings of the 4th European Congress of Biotechnology*, Vol. 2, Elsevier, Amsterdam, 1987, pp. 142–145.
4 P. G. Pietta, M. Pace and F. Menegus, *Anal. Biochem.*, 131 (1983) 533.
5 J. Horejsi and R. Smetana, *Acta Med. Scand.*, 155 (1956) 65.

6 S. Avrameas, *Immunochemistry*, 6 (1969) 43.
7 K. Ikura, K. Okumura, M. Yoshikawa, R. Sasaki and H. Chiba, *J. Appl. Biochem.*, 6 (1984) 222.
8 K. Weber and M. Osborn, *J. Biol. Chem.*, 244 (1969) 4406.
9 K. K. Andersson, Y. Benyamin, P. Dozou and C. Balny, *J. Immunol. Methods*, 25 (1979) 375.
10 H. D. Caldwell and C.-C. Kuo, *J. Immunol.*, 118 (1977) 437.
11 Y. Ikeda and M. Steiner, *J. Biol. Chem.*, 251 (1976) 6135.
12 M. Pace, D. Agnellini, P. G. Pietta, P. L. Mauri, F. Menegus and R. L. Berger, *Plant Physiol. (Life Sci. Adv.)*, 7 (1988) 115.

Journal of Chromatography, 539 (1991) 525–529
Elsevier Science Publishers B.V., Amsterdam

CHROM. 22 901

Use of immobilized triazine dyes in the purification of DNA topoisomerase I (Topo I) and terminal deoxynucleotidyl transferase (TdT) from calf thymus

ALGIMANTAS MARKAUSKAS*, VITALIS TIKNIUS and ROMAS MARCIŠAUSKAS
Institute of Applied Enzymology FERMENTAS, Fermentu 8, Vilnius-28, Lithuania (U.S.S.R.)

ABSTRACT

The interaction between TdT and Topo I, and twelve various triazine dyes immobilized on Sepharose CL-6B was studied. Yellow lightproof 2KT–Sepharose and Bordeaux 4ST–Sepharose were used to purify TdT and Topo I, respectively. The principal role of copper ions, complexed to the dye molecules, in the dye–protein interaction was evaluated.

INTRODUCTION

Terminal deoxynucleotidyl transferase (TdT) and DNA topoisomerase I (Topo I) from calf thymus gland are widely used in molecular biology. TdT is a unique DNA polymerase requiring no template and catalysing the addition of deoxynucleoside triphosphates at the 3′-end of poly- or oligodeoxynucleotide initiator and releasing inorganic pyrophosphate. This enzyme is generally used in genetic engineering for elongation of the DNA chains and for 3′-end labelling [1,2]. Topo I catalyses the relaxation of duplex DNA, knotting of single-stranded rings and intertwining of complementary single-stranded rings, and forms catenanes between one nicked and one closed circular duplex. This enzyme is employed in structural studies of DNA and in modelling of genetic processes [3].

In order to develop an efficient routine method for the purification of these proteins, a variety of adsorbents should be available. As the use of immobilized triazine dyes for this purpose has not previously been reported, we studied the interaction between these enzymes and adsorbents based on twelve triazine dyes, and two of them proved to be suitable for use in purifcation.

EXPERIMENTAL

Materials

All immobilized triazine dyes were kindly provided by the Laboratory of Adsorbent Synthesis and pBR 322 DNA by the Laboratory of Genetic Engineering of

0021-9673/91/$03.50

this Institute. Tris and EDTA were purchased from Serva (Heidelberg, Germany) and all other reagents from Merck (Darmstadt, Germany).

Preparation of initial extracts

A 500-g sample of thymus glands freed from debris and clotted blood were minced with a meat grinder and homogenized with an equal volume of 100 m*M* Tris–HCl (pH 6.8)–0.3 *M* KCl–2.5 m*M* K_3-EDTA–50 m*M* Na_2SO_3–1 m*M* PMSF–10% (v/v) ethylene glycol–14 m*M* 2-mercaptoethanol–10 m*M* KF–10 m*M* NAD five times for 30 s each in a Waring-type blender. After centrifugation at 30 000 *g* for 1 h, the supernatant was diluted with 50 m*M* Tris–HCl (pH 6.8)–2 m*M* K_3-EDTA–14 m*M* 2-mercaptoethanol–10% ethylene glycol to a volume of 1.4 l, and the 35–70% ammonium sulphate fraction precipitate was dissolved in 40 m*M* Tris–HCl (pH 8.0)–1.6 m*M* K_3-EDTA–14 m*M* 2-mercaptoethanol–10% ethylene glycol. This extract, dialysed overnight against the same buffer but containing glycerol instead of ethylene glycol, was applied to a Servacel DEAE-52 column (30 × 5 cm I.D.), and the flow-through fractions were collected. Further fractionation was done on a Bio-Rex 70 column (30 × 2.6 cm I.D.) in the same buffer. The column was developed with a 500-ml KCl gradient from 0 to 1 *M*. TdT activity eluted at 0.1–0.15 *M* KCl and Topo I at 0.18–0.22 *M* KCl. These preparations were used for further studies.

Screening procedure

A 0.15-ml aliquot of an appropriate adsorbent, equilibrated with 20 m*M* Tris–HCl (pH 8.0)–10 m*M* $MgCl_2$–0.1 m*M* K_3-EDTA–10 m*M* 2-mercaptoethanol–10% glycerol, and 0.5 ml of enzyme preparation dialysed against the same buffer, were thoroughly mixed in Eppendorf tubes. After incubation for 30 min in an ice-bath, the suspension was centrifuged for 30 s at 15 000 *g* and supernatants were collected for further analysis.

Enzyme assays

TdT activity was assayed according to Coleman [4] and Topo I as indicated by Ferro *et al.* [5].

Protein assay

A Bio-Rad Labs. protein assay kit was used to determine protein concentrations.

RESULTS

The supernatants after screening were subjected to analysis, and both protein concentration and enzyme activity were determined. The results are summarized in Table I. Two adsorbents were selected for further studies: Yellow Lightproof 2KT–Sepharose CL-6B and Bordeaux 4ST–Sepharose CL-6B (Fig. 1).

After optimization of the chromatographic conditions, the following parameters were obtained: Topo I, elution at 0.12–0.21 *M* KCl, purification 11.2-fold, yield 67%, specific activity (3–4) × 10^5 U/mg (Fig. 2); TdT, elution at 0.22–0.55 *M*, purification 10.5-fold, yield 80%, specific activity (5–7) × 10^4 U/mg (Fig. 3).

It should be noted that complexed Cu^{2+} ions are present in the molecules of both dyes thus selected, and that these ions play a crucial role in the affinity interaction. As

TABLE I

DATA ON DYE–ENZYME INTERACTIONS

Triazine dye immobilized on Sepharose CL-6B	TdT		Topo I	
	A[a]	B[b]	A[a]	B[b]
Red-Brown 2K	94.0	+	56.2	+
Scarlet 6S	68.2	+	42.5	+
Pharmacia Red	79.8	+	43.8	+
Pharmacia Blue	83.9	+	32.5	+
Orange 5K	77.5	+	62.4	+
Yellow Bright 5Z	81.6	+	34.7	+
Bordeaux 4ST	94.1	+	15.4	+
Scarlet 2Z	74.7	+	28.5	−
Golden 2KX	20.2	−	34.7	−
Active Orange KX	48.2	−	42.3	+
Scarlet 4ZT	19.7	−	51.2	−
Yellow Lightproof 2KT	24.6	+	19.5	−

[a] Fraction of protein bound (%).
[b] + = Target enzyme bound; − = target enzyme not bound.

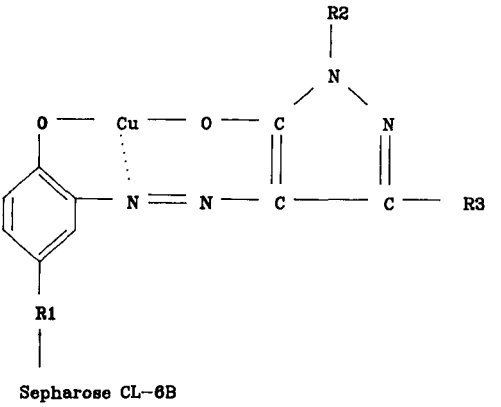

(1)

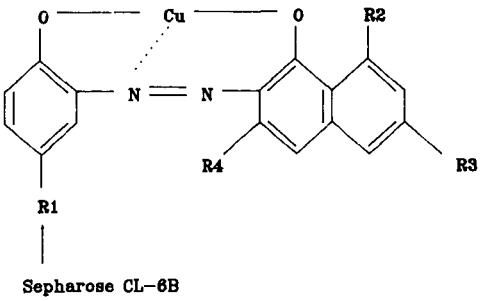

(2)

Fig. 1. Essential part of the chelating ring structure: (1) Yellow Lightproof 2KT; (2) Bordeaux 4ST. R1–R4 = reactive groups.

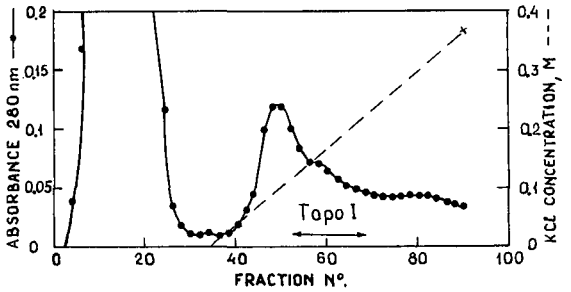

Fig. 2. Purification of Topo I on Bordeaux 4ST–Sepharose CL-6B. The 45-ml column was equilibrated with 20 m*M* Tris–HCl (pH 8.0)–10 m*M* $MgCl_2$–0.1 m*M* EDTA–10 m*M* 2-mercaptoethanol–10% (v/v) glycerol. KCl gradient from 0 to 0.4 *M*. Flow-rate, 15 ml/h.

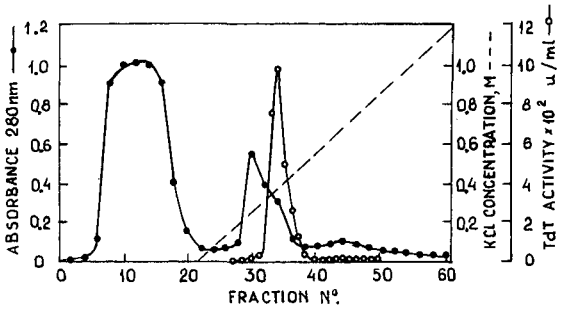

Fig. 3. Purification of TdT on Yellow Lightproof 2KT–Sepharose CL-6B. The 60-ml column was equilibrated with 20 m*M* Tris–HCl (pH 7.0)–2 m*M* $MgCl_2$–2 m*M* $ZnCl_2$–0.5 m*M* EDTA–14 m*M* 2-mercaptoethanol–10% (v/v) glycerol. KCl gradient from 0 to 1.2 *M*. Flow-rate, 20 ml/h.

TdT enzyme is sensitive to copper ions, we were forced to replace this ligand by zinc, and a Zn^{2+}/Mg^{2+}/EDTA ratio of 2:2:1 in the chromatographic buffer was found to be satisfactory, because in the absence of the transition metals we observed no interaction. The complete replacement of copper with zinc in the dye was accomplished by extensive washing of the adsorbent with several volumes of 100 m*M* EDTA (pH 5), deionized water and finally 15 m*M* $ZnCl_2$.

In contrast, Topo I is stable in the presence of copper complexed in the Bordeaux 4ST molecule. However, this enzyme showed only partial binding, but the addition of 10 m*M* $MgCl_2$ solved this problem. When the copper ions had been washed out with EDTA, the interaction, in contrast to that with TdT, was so strong that we were unable to elute the active enzyme under any conditions.

These results clearly demonstrate the pseudo-affinity nature of the interaction in both instances, *i.e.*, the interaction in the vicinity of active centre, and undoubtedly further studies are required to verify this conclusion.

REFERENCES

1 F. J. Bollum, in P. D. Boyer (Editor), *The Enzymes*, Vol. 10, Academic Press, New York, 3rd ed., 1974, p. 145.
2 R. L. Ratliff, in P. D. Boyer (Editor), *The Enzymes*, Vol. 14, Academic Press, New York, 1981, p. 105.
3 M. Gellert, *Annu. Rev. Biochem.*, 50 (1981) 879.
4 M. S. Coleman, *Arch. Biochem. Biophys.*, 182 (1977) 525.
5 A. M. Ferro, N. P. Higgins and B. M. Olivera, *J. Biol. Chem.*, 258 (1983) 6000.

Journal of Chromatography, 539 (1991) 531–533
Elsevier Science Publishers B.V., Amsterdam

CHROM. 22 908

Affinity purification of plasminogen by radial-flow affinity chromatography

YASMINE PLANQUES* and HÉLÈNE PORA
Cuno Europe, 1 Boulevard de l'Oise, 95030 Cergy-Pontoise (France)
and
FRANCO D. MENOZZI
Institut Pasteur, Laboratoire de Microbiologie Moléculaire, 1 Rue du Professeur Calmette, 59019 Lille (France)

ABSTRACT

A method for the purification of plasminogen using immobilized L-lysine on a membrane, the whole system being constructed in a radial flow cartridge, is described. Human plasma was applied to the cartridge at 20 ml/min. The results showed that under the chromatographic conditions chosen, in a single pass, >85% recovery of plasminogen was attained with a 110-fold increase in specific activity.

INTRODUCTION

With the recent advances in biotechnology, there is a large demand for purification methods that can achieve high product purity in a few simple steps. Affinity chromatography has become a method of choice as high purity can be obtained in a single step [1,2].

Plasminogen is the inactive precursor of the proteolytic enzyme plasmin, which is responsible for the dissolution of fibrin clots in the blood. The purification of plasminogen using L-lysine bound on Sepharose has been reported [3]. Although, the method proved to be satisfactory, the flow-rates were very low (75 ml/h) and it was time consuming. Bound L-lysine has been used in many other applications, and is a very useful ligand for the purification of plasmin and plasminogen of various species [4,5], plasminogen activator [6] and ribonucleic acids [7].

This paper describes a method for purifying plasminogen from human plasma with L-lysine immobilized on a radial-flow membrane cartridge system. The method provides a new means of obtaining large amounts of plasminogen within a few hours and could be easily extended owing to the linear scale-up capability of this system, which has been demonstrated previously using *p*-aminobenzamidine as a ligand [8].

0021-9673/91/$03.50

EXPERIMENTAL

L-Lysine coupling

A Zetaffinity 250 cartridge (Cuno, Cergy-Pontoise, France) containing modified cellulose was used as chromatographic medium. The hydroxyl derivative was used for ligand coupling. The activation of hydroxyl functions was accomplished with a 1.5% metaperiodate solution. Lysine was dissolved in 0.05 *M* sodium phosphate containing 0.25 *M* NaCl and recycled overnight through the cartridge. After reduction with $NaBH_4$, the cartridge was drained and the unbound reactive sites were blocked with 2% glycine ethyl ester hydrochloride solution.

Plasminogen purification from human plasma

The cartridge containing bound lysine was equilibrated with 0.1 *M* sodium phosphate (pH 7.4) containing 0.05 *M* NaCl and 0.01% Tween 80. After centrifugation and filtration, the plasma was diluted with equilibration buffer (0.5 v/v) and applied to the cartridge at 20 ml/min. The cartridge was washed with equilibration buffer until the absorbance at 280 nm reached the baseline, then elution was carried out with 0.2 *M* 6-aminocaproic acid in equilibration buffer. Before analysis, bound fractions were dialysed overnight at 4°C against 0.01 *M* 6-aminocaproic acid in equilibration buffer. The protein content was measured using the Bio-Rad protein assay and the plasminogen activity with the Kabi substrate S-2251. Purity was evaluated by 7.5% sodium dodecyl sulphate polyacrylamide gel electrophoresis.

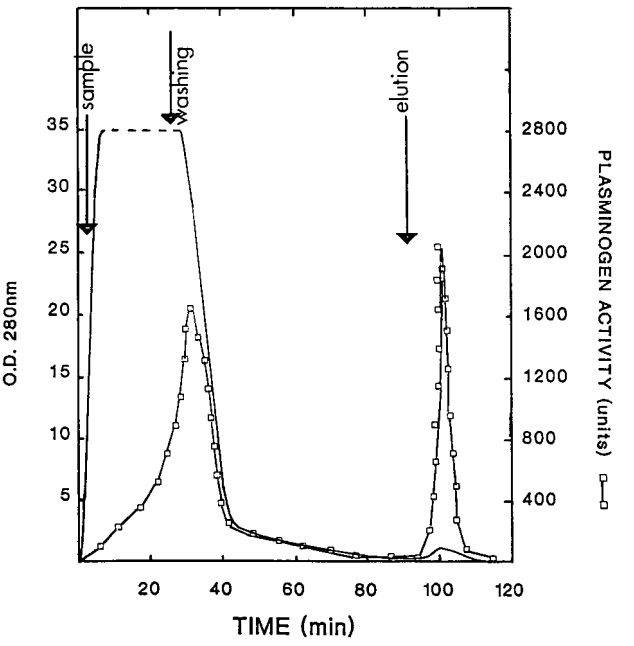

Fig. 1. Chromatogram of the purification of plasminogen from human plasma using lysine bound on a radial-flow cartridge. Chromatography was performed as described under Experimental.

TABLE I

RESULTS OF PLASMINOGEN PURIFICATION FROM HUMAN PLASMA USING LYSINE BOUND ON A RADIAL-FLOW CARTRIDGE

Device	Plasma volume (ml)	Plasminogen activity eluted (units)	Specific activity eluted	Purification	Total recovery (%)
No. 60 disc[a]	50	2452	406	100 ×	88
No. 250 capsule[b]	400	8948	358	144 ×	57
No. 250 capsule[c]	250	6045	410	124 ×	74

[a] Entire fractionation done at 4°C.
[b] 400 ml of plasma diluted to 600 ml in equilibration buffer.
[c] 250 ml of plasma diluted to 500 ml in equilibration buffer.

RESULTS AND DISCUSSION

The chromatograms (Fig. 1) shows that plasminogen was retained by the bound lysine. Electrophoretic analysis demonstrated that the eluted fractions were devoid of any visible protein contamination. The results in Table I show that in a single pass a very good increase of purity was obtained with satisfactory recoveries. This purification procedure is a very convenient method for fast and easy recovery of plasminogen, as a whole chromatographic cycle could be performed within 2 h.

This radial-flow chromatographic method has been used in many applications involving ion exchange and has proved to be extremely useful, particularly when the product of interest is present at low concentration in a very large sample, *e.g.*, monoclonal antibodies from hybridoma cell culture supernatant [9] or recombinant proteins [10]. Moreover, the linear scale-up capability of these radial-flow cartridges has already been demonstrated with ion exchangers [11] and affinity chromatography [8]. Hence the method described here could easily be scaled up to very large amounts within a short period of time.

REFERENCES

1 P. Cuatrecasas, *Adv. Enzymol.*, 36 (1972) 29.
2 S. Ostrove, *Methods Enzymol.*, 182 (1990) 357.
3 D. G. Deutsch and E. T. Mertz, *Science (Washington, D.C.)*, 170 (1970) 1095.
4 R. Gonzalez, M. Gronow, B. N. Violand and F. J. Castellino, *J. Biol. Chem.*, 252 (1977) 2175.
5 N. F. Paoni, B. N. Violand and F. J. Castellino, *J. Biol. Chem.*, 252 (1977) 7725.
6 R. Radcliffe and T. Heinze, *Arch. Biochem. Biophys.*, 189 (1978) 185.
7 D. S. Jones, H. K. Lundgren and F. T. Jay, *Nucleic Acids Res.*, 3 (1978) 1589.
8 S. H. Huang, S. Roy, K. C. Hou and G. T. Tsiao, *Biotechnology Prog.*, 4 (1985) 159.
9 F. B. Menozzi, P. Vanderpoorten, C. Dejaiffe and A. O. A. Miller, *J. Immunol. Methods*, 99 (1987) 229.
10 M. C. Casagli, M. G. Borri, C. d'Ettore, C. L. Caleoti and C. D. Liegro, *Prep. Biochem.*, 19 (1989) 23.
11 A. Jungbauer, F. Unterluggauer, K. Uhl, A. Buchacher, F. Steindl, B. Pettauer and E. Wenish, *Biotechnol. Bioeng.*, 32 (1988) 326.

Author Index Vol. 539

PUBLICATION SCHEDULE FOR 1991

Journal of Chromatography and Journal of Chromatography, Biomedical Applications

MONTH	D 1990	J	F	M	A	
Journal of Chromatography	535/1 + 2	536/1 + 2 537/1 + 2 538/1	538/2 539/1 539/2	540 541/1 + 2 542/1		The publication schedule for further issues will be published later
Cumulative Indexes, Vols. 501–550						
Bibliography Section				560/1		
Biomedical Applications		562/1 + 2 563/1	563/2	564/1	564/2 565/1 + 2	

INFORMATION FOR AUTHORS

(Detailed *Instructions to Authors* were published in Vol. 522, pp. 351–354. A free reprint can be obtained by application to the publisher, Elsevier Science Publishers B.V., P.O. Box 330, 1000 AH Amsterdam, The Netherlands.)

Types of Contributions. The following types of papers are published in the *Journal of Chromatography* and the section on *Biomedical Applications:* Regular research papers (Full-length papers), Review articles and Short Communications. Short Communications are usually descriptions of short investigations, or they can report minor technical improvements of previously published procedures; they reflect the same quality of research as Full-length papers, but should preferably not exceed six printed pages. For Review articles, see inside front cover under Submission of Papers.

Submission. Every paper must be accompanied by a letter from the senior author, stating that he/she is submitting the paper for publication in the *Journal of Chromatography*.

Manuscripts. Manuscripts should be typed in double spacing on consecutively numbered pages of uniform size. The manuscript should be preceded by a sheet of manuscript paper carrying the title of the paper and the name and full postal address of the person to whom the proofs are to be sent. As a rule, papers should be divided into sections, headed by a caption (*e.g.*, Abstract, Introduction, Experimental, Results, Discussion, etc.). All illustrations, photographs, tables, etc., should be on separate sheets.

Introduction. Every paper must have a concise introduction mentioning what has been done before on the topic described, and stating clearly what is new in the paper now submitted.

Abstract. All articles should have an abstract of 50–100 words which clearly and briefly indicates what is new, different and significant.

Illustrations. The figures should be submitted in a form suitable for reproduction, drawn in Indian ink on drawing or tracing paper. Each illustration should have a legend, all the *legends* being typed (with double spacing) together on a *separate sheet.* If structures are given in the text, the original drawings should be supplied. Coloured illustrations are reproduced at the author's expense, the cost being determined by the number of pages and by the number of colours needed. The written permission of the author and publisher must be obtained for the use of any figure already published. Its source must be indicated in the legend.

References. References should be numbered in the order in which they are cited in the text, and listed in numerical sequence on a separate sheet at the end of the article. Please check a recent issue for the layout of the reference list. Abbreviations for the titles of journals should follow the system used by *Chemical Abstracts.* Articles not yet published should be given as "in press" (journal should be specified), "submitted for publication" (journal should be specified), "in preparation" or "personal communication".

Dispatch. Before sending the manuscript to the Editor please check that the envelope contains four copies of the paper complete with references, legends and figures. One of the sets of figures must be the originals suitable for direct reproduction. Please also ensure that permission to publish has been obtained from your institute.

Proofs. One set of proofs will be sent to the author to be carefully checked for printer's errors. Corrections must be restricted to instances in which the proof is at variance with the manuscript. "Extra corrections" will be inserted at the author's expense.

Reprints. Fifty reprints of Full-length papers and Short Communications will be supplied free of charge. Additional reprints can be ordered by the authors. An order form containing price quotations will be sent to the authors together with the proofs of their article.

Advertisements. Advertisement rates are available from the publisher on request. The Editors of the journal accept no responsibility for the contents of the advertisements.

Ion Chromatography

Principles and Applications

by **P.R. Haddad,** *University of New South Wales, Kensington, N.S.W., Australia and* **P.E. Jackson,** *Waters Chromatography Division, Milford, MA, USA*

(Journal of Chromatography Library, 46)

Ion chromatography (IC) was first introduced in 1975 for the determination of inorganic anions and cations and water soluble organic acids and bases. Since then, the technique has grown in usage at a phenomenal rate. The growth of IC has been accompanied by a blurring of the original definition of the technique, so that it now embraces a very wide range of separation and detection methods, many of which bear little resemblance to the initial concept of ion-exchange separation coupled with conductivity detection.

Ion Chromatography is the first book to provide a comprehensive treatise on all aspects of ion chromatography. Ion-exchange, ion-interaction, ion-exclusion and other pertinent separation modes are included, whilst the detection methods discussed include conductivity, amperometry, potentiometry, spectroscopic methods (both molecular and atomic) and post-column reactions. The theoretical background and operating principles of each separation and detection mode are discussed in detail. A unique extensive compilation of practical applications of IC (1250 literature citations) is presented in tabular form. All relevant details of each application are given to accommodate reproduction of the method in the laboratory without access to the original publication.

This truly comprehensive text on ion chromatography should prove to be the standard reference work for researchers and those involved in the use of the subject in practical situations.

Contents: Chapter 1. Introduction. **PART I. Ion-Exchange Separation Methods.** Chapter 2. An introduction to ion-exchange methods. Chapter 3. Ion-exchange stationary phases for ion chromatography. Chapter 4. Eluents for ion-exchange separations. Chapter 5. Retention models for ion-exchange. **PART II. Ion-Interaction, Ion-Exclusion and Miscellaneous Separation Methods.** Chapter 6. Ion-interaction chromatography. Chapter 7. Ion-exclusion chromatography. Chapter 8. Miscellaneous separation methods. **PART III. Detection Methods.** Chapter 9. Conductivity detection. Chapter 10. Electrochemical detection (amperometry, voltammetry and coulometry). Chapter 11. Potentiometric detection. Chapter 12. Spectroscopic detection methods. Chapter 13. Detection by post-column reaction. **PART IV. Practical Aspects.** Chapter 14. Sample handling in ion chromatography. Chapter 15. Methods development. **PART V. Applications of Ion Chromatography.** Overview of the applications section. Chapter 16. Environmental applications. Chapter 17. Industrial applications. Chapter 18. Analysis of foods and plants. Chapter 19. Clinical and pharmaceutical applications. Chapter 20. Analysis of metals and metallurgical solutions. Chapter 21. Analysis of treated waters. Chapter 22. Miscellaneous applications. Appendix A. Statistical information on ion chromatography publications. Appendix B. Abbreviations and symbols. Index.

1990 798 pages
Price: US$ 191.50 / Dfl. 335.00
ISBN 0-444-88232-4

Elsevier Science Publishers
P.O. Box 211, 1000 AE Amsterdam, The Netherlands
P.O. Box 882, Madison Square Station, New York, NY 10159, USA